AD NUMBER

AD483820

NEW LIMITATION CHANGE

TO

Approved for public release, distribution unlimited

FROM

Distribution authorized to U.S. Gov't. agencies and their contractors; Administrative/Operational use; Jun 1966. Other requests shall be referred to Air Force Aero-Propulsion Laboratory, Research and Technology Division, AFSC, Wright-Patterson Air Force Base, OH 45433

AUTHORITY

AFAPL ltr, 12 Apr 1972

AFAPL-TR-65-122

CORONA ONSET VOLTAGE OF INSULATED AND BARE ELELECTRODES IN RAREFIED AIR AND OTHER GASES

WILLIAM G. DUNBAR

THE BOEING COMPANY
Aerospace Group

TECHNICAL REPORT AFAPL-TR-65-122

JUNE 1966

AIR FORCE AERO-PROPULSION LABORATORY
RESEARCH AND TECHNOLOGY DIVISION
AIR FORCE SYSTEMS COMMAND
WRIGHT-PATTERSON AIR FORCE BASE, OHIO

NOTICES

When Government drawings, specifications, or other data are used for any purpose other than in connection with a definitely related Government procurement operation, the United States Government thereby incurs no responsibility nor any obligation whatsoever; and the fact that the Government may have formulated, furnished, or in any way supplied the said drawings, specifications, or other data, is not to be regarded by implication or otherwise as in any manner licensing the holder or any other person or corporation, or conveying any rights or permission to manufacture, use, or sell any patented invention that may in any way be related thereto.

Copies of this report should not be returned to the Research and Technology Division unless return is required by security considerations, contractual obligations, or notice on a specific document.

CORONA ONSET VOLTAGE OF INSULATED AND BARE ELECTRODES IN RAREFIED AIR AND OTHER GASES

W. G. Dunbar
THE BOEING COMPANY
Aerospace Group

FOREWORD

It was recognized early in the X-20A (Dyna-Soar) program that electrical discharges, caused by corona and glow discharges, would induce electromagnetic interference into the vehicle electronic subsystems. During both boost and re-entry, the X-20A must pass through the 70,000- to 250,000-foot altitude zone in which corona is readily generated at low voltages.

Corona in this altitude zone was investigated from April 1959 to March 1963 by The Boeing Company during the USAF X-20A contract, AF33(657)-7132. When this contract was cancelled, experimental corona research had been completed, but no formal report had been written. In July 1965, the U.S. Air Force issued Contract AF33(615)-3020 to Boeing to document the results of the X-20A corona studies. The specific objectives were to (1) produce an assembled, condensed, analyzed, and documented high-altitude-corona report; (2) establish high-altitude-corona onset voltages; (3) determine how this onset voltage could be increased; and (4) recommend areas of investigation necessary to increase the minimum corona onset voltage. Experimental work on this contract was limited to the measurement of corona onset voltage in helium and helium-oxygen mixtures (1) between bare electrodes, (2) between twisted and spaced teflon insulated wires, and (3) between wired connector terminations.

The work on Contract AF33(615)-3020 was administered as Project NR 22087-NB "High-Altitude Corona," under the direction of the Air Force Aero-Propulsion Laboratory, Research and Technology Division, Wright-Patterson Air Force Base, Ohio, with Captain J. Priest as project engineer.

This document constitutes Boeing's final report in fulfillment of the requirements of Contract AF33(615)-3020. The analysis and technical writing in this document were accomplished by William G. Dunbar of The Boeing Company, Aerospace Group, Power Systems Unit. This report was submitted by the author 10 June 1966.

Publication of this report does not constitute Air Force approval of the report's findings or conclusions. It is published only for the exchange and stimulation of ideas.

PAUL W. MONTGOMERY, Major, USAF
Chief, Propulsion & Power Br
Aerospace Power Division

ABSTRACT

Electrical discharges caused by corona, glow discharges, and voltage breakdown were measured under conditions encountered in the X-20A (Dyna-Soar) aerospace vehicle when operating within the 70,000- to 250,000 altitude zone. Most measurements were made at the electric-power-system frequency (400-hertz) in gases (i.e., helium, nitrogen, oxygen, helium-oxygen mixtures, nitrogen-oxygen mixtures, and normal sea-level air at reduced pressure) used to pressurize X-20A vehicle compartments.

Test results show that at the minimum of the Paschen law type curve: (1) the corona onset voltage (that voltage at which the electrical discharge is initiated) can be increased by insulating the electrical terminals and by twisting or cabling the insulated wires; (2) the corona onset voltage between insulated wires is increased as the insulation is made thicker and insulation dielectric constant is made lower, and is decreased to that of bare wires as the wire diameter and wire spacing are increased; and (3) the corona onset voltage of components depends on the type of component, its wire connections, its installation, and the gaseous environment.

The corona onset voltage of round, bare, nichrome wires is less at temperatures over 500°C than at temperatures between -60°C and 150°C. The corona onset voltage drops to nearly zero when contaminants such as molybdenum-trioxide vapor permeate the air space between wires at temperatures above 500°C and pressures above 1.0 torr.

CONTENTS

ILLUSTRATIONS

TABLES

ILLUSTRATIONS

ILLUSTRATIONS (Cont)

TABLES

I. INTRODUCTION

Many spacecraft electric-power-subsystem components are required to operate in various low-pressure and/or high-temperature environments during launch, flight, and reentry. Some combinations of low pressure and high temperature are in a regime where corona readily forms on the conducting parts of a 115/200-volt power subsystem. Such corona creates radio interference, and if allowed to persist, will deteriorate insulation.

Much of this document is the result of an effort to assemble, condense, and analyze the high-altitude-corona onset voltage data acquired during the design and development phase of the X-20A space vehicle. The X-20A winged vehicle was designed to attain orbital velocities and to withstand reentry heating. Some of the electrical equipment was located in compartments where, during flight, it could be exposed to low-pressure air, nitrogen, oxygen, or nitrogen-oxygen mixtures. Other electrical equipment was located in the unpressurized air-filled nose and wing compartments, where high temperatures would exist during boost and reentry. These high-temperature compartments were constructed of disilicide-coated molybdenum. Hence, electrical components were exposed to high-temperature molybdenum trioxide-air mixtures when coating failures occurred.

The corona onset voltage in helium-oxygen mixtures becomes important because these gases are proposed for manned spacecraft atmospheres. The optimum helium-to-oxygen ratio has not yet been established; it may vary from mission to mission. Corona onset voltage may be a consideration in selecting the optimum ratio, because often the corona onset voltage in gas mixtures is lower than the onset voltage in either pure component. For these reasons, the original X-20A data has been supplemented with data obtained from tests in helium-oxygen mixtures.

Much of the corona data obtained during X-20A development is also applicable to other spacecraft. One objective of this document is to present this corona data in a form which is useful to design of spacecraft. The theoretical aspects of corona are discussed in the section entitled "Electrical Characteristics of Corona." The "Test Equipment and Procedures" section pertains to the experimental work done on the X-20A program and the helium-oxygen research. The analyzed and summarized data from tests appear in Section III, "Corona Test Data." Detailed test data are located in the appendixes.

II. DESCRIPTION OF CORONA AND ITS OCCURRENCE

In this section is discussed the electrical properties of corona, which is the faintly luminous and audible glow surrounding electrically energized electrodes at voltages slightly below or coincident with the sparkover voltage. Theoretical studies and experiments on corona carried out in the past are referenced where applicable.

Corona is an audible, luminous, voltage discharge resulting from the ionization of gas surrounding a conductor, around which exists a voltage gradient exceeding a critical value (References 1 and 2). In a strict sense, the word "corona" includes only those electrical discharges occurring at near sea-level pressures. Glow discharge and voltage breakdown better describe the electrical discharges at pressures below 20 torr. However, because corona is associated with a glow, and occurs at the same onset potential as glow discharge and voltage breakdown, the word "corona" is used throughout this report to identify any electrical discharge.

Corona within an electrical-power system consumes power, generates spurious high-frequency voltages that produce interference in communication and electronic equipment, deteriorates insulation in the vicinity of the discharge, and disassociates some gases, creating noxious gases and odors. Corona can occur whenever the potential between electrodes is greater than the minimum voltage expressed by the Paschen law curve.

This law states: "If the length of the discharge gap (between electrodes) and the gas pressure (at constant temperature) are altered in such a way that their product is unchanged, the magnitude of the breakdown voltage remains constant" (Reference 3).

Loeb (Reference 4) describes partial voltage breakdown ca[illegible]d by gaseous electrical discharges as:

"A manifestation of discharge or breakdown at the electrodes is the emission of light, sometimes accompanied by audible noise and by current fluctuations which can be picked up inductively and which manifest themselves in radio interference. The peculiar forms of these localized and partial breakdowns have led to their being characterized by such names as corona and brush discharge and at lower pressures glow discharge."

The terms glow, brush, and corona [illegible] different visual forms of the same phenomenon. At low pressure, the [illegible]osity is general and diffuses over the surface of the electrodes, as one [illegible] at from high diffusion of electrons at low pressures; hence, glow discharge. [illegible] sea-level atmospheric pressure, the luminosity at the negative electrode is localized at points in small areas, whereas at the positive electrode the luminosity sometimes spreads as a thin film over

the high field area. This phenomenon is commonly called corona. Under other conditions, the luminosity extends out into the interelectrode gap in the form of a brush of diverse geometry — originally called the brush discharge. The terms brush corona, impulse corona, and streamer corona are descriptions of the different visual forms of an electrical discharge.

"Voltage breakdown" is the temporary or permanent loss of normal insulating properties. It is normal design practice to provide a dielectric material or dielectric material system with a dielectric strength which can withstand an electric field higher than the electric field at the surface of the electrode. Voltage breakdown results when the dielectric material deteriorates. Heat and corona frequently cause deterioration of dielectric materials.

CORONA ONSET VOLTAGE

When corona is experimentally measured, two terms are used to describe the presence of corona — corona onset voltage (COV) and corona offset voltage. Corona onset voltage is the lowest potential at which ionization by collision becomes a cumulative process; i.e., the potential at which self-sustained corona first starts. The COV is determined by increasing the applied voltage between electrodes until corona-current induced signals appear on the screen of an oscilloscope or similar detector. That voltage is then held constant for a period of time to determine if the pulses are sustained. If the pulses are not sustained, the voltage is increased in small increments until sustained corona is obtained. Corona offset voltage is the voltage at which corona is extinguished. The offset potential is determined by decreasing the applied voltage across the specimen until corona signals disappear from the oscilloscope screen or detector.

When corona is present, there is a self-sustained electrical discharge and, consequently, a release of energy. This energy tends to heat the interelectrode gas and any nearby insulation surfaces. Any temperature rise will change the offset voltage, thus giving inconsistent experimental data. Therefore, the corona onset voltage measurement is generally more repeatable than the corona offset voltage measurement.

Self-sustained corona depends on the stripping of electrons from neutral atoms and the ionization of other atoms by these electrons. To be effective ionizers, these stripped electrons must gain a certain minimum kinetic energy from acceleration in the electric field. Attainment of ionization energy depends on the electric-field strength and the mean free path of the electron. The mean free path is inversely proportional to the gas density; thus COV is a function of gas composition and density.

GAS PRESSURE-DENSITY RELATIONSHIP

The density of a gas is a function of temperature and pressure or altitude. Pressure, volume, and temperature of a perfect gas are related by the equation,

$$PV = NRT \qquad (1)$$

where: P = pressure in torr

V = volume in cubic centimeters

T = absolute temperature in degrees Kelvin

N = number of moles

R = work per degree Celsius per mole

The gas density is defined as the number of molecules per cubic centimeter at pressure P.

As gas density is increased from standard temperature and pressure, the COV is increased because at higher densities the molecules are packed closer, and a higher electric field is required to accelerate the electrons to ionizing energy within the mean free path. The COV decreases as gas density is decreased from standard pressure and temperature because the longer mean free path permits the electrons to gain more energy prior to collision. As density is further decreased, the COV decreases until a minimum is reached. The pressure corresponding to minimum COV depends on the spacing of the electrodes; for a one-centimeter spacing at room temperature this pressure occurs between 0.5 and 1.0 torr. A representative minimum COV for air is 326 volts d.c.; the COV for the same contact configuration at standard atmospheric conditions is 31 kilovolts.

As density is further reduced, the COV rises steeply because the spacing between gas molecules becomes so large that although every electron collision produces ionization, it is hard to achieve enough ionizations to sustain the chain reaction. Finally, the pressure becomes so low that the average electron travels from one electrode to the other without colliding with a molecule. This is also the reason why the minimum COV varies with spacing — as the spacing is increased, the minimum COV occurs at lower pressures (Reference 5).

Corona, under normal conditions, has no sharply defined starting voltage because its initiation depends on an external source of ionization. There is generally a time delay between the application of voltage and corona. This time delay varies statistically and is a function of the difference between the applied voltage and the "critical voltage." Ultraviolet and higher-energy radiation reduce the time delay considerably.

Below the critical voltage, there is a potential, Vg, where pulses of corona start but are not self-sustaining, hence are extinguished. The region from Vg to the critical voltage is called the "Geiger-counter regime" (Reference 6). The frequency of the pulses in this region generally depends on the intensity of the external ionizing agents present.

When radioactive Cobalt-60, a gamma emitter, is used as an ionizing material, it affects corona in three ways: first, it lowers the corona onset voltage slightly; second, it raises the intensity of the intermittent corona; and third, it may alter the mechanical and electrical properties of the insulation to make the material more or less corona resistant. Irradiated polyethylene is an example of a material which is changed by radiation to be more corona resistant. Its increased corona resistance after irradiation results from an increase in ability to shrink and bond to itself to form a structure with fewer voids (Reference 7).

The COV of a test specimen as a function of gas density and spacing is shown in Figure 1. The general shape of this curve, which is defined by Paschen's law and is referred to as the Paschen law curve, has been known for many years. Paschen curves have been published for many gases and spacings between bare-metal electrodes. The COV as a function of gas density and spacing is different for each gas and gas mixture and is affected by the electrode material and electrode configuration. The COV is always the same for a given gas and gas density, regardless of what combination of pressure and temperature produce that density, for electrode spacings between 0.5 and 25 millimeters and temperatures below 500°C.

The COV may be related to temperature and altitude by using the U.S. Standard Atmosphere, which gives the air-density factor as a function of altitude. Thus, for corona test purposes, it is possible to simulate any altitude and temperature in a room-temperature chamber containing gas at an appropriate pressure. However, this simulated test environment ignores higher-order effects from chemical and thermal dielectric deterioration, which would occur at a temperature other than room temperature. A U. S. Standard-Atmosphere chart is partially reproduced in Appendix V (Table V-1 and Reference 8).

The test conditions for simulating a given operating altitude and temperature can be calculated by using this relationship derived from the ideal gas law:

$$P_t = P_o \left(\frac{273 + t_t}{273 + t_o} \right) \quad \text{Constant Volume} \qquad (2)$$

where:

t_o = operating temperature in degrees Celsius

t_t = test temperature in degrees Celsius (usually room temperature)

P_o = operating pressure in torr

P_t = test-chamber pressure in torr

The COV, as a function of gas pressure and temperature, for round nichrome wires having a fixed spacing is shown in Figure 2. For each constant temperature curve shown, the COV follows Paschen's law in the low-pressure region, decreasing to a minimum voltage at a predictable pressure, followed by an increase in COV as the pressure is further reduced. There is some variation in the minimum COV at temperatures between 500 to 1100°C, but little or no change from 23 to 500°C.

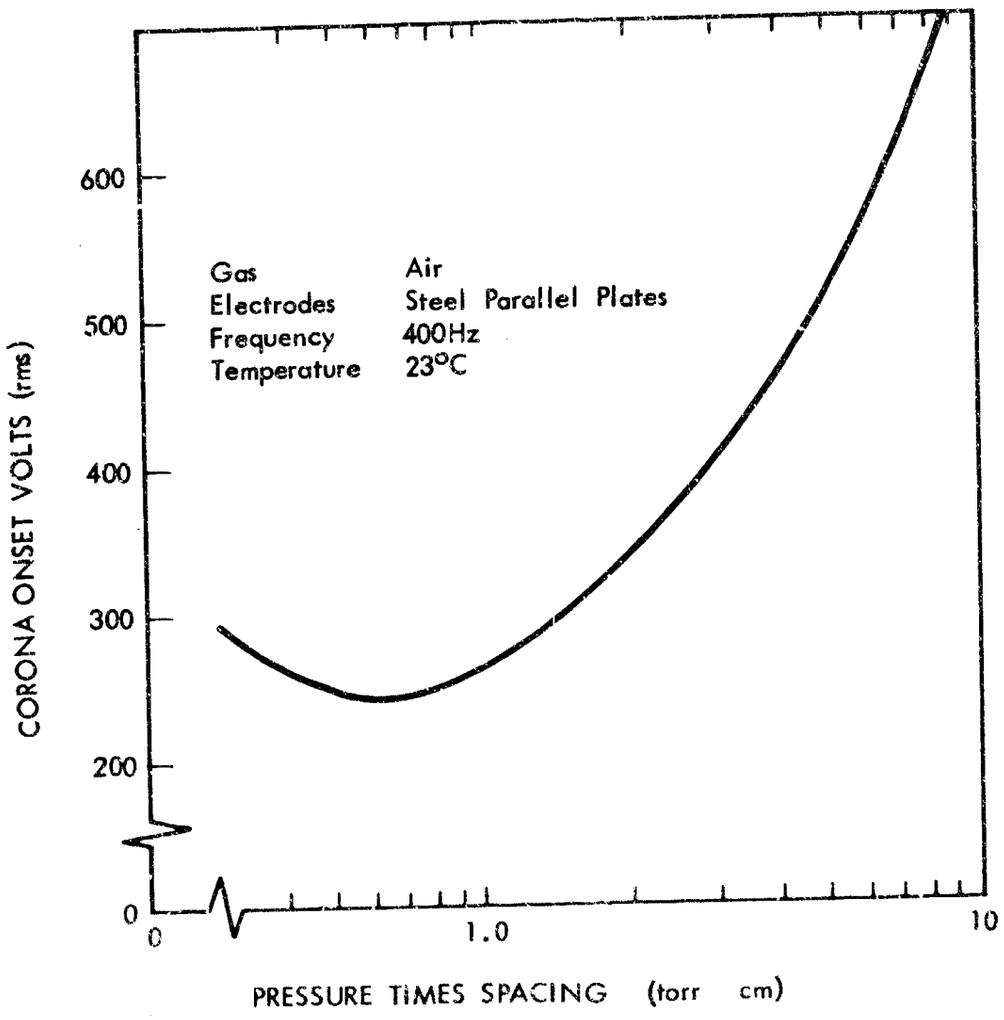

Figure 1: CORONA ONSET VOLTAGE AS A FUNCTION OF PRESSURE TIMES SPACING

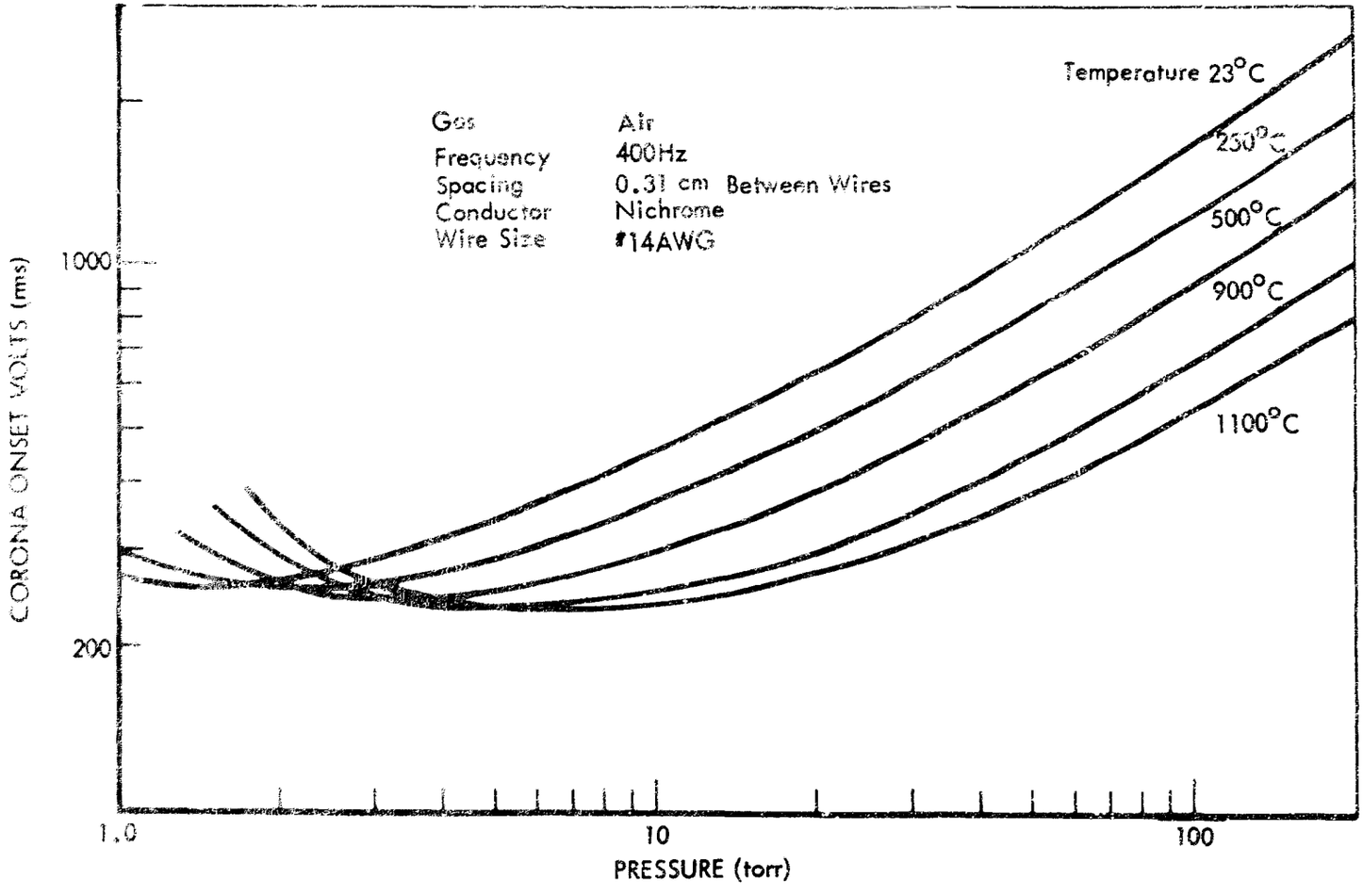

Figure 2: CORONA ONSET VOLTAGE AS A FUNCTION OF TEMPERATURE AND PRESSURE FOR PARALLEL WIRES IN A HEATED CHAMBER

FACTORS AFFECTING CORONA

At near-sea-level pressure, the COV between bar electrodes increases as electrode spacing is increased. Between sea-level and near-zero pressures, there is a pressure at which the COV is at a minimum for any given electrode spacing. For each electrode spacing there is a unique pressure at which minimum COV occurs (Figure 5). Thus, the minimum COV will occur over a wide range of altitudes in the electric system of an aircraft or space vehicle having many components with a variety of spacings between conductors, contacts, and terminations. At constant temperature and pressure, minimum COV occurs at a point directly proportional to the electrode spacing.

The volume of gas between a pair of parallel-plate electrodes varies directly with spacing. Hence, the following relationship can be derived from the gas law for parallel-plate electrodes at constant temperature:

$$P_2 = P_1 \frac{d_1}{d_2} \tag{3}$$

where: P_1 = original pressure in torr

P_2 = new pressure in torr

d_1 = original spacing in centimeters

d_2 = new spacing in centimeters

This implies that the pressure at which the COV is a minimum for electrodes of fixed configuration is a function of electrode spacing. The peak-to-peak 400-hertz COV for a gap is approximately the d.c. COV. As the frequency is increased, a point will be reached where the positive ions have insufficient time to cross the gap in a half-cycle, and then COV will tend to increase. In this report, one test involves X-band frequencies; all other data is for the frequency range from d.c. to 400-hertz, where the COV is not affected by frequency.

At near-sea-level pressures, the COV between bare electrodes is increased as the electrode configuration is changed from points to planes. However, at altitudes corresponding to the lowest COV, the onset voltage is affected only slightly by electrode configuration (Figure 4). A common rule of thumb in making parallel-plate electrodes is that the ratio of electrode diameter to spacing should be 10:1.

VOLTAGE DISTRIBUTION IN GAS-SOLID DIELECTRICS

Past work has shown that the corona onset voltage in solids is many times higher than in gases. Also, it has been shown that in solids, as in gases, the start of cumulative ionization is the beginning of dielectric breakdown, and solid insulations generally have much greater dielectric strength than gaseous insulations. Thus, corona should occur first in the gas surrounding a homogeneous solid

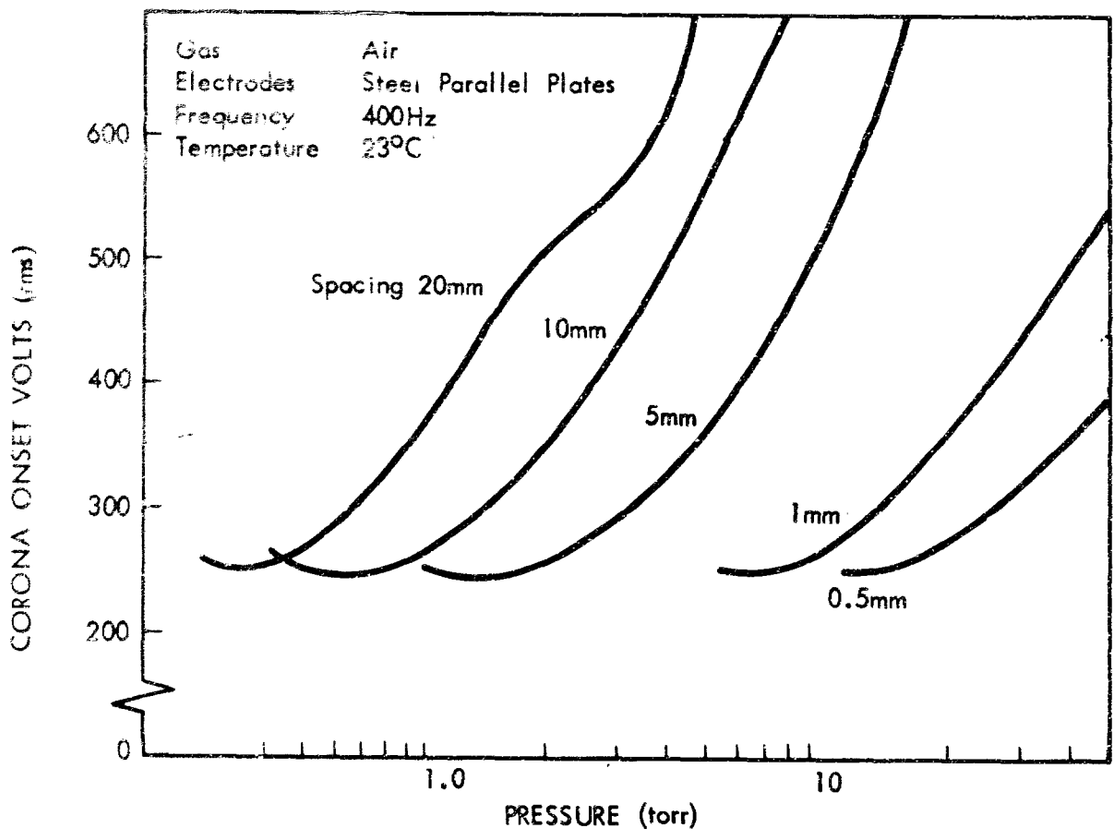

Figure 3: CORONA ONSET VOLTAGE BETWEEN PARALLEL PLATES AT SEVERAL SPACINGS

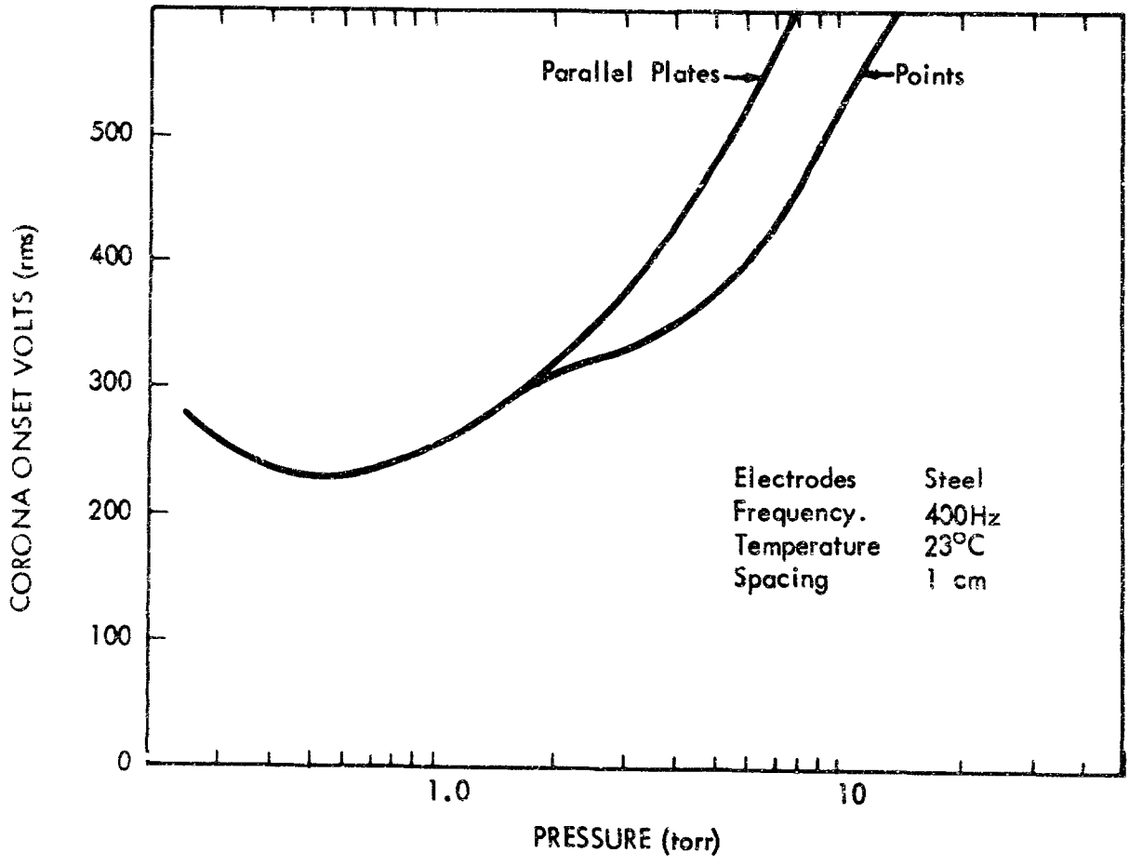

Figure 4: CORONA ONSET VOLTAGE BETWEEN POINTS AND PLATES IN AIR

dielectric. The corona onset voltage in gases can be determined by using established curves for various gap distances and electrode configurations. The remaining problem is one of establishing how the applied voltage distributes itself between the gas and solid portions of the dielectric path.

Halleck (Reference 9) has shown that when a voltage is applied to two capacitors in series, the applied voltage, V, will be divided between the two capacitors by:

$$V = V_1 + V_2 \tag{4}$$

where: V = voltage across the two capacitors

V_1 = voltage across the solid dielectric capacitor

V_2 = voltage across the gas dielectric capacitor

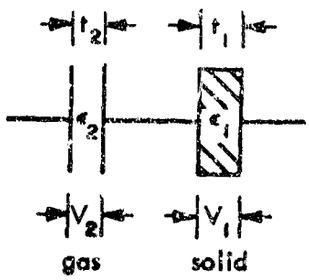

The voltage gradient, E, across each capacitor is then:

$$E_1 = \frac{V_1}{t_1} \tag{5}$$

$$E_2 = \frac{V_2}{t_2} \tag{6}$$

where: t_1 = thickness of the solid dielectric

t_2 = thickness of the gas dielectric

It follows from the definition of the dielectric constant, ϵ, that

$$E_1 \epsilon_1 = E_2 \epsilon_2 \tag{7}$$

Substituting into Equation 1 then gives:

$$V = E_2 \left(t_1 \frac{\epsilon_2}{\epsilon_1} + t_2 \right) \tag{8}$$

$$V = E_2 t_2 \left(\frac{\epsilon_2}{\epsilon_1} \frac{t_1}{t_2} + 1 \right) \tag{9}$$

$$V = V_2 \left(\frac{t_1}{t_2} \frac{\epsilon_2}{\epsilon_1} + 1 \right) \tag{10}$$

Let ϵ_2, the dielectric constant of the gas-dielectric capacitor, be 1.0 which is the approximate dielectric constant of most gases.

Then V_2, the voltage across the gas capacitor becomes:

$$V_2 = \frac{V}{\frac{t_1}{t_2 \epsilon_1} + 1} \tag{11}$$

Measurements show that the breakdown voltage in a gas dielectric uniform field is the same as the corona onset voltage. Substituting the corona onset voltage, V_{cs}, for V_2 then gives limiting voltage for corona-free operation.

$$V = V_{cs} \left(1 + \frac{t_1}{t_2 \epsilon_1} \right) \tag{12}$$

Similarly, an equation can be derived for two solid dielectrics in series with one air gap:

$$V = V_{cs} \left(\frac{t_1}{t_2 \epsilon_1} + 1 + \frac{t_3}{\epsilon_3 t_1} \right) \tag{13}$$

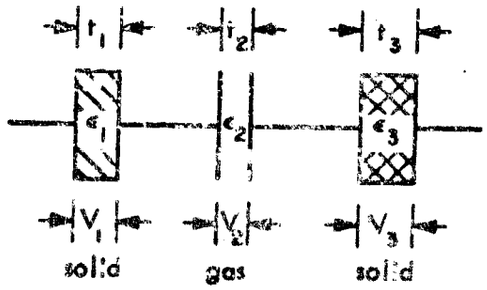

where: ϵ_3 = dielectric constant of the second solid dielectric

t_3 = thickness of the second solid dielectric

A condition sometimes encountered in practice is two gas gaps in series with a single solid dielectric. The appicable equation is:

$$V = V_{cs} \left(\frac{t_1}{t_2 \epsilon_1} + 1 + \frac{t_3}{t_2} \right) \quad \text{or} \tag{14}$$

$$V = V_{cs}\left(\frac{t_1}{t_4\,\epsilon_1} + \frac{t_2}{t_4} + 1\right) \tag{15}$$

and in the case where the air-gap thicknesses are equal:

$$t_2 = t_4$$

$$V = V_{cs}\left(\frac{t_1}{t_4\,\epsilon_1} + 2\right) \tag{16}$$

where: t_4 = thickness of second gas gap

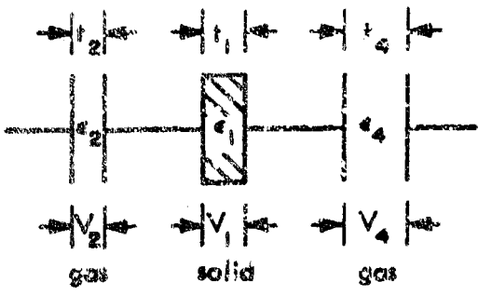

The voltage applied to two insulated wires will divide into three components: the voltage across each of the two wire insulations, and the voltage across the space between the insulations. This voltage distribution is unlike that encountered in series capacitors where the voltage across the air capacitor is proportional to the voltage across the solid-insulation capacitor for all applied voltages. With parallel wires, the thickness of the insulation is constant around the wire, but the thickness of the gap between wires varies from a minimum in the space between the wires to a maximum from the far side of one conductor to the far side of the other conductor. This results in a nonlinear electric field shown in Figure 5.

The analysis of the field about a pair of insulated wires can be simplified by assuming that the wires are of infinite length, thus reducing the analysis to a two-dimensional field. Assuming an infinite ground plane between the two wires does not alter the field but further simplifies the analysis. Curvilinear squares can then be calculated, with two sides of each square representing the electric field and the other two sides representing equipotential lines. The field lines then map into circles emanating normal to the conductor and terminating normal to the equipotential ground plane. With a two dielectric media, the wire insulation and the gas, the following conservation-of-energy principle applies everywhere in the media:

$$\oint \bar{E} \cdot d\bar{S} = 0 \tag{17}$$

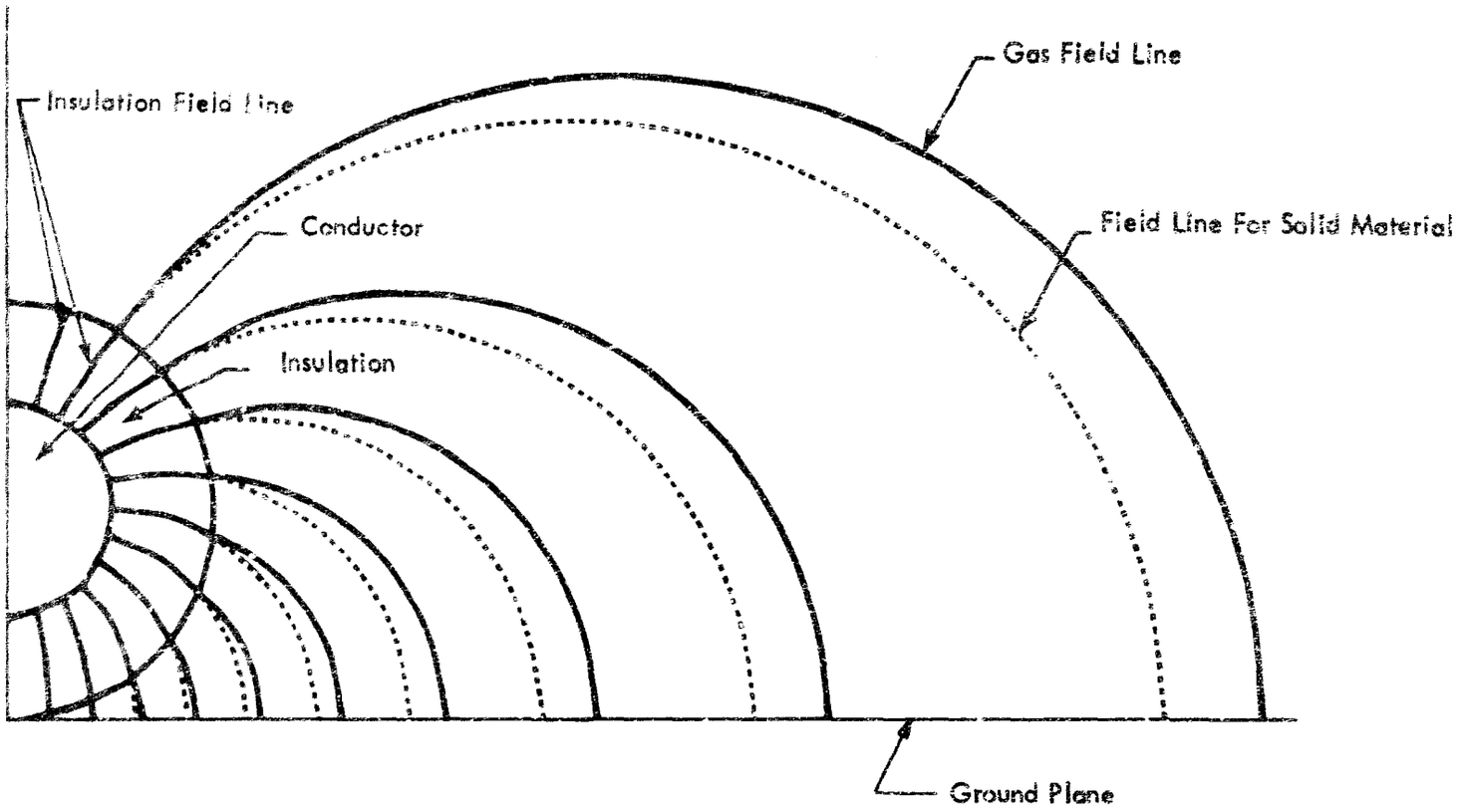

Figure 5: ELECTROSTATIC FIELD PLOT

where: $\bar{E}$ = electric field intensity

$\bar{S}$ = field direction line

As a result a field line passing from the solid insulation to the gas is discontinuous at the interface.

In terms of the angles between the direction lines and the tangent to the boundary

$$\bar{E}_1 \epsilon_1 = \bar{E}_2 \epsilon_2 \tag{18}$$

or

$$\bar{D}_1 = \bar{D}_2 \tag{19}$$

where: $\bar{D}$ = displacement vector

Then

$$\bar{D}_1 \sin \alpha_1 = \bar{D}_2 \sin \alpha_2 \tag{20}$$

or

$$\bar{E}_1 \epsilon_1 \sin \alpha_1 = \bar{E}_2 \epsilon_2 \sin \alpha_2 \tag{21}$$

The angles are shown in the sketch.

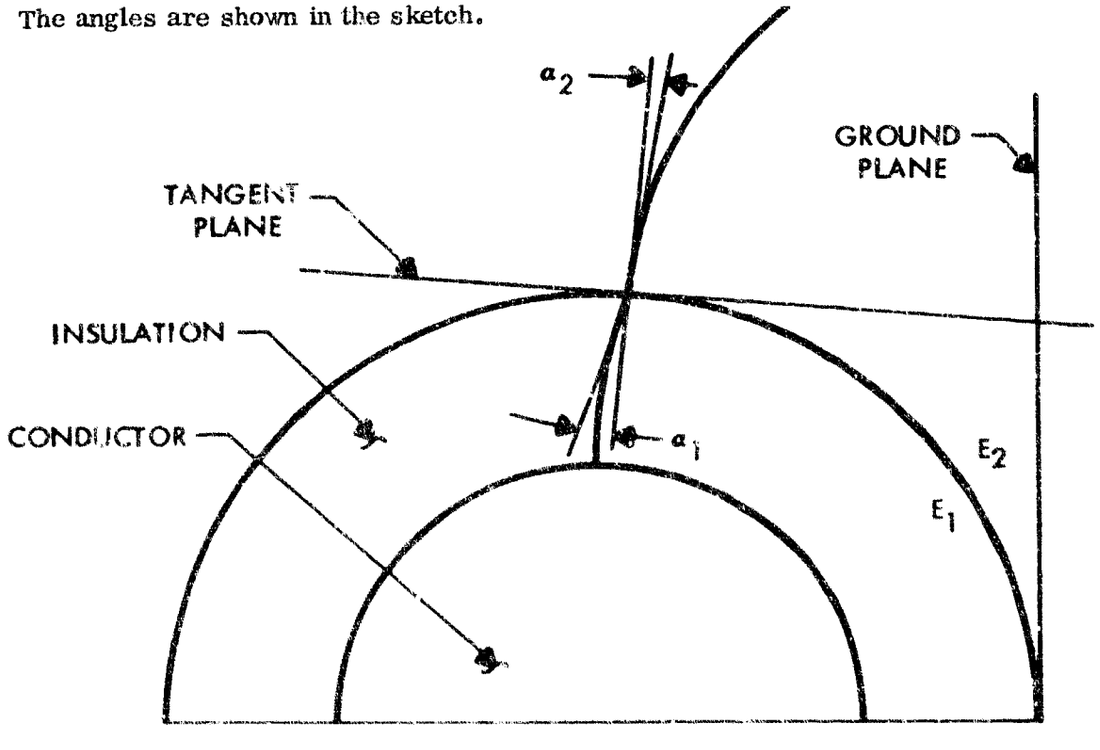

The continuous components of $\bar{E}$ are

$$\bar{E}_1 \cos \alpha_1 = \bar{E}_2 \cos \alpha_2 \tag{22}$$

then, by dividing and rearranging:

$$\frac{\tan \alpha_2}{\tan \alpha_1} = \frac{\epsilon_1}{\epsilon_2} \tag{23}$$

The field lines of a gas-solid insulation system for a pair of closely spaced wires are shown in Figure 5. The mathematical equations for these field lines are derived in Appendix III.

ELECTRODE INSULATION

Corona will occur adjacent to an electrode in a localized area where the electric field is the highest. With a gas-solid dielectric combination, corona will occur when the dielectric strength of the gas is exceeded, provided the corona onset voltage is much greater in the solid than in the gas.

Two precautions must be observed when using gas-solid insulation. First, the electric field may be highest at the gas-solid interface. Corona may occur here during momentary overvoltage, resulting in charring of the insulation or carbon tracking. Sometimes the introduction of solid insulation having a high dielectric constant may actually lower the electrode potential at which corona occurs. Second, in applying insulation to a wire or electrode, it is important that there be no air spaces between the insulation and the conductors. The reason is that when materials of different dielectric constant are placed in an electric field the voltage divides inversely as the dielectric constant; that is, the material with the higher dielectric constant will have the lower voltage gradient across it. Because the lowest dielectric-constant material is gas, which also has the lowest dielectric strength, this voltage division becomes undesirable. Thus, a good insulating material should have a low dielectric constant and a high breakdown strength if it is to be used in places having air pockets or gas layers (Reference 5).

Mercier and Elliott in "Analysis and Elimination of Corona Effects" (Reference 10) state: "Since corona occurs when air is overstressed, it is possible to eliminate this corona by eliminating the air gap either electrically or mechanically. In eliminating an air gap electrically, both surfaces bordering the air gap may be coated with a conducting or metalized paint, or metal foil. The two conducting surfaces are then tied together electrically to eliminate the voltage across the air gap. The air gap can be eliminated mechanically with a filler, such as transformer oil, epoxy casting resin, or petrolatum."

It is difficult to eliminate all voids in solid insulation and all air spaces between an electrode and solid insulation. Some voids have been eliminated by using irradiated polyethylene, which has the ability to shrink and bond to itself to form a structure with few voids (Reference 7).

III. TEST EQUIPMENT AND PROCEDURE

The X-20A corona tests were designed to establish from measurements the COV of several electric-power-system components in the environments of the space vehicle. The IEEE Insulation Committee recognized three circuits for detecting corona; all three circuits were investigated for use in the X-20A program to obtain accurate reproducible results. The three corona-detecting methods are summarized in Table 1, which is reproduced from a paper by T. W. Dakin and J. Lim of Westinghouse (Reference 11).

X-20A TEST APPROACH

The method adopted for the X-20A program was the one in which the voltage drop across a resistor in series with the ground lead is measured (Section 2.a(1) of Table 1). This simple method produced consistent results and was insensitive to outside interference. The amplifier and oscilloscope provided a sensitivity of 500 microvolts per centimeter, which was adequate for all electrodes tested and all of the environments.

The electrodes were energized from either a 15,000-volt (rms), 1.5-kva, 400-hertz single-phase transformer or a 1000/500-volt, 1.0 kva, 400-hertz single-phase transformer. The transformer was connected to a General Radio 20-ampere, 0/130-volt (rms), 400-hertz variac. The variac was supplied by a 400-hertz, 115/200-volt, three-phase laboratory power source.

The presence of corona was detected by the voltage drop across a 96-ohm resistor connected in series with the ground lead to the electrodes. The signal from this resistor was fed through a high-pass filter to attenuate the 400-hertz sine-wave signal, its first five harmonics, and all induced spurious voltage signals having frequencies less than 2.2 kilocycles.

This filtered signal was examined for corona voltage with a Tektronix 545A oscilloscope, using a type L plug-in preamplifier. The corona detection circuit is shown in Figure 6.

A three-phase corona-detecting circuit was used to test several X-20A components. This circuit used matched 1000/500-volt, 1.0 kva, 400-hertz transformers and variacs (Figure 7).

The various electrode configurations and electric-power-subsystem components were tested in a chamber evacuated by either a W. M. Welch Duo-Seal vacuum pump or a 47 cubic-foot-per-second Kinney Model KS-47 vacuum pump. The pressure inside the vacuum chamber, down to 5 torr, was read from a Wallace and Tiernan Model FA-173 absolute-pressure gage. The pressure, when below 5 torr, was read from a universal vacuum gage manufactured by Todd Scientific Company. The voltage across the electrodes was measured with calibrated-certified electrostatic voltmeters manufactured by the Rawson Electrical Company.

Table 1. CORONA DETECTION

1. Power-Frequency Bridge Methods

   a. Direct balance of the bridge, wherein the increased tan δ at higher voltages indicates the power loss due to the sum of corona discharges. The angle δ is the power factor angle against the j axis.

   b. Observation of the bridge unbalance voltage due to the corona as a Lissajous figure, where the area of the figure indicates the corona power loss, if other losses are balanced out.

2. Measurement of the Voltage Produced Across a Resistor by the Corona Discharge. Several modifications have been used:

   a. A resistor is connected in series with the ground lead to the test specimen. The voltage drop is measured using a

      (1) Wide-band amplifier, or

      (2) Narrow-band amplifier.

   b. A resistor is connected in series with a coupling capacitor connected to the high-voltage terminal of the test specimen. Again the voltage drop is measured using a

      (1) Wide-band amplifier, or

      (2) Narrow-band amplifier (essentially like the NEMA, electromagnetic interference).

3. Measurement of the Voltage Drop Produced Across an Inductor by the Corona Discharge

   a. An inductor is connected in series with the ground lead to the test specimen. The voltage drop is measured using a

      (1) Wide-band amplifier, or

      (2) Tuned narrow-band amplifier.

   b. An inductor is connected in series with a coupling capacitor to the test specimen. The voltage drop is measured using a

      (1) Wide-band amplifier, or

      (2) Tuned narrow-band amplifier.

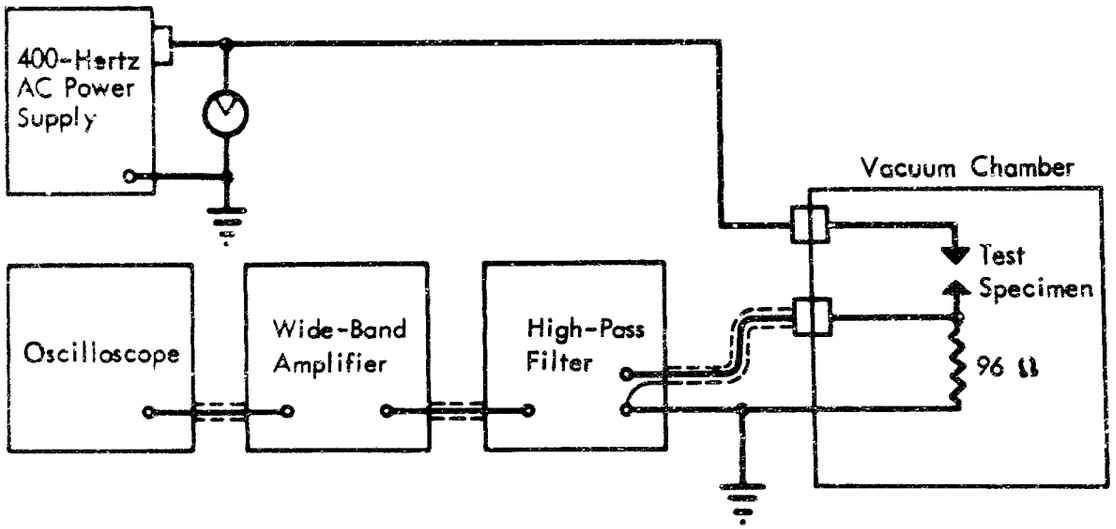

Figure 6: CORONA DETECTION CIRCUIT

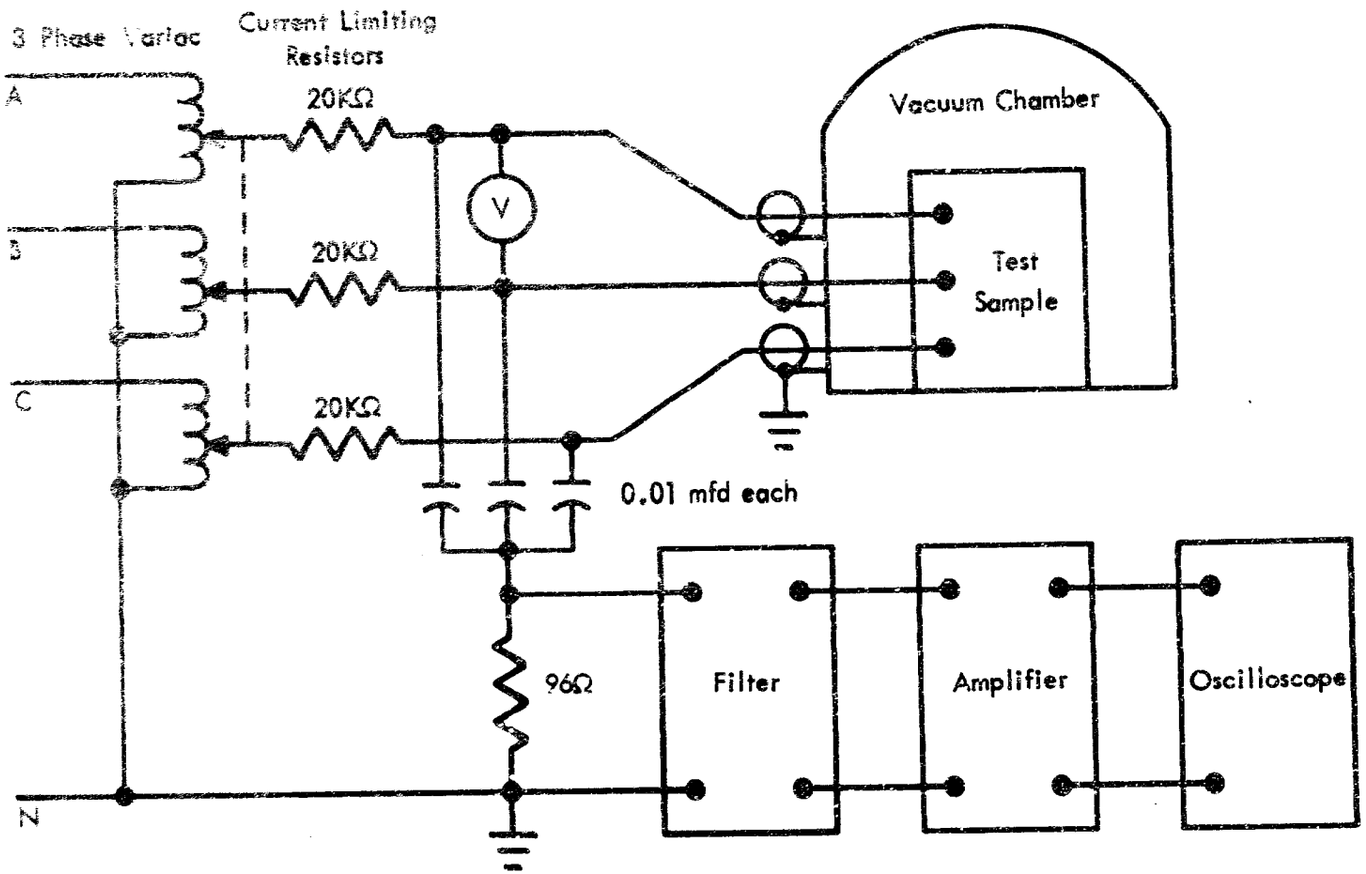

Figure 7: THREE-PHASE CORONA DETECTION CIRCUIT

For testing bare electrodes and X-20A components, three vacuum chambers were actually used: one for testing 5-centimeter-diameter parallel-plate electrodes, pointed electrodes, and 0.64-centimeter round-rod electrodes; another for testing high-temperature wires; and the third, for testing X-20A components and wiring. Dry, filtered gases at 24°C were used for all bare-electrode tests.

Three of the electrode pairs are shown in Figure 8. The knurled sections of the electrodes were machined off prior to testing. Figures 9 and 10 show test setups having pointed and parallel-plane electrodes in the vacuum chambers.

Equipment used for corona tests in helium-oxygen mixtures included a vacuum chamber, vacuum pump, helium and oxygen gas supply, corona-detection instruments, and power supply. This equipment is shown in Figure 11. COV was determined by slowly varying the power supply voltage as shown in Figure 12. Twisted wires and a connector were tested in the T-shaped vacuum chamber shown in Figure 13.

A shield is placed over the bell jar during test to protect the equipment and operating personnel in case the bell jar fails. A micrometer on the left end of the bell jar is used to space the electrodes before and during the testing.

HIGH-TEMPERATURE TESTS

High-temperature corona measurements were obtained in an oven, made of lightweight firebrick, enclosed in a vacuum chamber. The parallel wires being tested were centered within a 7.5-centimeter-diameter thin-wall stainless-steel tube that was placed inside the oven. The stainless-steel tube was grounded at each end to isolate the test specimens from interference from the high-current low-voltage direct-current power supply used to energize nichrome heating elements. The temperature was measured with an optical pyrometer and with thermocouples installed on the stainless-steel tube.

The test wires were spaced with porcelain insulators — one fixed and the other spring-loaded to provide wire tension. The insulators were cooled to limit leakage current through the insulators. All sharp metal edges were glass-taped to prevent corona from forming in areas not under test. One end of the oven is shown in Figure 14.

During testing, the oven was held at each test temperature for at least 15 minutes prior to corona measurements to stabilize the temperature in the stainless-steel tube and the parallel wires. Even then the wire ends were cooler than the midsections of the wires, due to radiation and conduction to the cold insulators. Therefore, the only truly valid readings were those taken at the minimum and above the minimum pressures of the Paschen law curve. Corona onset voltages observed at pressures lower than the pressure at the Paschen law minimum were ambigous with respect to the density of the gas surrounding the conductor where the corona occurred. The vacuum chamber for this test was 90 centimeters in diameter and

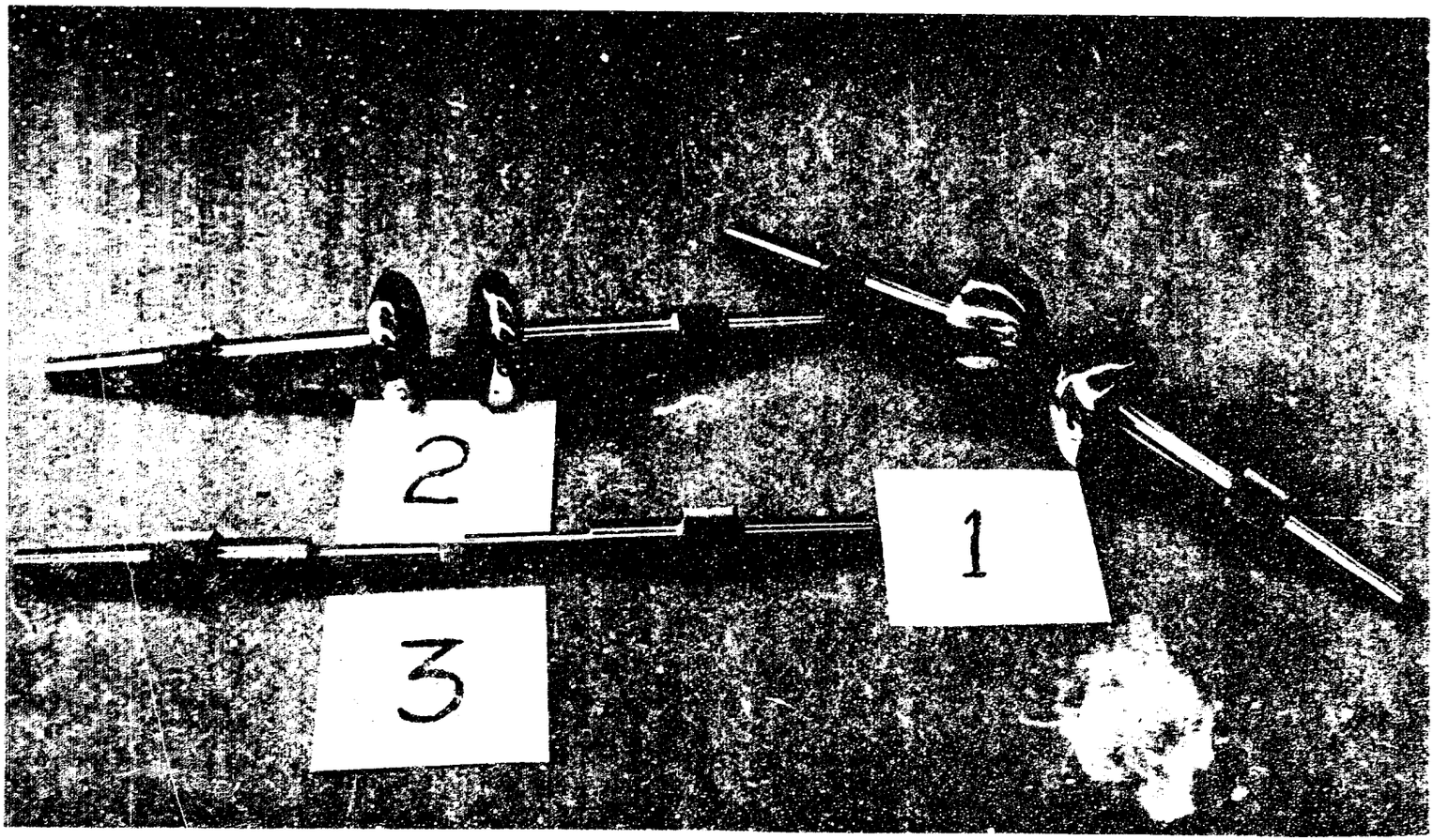

Figure 8: TEST ELECTRODES

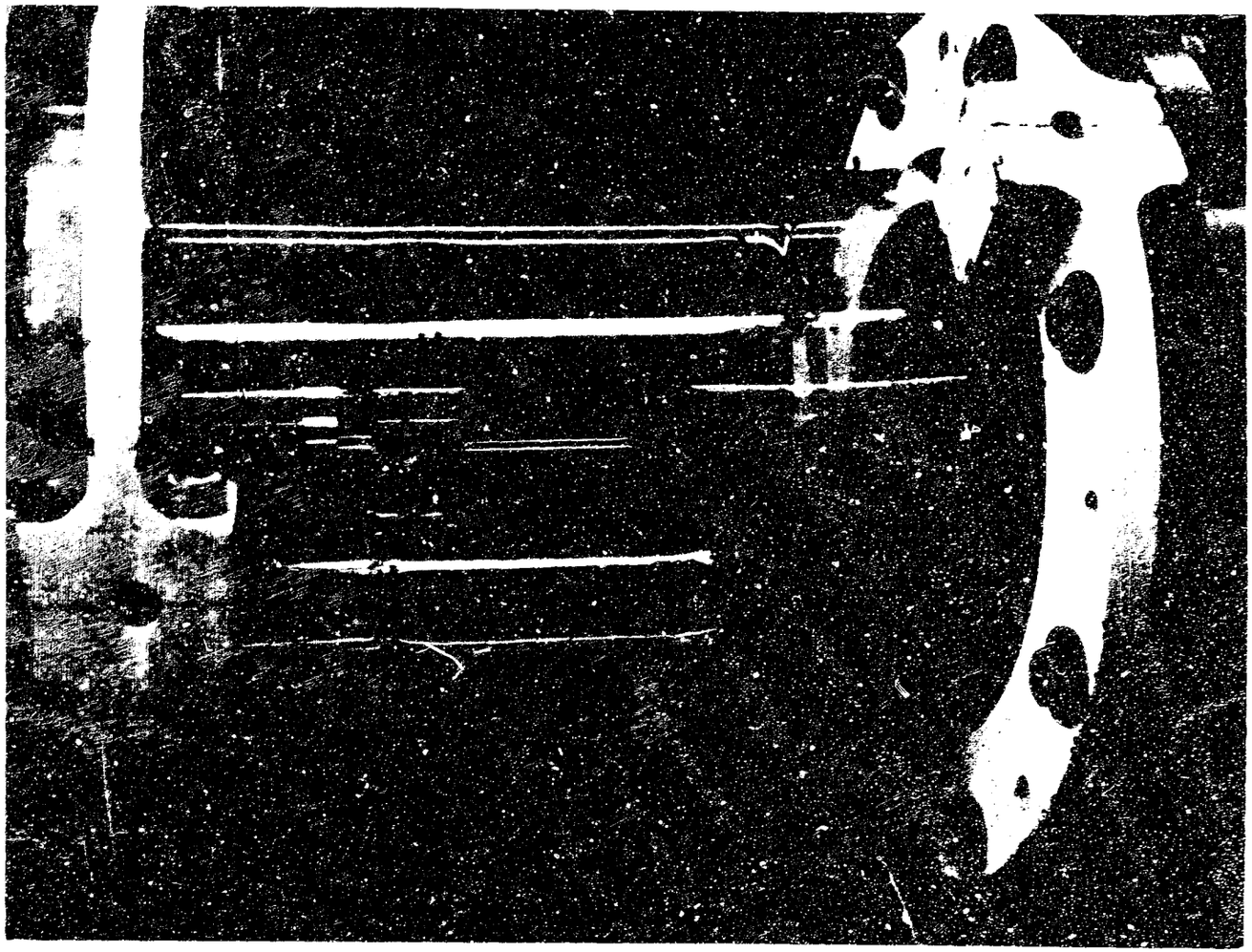

Figure 9: POINTED ELECTRODES IN TEST CHAMBER

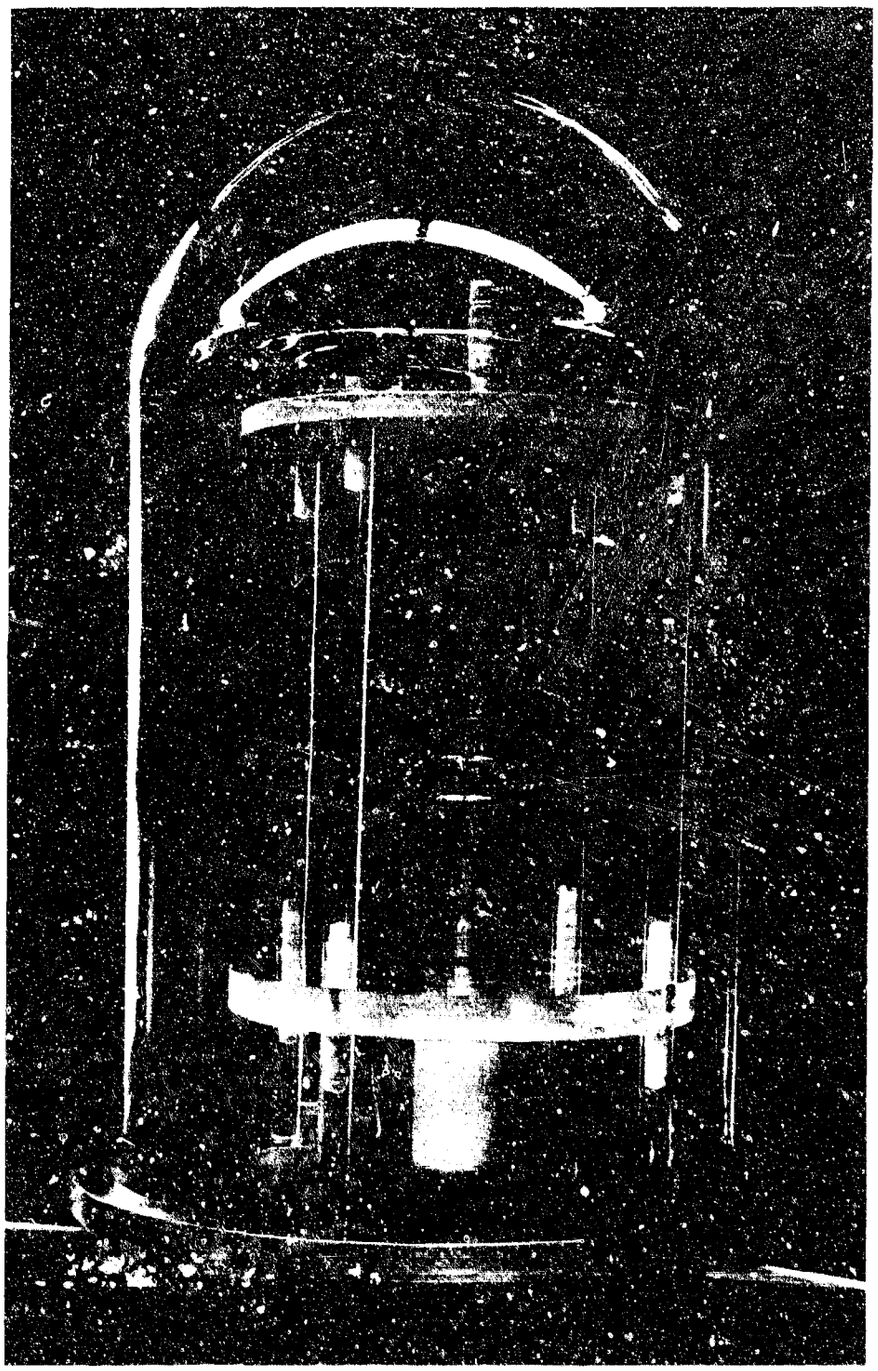

Figure 10: PARALLEL – PLATE ELECTRODES IN VACUUM CHAMBER

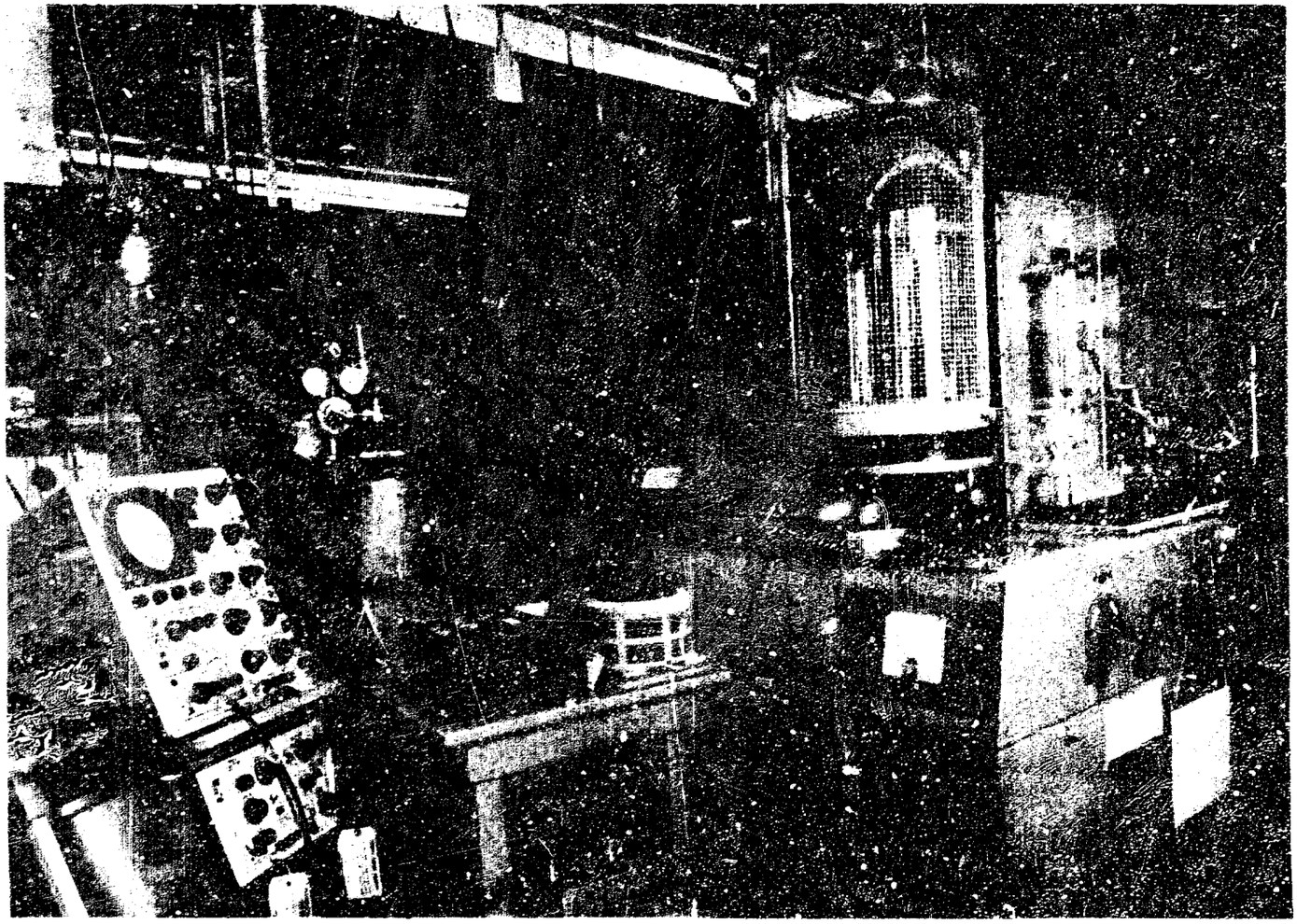

Figure 11: CORONA TEST SETUP FOR HELIUM-OXYGEN MIXTURES

Figure 12: ADJUSTING VOLTAGE DURING CORONA MEASUREMENT

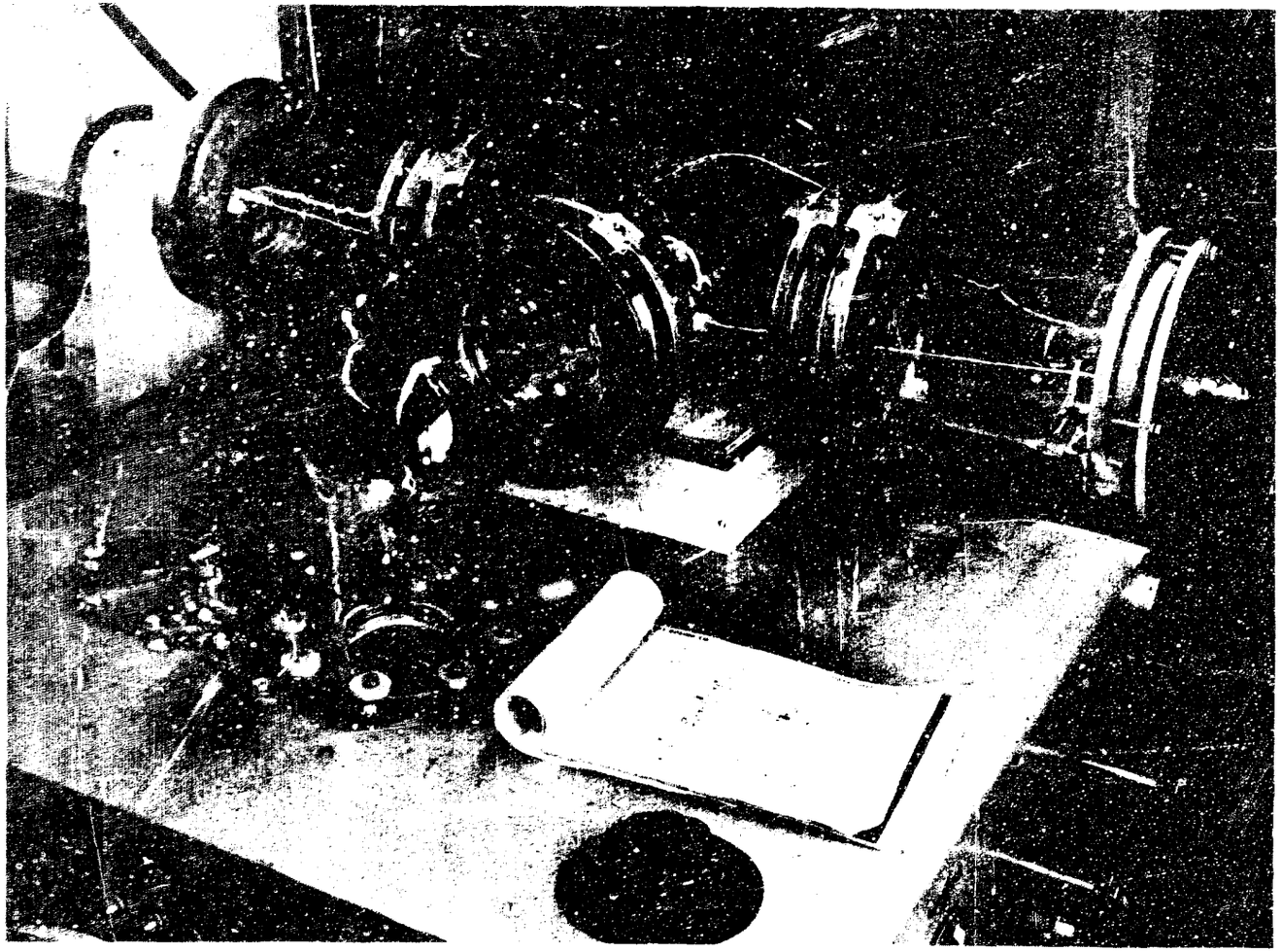

Figure 13: WIRE AND CONNECTOR CORONA TEST

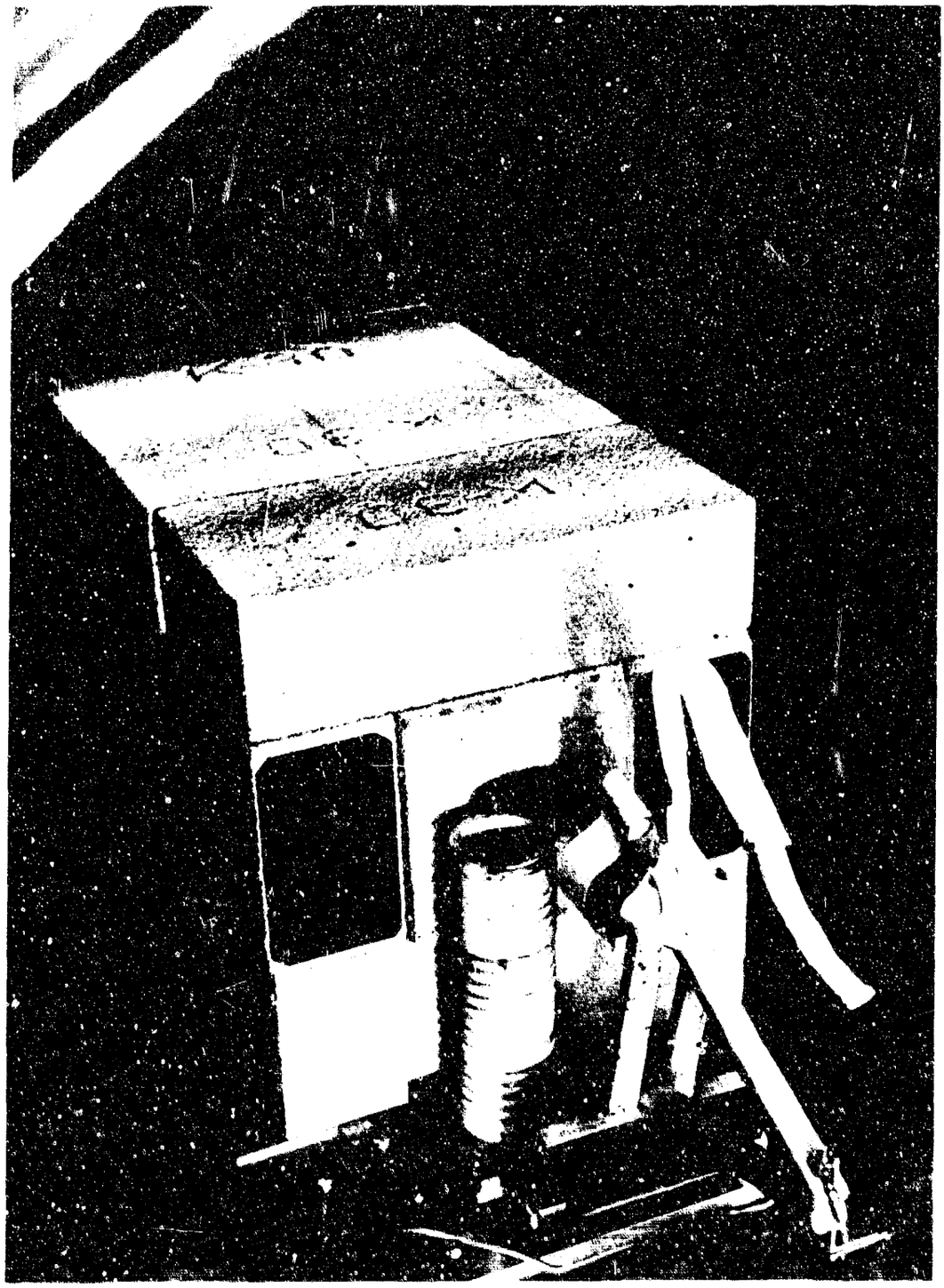

Figure 14: HIGH TEMPERATURE OVEN

150 centimeters long (Figure 15). Electrical connections and cooling-water feedthroughs are shown in Figure 16. The vacuum-chamber high-voltage feedthrough was made of teflon and spaced at least 10 centimeters from the grounded tank. The corona onset voltage, as a function of pressure, for the vacuum-chamber feedthrough is shown in Figure 17. The feed-through corona onset voltage represents an upper limit for valid corona-voltage readings.

CONTAMINATION TESTS

The equipment used for the high-temperature wire tests was also used in measuring the corona onset voltage between high-temperature bare wires in molybdenum-trioxide vapor. Contamination was obtained by either heating molybdenum decals or molybdenum wires. The vacuum chamber was thoroughly cleaned and the oven replaced after each run. Molybdenum-trioxide crystal growth is shown in Figure 18.

COMPONENT TESTS

Electric components were bolted to a stainless-steel baseplate containing feedthroughs for instrumentation of pressure, temperature, and voltage. Feedthroughs for power were available for those components requiring activation during test. A glass bell jar, 30 centimeters in diameter and 45 centimeters high, formed the vacuum enclosure.

TEST PROCEDURE

The equipment was assembled as shown schematically in Figure 6. The electrodes were checked for scars, etching, burning, corrosion, cleanliness, spacing, and alignment prior to installation in the test chamber. When a gas other than air was used, the chamber was purged three times by exhausting to less than 0.05 torr and refilling to 700 torr with the test gas. The chamber was externally heated during the first purge to evaporate finger prints and/or oxides that collected on the electrodes, endbells, and glassware.

When changing from atmospheric air to the test gas, the chamber was purged three or more times by evacuating to 0.02 torr and then repressurizing to 700 torr with the test gas. The pressure was then decreased to a standard gas pressure where the COV was checked at a known density-spacing-COV value. If the test point was correct, the system was pressurized with the correct amount of gas for subsequent tests. The same procedure was followed for pure gases and gas mixtures.

Chamber pressure was held constant for at least 3 minutes prior to any measurement of corona onset voltage. Then a 400-Hz a.c. voltage was applied between the test electrodes and increased from zero to just below the expected onset voltage. From this point the voltage was increased manually at a rate of 20 volts per minute until sustained corona discharges appeared. The voltage was then reduced below the threshold of corona onset and the process repeated. Temperature was

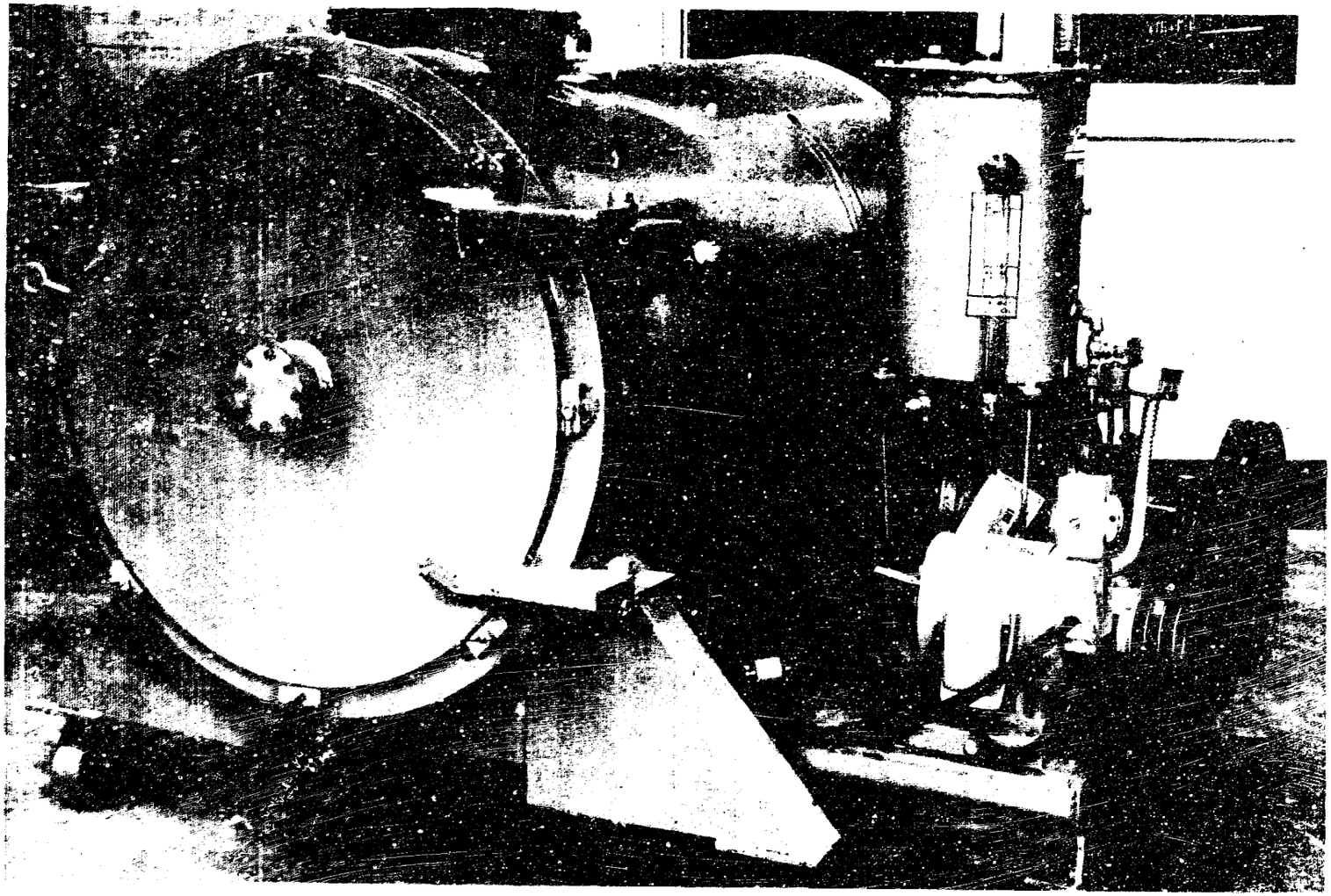

Figure 15: VACUUM CHAMBER

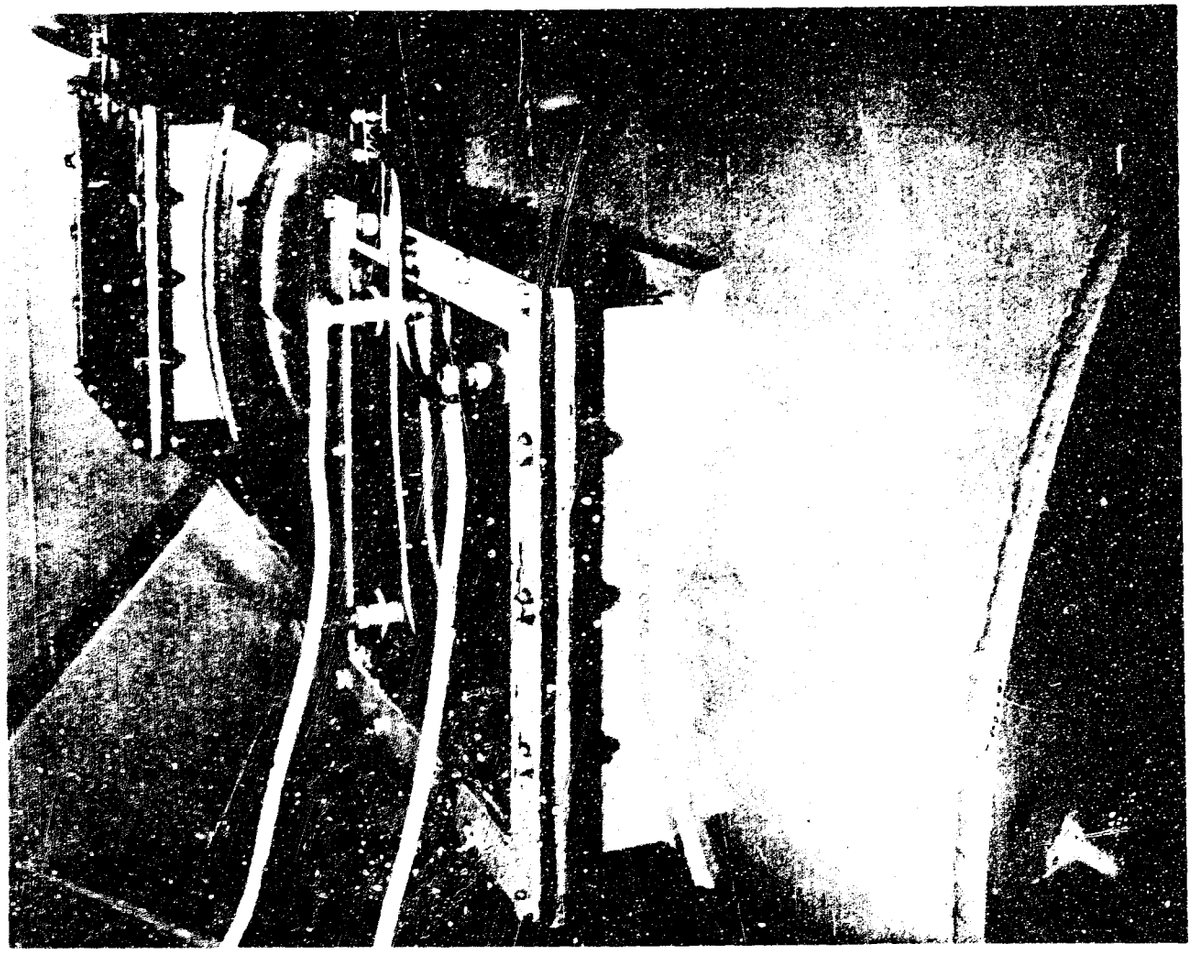

Figure 16: COOLING AND INSTRUMENTATION FEEDTHROUGHS UNDER VACUUM CHAMBER

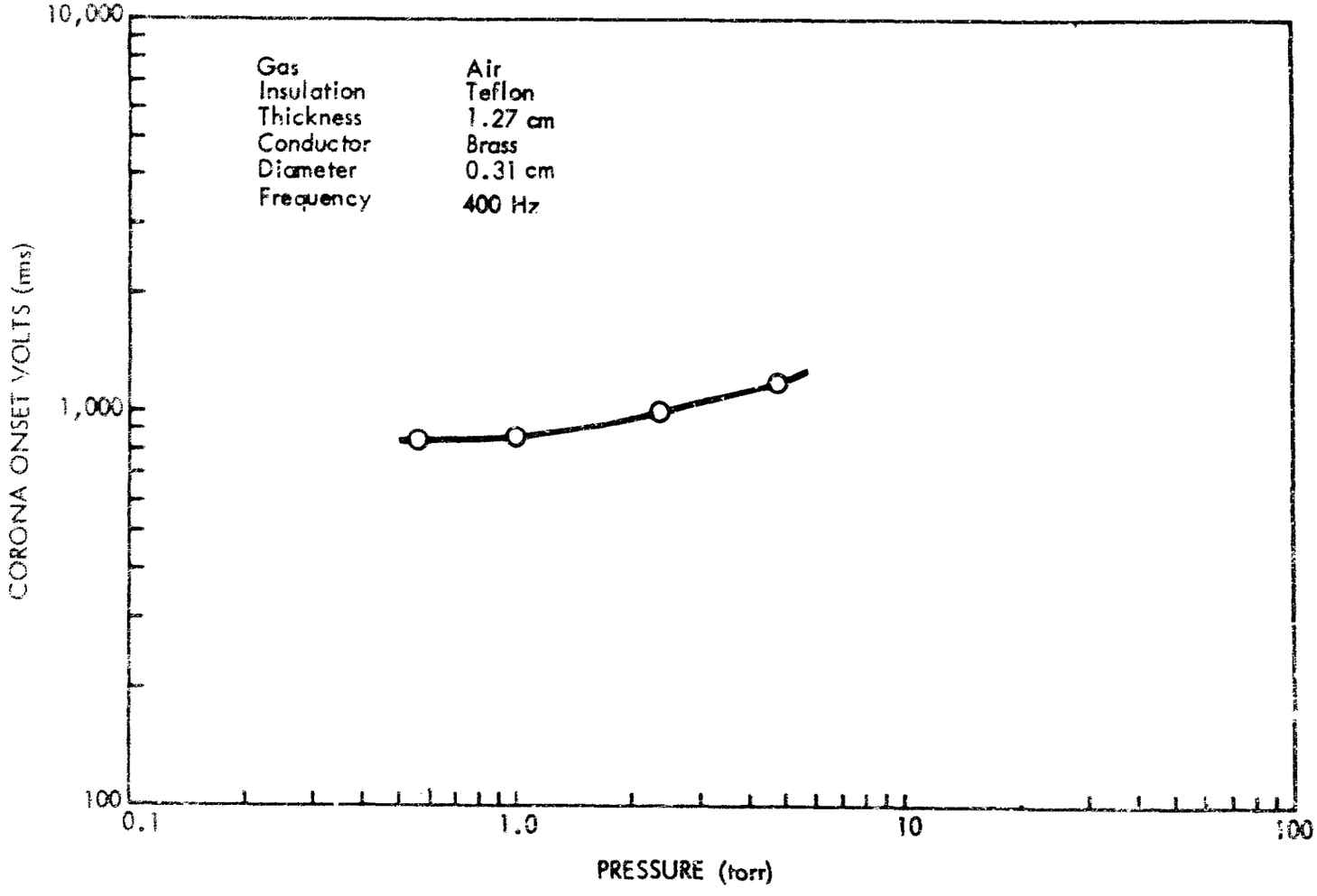

Figure 17: CORONA ONSET VOLTAGE OF TEST CHAMBER FEEDTHROUGH

Figure 18: MOLYBDENUM TRIOXIDE CRYSTAL ON A CABLE

recorded and adjusted every 15 minutes throughout the test. The chamber was purged several times during each test to eliminate the effect of ozone and other test-generated impurities.

Several points were taken at the minimum of the Paschen law curve for each pressure, spacing, electrode configuration, and gas. The COV curve for each test included the lowest voltage points at each pressure. Data obtained at Boeing with standard configurations and test conditions agreed with published data within 1 percent.

VERIFICATION OF TEST APPARATUS

The vacuum chamber was first checked for leaks and stability of electrode spacing. The leakage rate was found to be less than 0.1 torr in 24 hours. The electrode-spacing change was less than 0.0025 cm between atmospheric pressure and 0.02 torr.

The objective of the tests was to detect the presence of either corona or voltage breakdown, rather than the magnitude of the corona. The minimum detectable corona display on the oscilloscope was evaluated by measuring the electromagnetic interference (EMI) transmitted from one insulated wire to another. It was found that a 1-millimeter deflection of the oscilloscope beam represented corona that produced an interference level well below the allowed EMI limit for the X-20A electrical subsystem. A 5- to 50-millimeter indication on the oscilloscope indicated interference that exceeded the EMI requirement by one or more magnitudes.

An IEEE subcommittee on gaseous insulation has developed a portable test cell for screening gaseous dielectrics (Reference 12). The cell accommodates square rods, plates, round rods, and other electrode configurations. The test circuit and vacuum chamber used at Boeing deviated from the IEEE standard test cell, but the electrodes were as specified. For example, the 400-Hz voltage breakdown and corona between 6.4-millimeter round-steel rods at fixed spacings of 0.5 to 5, 10, and 20 millimeters were measured at room temperature in air and various pressures. The results of this test are shown in Figure 19. The voltage breakdown between 5-centimeter-diameter parallel-plate electrodes was measured at room temperature (24°C) in air at various pressures. Air was filtered and dried to a dewpoint of lower than -100°C. The knurled section of each test electrode (Figure 8, Set 2) was machined off prior to use. Data taken with these 5-centimeter electrodes compares well with the data of References 3, 13, 14, 15, 16, and 17, as shown in Table 2.

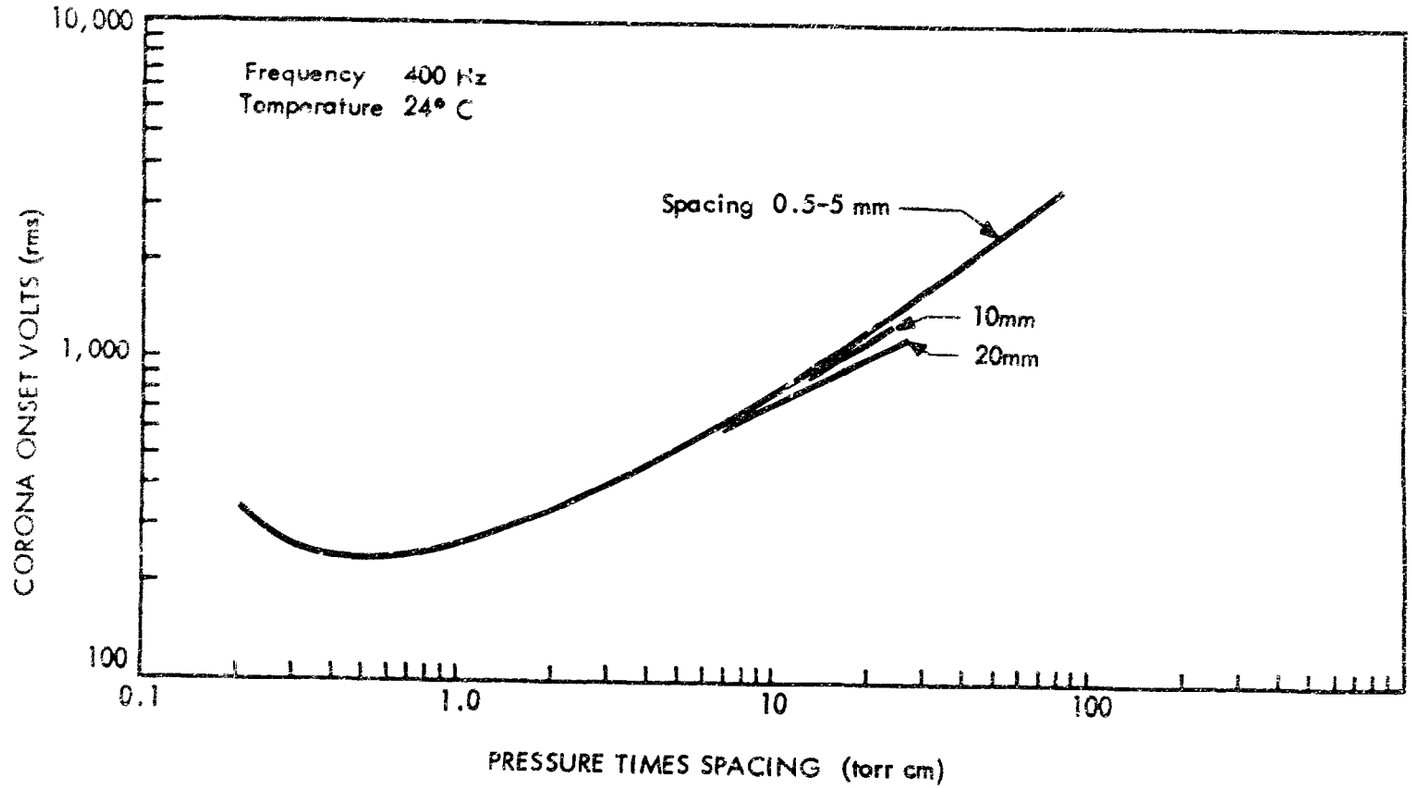

Figure 19: CORONA ONSET VOLTAGE BETWEEN RODS IN AIR

Table 2. VOLTAGE BREAKDOWN BETWEEN PARALLEL PLANES IN AIR AT 23°C — SPACED ONE CENTIMETER

Pressure (mm Hg)	Breakdown Voltage		
	Measured (d.c.)	Calculated (a.c.)	Measured (a.c.)
0.6	323	238	232
1.0	362	256	260
2.0	470	332	337
5.0	740	523	520
10.0	1,080	762	770
25.0	1,760	1,242	1,180
50.0	3,300	2,330	2,400
100.0	5,600	3,960	4,050
200.0	10,000	7,070	7,000
500.0	23,000	16,200	16,000
746.0	30,400	21,400	21,700

IV. TEST DATA

The test data presented in this report are normalized with respect to pressure and spacing by using pressure times spacing (torr-cm) as the independent variable. Therefore, to find the minimum COV for a given electrode configuration it is only necessary to multiply the gas pressure by the electrode spacing and read the minimum COV from the curve. The spacing or pressure limitations at a given voltage can be determined by reversing the procedure.

Gases most commonly investigated by others have been argon, carbon dioxide, helium, hydrogen, neon, nitrogen, and oxygen. Some of the corona-onset-voltage curves in air, carbon dioxide, helium, nitrogen, and sulphur hexafluoride are shown in Figure 20, and the minimums are summarized in Table 3. The curves show that the COV, as a function of pressure and spacing, is unique for each gas or gaseous mixture.

There were four areas in the X-20A vehicle where corona could have been a problem: the electronics compartment, pressurized with nitrogen; the crew compartment, pressurized with 60-percent nitrogen and 40-percent oxygen (by volume); the unpressurized air-filled wiring ducts between compartments; and the generator compartment, pressurized with a gas specified by the vendor. Normally the pressurized compartments do not have corona problems; however, a valve malfunction, broken gas line, a break in the compartment, or a malfunction in the pressurization subsystem could depressurize such compartments when the vehicle is at high altitudes. Thus a variety of gases and gas mixtures were used in corona testing.

Manned space vehicle atmospheres must be compatible with the physiological requirements of the crew. Environments considered for crew compartments include pure oxygen for the Mercury, Gemini, and Apollo; nitrogen-oxygen mixtures for the X-20A; and helium-oxygen, neon-oxygen, and nitrogen-oxygen mixtures for future vehicles. In the two-gas atmospheres considered, oxygen partial pressure, P_{O_2}, is usually held at 180 torr (3.5 psia). This is physiologically nearly optimum, and allows crew transition from a two-gas atmosphere to an emergency pure-oxygen atmosphere without change in P_{O_2}. Diluent partial pressures of helium, neon, or nitrogen are then established to provide the required total cabin pressure. Proposed diluent partial pressures range from 180 to 580 torr (References 18, 19, 20, 21, and 22).

Needle-point and parallel-plate electrodes provide two extremes in electric-field intensity. Parallel plates have well-defined uniform fields, whereas needle points have extreme nonuniform fields. The corona characteristics of electrical components vary between these extremes. Screw threads, nut tips, very thin wires, and poor solder joints are examples of points. Relay contacts, large parallel bars, and variable-capacitor plates are examples of parallel plates. Therefore, both needle and parallel-plate electrodes were used in the corona tests.

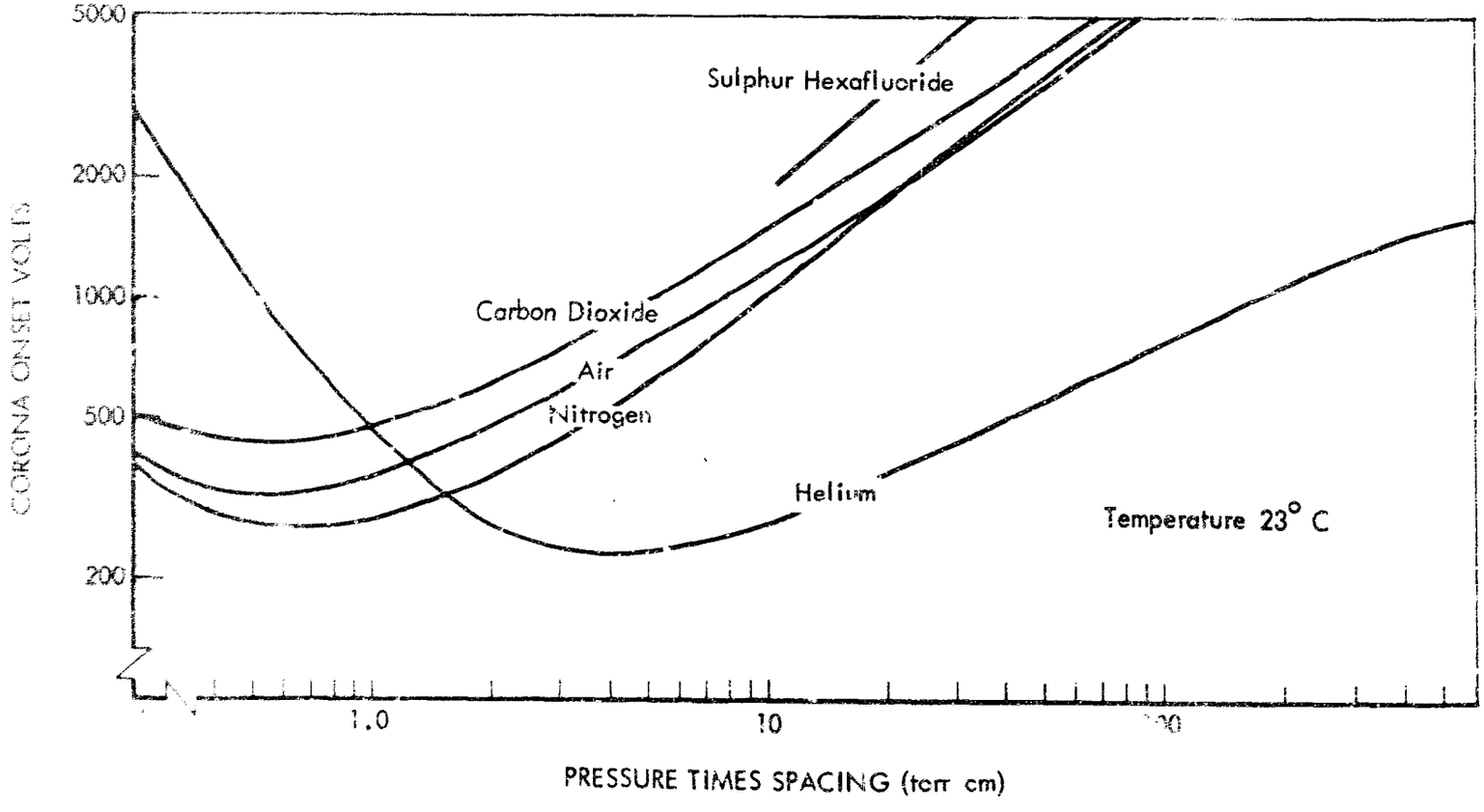

Figure 20: DIRECT CURRENT BREAKDOWN VOLTAGE BETWEEN PARALLEL PLATES

Table 3: BREAKDOWN VOLTAGE BETWEEN BARE ELECTRODES SPACED ONE CENTIMETER

Gas	Minimum at Critical Pressure Spacing		Breakdown Voltage at 1 Atmosphere	
	Volts (a.c.)	Volts (d.c.)	Kilovolts (a.c.)	Kilovolts (d.c.)
Air	223	315	23	33
Ammonia	---	---	18.5	26
Argon	196	280	3.4	4.8
Carbon Dioxide	305	430	24	28
Freon 14	340	480	22.8	32
Freon 114	295	42.	64	90
Freon 115	305	430	64	90
Freon 116	355	500	--	--
Freon C 138	320	450	--	--
Helium	132	189	1.3	1.63
Hydrogen	290	---	12	17
Nitrogen	187	265	22.8	32
Oxygen	310	440	--	--
Sulfur Hexafluoride	365	520	67	95

It is anticipated that space vehicles, as in the X-20A, will require electric-power quality as specified in MIL-STD-704. This specification allows excursions up to 190/330 volts (rm) from the 115/200-volt, 400-Hz power supply; therefore, most of the corona testing was done with 400-Hz a.c. in this voltage range.

As shown here, the minimum COV in nitrogen is 190 volts (rms) between bare electrodes, creating a definite possibility of corona between lines and ground if a gas-filled compartment is depressurized. Continuous corona could exist in three-phase circuits where conductors are spaced between 0.1 and 5 centimeters and where the nitrogen pressure is between 0.1 and 7.6 torr.

Most of the corona onset voltage measurements were made with 400-hertz a.c., the normal power frequency for the X-20A electric power system, rather than direct current. A generalized formula for comparing direct-current corona data with the alternating-current data is:

$$V_{\text{rms a.c.}} = \frac{1}{\sqrt{2}} V_{\text{d.c.}} \text{ or } 0.707\, V_{\text{d.c.}} \qquad (24)$$

This formula can be used only when the electric field is uniform. Data have been published on the direct-current breakdown voltage of pointed electrodes and for wires surrounded by coaxial cylinders in several gases and different pressures. In some gases, the curves at the minimum voltage or critical pressure for point-to-plane and for wire-to-coaxial cylinder configurations show lower breakdown voltages when the wire or point is negative to the other electrode. The direct-current COV for a wire-to-coaxial cylinder, taken from Reference 3, is shown in Figure 21. Thus, the above equation cannot be used for converting a.c. COV to d.c. COV in point-to-plane and wire-to-coaxial shield configurations.

Most of the Boeing data were taken with alternating current; hence, the corona onset voltage always corresponds to the d.c. polarity that has the lower COV.

CORONA ONSET VOLTAGE IN GASES BETWEEN BARE ELECTRODES

The direct-current corona onset voltage and breakdown voltage between electrodes of many configurations in air, helium, nitrogen, oxygen, and other gases are known at room temperature (Figure 20). A literature survey failed to produce adequate information on the COV and breakdown voltage in ammonia, carbon dioxide, oxygen, and nitrogen-oxygen mixtures; consequently, these data were obtained by Boeing in the laboratory.

Ammonia, carbon dioxide, helium, and nitrogen were investigated from the standpoints of dielectric constant, dielectric strength, and compatibility with other materials. It was found that these gases have a dielectric constant between 1.000 and 1.008 at room temperature and pressure (20°C and 760 torr). The dielectric strengths of the gases at normal temperature and pressure are shown in Table 4.

Table 4: DIELECTRIC STRENGTH OF GASES AT ROOM TEMPERATURE AND PRESSURE

	Relative Dielectric Strength (Referenced to Dry Air)	
Gas	d.c.	a.c. (less than 10,000 megacycles)
Air, dry	1.0	1.0
Ammonia, commercially dry	0.94*	1.35*
Ammonia over NH_4OH	0.85	---
Carbon Dioxide	0.91	1.10
Helium	0.13	0.043*
Nitrogen	1.03	1.0
Mixture of Nitrogen, 75%; Ammonia, commercially dry, 25%	0.83*	---

* From experimental data using parallel plates.

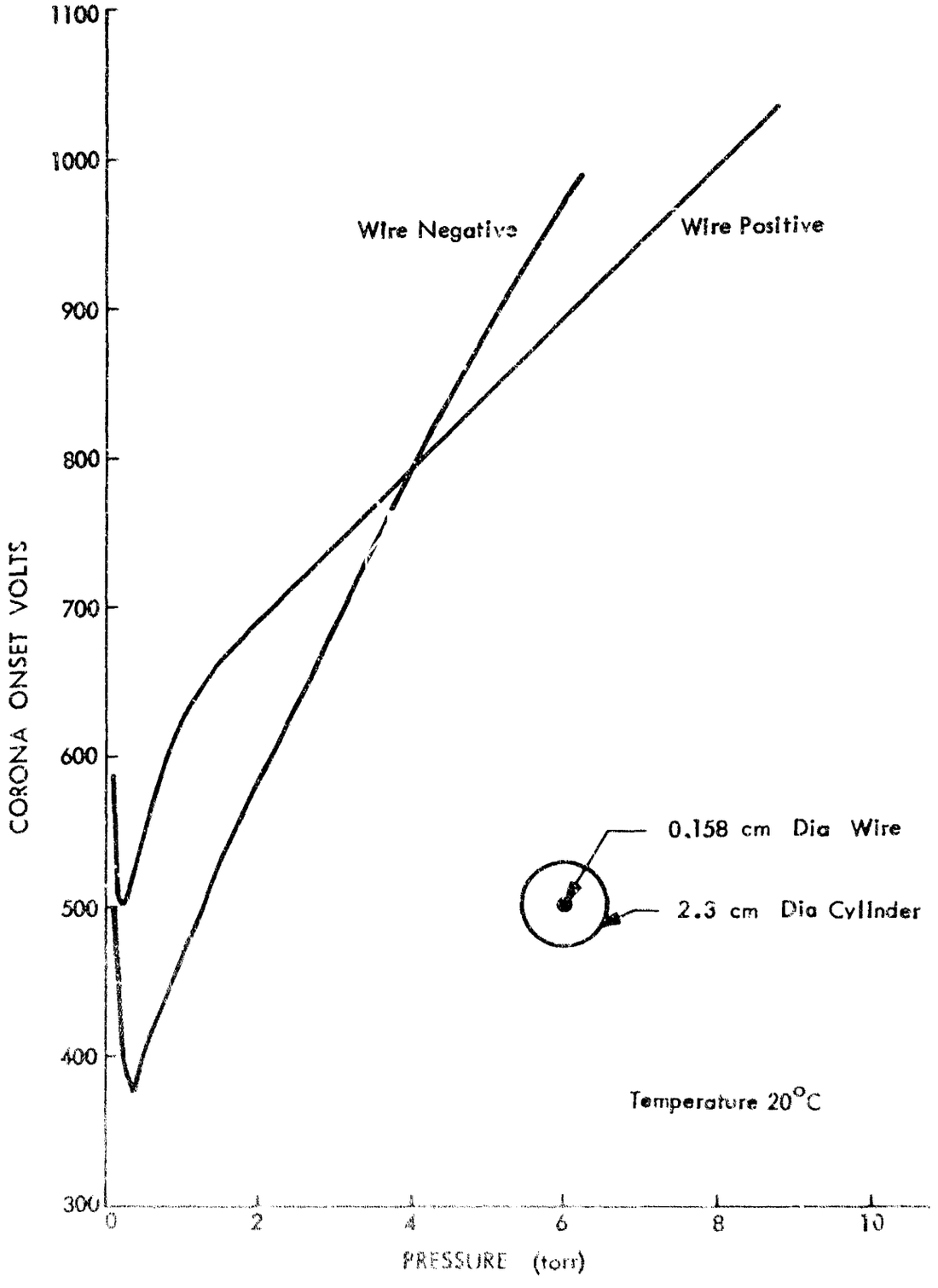

Figure 21 DIRECT CURRENT BREAKDOWN VOLTAGE OF AIR BETWEEN A WIRE AND A COAXIAL CYLINDER

AMMONIA

Air, cooled by ammonia, is presently used as an electronic atmosphere in the IM-99 missile. However, ammonia is one of the few gases that can be used as both an evaporating coolant and as a pressurizing gas for some electrical subsystems and components; therefore, it was investigated. Ammonia is generally considered corrosive. However, the corrosion rate of pure ammonia gas at 25°C is less than 0.020-inch per year on materials that it attacks quite readily, such as copper, aluminum alloys, zinc, and galvanized surfaces (Reference 23). This is a low corrosion rate for some uses, but is high when compared to corrosion in inert gases. Excellent resistance to ammonia is offered by Kel-F, Koroseal, natural rubber, polyethylene, silicone rubber, Teflon, Tygon, and white asbestos. Corrosion rates in ammonia at room temperature and pressure are shown in Table 5.

A curve of d.c. breakdown voltage in ammonia between 2.5-centimeter-diameter parallel electrodes spaced 0.25 centimeter apart is shown in Figure 22. Since these plates are closely spaced (0.1 spacing-to-diameter ratio), the breakdown voltage is essentially the same as for parallel plates. Other ammonia data at 9600 megacycles appears in Appendix I.

CARBON DIOXIDE

Carbon dioxide (CO_2) is a useful pressurizing gas because it can be stored as a high-density comparatively low-pressure gas, solid, or liquid. Furthermore at a given pressure it is a better heat-transfer agent than air. This makes it possible to transfer a given amount of heat with less blower power and lower compartment pressure, thus reducing gas loss from leaks.

The electrical properties of CO_2 are comparable to those of air. The dielectric constant of CO_2 at 1 atmosphere and 23°C is about that of air. The dielectric strength of CO_2 at 1-atmosphere pressure, for alternating voltages up to 10,000 megacycles, is less than the strength of air — 0.91 for CO_2 versus 1.0 for air. However, at critical pressures, the COV is greater for CO_2 — 230 volts (rms) for air, 310 volts (rms) for CO_2.

Although an inexpensive gas, carbon dioxide has drawbacks. For example, CO_2, like ammonia, absorbs infrared energy. Below 10,000 megacycles per second, CO_2 attenuates signals slightly more than air. Brush-type direct-current motors may not operate properly in a CO_2 atmosphere; even with high-altitude brushes the motor will operate satisfactorily for only a short time.

The corona onset voltage as a function of CO_2 pressure and electrode spacing, for plates, points, and rod electrode configurations is shown in Figure 23. The COV between parallel plates for carbon dioxide and air is compared in Figure 20.

It is interesting to note that a combination of CO_2 and water is less corrosive than an equivalent air-water combination.

Table 5: CORROSION RATES FOR AMMONIA AND AMMONIA-WATER SOLUTIONS (REFERENCE 19)

Material	Ammonia (%)	Temp. (°F)	Corrosion Rate (in. per yr)
Steel, Cast Iron, Ni Resist; 12 Cr Steel; 17 Cr Steel; Worthite; Durimet 20; 18-8 Stainless Steel	100	75	0.002
	10-30	212	0.020
Copper, Tin, Bronze, Al Bronze, Red Brass, Silicon Bronze	10-40	75	0.050
	100	75	0.002
Yellow Brass	10-40, 90	75	0.050 stress cracks
	100	75	0.002
316 Stainless	10-30	175	0.020
	100	75	0.002
Monel	10-30	75	0.050
	100	700	0.050
	100	500	0.020
	100	75	0.002
Nickel	10-30	75	0.050
	100	700	0.050
	100	500	0.020
Inconel	10-30	75	0.002
	100	700	0.020
Hastelloy (A, B, C, D)	10-40	75	0.002
	10-100	212	0.020
	100	600	0.020
Aluminum	10-30, 100	75	0.002
	10-30, 100	125	0.020
	100	212	0.020
Lead	10-30, 100	75	0.020
	100	212	0.020
Gold, Platinum, Tantalum	10-30, 100	212	0.002
Silver	10-30	75	0.050
	100	75	0.020
Silicon Irons	10-30	75	0.020
	100	212	0.020
Glass and Stoneware	10-30, 100	212	0.002
Rubber	10-30, 100	75	0.002
Asbestos	10, 20	75	0.002
Plastic (Haveg)	10, 40	212	0.002
Karbate	10-30, 100	212	0.002
Concrete	100	75	0.002
Wood	100	75	between 0.020-0.050
Titanium, Zirconium	30	75	0.002

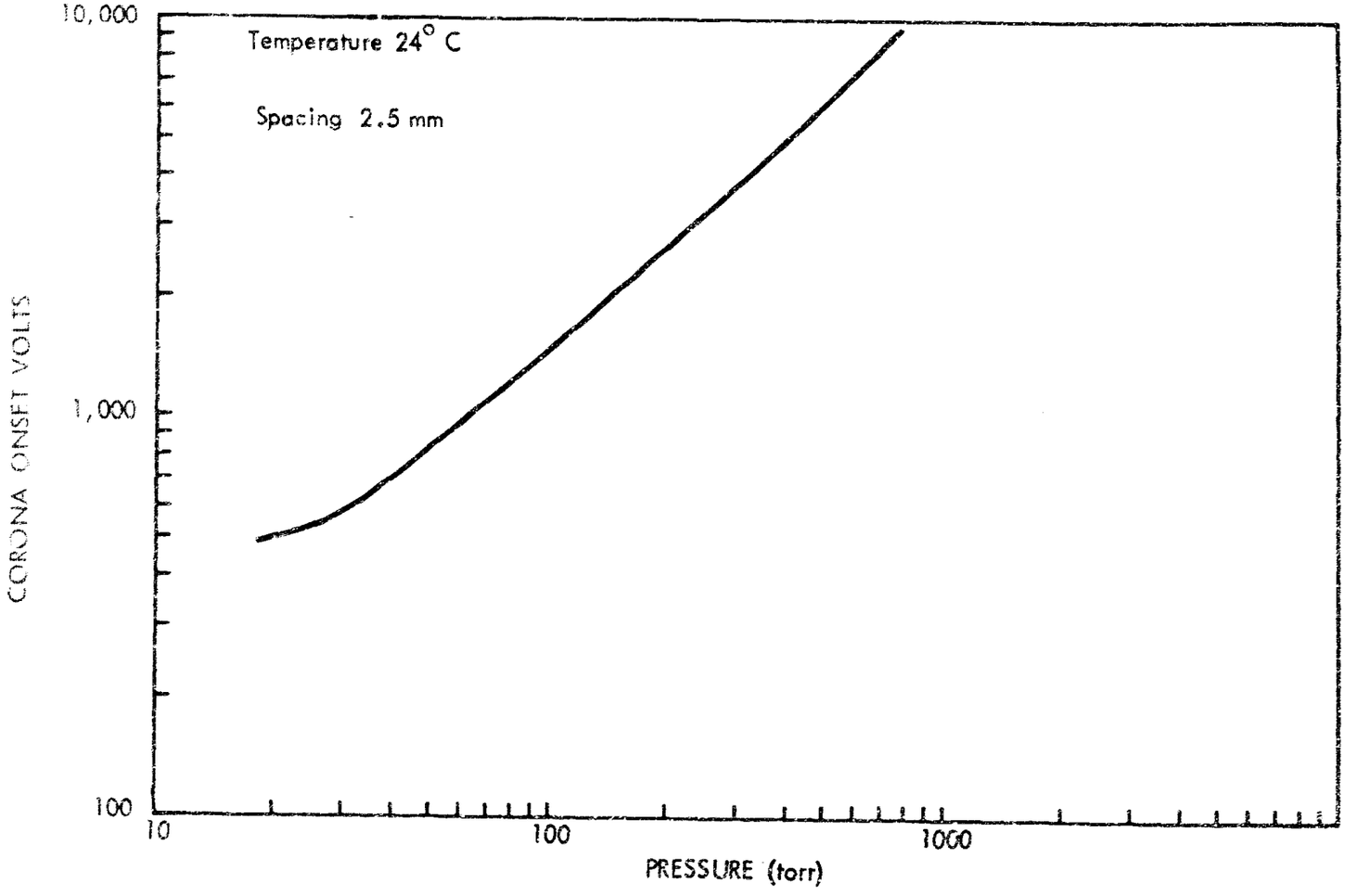

Figure 22: DIRECT CURRENT BREAKDOWN VOLTAGE BETWEEN PARALLEL PLATES IN AMMONIA

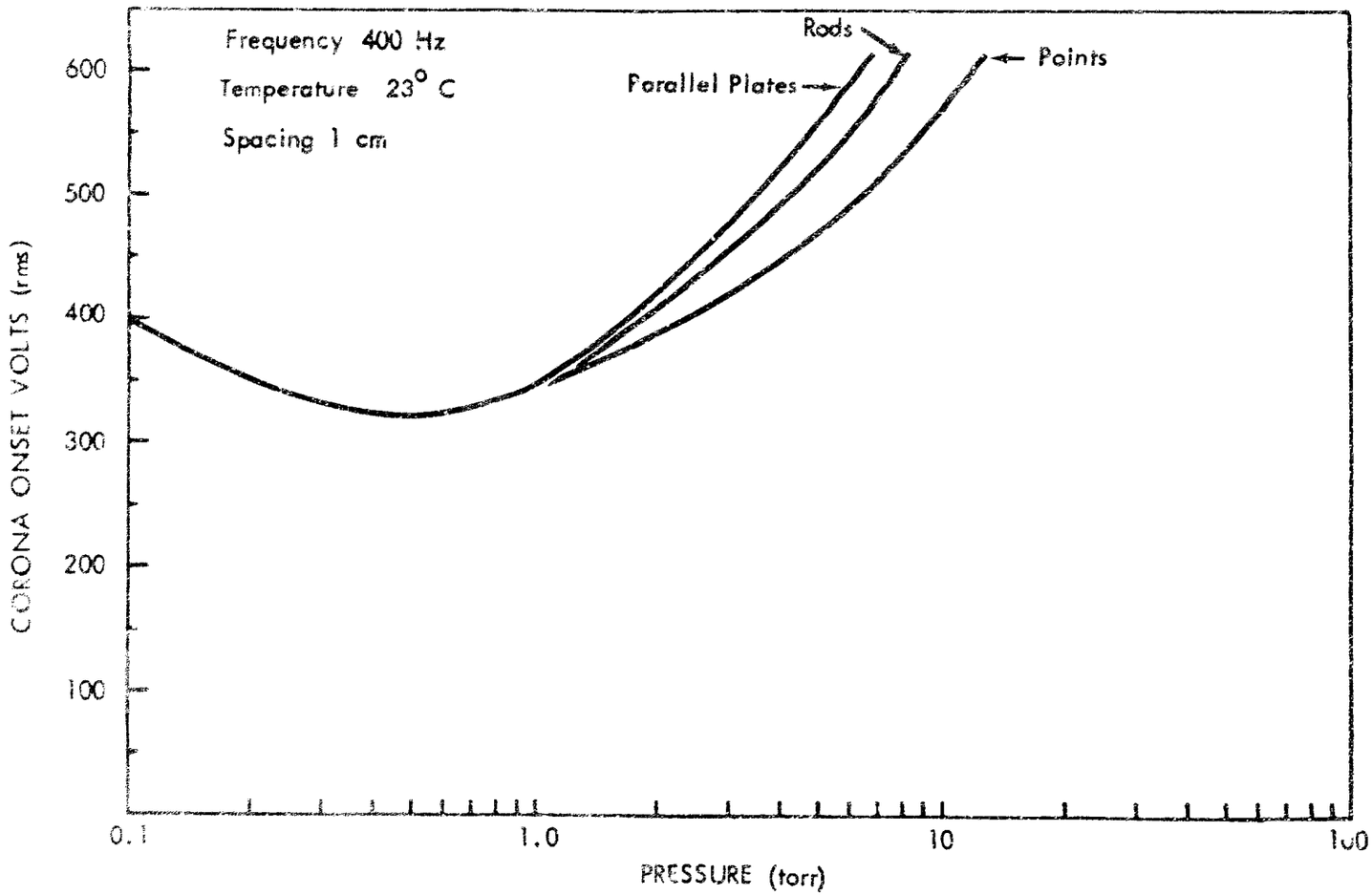

Figure 23:PARALLEL PLATES, POINTS AND RODS IN CARBON DIOXIDE

HELIUM

Helium is the lightest inert gas used for pressurization and environmental cooling. It has good electrical properties when pressurized and is inert with respect to combustion and corrosion. However, practical helium storage requires high-pressure leak-free vessels. The minimum corona onset voltage in helium is much lower (about 132 volts rms) than in other gases at the critical pressure-spacing dimension.

More data is available on helium than on most other pure gases (References 3, 4, 13, 14, 15, 17, and 24). Corona onset voltage as a function of pressure and spacing between parallel plates, rods, and pointed electrodes is shown in Figure 24. Helium was not considered seriously as a pressurizing and cooling gas for X-20A because of its containment problem and low corona-onset-voltage characteristics. Mixtures of helium and oxygen are being considered for future space vehicles. Corona characteristics of some of these mixtures are shown in Figure 25.

NITROGEN

Nitrogen was the pressurization gas selected for the X-20A electronic compartment, and a nitrogen-oxygen mixture was selected for the pilot's compartment. Extensive COV tests were conducted in pure nitrogen and mixtures of nitrogen and oxygen. Figure 20 shows that pure nitrogen has a lower minimum breakdown voltage than air; therefore, those compartments using nitrogen or nitrogen-oxygen were especially susceptible to corona.

The gas pressure that must be maintained within a nitrogen-filled compartment will depend upon the voltage, electrode material and configurations, and the spacing between electrodes. There will be no breakdown, regardless of pressure, if all voltages in nitrogen are below 180 volts (rms) a.c. or 250 volts d.c.

MANNED SPACECRAFT ATMOSPHERE

Atmospheres composed of oxygen and various inert gas diluents have been investigated for manned spacecraft. The better diluents appear to be helium, neon, and nitrogen. Nitrogen was chosen for the X-20A, and helium and nitrogen are being considered for the Manned Orbiting Laboratory (MOL). Neon as a diluent has been used successfully in diving work by the Royal Navy and in experimental space chambers (Reference 20). Neon has not yet been used in spacecraft. The Mercury, Gemini, X-15, and Apollo vehicles all use low pressure oxygen without diluents for the breathing atmosphere.

When pure oxygen is used for breathing, the cabin is usually pressurized to 260 torr (5.0 psia). The Earth's atmosphere, containing 21-percent oxygen, provides 160 torr (3.1 psia) partial pressure of oxygen. Most spacecraft using diluted oxygen are based on 160 torr (3.5 psia) partial oxygen pressure, with approximately 360 torr (7.5 psia) total cabin pressure. Atmosphere selection for manned spacecraft is influenced by:

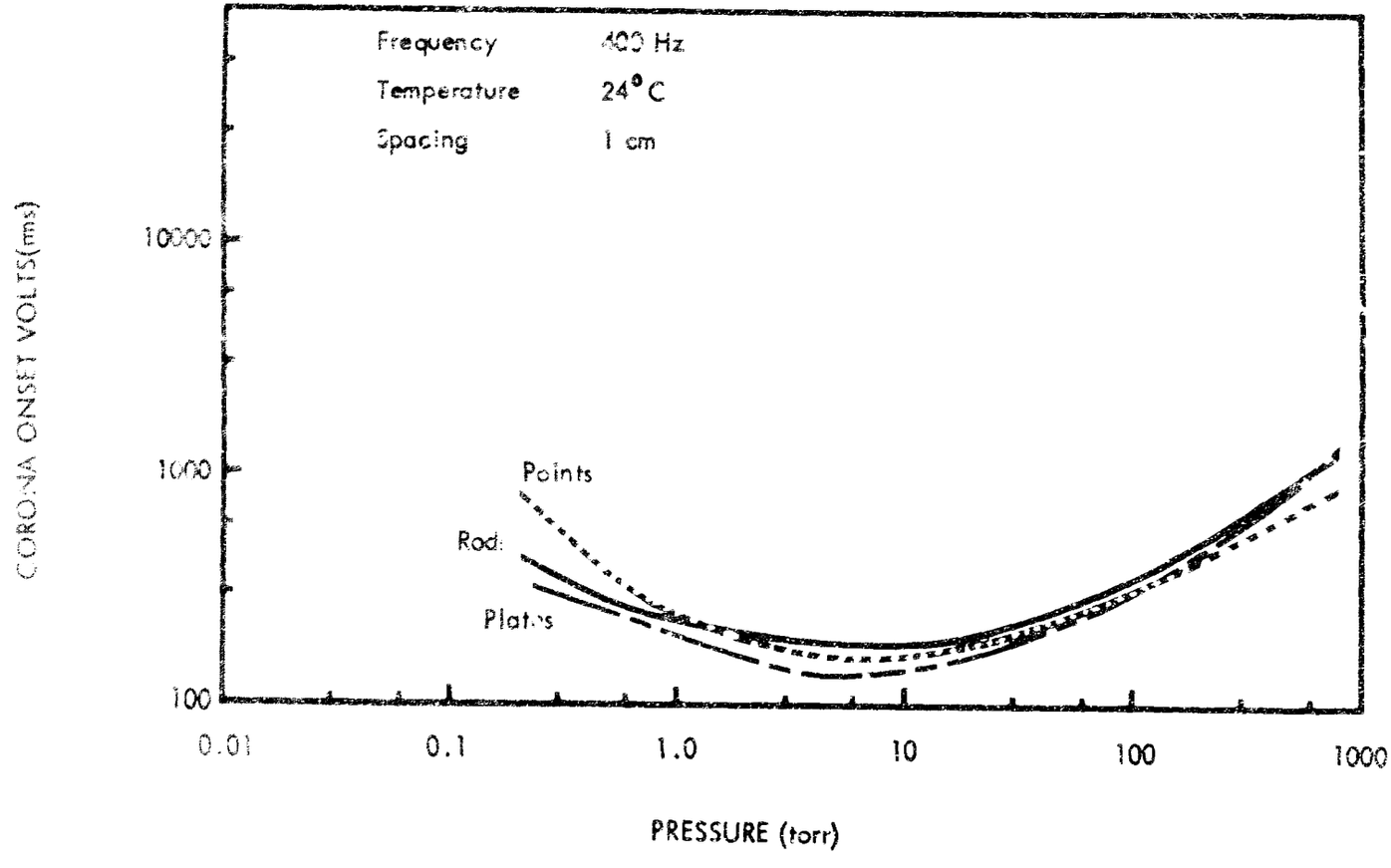

Figure 24: PARALLEL PLATES, POINTS AND RODS IN HELIUM

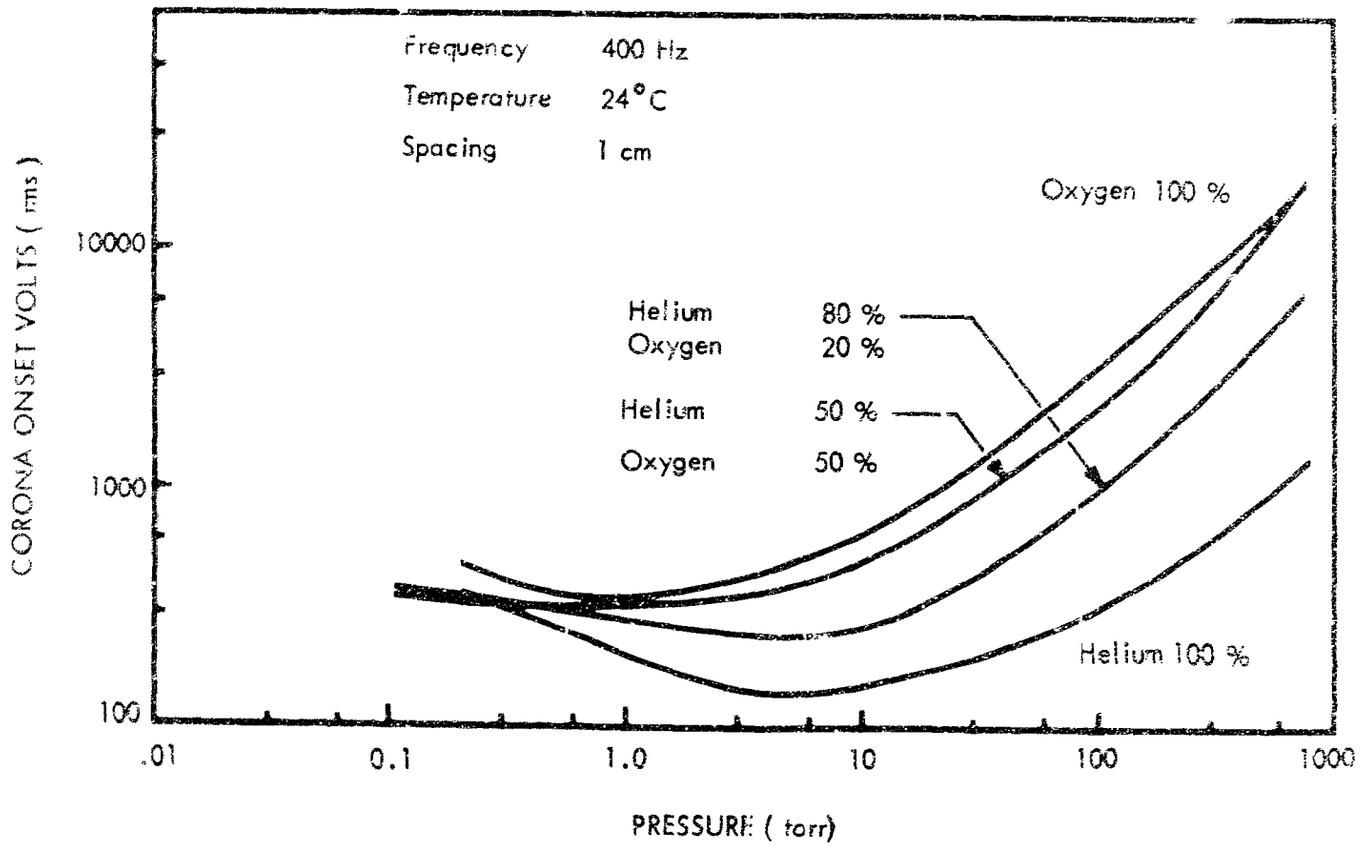

Figure 25: CORONA ONSET VOLTAGE OF HELIUM - OXYGEN GASES AND GAS MIXTURES BETWEEN 5.0 - cm DIAMETER PARALLEL PLATES

- The leak rate, and tank and structural weight required to contain the gases for replenishment;
- The electric power required to circulate, decontaminate, and monitor the atmosphere;
- Flammability of materials in the gaseous mixture;
- The physiological and pathological effects on the astronaut;
- Spacecraft gas requirements, other than life support.

Gas escapes from the spacecraft through small capillary-type holes, less than 10 microns in diameter, and through larger holes caused by meteorite penetrations. The helium flow through a capillary-type hole less than 0.1 micron is about 7.5 times greater than for air at normal spacecraft pressures. However, this higher flow rate would require less helium than air or nitrogen by weight.

A typical spacecraft 3 meters in diameter and 6 meters long pressurized to 360 torr would have a total leakage of about 0.5 kilogram of helium-oxygen atmosphere per day through capillary holes. This leakage is insignificant compared to leakage through larger holes where the flow rate is approximately the same for all gases. As a result, the weight of a spacecraft pressurized with helium-oxygen is less than if either a nitrogen-oxygen or a neon-oxygen mixture were used (Reference 21).

The flammability in two-gas atmospheres is greatly reduced if oxygen is diluted with at least an equal volume of inert gas.

The electric power required for atmosphere circulation depends on temperature, pressure, and compartment configuration. Less power is used if the diluents are helium or neon rather than nitrogen, primarily because of differences in thermal conductivity. Power for decontamination and monitoring of gas supplies is not affected by the diluent selection.

The important advantage of helium and neon diluents is that their use minimizes the possibility of nitrogen narcosis, and reduces other physiological difficulties (References 19 and 22) and overall weight.

HELIUM-OXYGEN MIXTURE

A gaseous mixture of helium and oxygen has been suggested for the MOL crew compartment. During flight, cabin depressurization or equipment malfunctions can cause pressures to vary from nominal cabin pressure to the vacuum of space. Failure in piping, control valves, or pressure vessels could change the cabin atmosphere mixture to either nearly pure helium or oxygen.

Corona in helium and oxygen mixtures was explored by measuring the corona onset voltage between a pair of 5.0-centimeter parallel-plate electrodes spaced 1.0 centimeter apart. Spacings of 2.0 and 9.2 centimeters were also tested in pure gases; no noticeable change in the Paschen-law voltage pressure spacing relationship was found.

Curves developed from the test data obtained with parallel-plate electrodes are shown in Figure 25. In these curves the COV is plotted as a function of pressure times spacing for pure helium, pure oxygen and gas mixtures. The curves in Figure 24 show the corona onset voltage for parallel plates, round rods and points spaced one-centimeter apart. Curves showing the COV as a function of the proportion of helium in oxygen appear in Appendix I. The percentage helium (by volume) in oxygen was measured at constant temperature.

These data show, for example, that corona can appear on the bare electrodes of a 200-volt (rms) line-to-line power subsystem if the surrounding gas contains more than 80-percent helium by volume. Such a subsystem would require corona protection in the form of special ground planes and/or insulation.

NITROGEN-OXYGEN MIXTURES

The equipment in the crew compartment of the X-20A had to operate successfully in all nitrogen-oxygen mixtures and in all pressures ranging from sea-level atmosphere to the vacuum of space. Before each flight, the crew compartment was filled with air at 1 atmosphere. During flight, air leaking out was to be replaced with a mixture of dry, filtered nitrogen and oxygen. Failures in the pressure walls or control valves would result in slow or rapid depressurization. Malfunctions in gas supply apparatus could vary the mixture to either pure nitrogen or pure oxygen.

The nitrogen and oxygen mixtures were explored by measuring the corona onset voltage between a pair of 6.4-milimeter-diameter rods. Parallel-plate electrodes were tried, but large random errors occurred when the parallel plates were closely spaced. Larger spacings were attempted, but with them COV occurred at gas pressure below 1 torr, where the gas pressure could not be held within an acceptable tolerance.

Two sets of curves were developed from the test data. One set shows the COV as a function of the proportion of nitrogen and oxygen. In these tests, the electrode spacing and total pressure were held to within 1.0 percent of the values shown on the curves. In the second set of curves Figure 26, COV versus pressure times spacing are plotted for three gas mixtures and for the pure gases. These data show that the COV cannot be determined for a gas mixture by linear extrapolation or interpolation from known mixtures. They also show that there are pressures and spacings where the COV of some mixtures is less than that of either component gas.

These data show that corona will appear on the bare electrodes of a 200-volt (rms) line-to-line power subsystem if a gaseous mixture having more than 95-percent nitrogen is critical. If a subsystem must operate in such an environment, then corona protection must be designed into its components.

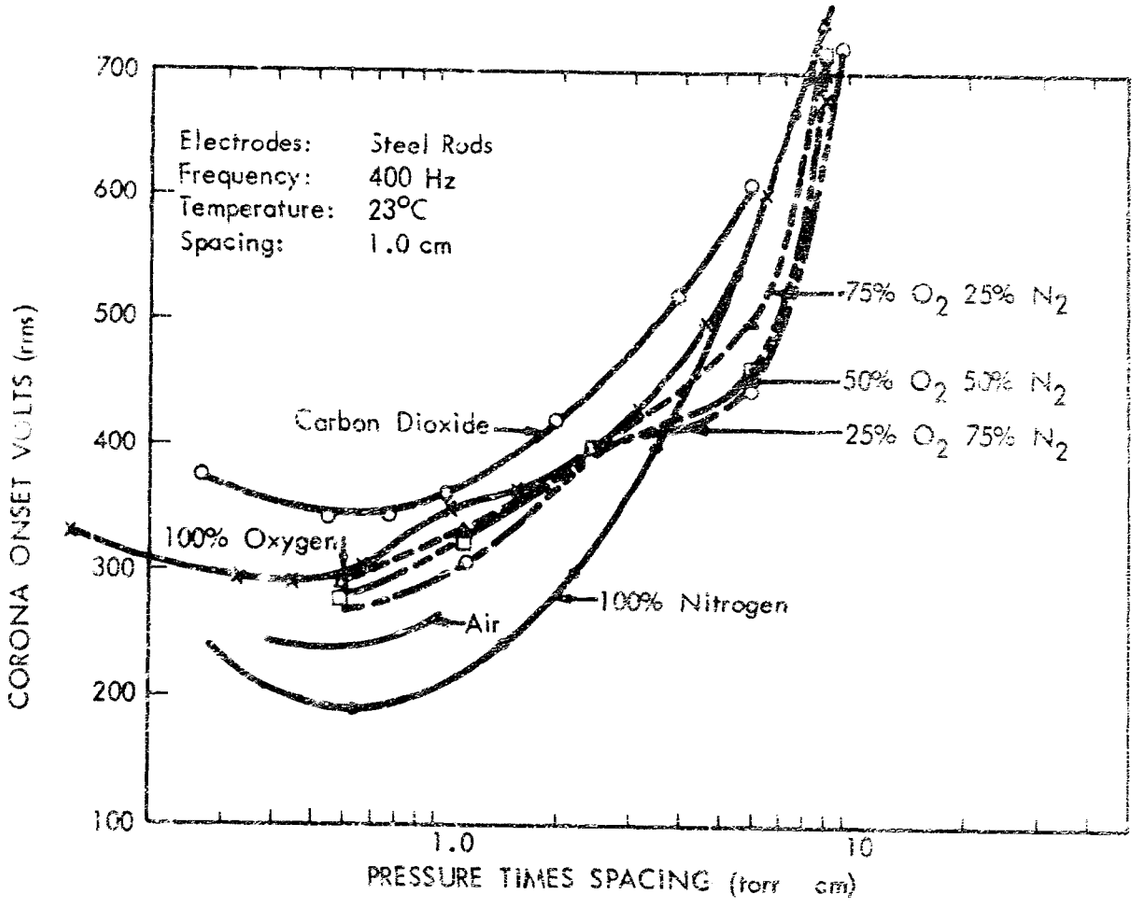

Figure 26: CORONA ONSET VOLTAGE OF GASES AND GAS MIXTURES BETWEEN 0.64 - CM DIAMETER ROUND RODS

HIGH TEMPERATURE

The X-20A was designed with some electric conductors located outside of environmentally controlled compartments. These conductors were exposed to temperatures over 1000°C, radiation fields, and pressures approaching 0 torr. It was necessary to ensure that corona and insulation losses in these conductors would be within acceptable limits. Therefore, the electrical characteristics of both bare and insulated parallel-wire circuits were measured in these extreme environments.

Power wires in aerospace vehicles are usually twisted or cabled. However, the very low resistance of available insulating materials at 1000°C made it necessary to consider, for the X-20A, wires held in place by either ceramic spacers or solid sheathed and swaged ceramic insulation. To determine the effectiveness of this approach, two spaced No. 14 AWG nichrome-V wires were tested for COV in the vacuum oven previously described. The wires were heated before testing to facilitate straightening the wires by applied tension and to form an oxide coating on the conductors so all tests would be with conductors having the same physical properties. The wires were checked for spacing, tension, and uniformity after each heating cycle.

The 400-hertz corona-onset voltage in air, between wires at fixed spacings of 3.2, 6.4, and 25 millimeters, was measured in the heated altitude chamber at pressures from sea level to 0.2 torr, and at oven temperatures of 23, 250, 500, 700, 866, and 1100°C. Data were recorded for both decreasing and increasing pressures. The pressure was held constant before any corona reading was taken.

Figure 27 shows the test results plotted with COV as a function of pressure and temperature for each spacing. It will be noted that the minimum breakdown voltage is lower at the higher temperatures for each spacing tested. The temperature varied along the length of the tested wire. For example, when the central portion of a wire was at 596°C, the end of the wire connected to the fixture outside the oven was at 100°C. Therefore, there is an ambiguity in the experimental results with respect to the COV at high temperatures. At pressures below 1 atmosphere, the lowest COV corresponds to the spacing and its related pressure and temperature in the central or hottest portion of the wire.

A second influence was also observed: that of high-temperature electron mobility. This effect causes the COV to be lower than expected for a given temperature.

The minimum corona onset voltage varied from 265 volts (rms) a.c. at room temperature down to 230 volts (rms) a.c. at 1100°C. Such corona onset voltages are probably too low for reliable operation of a 115/208-volt three-phase power circuit. Since wider spacing of the conductors will not reduce corona and glow discharges at low pressure, the only way to eliminate them is to use high-temperature ceramic insulation.

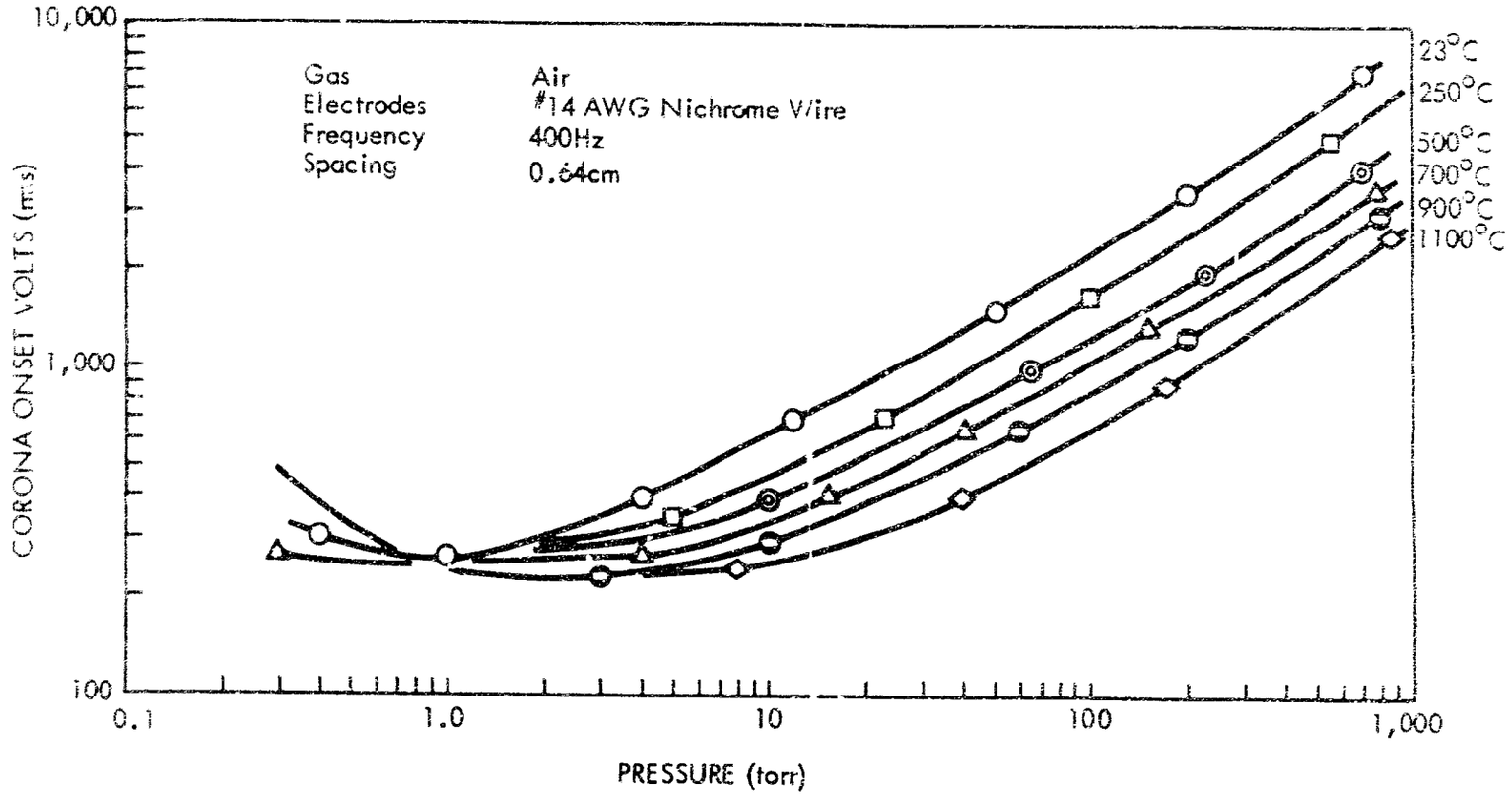

Figure 27: CORONA BETWEEN NICHROME WIRES IN HEATED CHAMBER

[illegible] tests indicated that metal-sheathed, solid-ceramic-insulated wire was [illegible] for instrumentation and power wire operating in temperatures above [illegible] tests at Boeing (Reference 25) indicated that:

a) Organic insulation has limited life in temperatures over 500°C;

b) Inorganic insulators, other than ceramic, begin to conduct at high temperatures;

c) Fibrous or spaced-beaded insulation within a solid or braided sheath became plated with oxides of the sheath and/or conductor at high temperatures, resulting in short circuits;

d) Solid metal sheaths protected the wire from ionized gases and foreign materials and structurally contained the ceramic insulation.

CORONA MEASUREMENTS BETWEEN MOLYBDENUM WIRES

When subjected to high temperature, molybdenum and tungsten sensors, wiring, and other parts must be protected from oxidation by either an inert atmosphere or evacuation to less than 0.01 torr. Likewise, nonoxidizing conductors should not be located in the vicinity of unprotected molybdenum in a high-temperature atmosphere containing oxygen because the molybdenum will oxidize, releasing molybdenum trioxide MoO_3 by evaporation. This oxide may penetrate the wire sheathing and contaminate the interelectrode spaces in the wires, thus inducing corona and creating radio noise.

It has been established that time, temperature, and oxygen pressure determine the quantity of molybdenum trioxide formed (Reference 26). Below 500°C, a parabolic oxidation law is followed; little or no trioxide forms. Above 500°C, the MoO_3 begins to evaporate; at 600°C, evaporation rate of MoO_3 becomes significant. At 770°C, the rate of evaporation of MoO_3 equals the rate of formation, and evaporation becomes rapid as the temperature is increased.

The 400-hertz corona onset voltage was measured between molybdenum-titanium wires, spaced 6.4-millimeters apart, at atmospheric pressure and at temperatures exceeding 500°C in air. The wires did not corrode at temperatures below 500°C, but the wires showed appreciable corrosion when heated above 500°C. At 1100°C, the corrosion layer became thick and MoO_3 crystals formed on the wires. The numerous MoO_3 molecules in the air between the wires carried conduction current when a voltage exceeding the corona onset voltage was applied to the wires. Curves showing the corona onset voltage at several temperatures between parallel wires made of molybdenum alloy (containing 0.5-percent titanium), as a function of pressure, appear in Figure 28. Experiments were also conducted using No. 18 AWG nickel-clad copper wires and No. 14 AWG nichrome wires in an oven contaminated with molybdenum. Results of these experiments are shown in Appendix H.

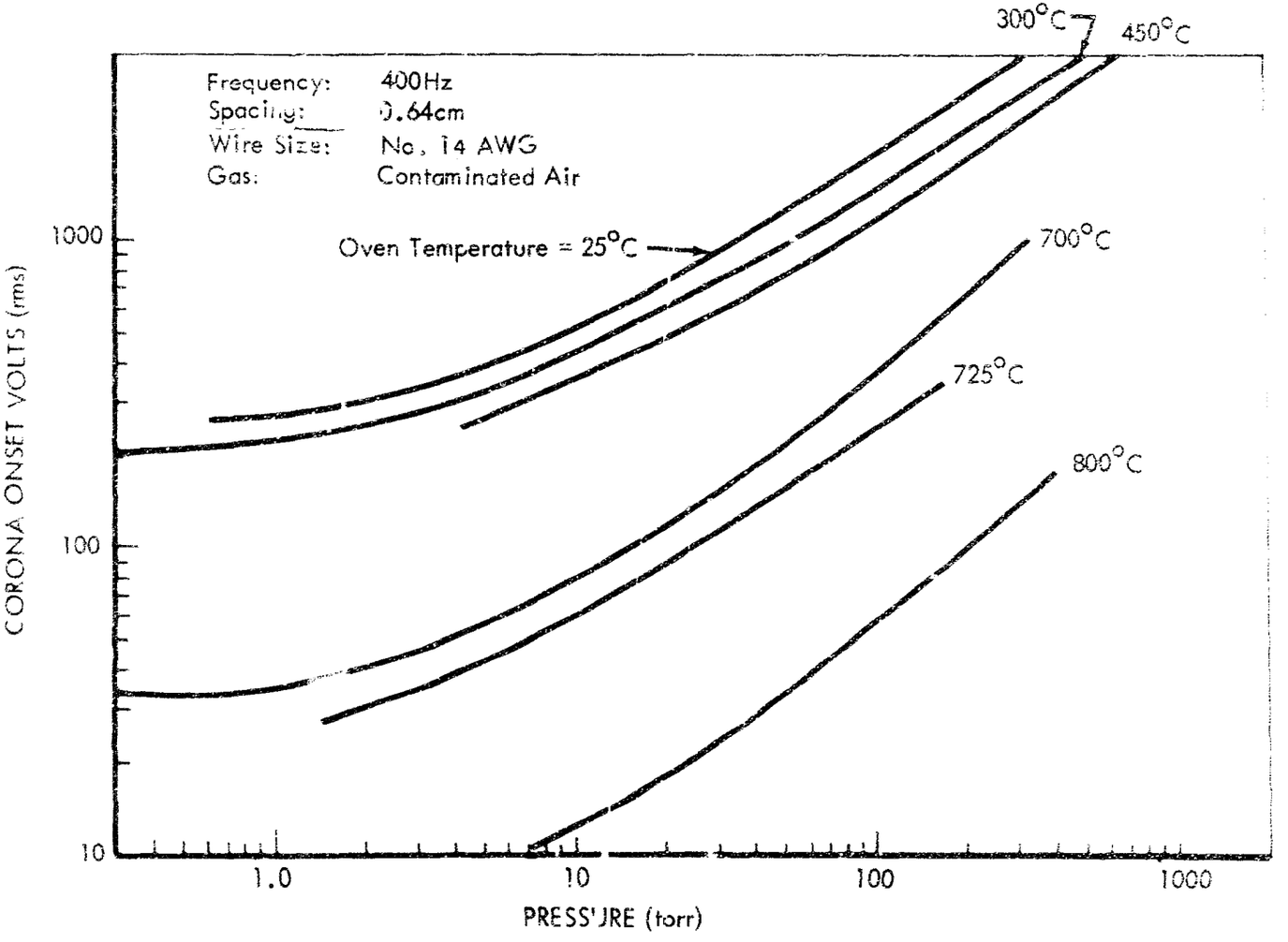

Figure 28: CORONA ONSET VOLTAGE OF NICKEL-CLAD WIRES IN A MOLYBDENUM CONTAMINATED OVEN

Crystals of MoO_3 formed at atmospheric pressure are yellowish and appear on the surfaces of the wires. Crystals formed at low pressures are long, flat, and clear. These crystals are found on all surfaces in the surrounding area. Very few crystals appeared on the parallel wires at low pressures, but the oven had crystals on all surfaces of the brickwork. Formation of MoO_3 crystals at the end of an oven is shown in Figure 18.

If molybdenum wiring must be used, it should be protected by keeping it at less than 500°C or in a hard vacuum (10^{-4} torr or less). Conductors should not be placed in the vicinity of unprotected molybdenum because the MoO_3 will contaminate the area.

Molybdenum can be chromium plated to prevent oxidation. However, if the molybdenum member is stressed, the chromium may crack and the molybdenum will oxidize releasing MoO_3. Rhodium and platinum can also be used as coatings to prevent the oxidization.

Tungsten, like molybdenum, oxidizes, and the resulting oxide evaporates at temperatures above 400°C. Consequently, tungsten should be treated with the same precaution as molybdenum.

INSULATED WIRES

The minimum COV of a wire sample is shown in Figure 29. Two factors are significant. First, the insulation around the wire has increased the corona onset voltage above that for bare wires spaced 6.4 millimeters apart — from 265 to 320 volts (rms) a.c.. This 320 volts (rms) is above the operating voltage of a 115/200-volt electric-power subsystem, but slightly below the maximum ceiling voltage allowed during transients. Second, twisting or closely spacing the wires further increased the minimum corona onset voltage by another 50 to 370 volts (rms). The higher COV of the twisted wire comes from the difference in the length of air path between the insulations.

All tests have indicated that the minimum corona onset voltage of a twisted pair is always greater than that of a spaced pair, and that the difference in minimum COV between a twisted pair and a spaced pair depends on the dielectric constant of the insulation, thickness of insulation, wire size, and voltage stress.

The wires described in Table 6 were tested for corona onset voltage. The COV at the minimum of the Paschen law curve for these wires is shown in Figure 30. In electric-subsystem design it is important that the minimum COV of the wire be greater than the maximum voltage allowed on the subsystem.

COMPONENTS

In measuring the corona onset voltage of electric components, it is important that the minimum COV of the connecting wire is equal to or greater than that of the component being tested.

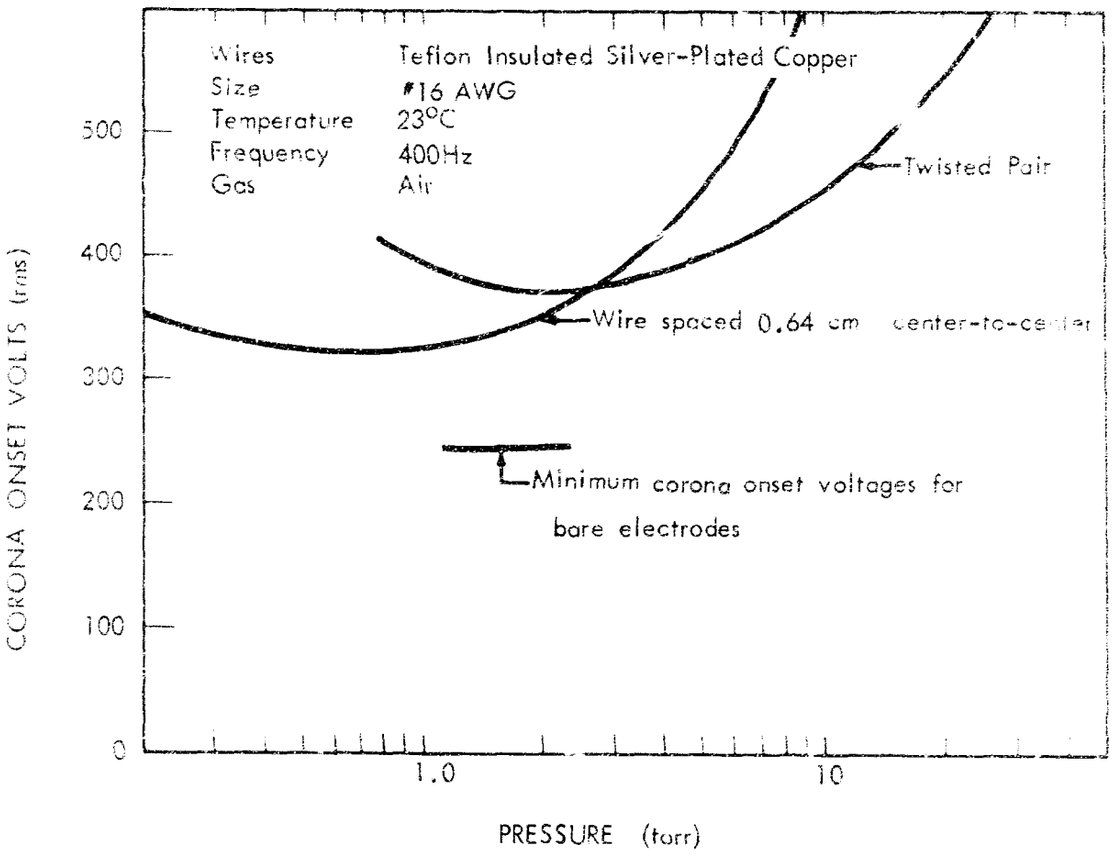

Figure 29: CORONA ONSET VOLTAGE OF TWISTED AND SPACED WIRES

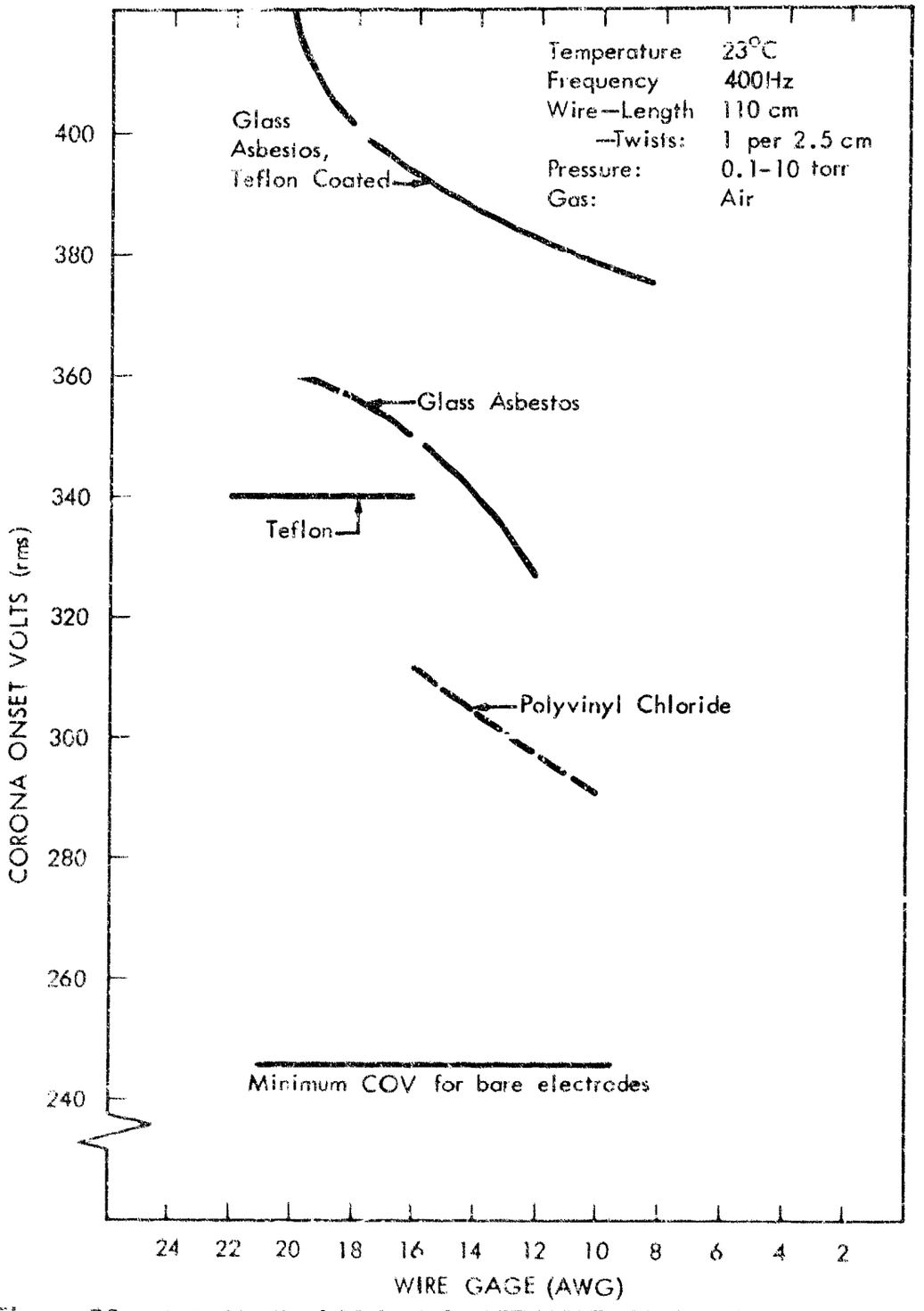

Figure 30: MINIMUM CORONA ONSET VOLTAGE OF SEVERAL WIRE TYPES AND SIZES

Table 6: DESCRIPTION OF WIRE TEST SAMPLES

SAMPLE NUMBER	WIRE GAGE	Primary	Barrier	Outer Jacket	Thickness (in.)
1	16	PVC	Glass	Nylon	0.025
	10		Braid		0.036
2	20	Asbestos	Glass	Teflon	0.042
	16		Braid	and	0.045
	12			Fiberglass	0.052
3	22	Teflon			0.022
	20	(TFE)			0.025
	16				0.035
4	20	Teflon	Teflon	Teflon	0.030
	18	(TFE)	and	(TFE)	0.032
	8		Fiberglass		0.040

Four corona onset voltage tests were made on a 55-pin mated connector. The connector shell was grounded and the connecting wires and unwired pins were encapsulated with 13 millimeters or more of silicone rubber.

In the first test, a pair of No. 22 AWG teflon-insulated wires, spaced 6.4 millimeters apart, were connected to adjacent connector pins and then fed through the chamber wall to the voltage source. The second test was the same as the first except that the connecting wires were twisted. In the third test, one wire was disconnected from its pin and then reconnected to the same pin circuit on the mating half of the connector. The fourth test was made with the wires in the same physical position, but the connector was removed and its space was filled with silicone rubber. This was to demonstrate that the connector, rather than the wires, was responsible for the observed minimum COV.

The test results (Figure 31) show that the true COV of the connector was obtained in the third test. The curves from the first and second tests correspond to spaced and twisted wires as shown in Figure 29. Results of the fourth test were the same as for conductors spaced 5 centimeters apart — the minimum spacing measured between conductors inside the altitude chamber. If insulation voids had existed between adjacent connector pins, the COV would have been that of bare pins in the encapsulated gas.

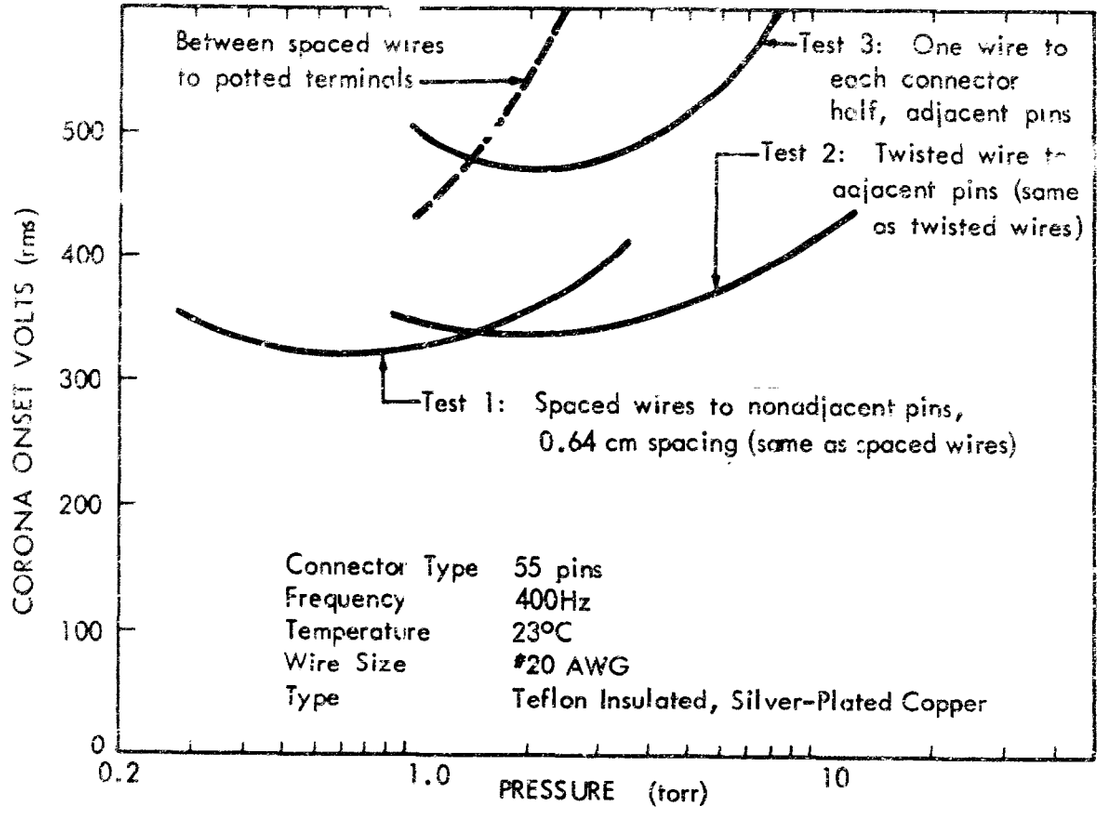

Figure 31: CORONA ONSET VOLTAGE FOR WIRED CONNECTOR

V. RECOMMENDED FUTURE RESEARCH

The contract requires that the final report include recommended areas of investigation necessary to increase the minimum corona onset voltage. It is recommended that further investigation be conducted on ground planes, hermetic sealing, and foam and solid insulation.

Two other recommended studies, which are not directly associated with increasing the corona onset voltage, are corona onset in neon-oxygen mixtures, and high-temperature corona.

GROUND PLANES

Tests conducted during X-20A development show that twisted wires have a higher corona onset voltage than spaced wires.

The electrostatic field between a single wire and a ground plane is the same as that between one wire of a twisted pair and the half-plane of the twisted wires. The only difference is that the twisted wires are about as close to each other as possible. In general, placing insulated electric wire or electrical components close to the ground plane will increase the corona onset voltage.

The closeness of ground planes and the resulting corona onset voltage can be improved by wrapping the electric components or cabling with conducting shields and using conducting fillers such as carbon-black impregnated plastics to fill voids between insulated wires and ground planes.

It is predicted that with the installation of the ground planes and the encapsulation of wiring with conducting fillers the critical corona onset voltage of twisted wires in air can be raised from 340 volts rms to about 500 volts rms.

The required research involves investigations into how much conductivity is required in shields and conducting fillers determining how shields and conducting fillers can be prepared and applied in practice, and testing wire, shields, and conducting fillers to verify improvement in corona onset voltage.

HERMETICALLY SEALED COMPONENTS

Space flight experience has demonstrated that hermetic seals tend to leak. Even if no cracks or flaws develop during assembly, test, and boost, the leakage will occur, although it may take several months before it is significant. As the gas in the hermetically sealed compartment leaks out, the pressure declines, ultimately reaching a value corresponding to the minimum in the Paschen law curve where corona can occur. The leakage becomes very slow at low pressures, hence operation near the Paschen law minimum can persist for a long time.

Hermetic sealing is a useful method of avoiding corona in critical spacecraft components, particularly those that must operate during the changing pressure that occurs as the vehicle is boosted from Earth. There are several approaches to overcoming the leakage problem. One is to use a pressurizing gas having large molecules that will not escape readily.

Gases such as carbon dioxide, sulfur hexafluoride, and vapors of chlorofluorohydrocarbons have the required large molecules. However, they need to be evaluated with respect to other characteristics, such as formation of corrosive products when heated by arcs at electrical contacts.

Another possibility is the use of sponge-stored fluorinated hydrocarbons, which also have satisfactorily large molecules. It may be possible to retain in a sponge liquid Freon that evaporates and replaces the gas that leaks out. Again, the characteristics of such pressurizing gases must be carefully evaluated for compatibility with electric sparks, insulation, hermetic-seal materials, and dissociation products.

FOAM-SOLID INSULATION

Because foams are light in weight, they are desirable insulating and potting materials for spacecraft. Unfortunately, foamed packages have failed as the foam outgassed in space. These failures tend to occur between 1 hour and 20 days after launch. Repeated failures of this type have resulted in hesitancy to use foams for spacecraft.

A foam is analogous to a matrix of capacitors composed of gas, having a dielectric constant of around 1.0, and webs of plastic having a different dielectric constant. As the entrapped gas leaks out of the bubbles constituting the foam, the Paschen law minimum conditions are obtained in different bubbles at different times. Those bubbles near sharp conducting edges would be most susceptible to corona.

It is possible that foam can be used as a spacecraft insulation if sharp edges of conductors, which cause high dielectric stress, are first coated with solid plastic. However, the dielectric and corona characteristics of foam insulations must be understood before design guides for foam- and solid-insulation assemblies can be developed. A necessary step in acquiring this understanding is the development of a mathematical model for the dielectric characteristics of foam and solid insulation. The foam will have a variety of bubble sizes; hence, the model will be so complex that it can best be handled with a computer.

The final design criteria developed from the mathematical model will have to be checked with tests in vacuum, with corona formation being one of the more important measurements.

OXYGEN-INERT GAS MIXTURES

The corona onset voltage in oxygen-inert gas mixtures becomes important because such mixtures are proposed for pressurizing manned spacecraft. Helium, krypton, neon, nitrogen, and xenon are being considered as diluents for oxygen. Corona data for nitrogen-oxygen and helium-oxygen mixtures are reported in this document.

All diluent gases proposed for space cabin atmospheres form many tiny bubbles in human fat tissue and the circulating blood upon decompression. Studies reported by Roth (References 18, 20, and 22) indicate that decompression sickness (dysbarism) occurs about 1/4 as often when helium is used as a diluent in place of nitrogen, and 1/6 as often when neon is used. Neon has been used for diluting oxygen by the Royal Navy (Reference 20) and was found to decrease lung damage in explosive decompression. Use of helium also decreases the hazard of ebullism, the formation of water vapor and gas bubbles at altitudes about 70,000 feet.

Some gas mixtures (for example ammonia-nitrogen, hydrogen-nitrogen, and neon-argon mixtures) have a minimum corona onset voltage that is less than that of either of the two component gases. The corona onset voltage at the critical pressure-spacing in some gas mixtures is less than 90 percent of the corona onset voltage in the lower of the two gases. Thus, some oxygen-neon mixtures, for example, could have corona onset voltages below 115 volts rms a.c. at the critical pressure-spacing relationship.

The gas mixture may be fixed during normal vehicle operation. However, compartment leaks, inert gas or oxygen supply malfunction, and opening locks to space may change the gas pressure and/or composition. Slow leaks in the vicinity of bulkhead connectors may pressurize continuously the connector terminals on the space side of the bulkhead at a pressure corresponding to the minimum corona onset voltage, thus creating electromagnetic interference. It is recommended that the experimental work with helium-oxygen mixtures be duplicated using neon-oxygen mixtures.

HIGH-TEMPERATURE CORONA

The testing during the X-20A program indicated that contamination of the atmosphere from the release of absorbed gases and from the oxidation of nearby spacecraft structures significantly reduced the corona onset voltage at temperatures over 500°C. This work also indicated that there were three additional mechanisms that stimulated corona formation: (1) thermal electron emission from metallic and other surfaces; (2) magnetic fields from current-carrying conductors; and (3) electron and ion emission from arcs.

The No. 3 mechanism may have been responsible for reported failures of power switchover relays, where arc-generated electrons could have reduced corona onset voltage to the 12 to 50 volt level. Theoretical analysis and experimental work would be required to evaluate the effects of these additional factors on corona onset voltage.

VI. CONCLUSIONS

The corona research accomplished in the X-20A program, supplemented by analyses and tests conducted on Contract AF33(615)-3020, leads to the following conclusions:

- Corona is undesirable in aerospace vehicles because it consumes power, creates electromagnetic interference, deteriorates insulation, and, under certain conditions, develops into power-subsystem faults.
- There are clearly defined conditions of temperature, pressure, gas composition, and electrode configuration in which corona will occur at a given voltage stress. There is a gas density and electrode spacing at which the corona onset voltage will be a minimum. Higher or lower densities and different electrode spacings will result in increased corona onset voltage. To some extent, electrode spacing and electrode configuration lose their significance at the minimum corona onset conditions.
- It is possible to design a corona-free, 115/200-volt, 400-Hz electric-power subsystem for a spacecraft with a low-pressure air atmosphere, provided that no part of the subsystem is exposed to temperatures above 300°C. Particular care must be taken in predicting the effects of abnormal pressure and/or pressurizing gas composition occurring during pressurization malfunctions.
- Design of a high-temperature corona-free electric-power subsystem would be a risky venture at this time. It is known, for example, that the corona onset voltage of conductors near molybdenum in air can be reduced to virtually zero by the release of molybdenum trioxide gas. All the corona hazards may not yet have been identified.
- Spacecraft atmospheres composed of mixtures of either helium and oxygen or nitrogen and oxygen will have higher corona onset voltages than would be obtained in low-pressure air, provided the mixture contains at least 25 percent oxygen by volume.
- Important work remains to be done in investigation of ground planes, hermetic sealing, use of foam and solid insulation, corona onset in neon-oxygen mixtures, and high-temperature corona.

Appendix I

POINTS, RODS, AND PLATES IN VARIOUS GASES

The corona onset voltage in air, ammonia, carbon dioxide, nitrogen, oxygen, helium-oxygen mixtures and nitrogen-oxygen mixtures, between points, round rods, and parallel plates at room temperature appear in this appendix. The test data were obtained with the equipment and test procedure discussed in Section III. Each data point actually represents a group of laboratory readings. The data are plotted in Paschen law type curves with pressure-spacing values as the independent variable.

At moderate pressures, the corona onset voltage will become lower as gas pressure is reduced because the longer mean-free-path between electrodes permits electrons to be accelerated more readily to ionizing potential. Reduction of the gas pressure below the Paschen law minimum normally results in a higher corona onset voltage because the interelectrode gap no longer contains enough gas molecules to sustain ionizing collisions. However, with uninsulated electrodes the interelectrode gap includes the distance between the electrode shafts. Thus the minimum corona onset voltage can be expected to be a broad plateau extending from the pressure at which collisions cease to occur between the closest spaced electrode areas to the pressure where electrons traveling between the widest-spaced electrode surfaces cease having collisions. This phenomena is evident in all curves and is best illustrated in Figures I-1 through I-6, where the parallel-plate electrode spacing is varied from 0.5 millimeter to 20 millimeters.

Experimental corona onset voltage test data in ammonia, carbon dioxide, nitrogen, oxygen, helium-oxygen mixtures, and nitrogen-oxygen mixtures are shown in Figures I-7 through I-29. The helium used was supplied by the United States Government Bureau of Mines, and was Grade A. The distributor was Air Reduction Pacific Company, Seattle, Washington. The helium had a purity of 99.995 and a dew point of -70°C (less than 3.53 parts per million water).

LIST OF FIGURES — APPENDIX I

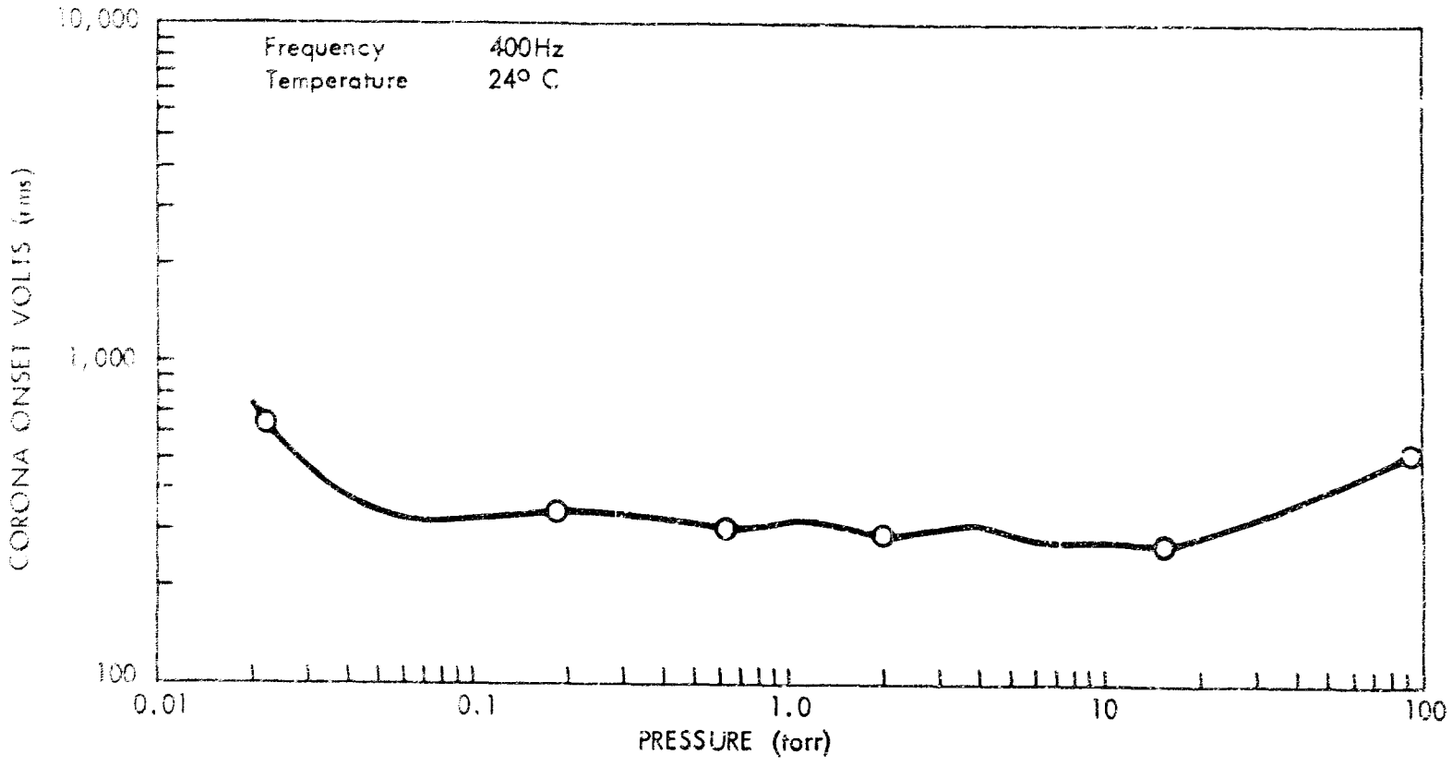

Figure 1-1: PARALLEL PLATES IN DRY AIR — 0.5-mm SPACING

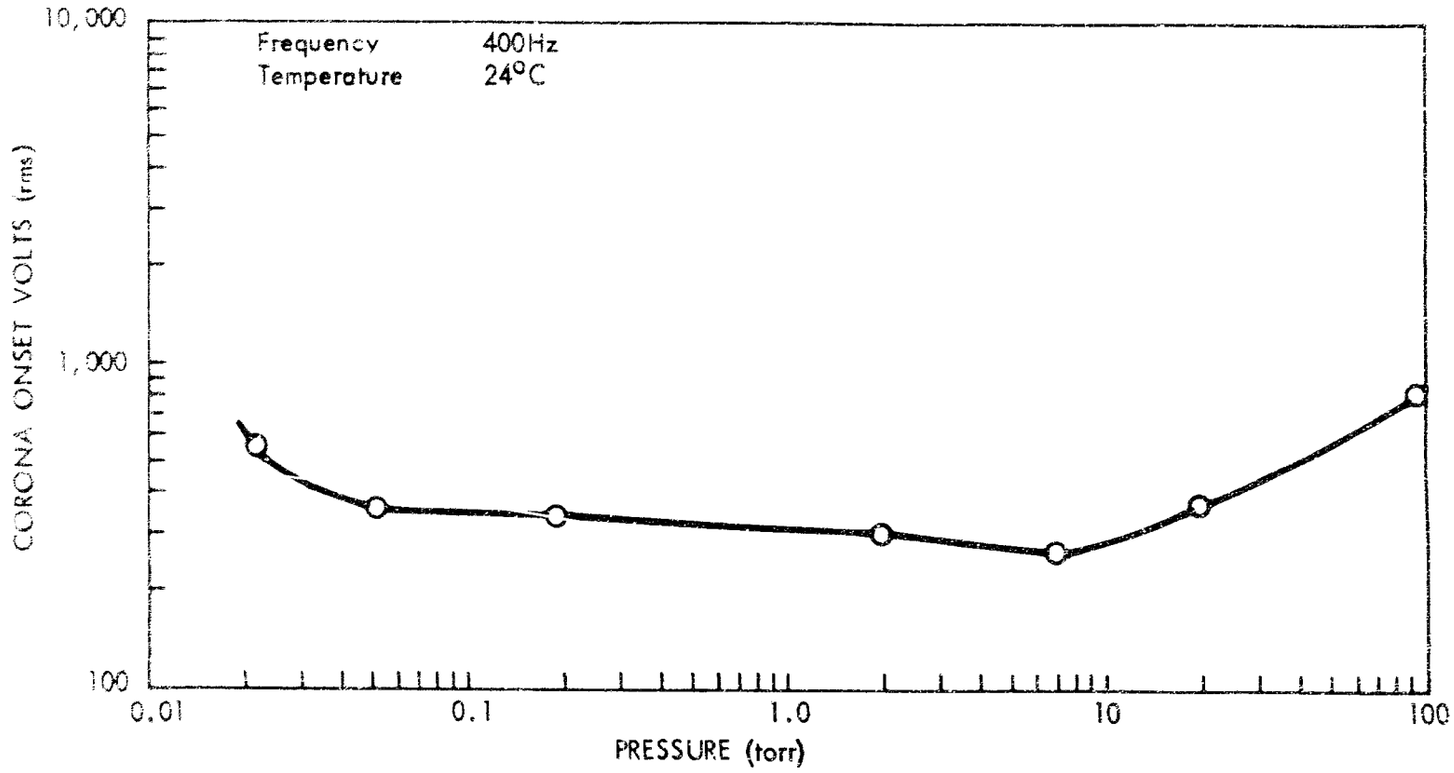

Figure 1-2: PARALLEL PLATES IN DRY AIR — 1-mm SPACING

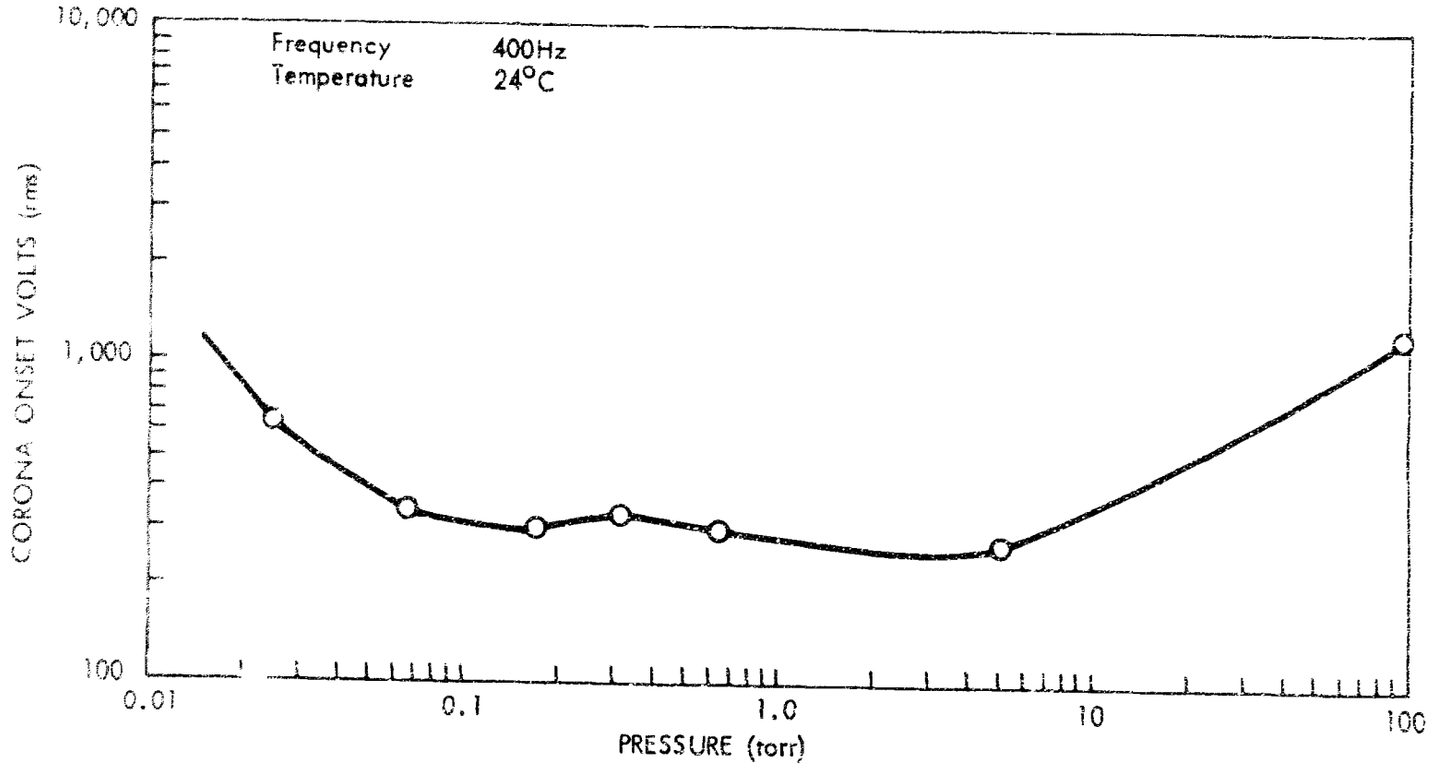

Figure 1-3: PARALLEL PLATES IN DRY AIR — 2-mm SPACING

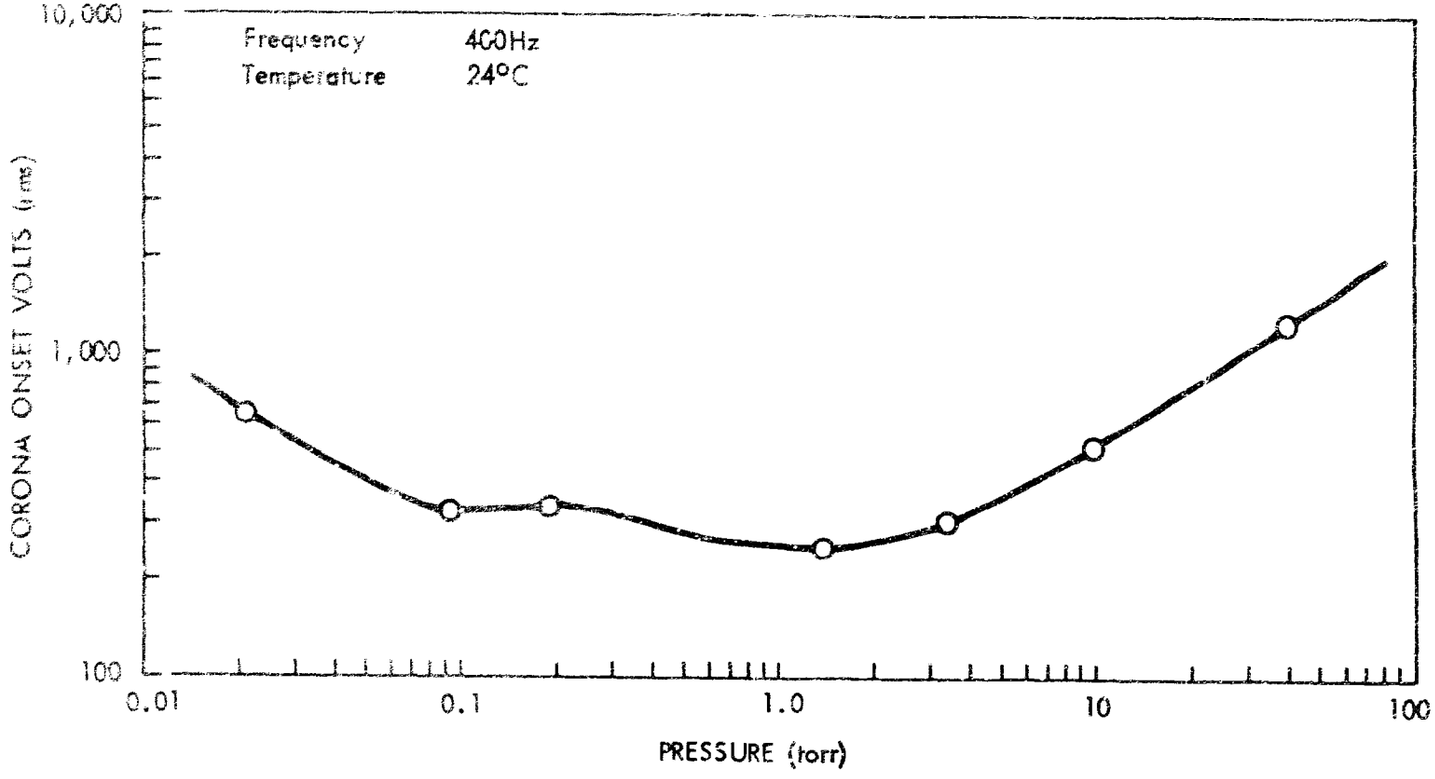

Figure 1-4: PARALLEL PLATES IN DRY AIR — 5-mm SPACING

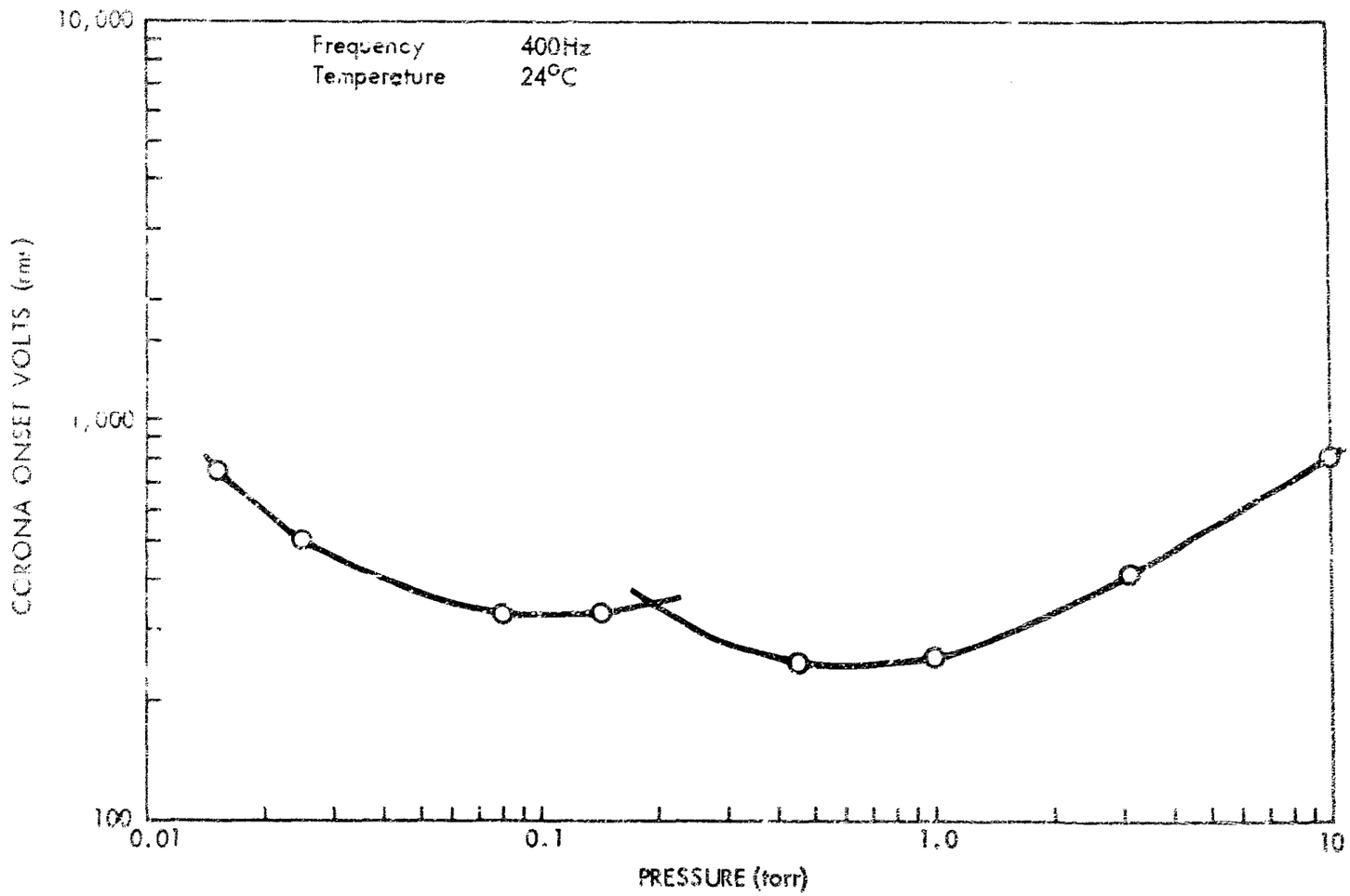

Figure 1-5: PARALLEL PLATES IN DRY AIR — 10-mm SPACING

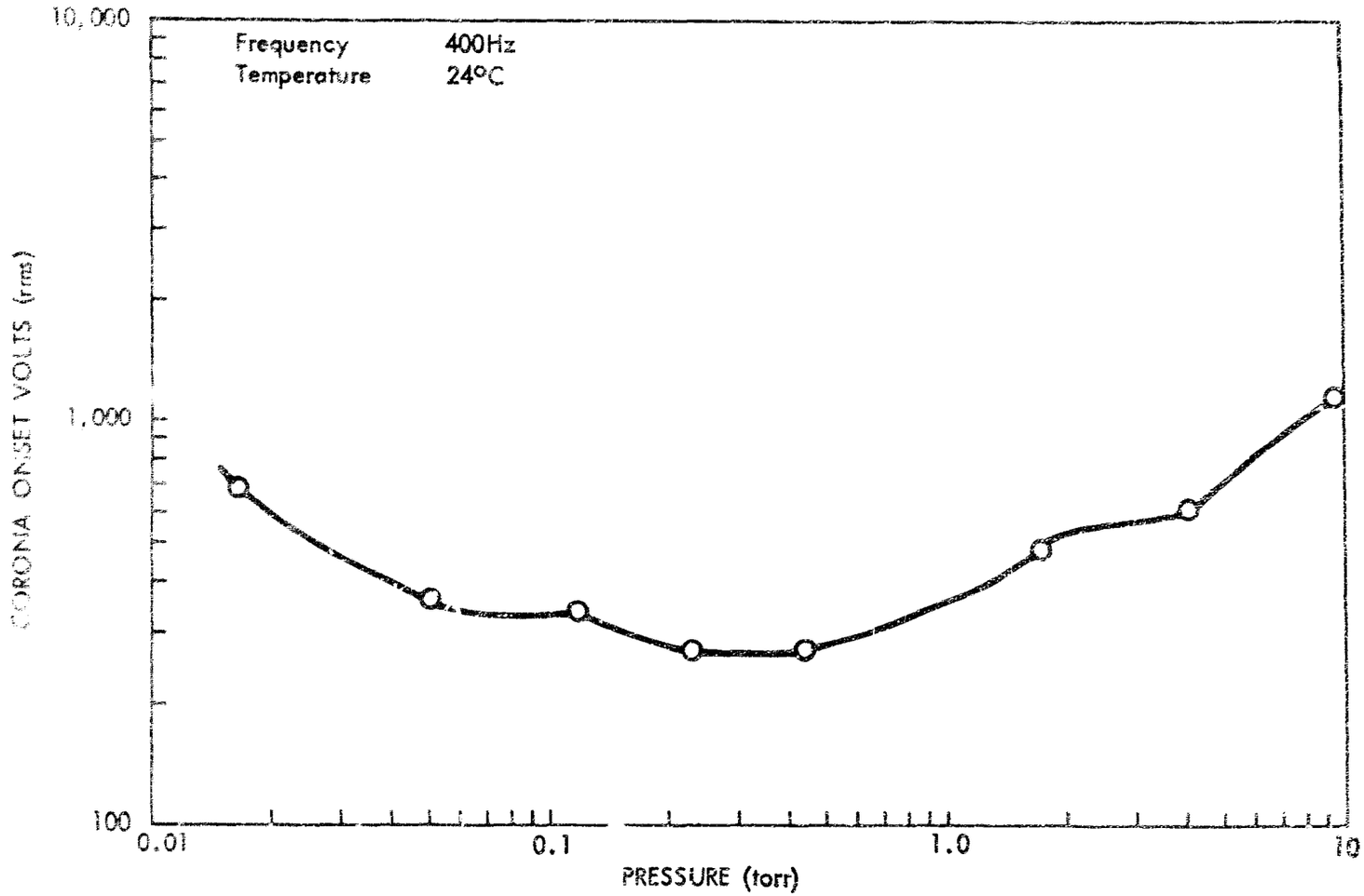

Figure 1-6: PARALLEL PLATES IN DRY AIR — 20-mm SPACING

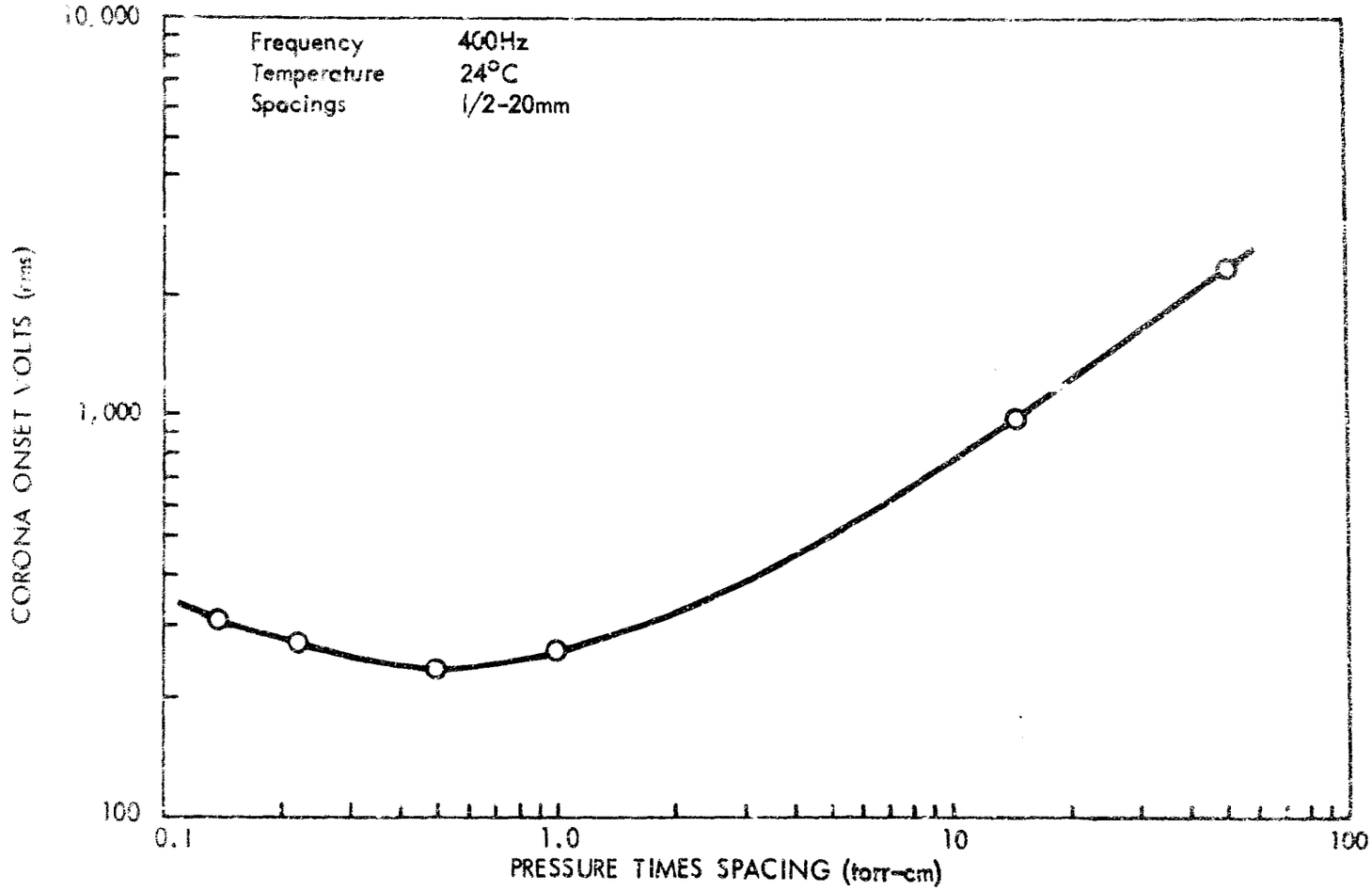

Figure 1-7: PARALLEL PLATES IN DRY AIR

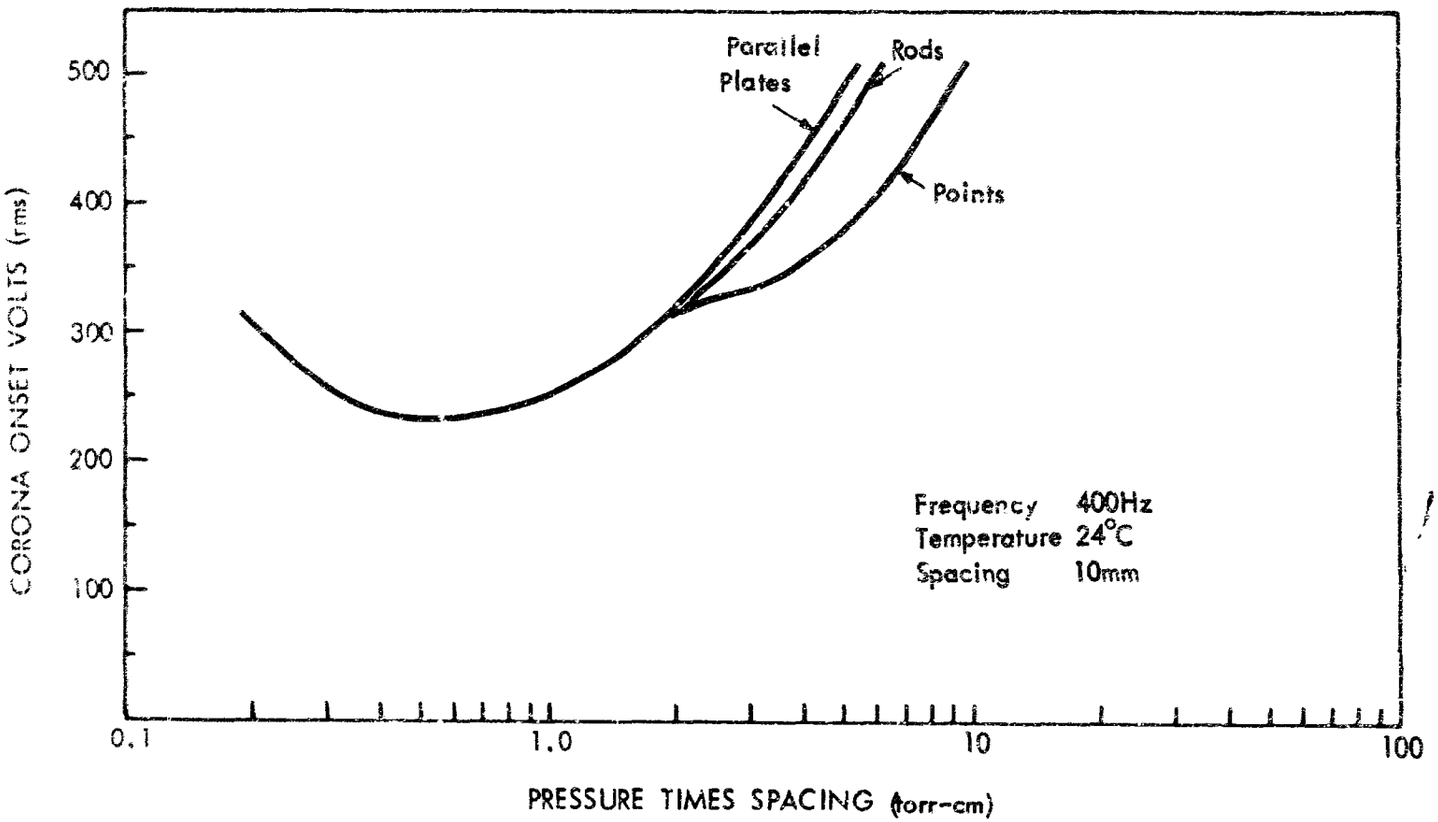

Figure I-8: PARALLEL PLATES, POINTS AND RODS IN DRY AIR

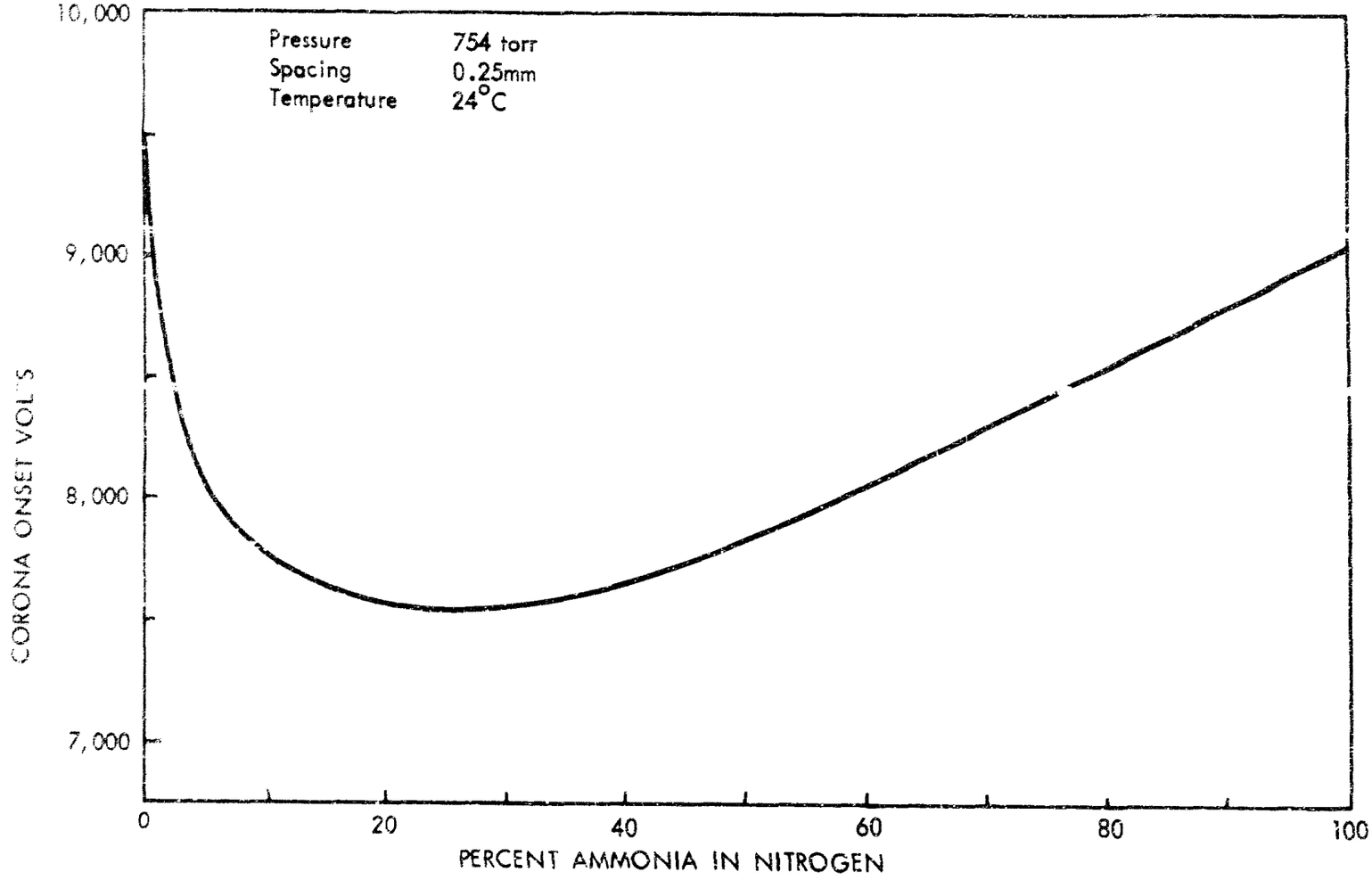

Figure I-9: PARALLEL PLATES IN AMMONIA-NITROGEN MIXTURES WITH DIRECT CURRENT

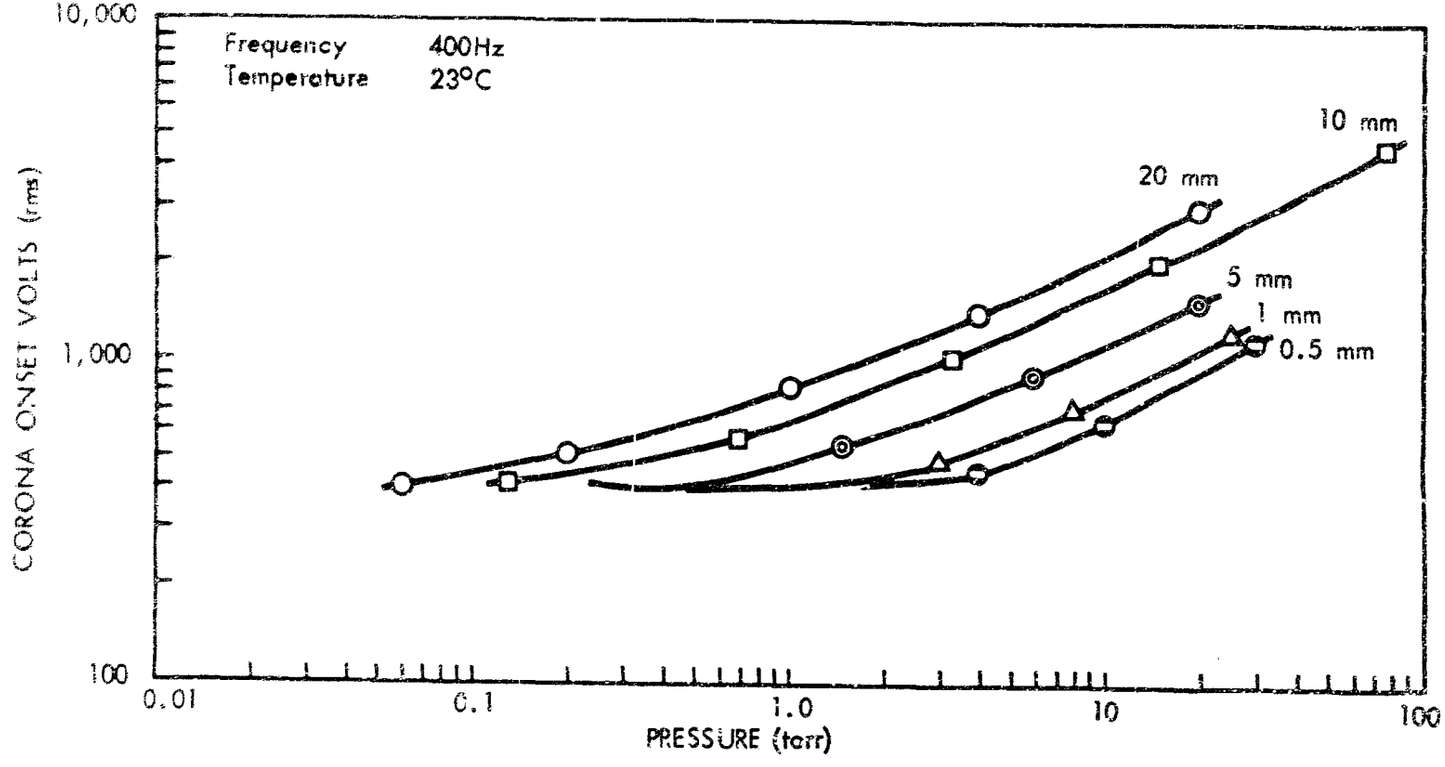

Figure 1-10: POINTED ELECTRODES IN CARBON DIOXIDE

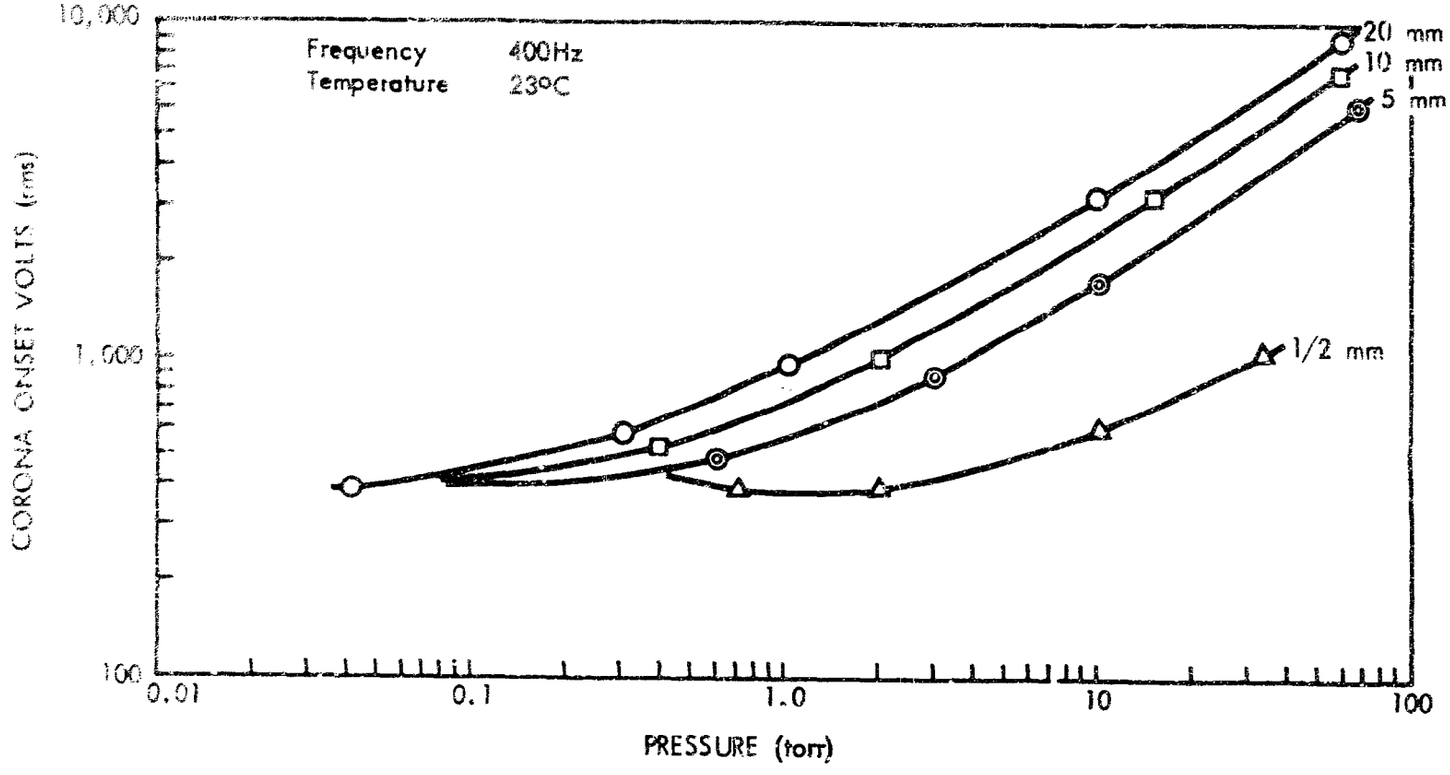

Figure I-11: ROUND RODS IN CARBON DIOXIDE

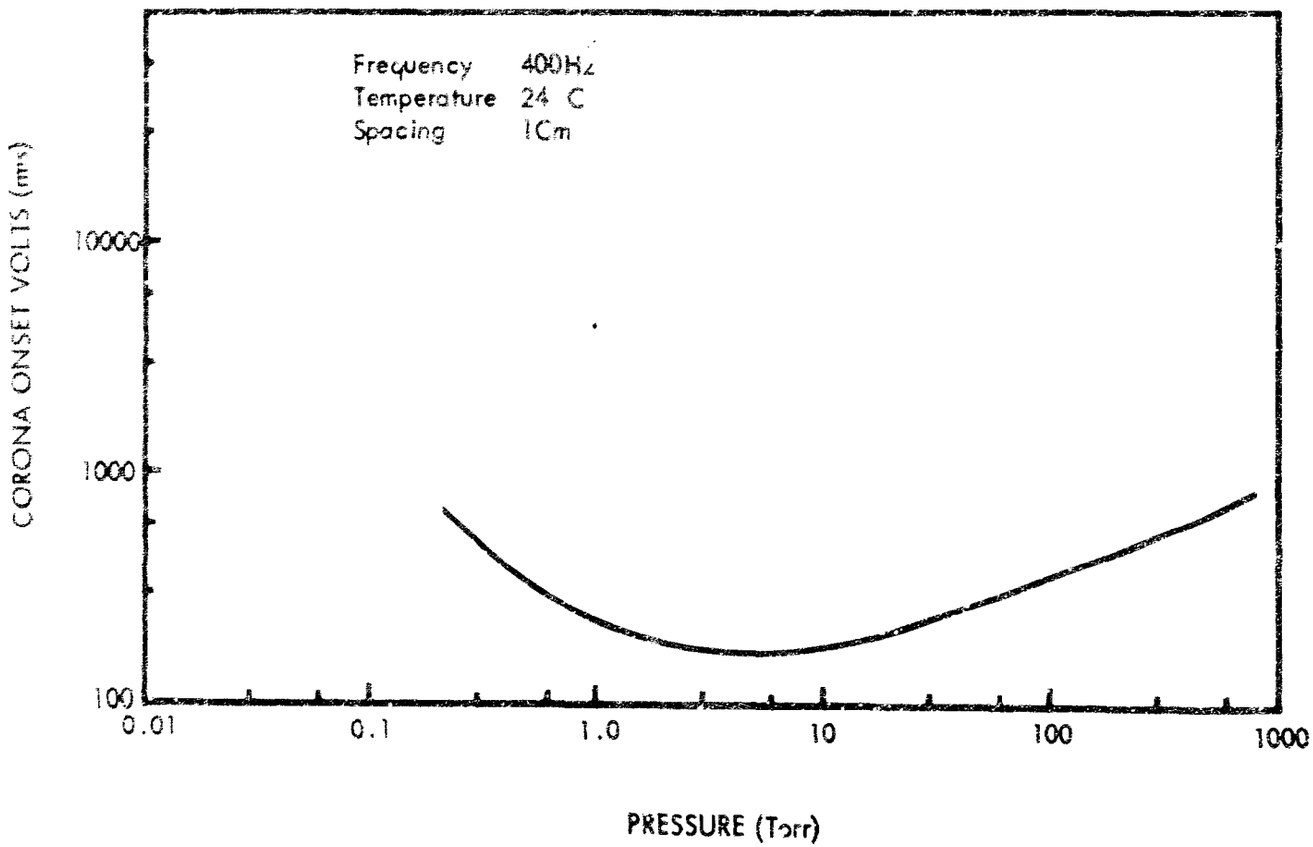

Figure I - 12: POINTED ELECTRODES IN HELIUM

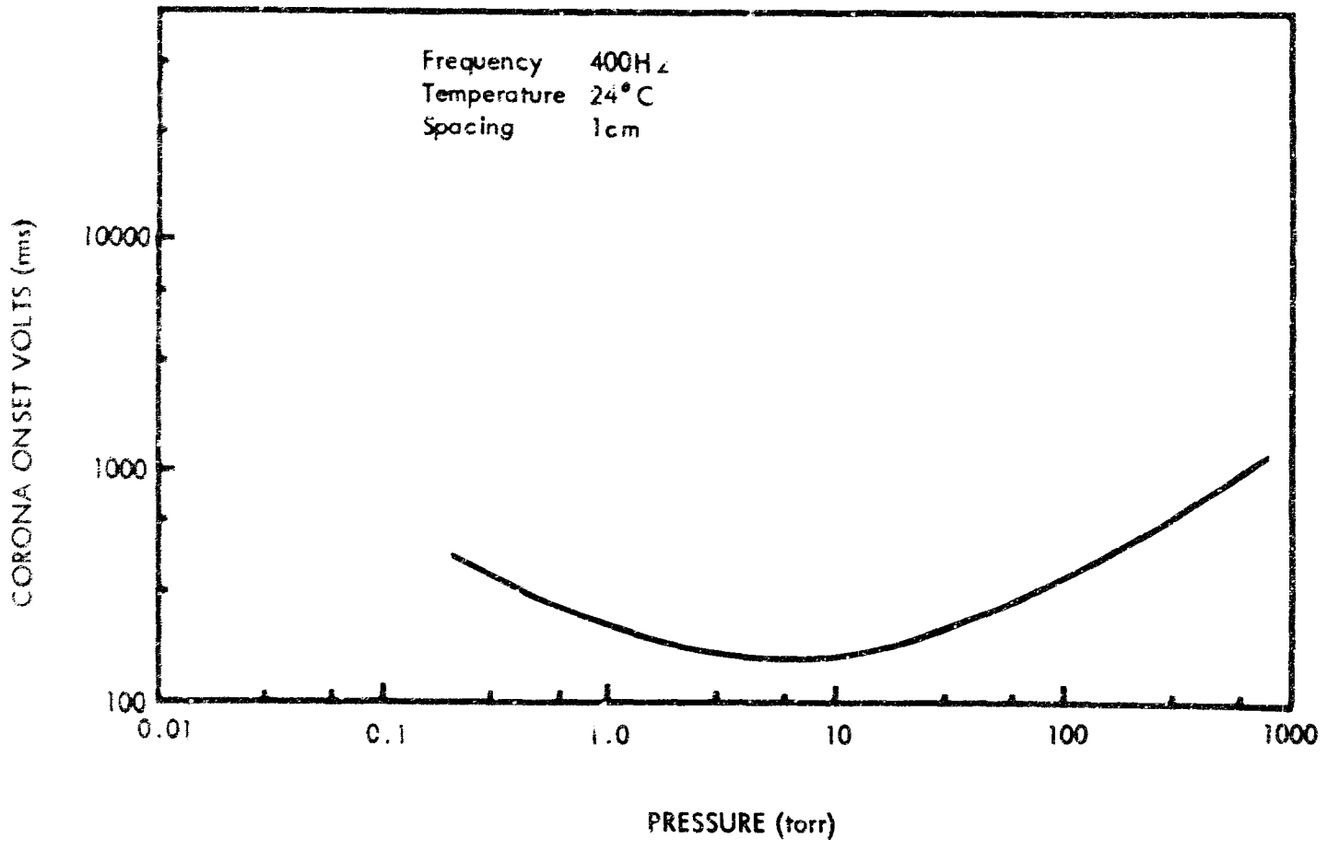

Figure I - 13: ROUND RODS IN HELIUM

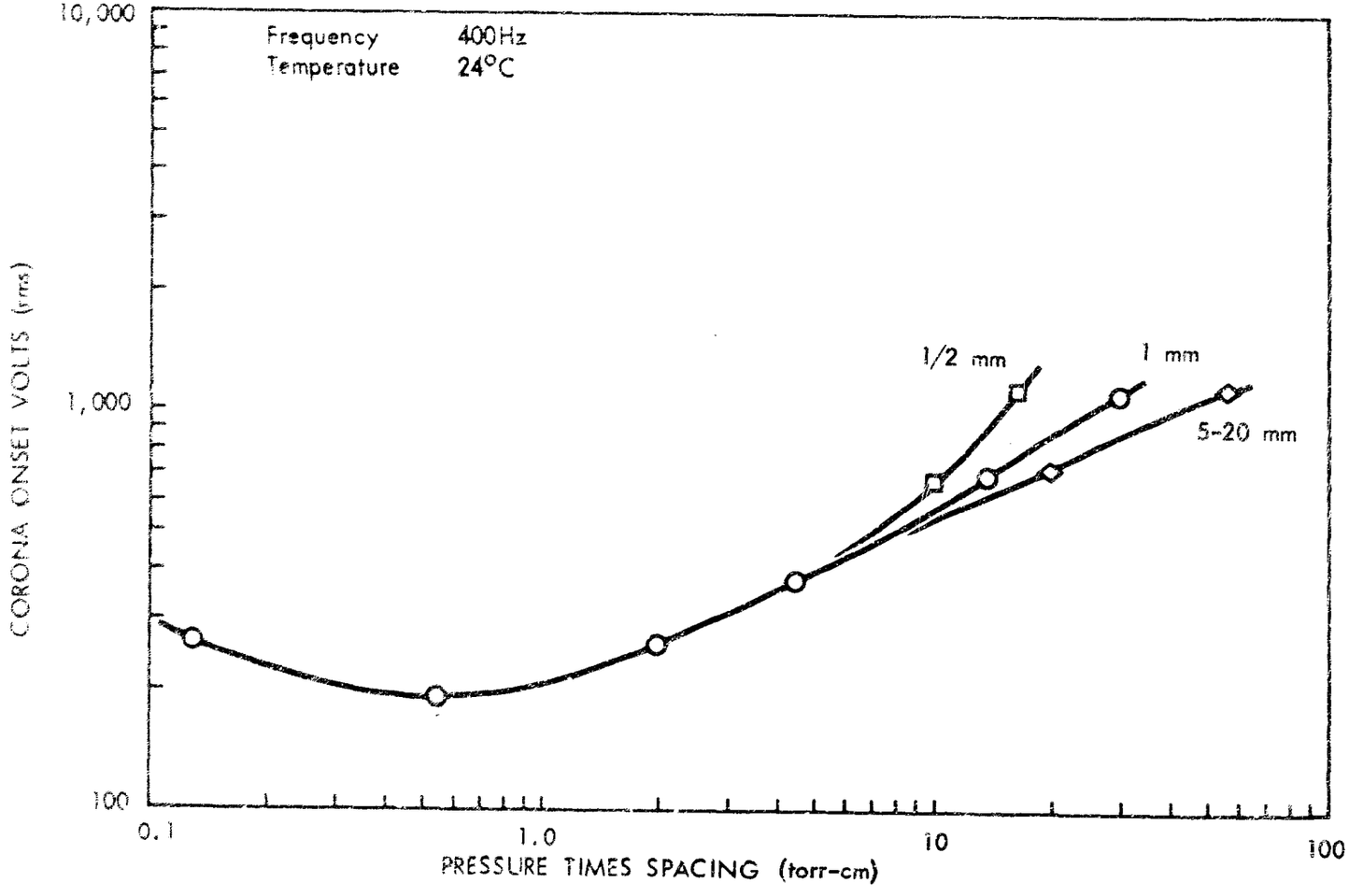

Figure 1-14: POINTED ELECTRODES IN NITROGEN

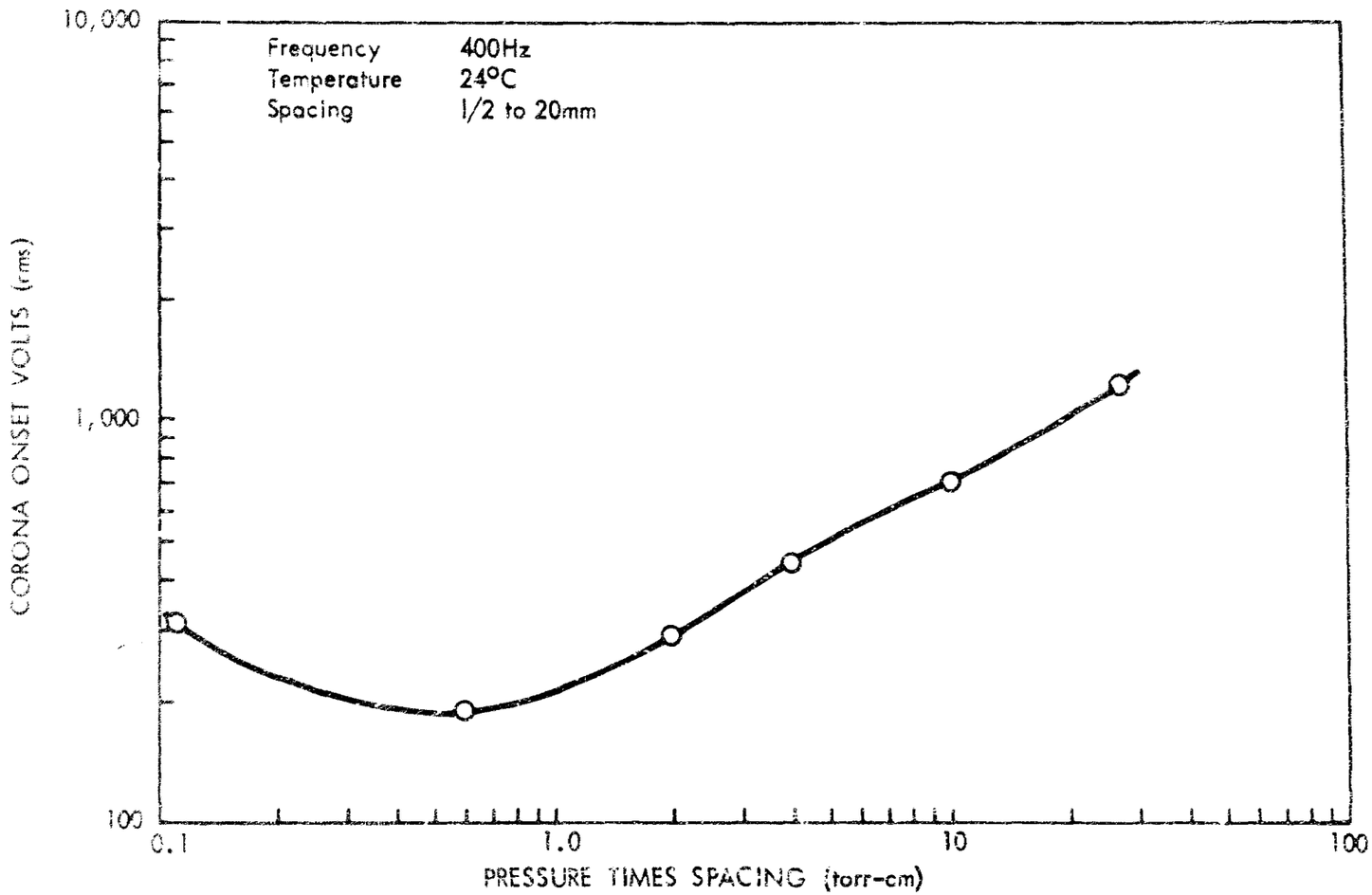

Figure I-15: ROUND RODS IN NITROGEN

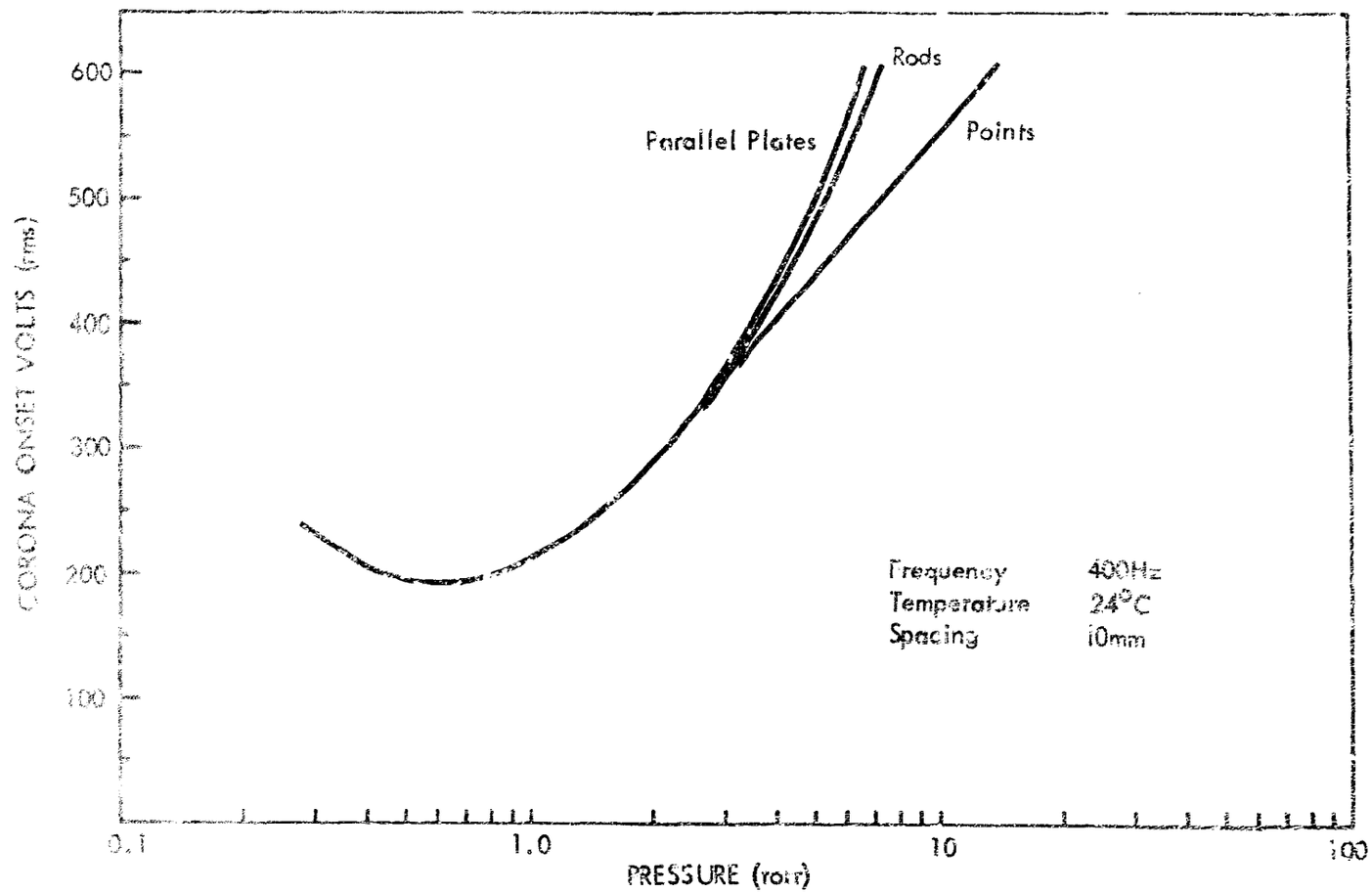

Figure 1-15: PARALLEL PLATES, POINTS, AND RODS IN NITROGEN

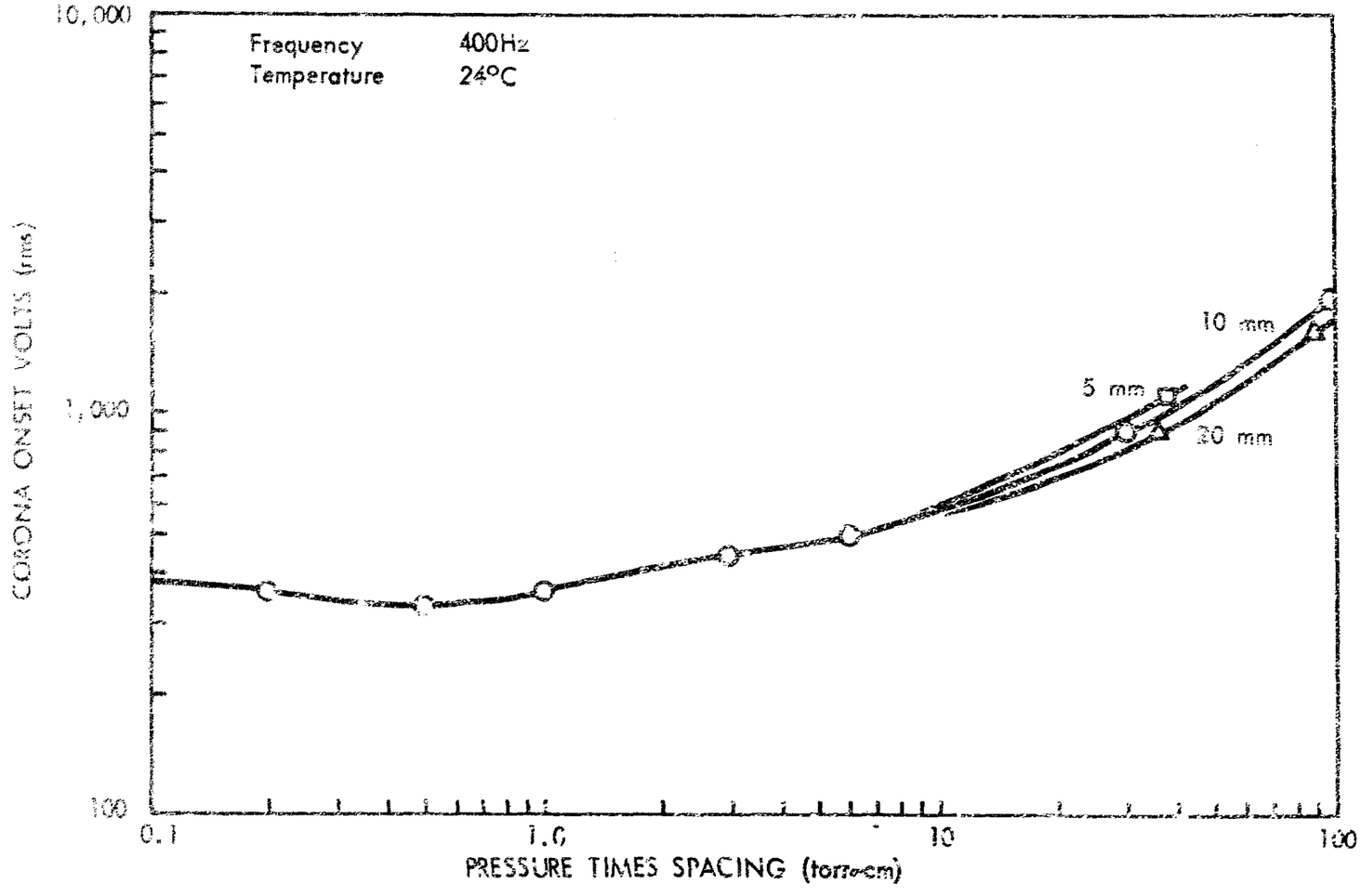

Figure 1-17: POINTED ELECTRODES IN OXYGEN

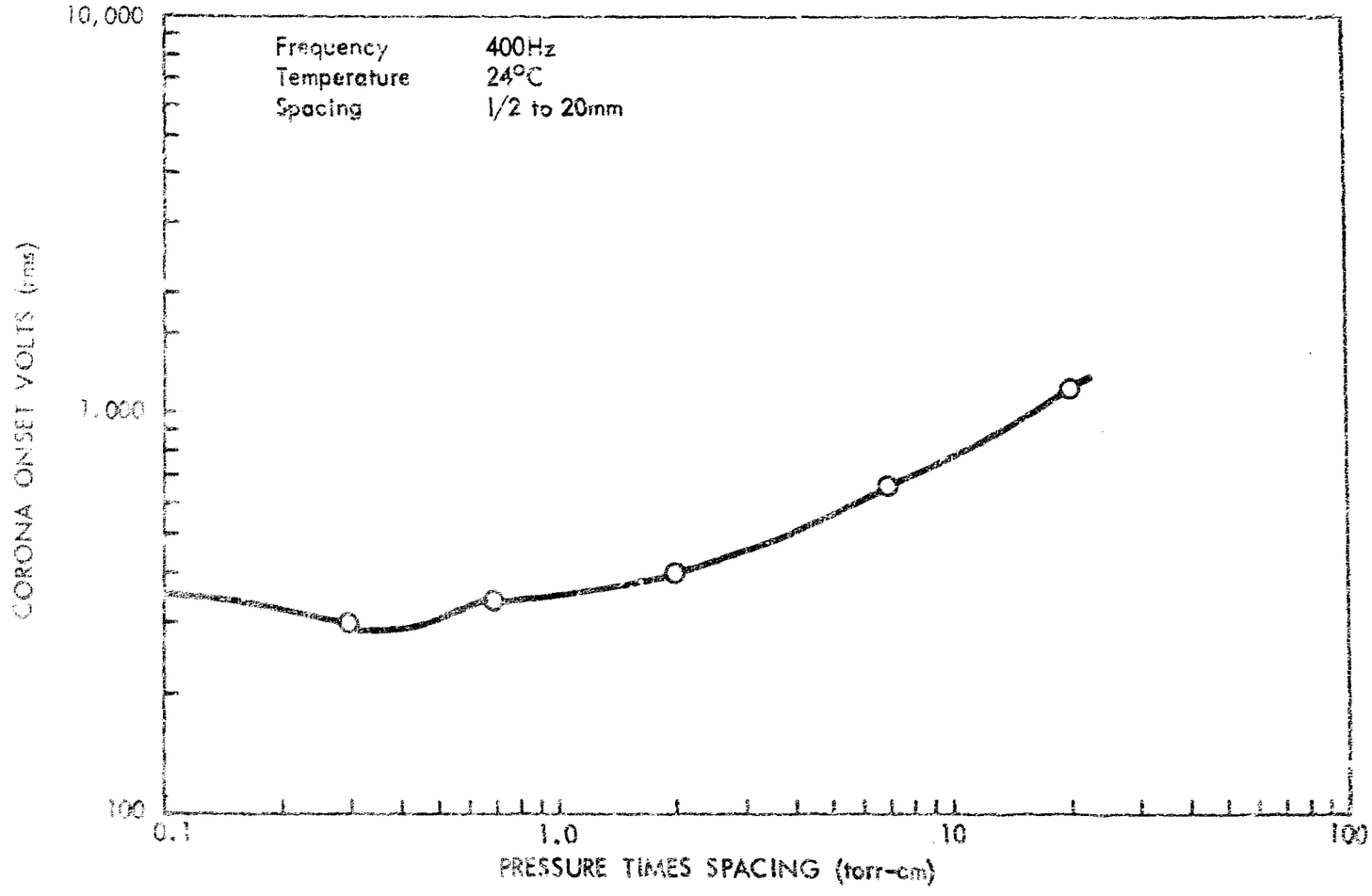

Figure I-18: ROUND RODS IN OXYGEN

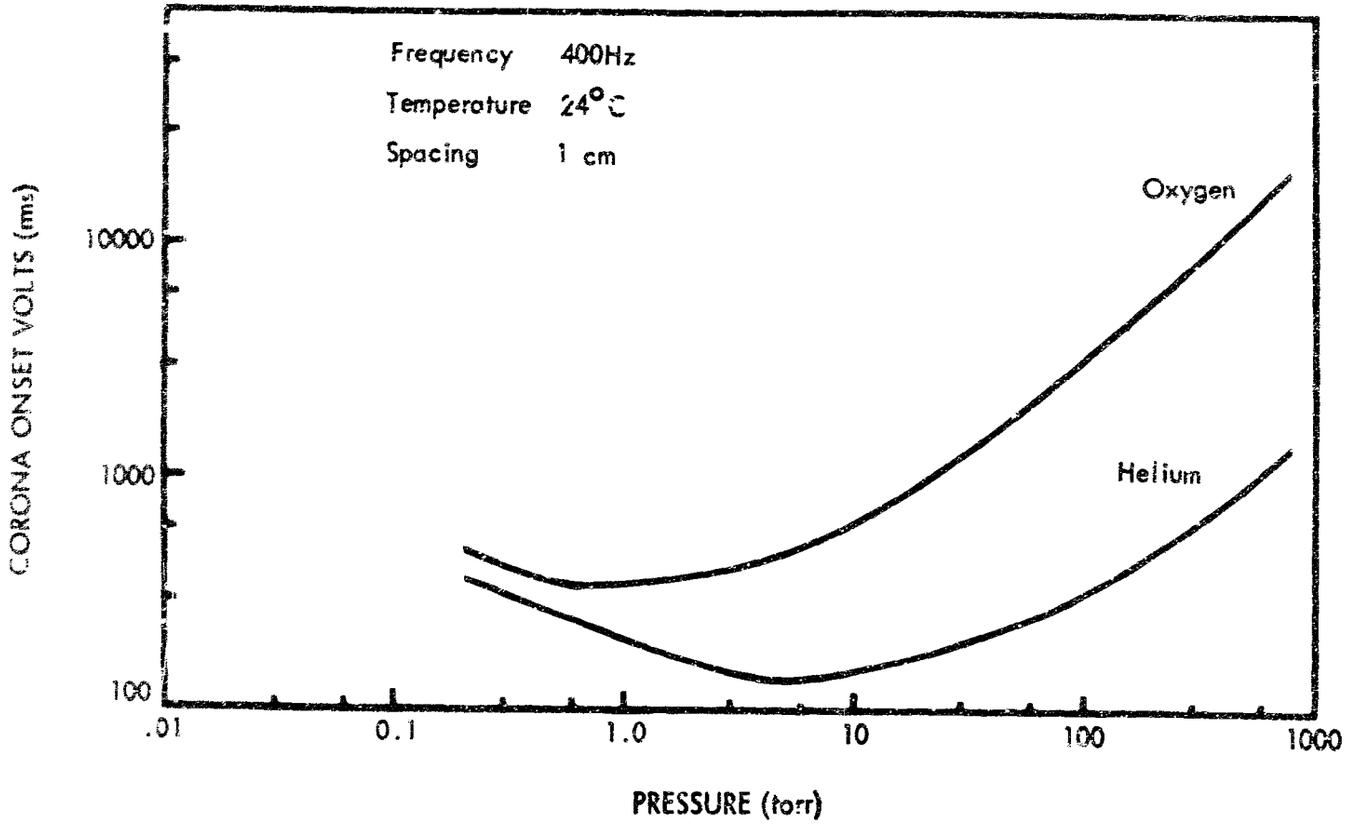

Figure I - 19: PARALLEL PLATES IN PURE HELIUM AND IN PURE OXYGEN

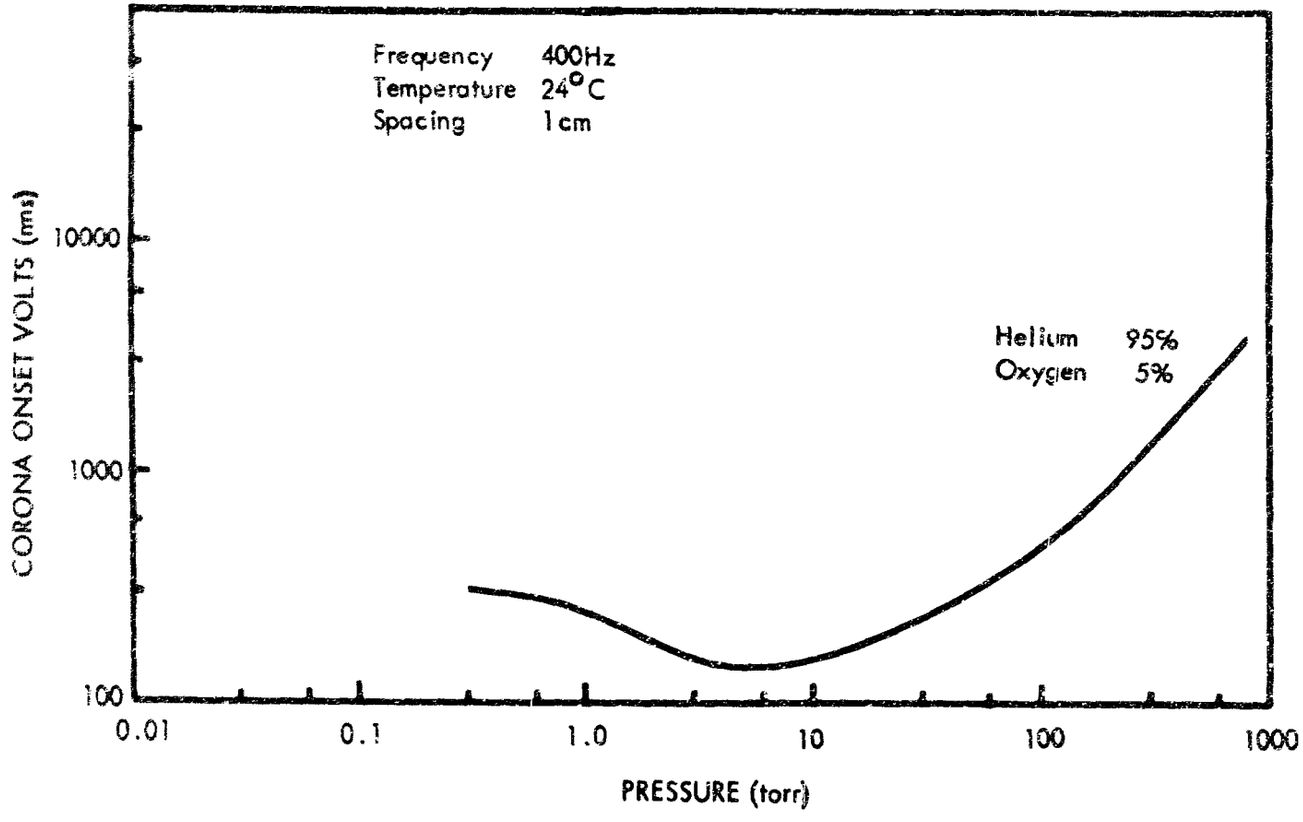

Figure I - 20: PARALLEL PLATES IN 95% HELIUM - 5% OXYGEN MIXTURE

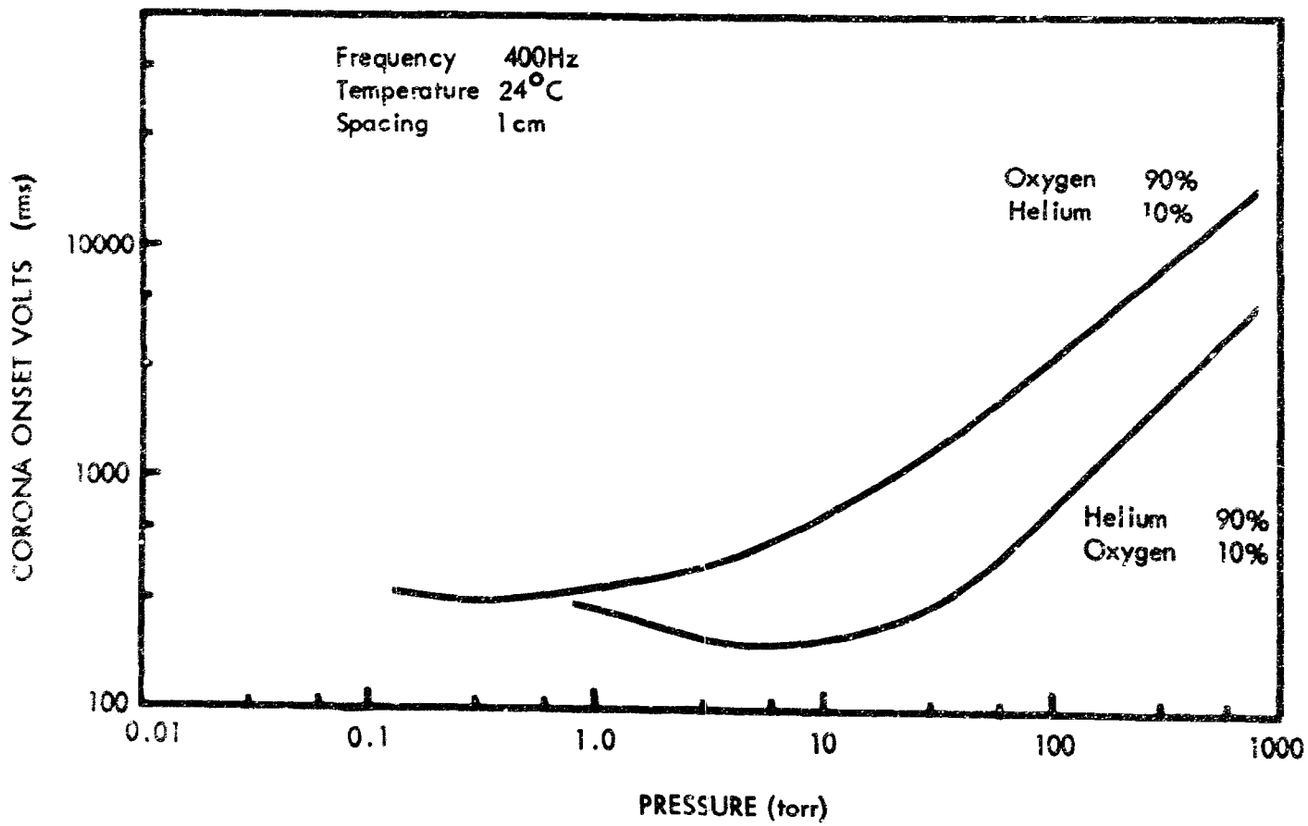

Figure I - 21: PARALLEL PLATES IN HELIUM - OXYGEN MIXTURES, 90-10 PERCENTS

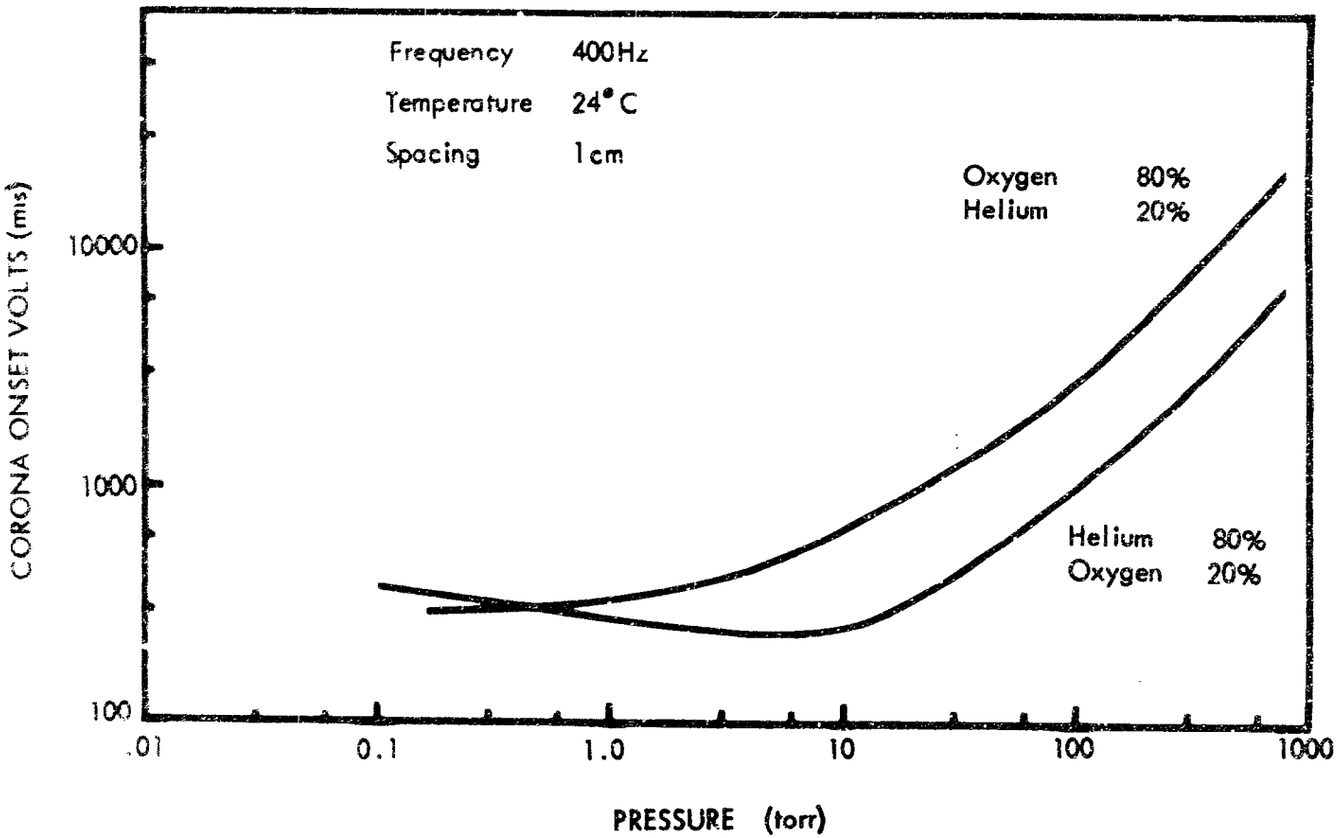

Figure I - 22: PARALLEL PLATES IN HELIUM - OXYGEN MIXTURES, 80-20 PERCENTS

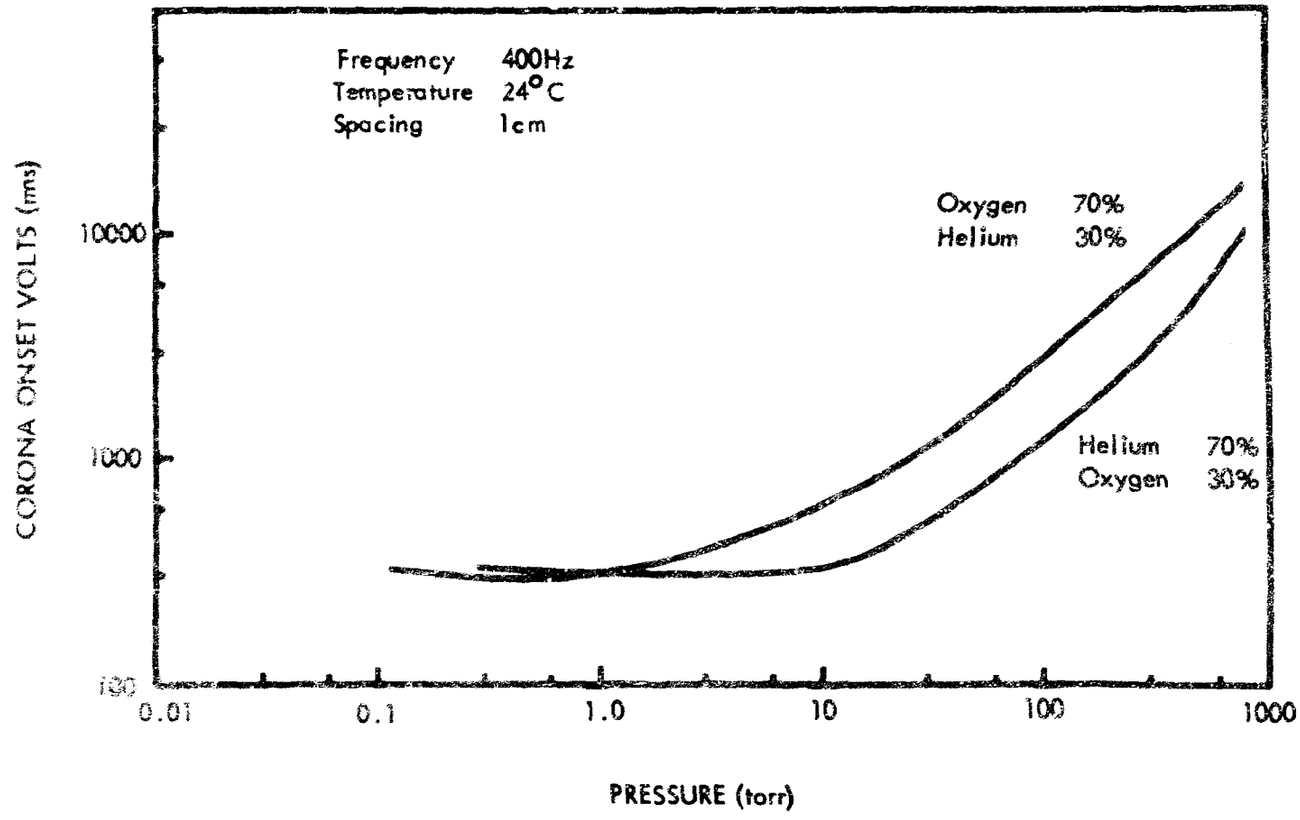

Figure I - 23. PARALLEL PLATES IN HELIUM - OXYGEN MIXTURES, 70-30 PERCENTS

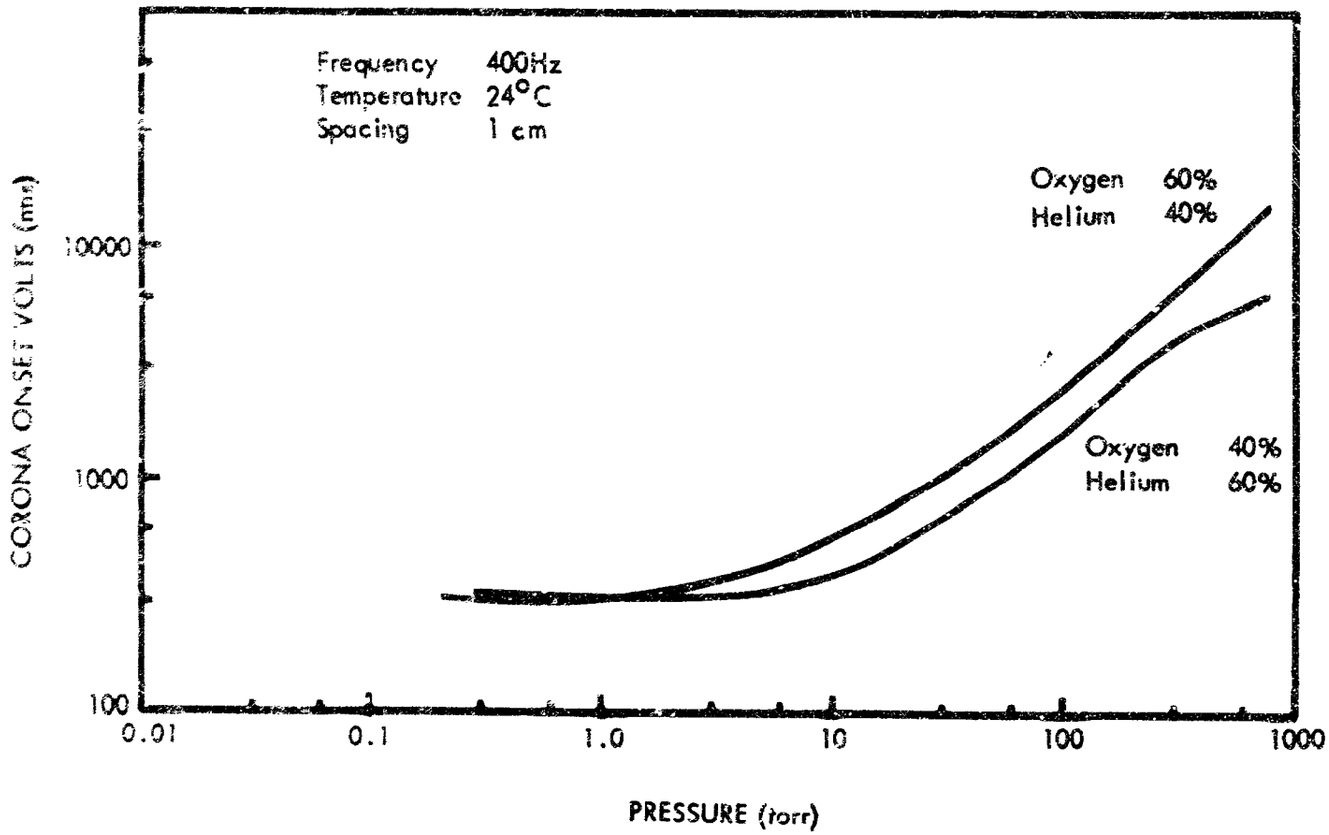

Figure I - 24: PARALLEL PLATES IN HELIUM - OXYGEN MIXTURES, 60-40 PERCENTS

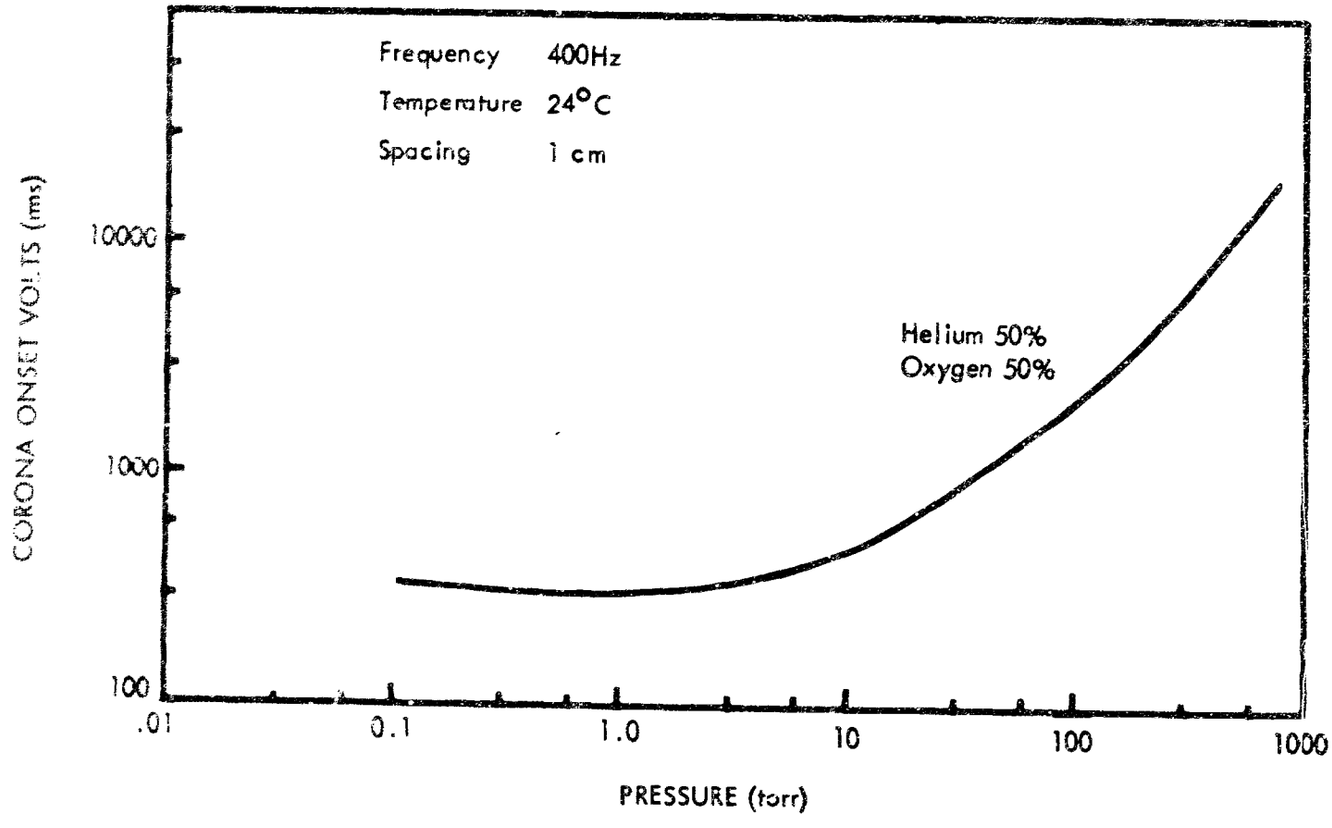

Figure I - 25: PARALLEL PLATES IN HELIUM - OXYGEN MIXTURES, 50-50 PERCENTS

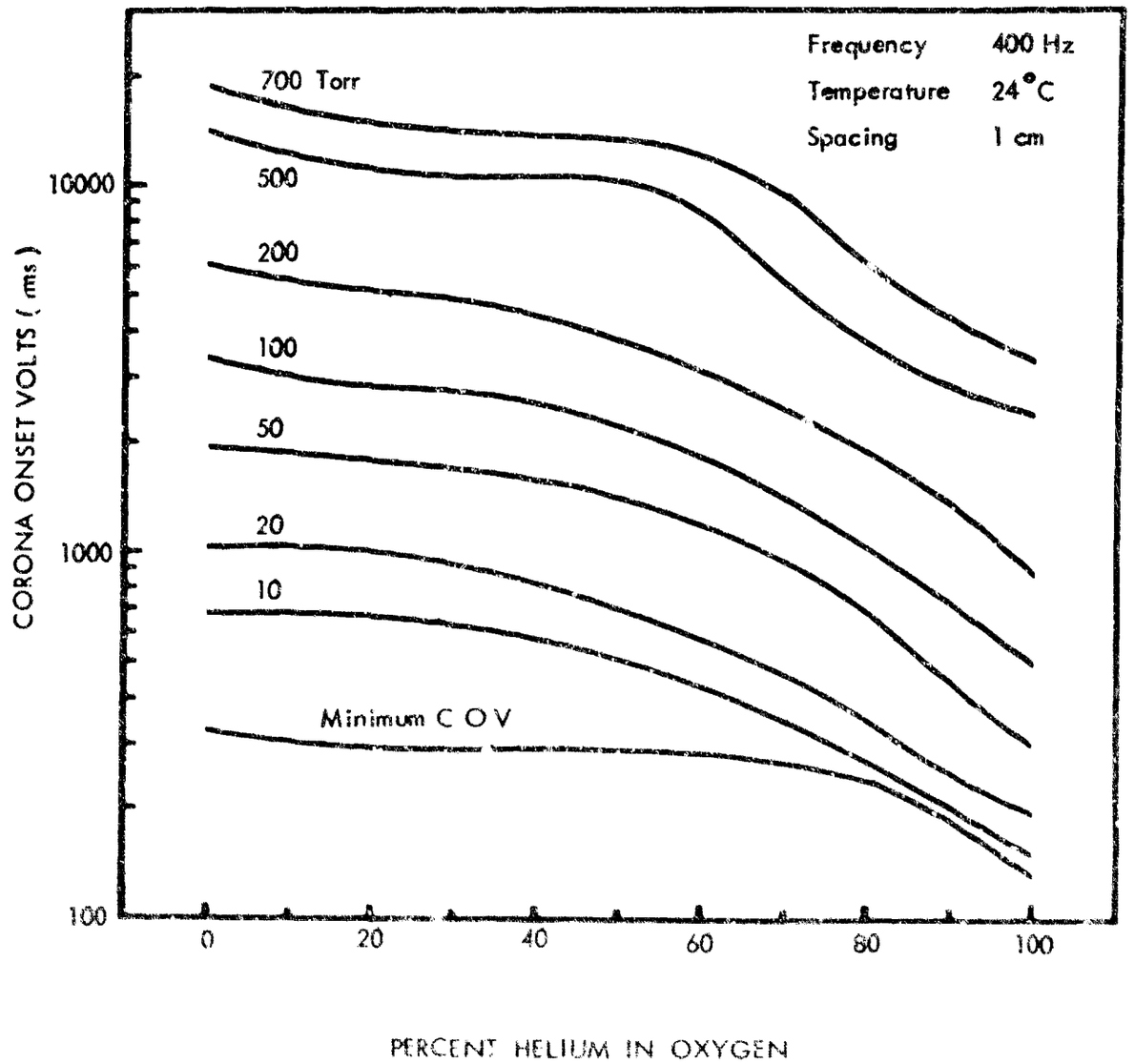

Figure 1 - 26: PARALLEL PLATES IN HELIUM - OXYGEN MIXTURES

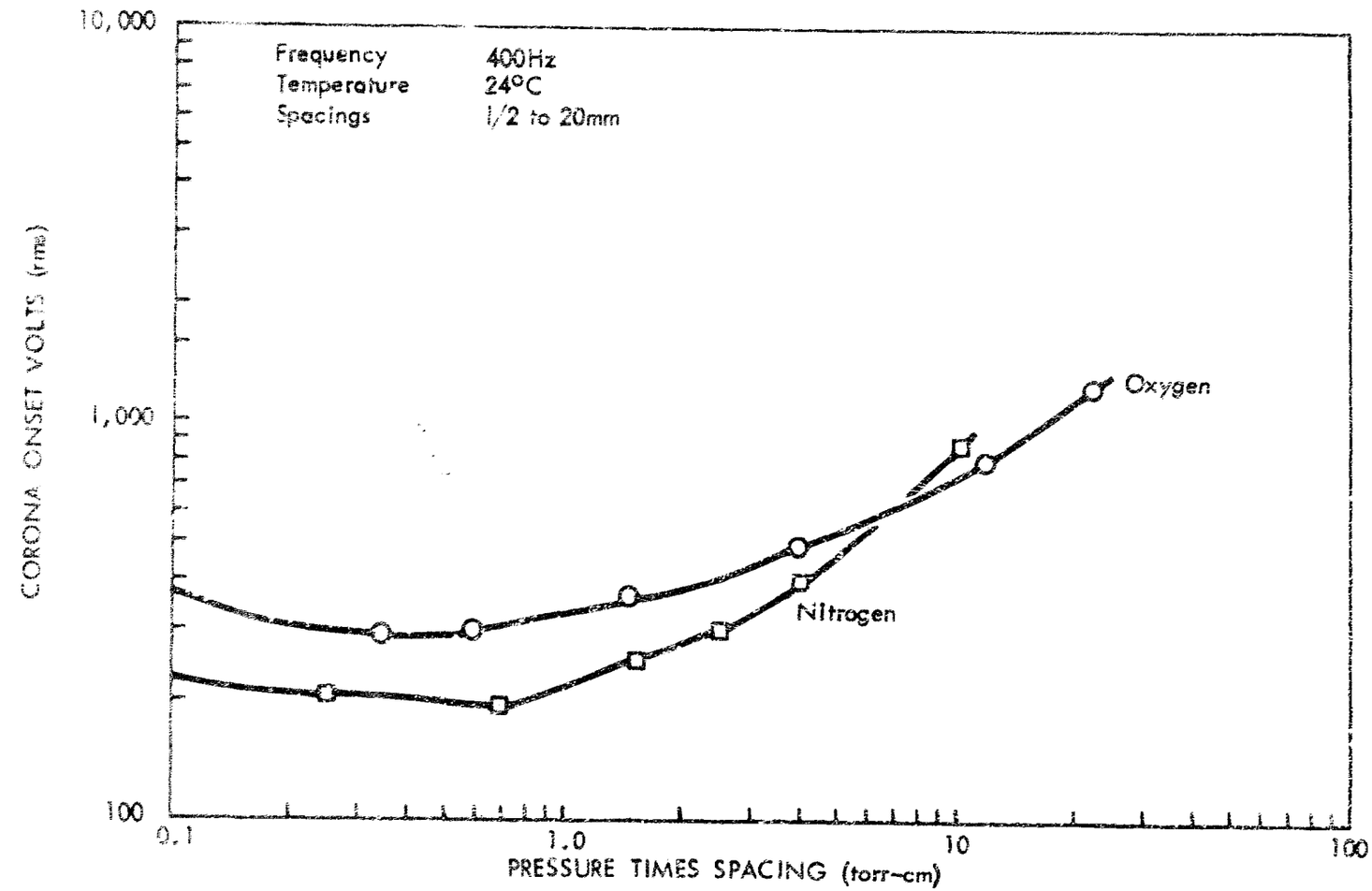

Figure I-27: PARALLEL PLATES IN NITROGEN AND OXYGEN

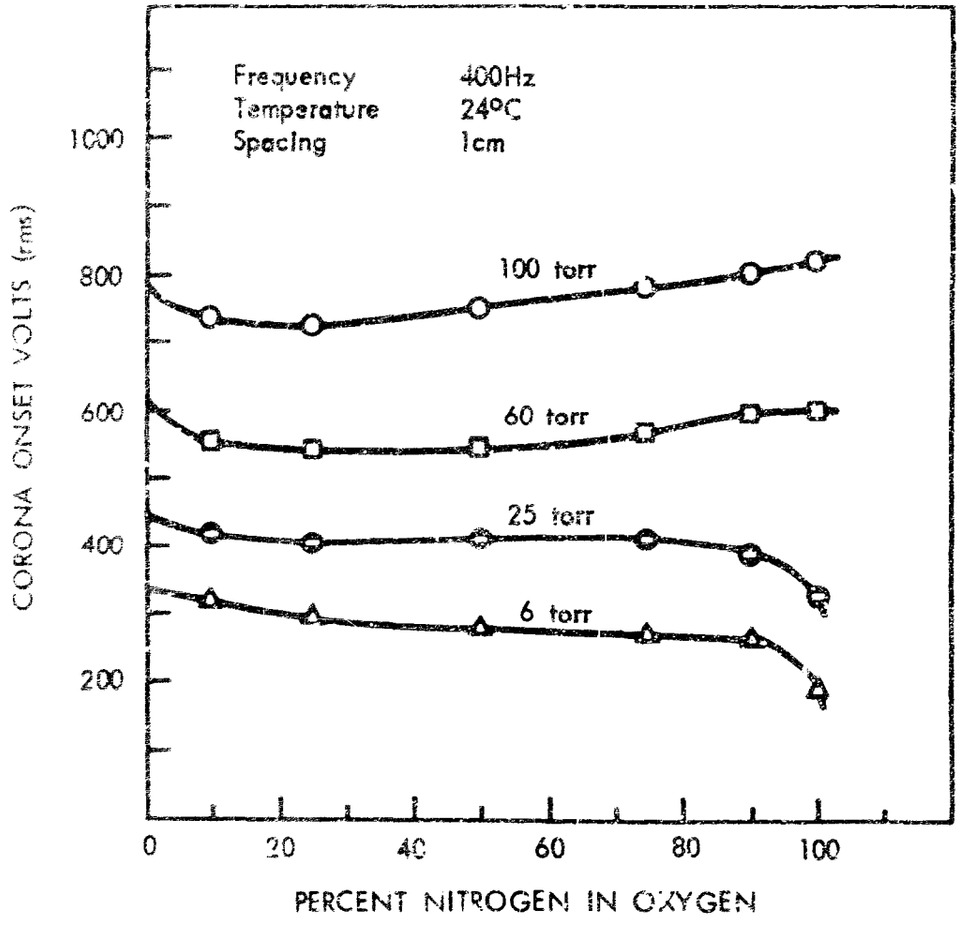

Figure 1-28: ROUND RODS IN NITROGEN-OXYGEN MIXTURES

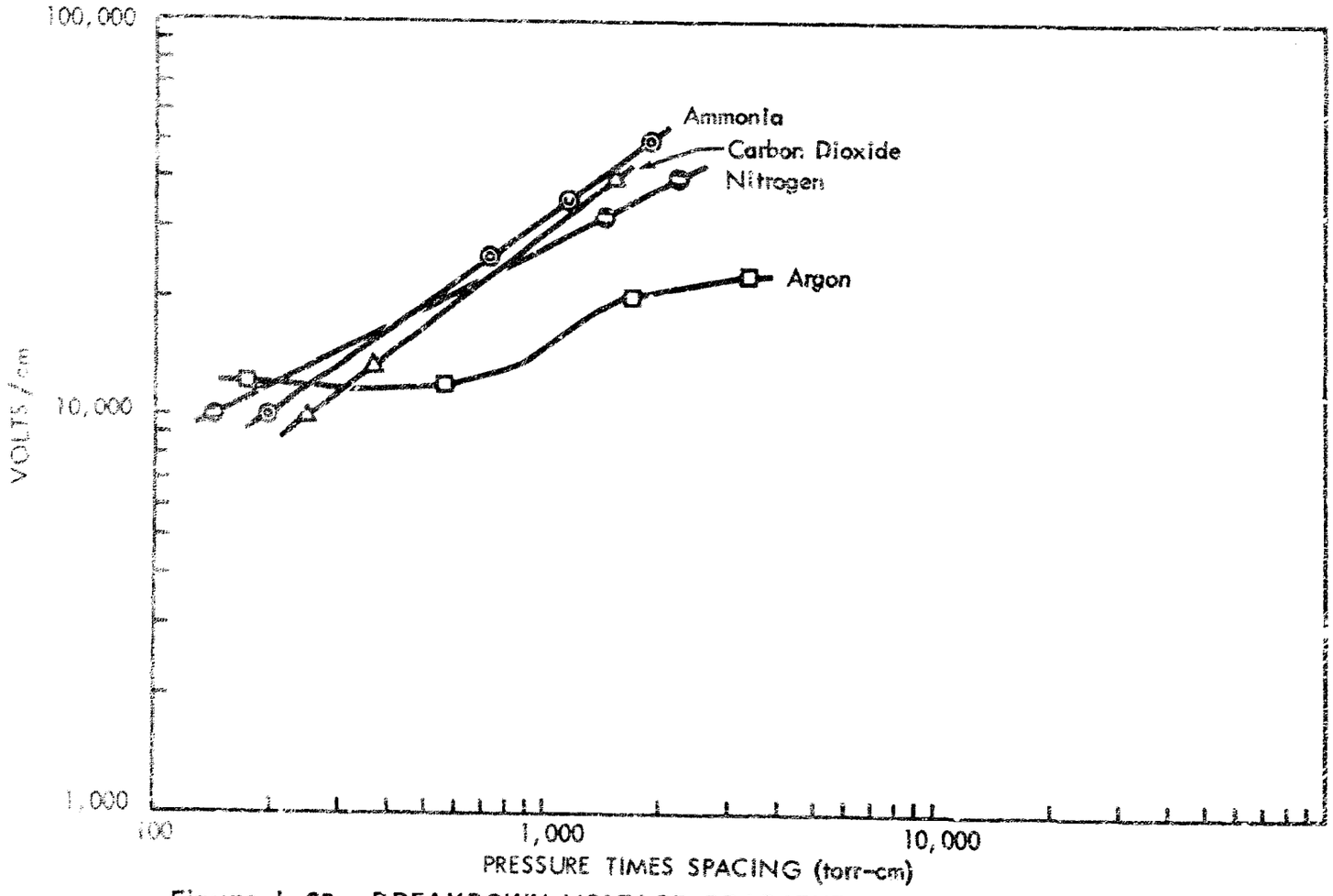

Figure I-29: BREAKDOWN VOLTAGE GRADIENT BETWEEN PARALLEL PLATES IN GASES AT 24°C AND 9600 mc

Appendix II

HIGH-TEMPERATURE AND CONTAMINATION TESTS

Two sets of related test data are shown in this appendix:

1) The corona onset voltage between parallel wires in a high-temperature oven;

2) The corona onset voltage between parallel wires in a high-temperature molybdenum-contaminated oven.

The high-temperature corona onset voltage was measured with parallel, spaced round, bare nichrome wires; teflon-insulated wires; and ceramic-insulated wires in air. The "wire spacing" was the minimum distance between the wires. These data are shown in Figures II-1 through II-7.

The test data from the molybdenum-trioxide contaminated oven are plotted with COV as a function of temperature and pressure and with the change in insulation impedance as a function of temperature and pressure. The insulation was a high-temperature asbestos-insulated braided sheath which formed a coaxial cable. When tested at temperatures below 400°C, the impedance was approximately the capacitive reactance of the insulation; however, the insulation resistance dropped rapidly as oven temperature was further increased. At 500°C a new effect became prominent — the subliming molybdenum-trioxide, which penetrated the insulation and lowered its resistance to nearly zero. These data are shown in Figures II-9 through II-13.

The oven-temperature time profile for a two-cycle test is shown in Figure II-8. The oven was allowed to cool for four hours between cycles to allow time for measurement of the resistance of the cold cable insulation. Molybdenum-trioxide at temperatures below 400°C is crystalline and its resistance was so high that its conductivity could not be detected by ohmic measurements.

LIST OF FIGURES — APPENDIX II

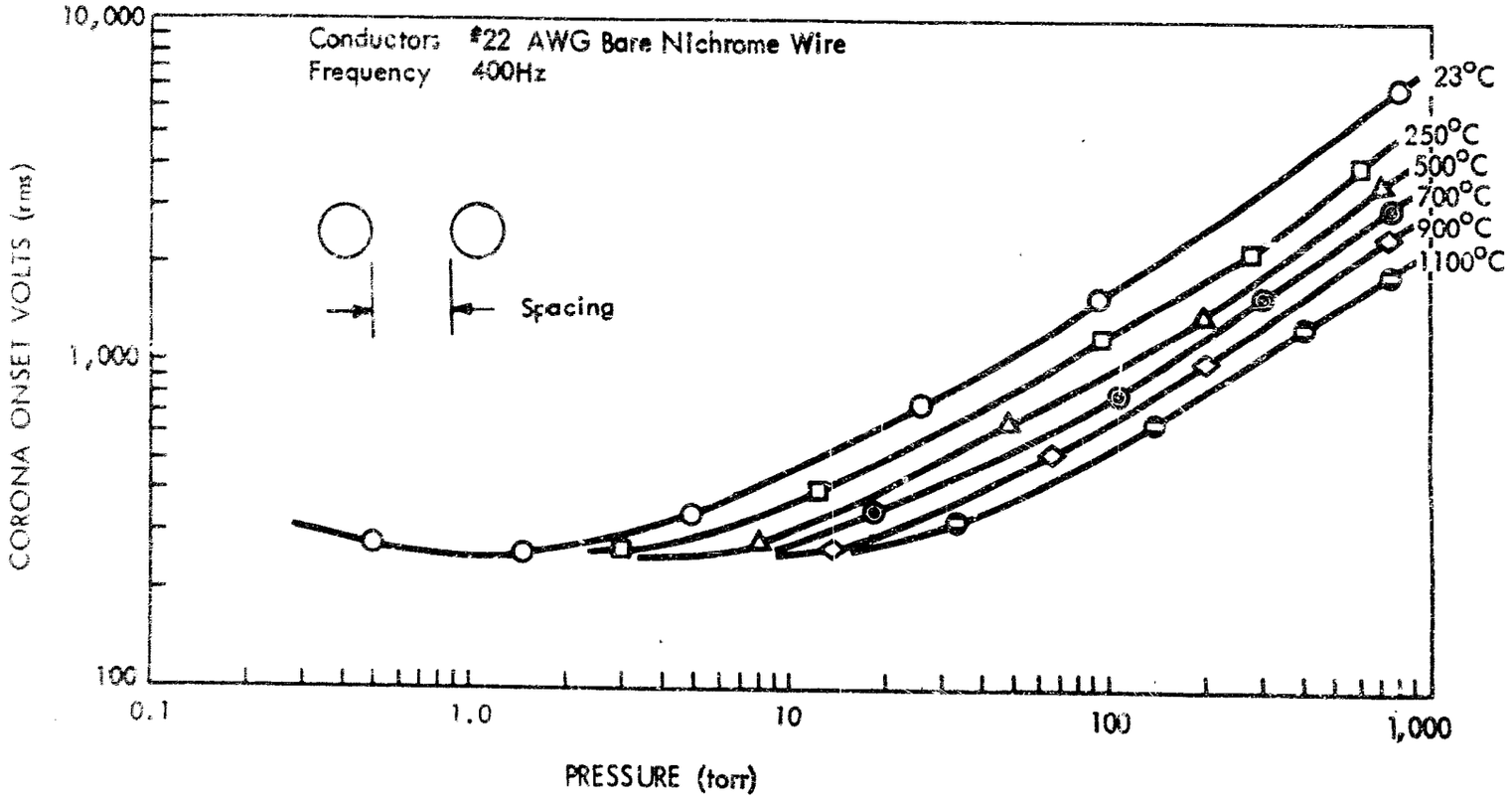

Figure II-1: NICHROME WIRES SPACED 3.2 mm IN AIR UP TO 1100°C

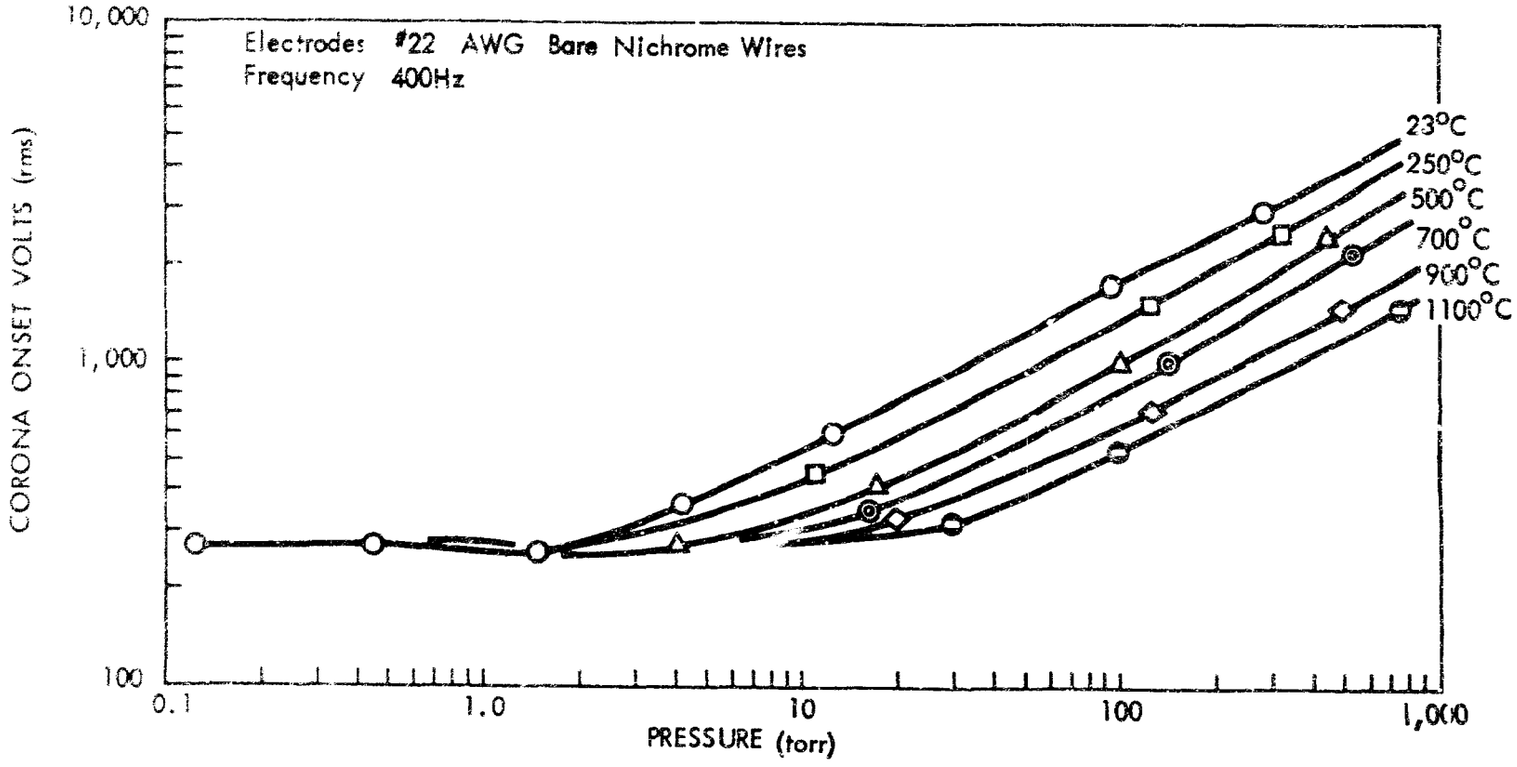

Figure II-2: NICHROME WIRES SPACED 6.4 mm IN AIR UP TO 1100°C

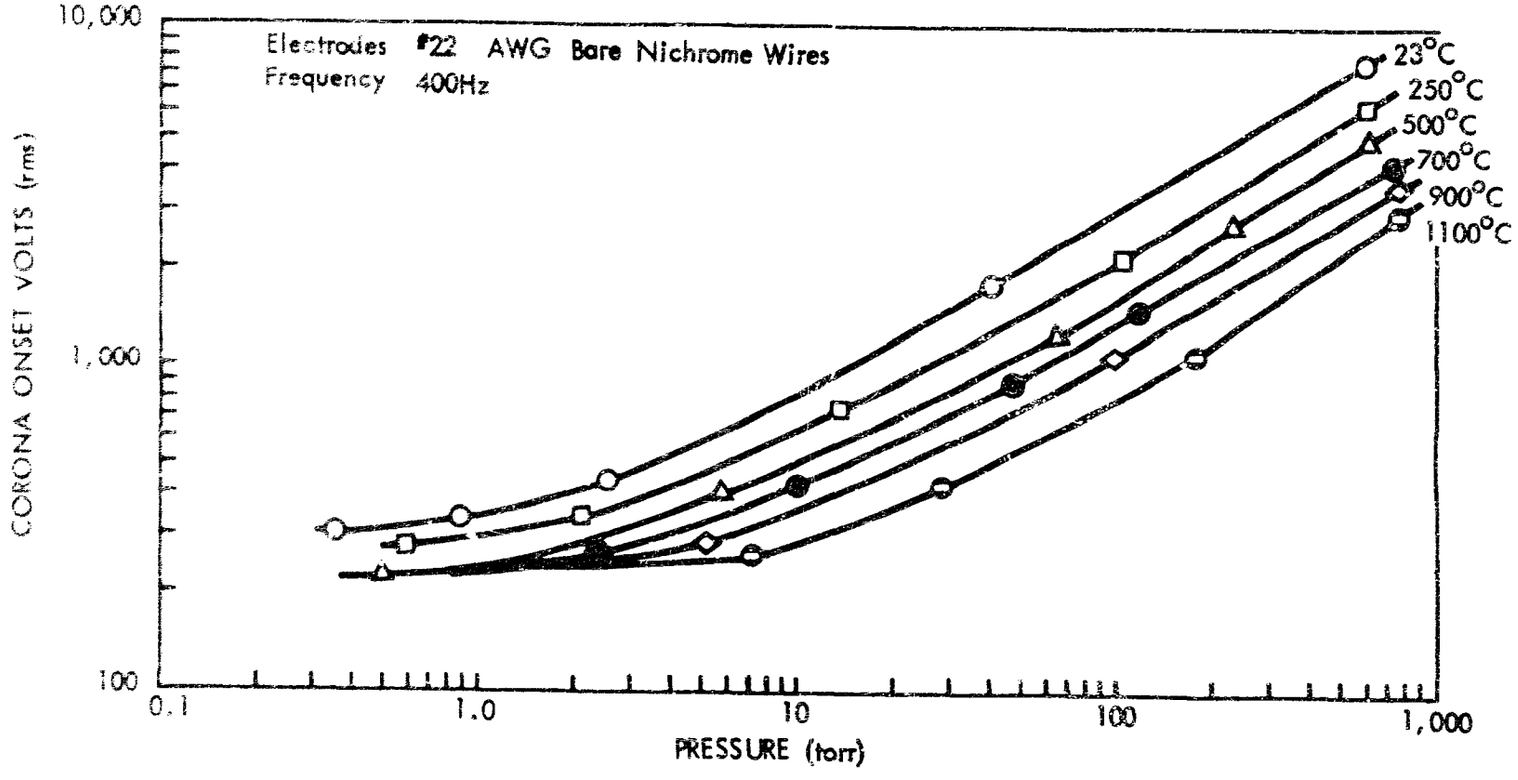

Figure II-3: NICHROME WIRES SPACED 25 mm IN AIR UP TO 1100°C

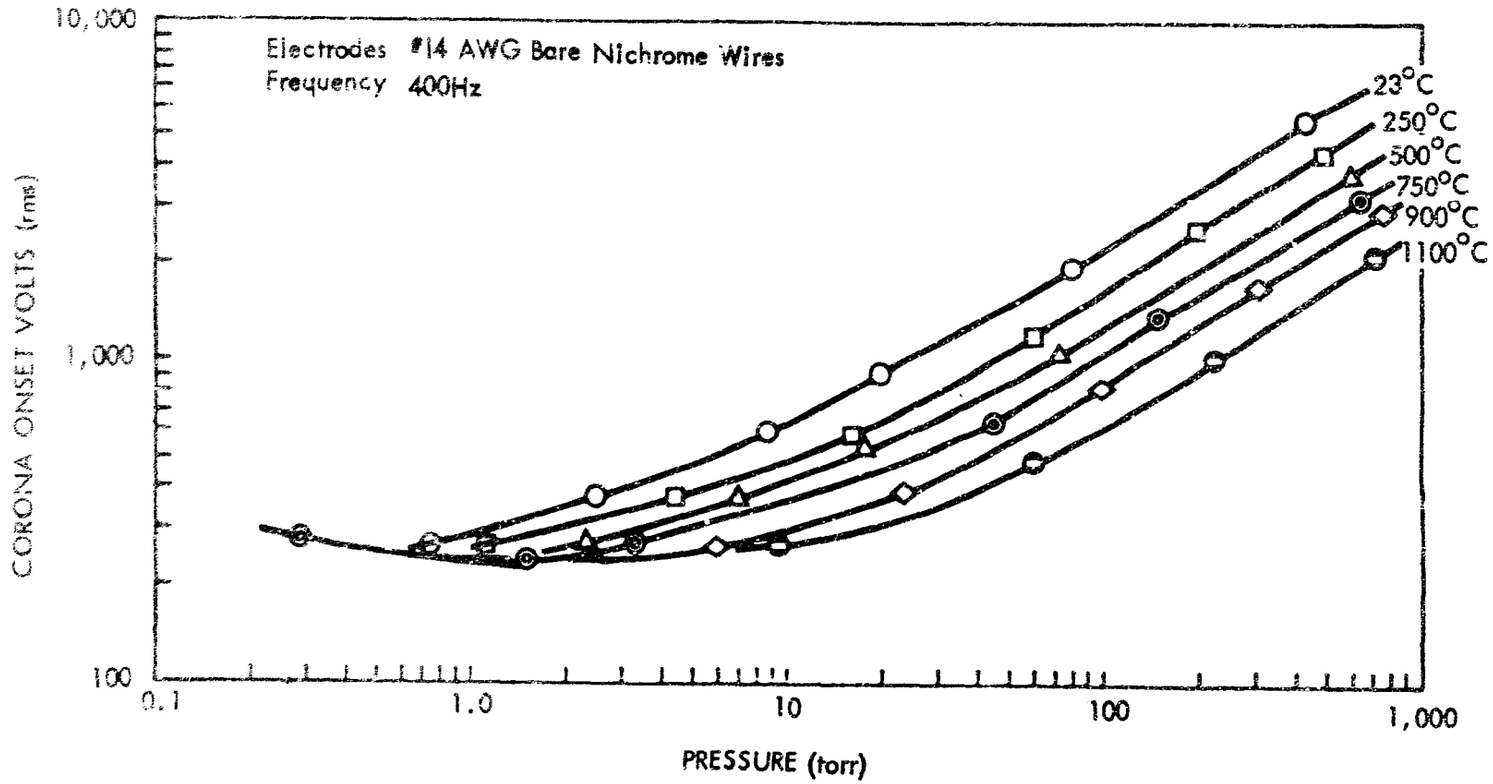

Figure 11-4: NICHROME WIRES SPACED 6.4 mm IN AIR UP TO 1100°C

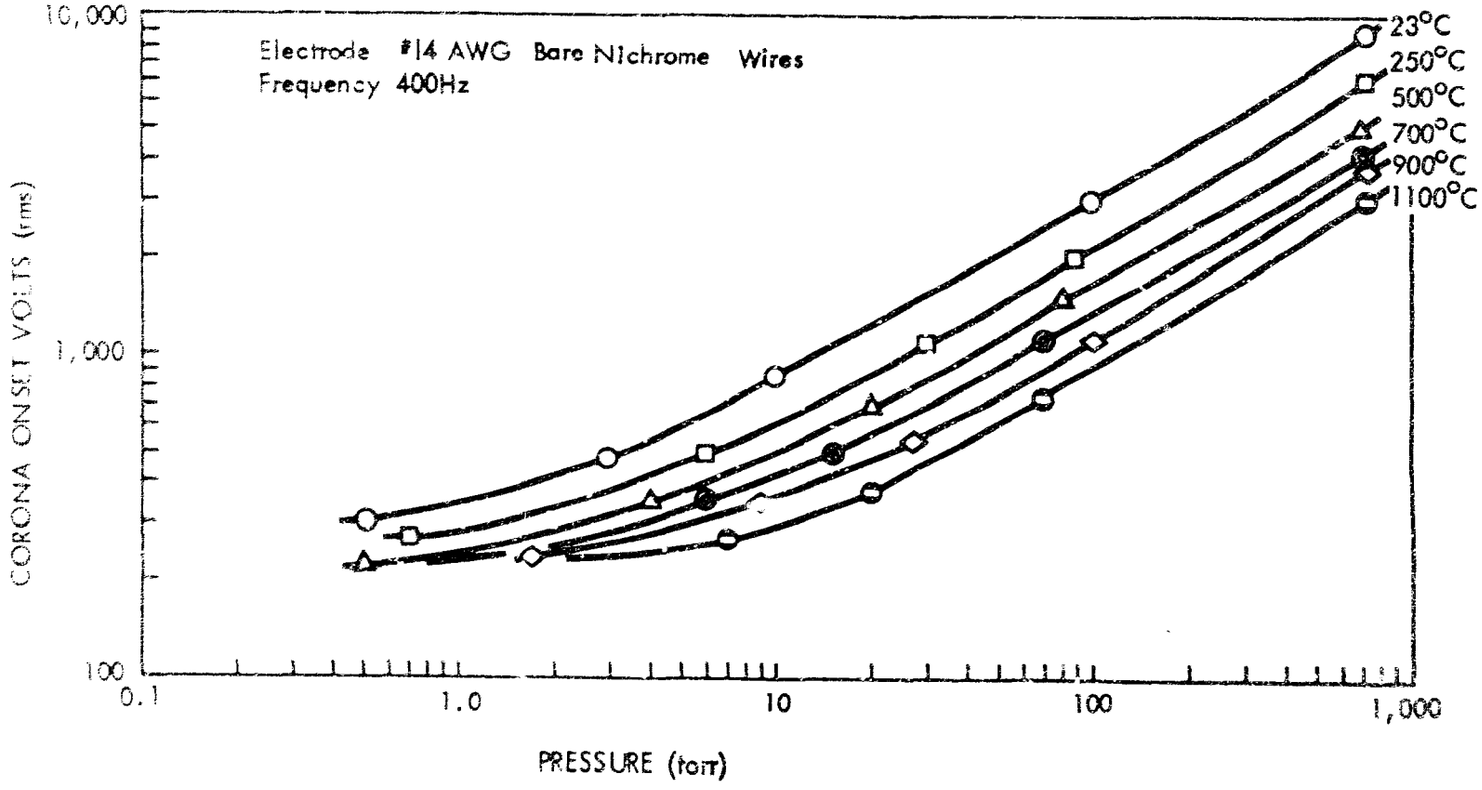

Figure II-5: NICHROME WIRES SPACED 25 mm IN AIR UP TO 1100°C

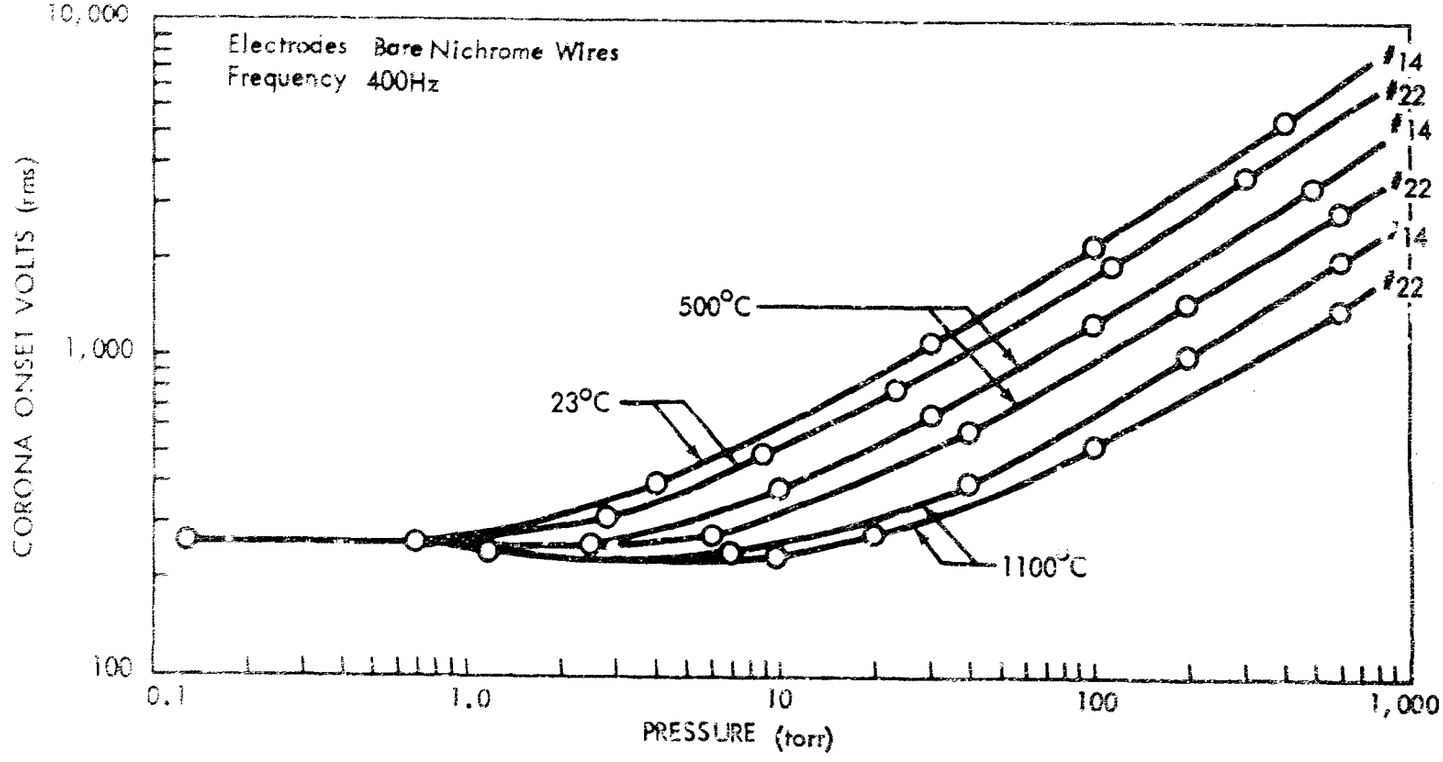

Figure 11-6: NICHROME WIRES SPACED 6.4 mm IN AIR UP TO 1100°C

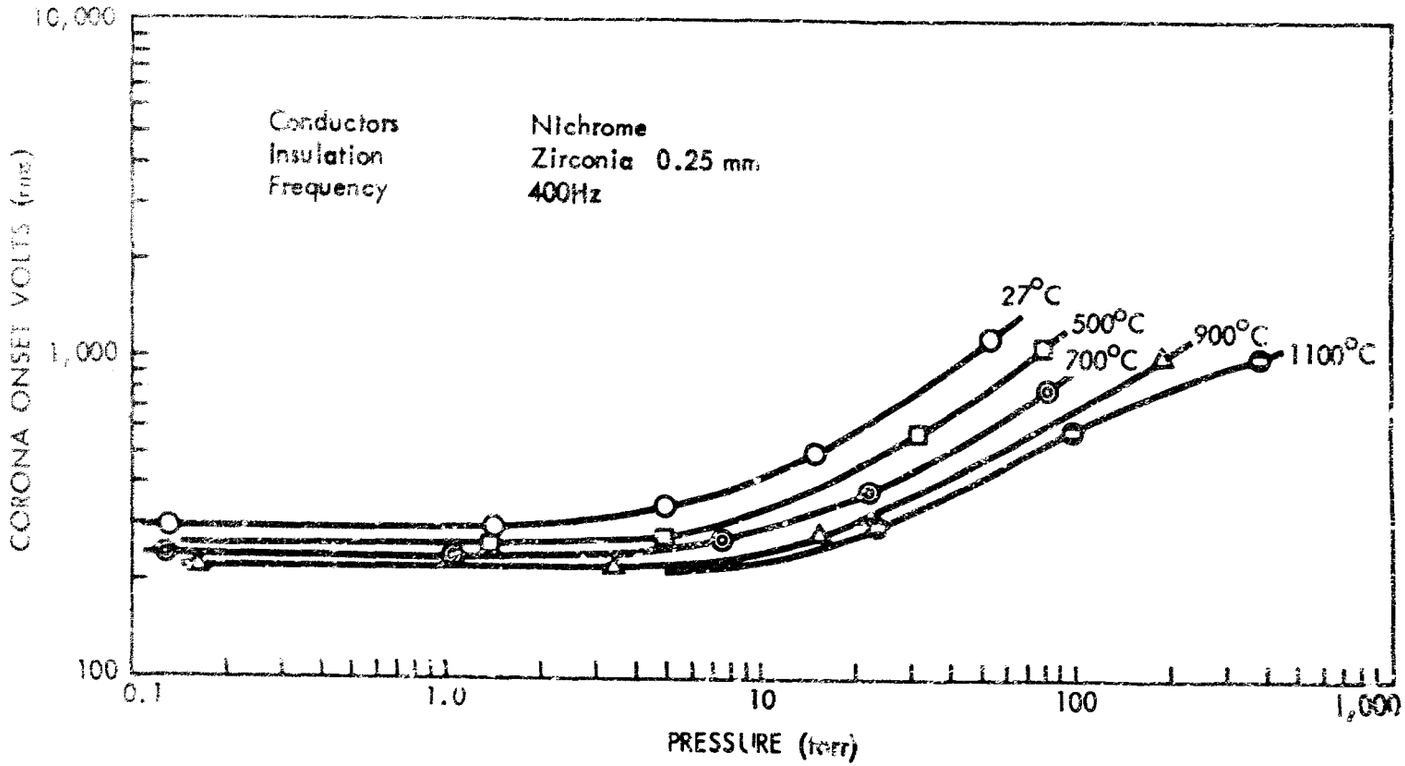

Figure II-7: ZIRCONIA INSULATED WIRES SPACED 6.4 mm IN AIR

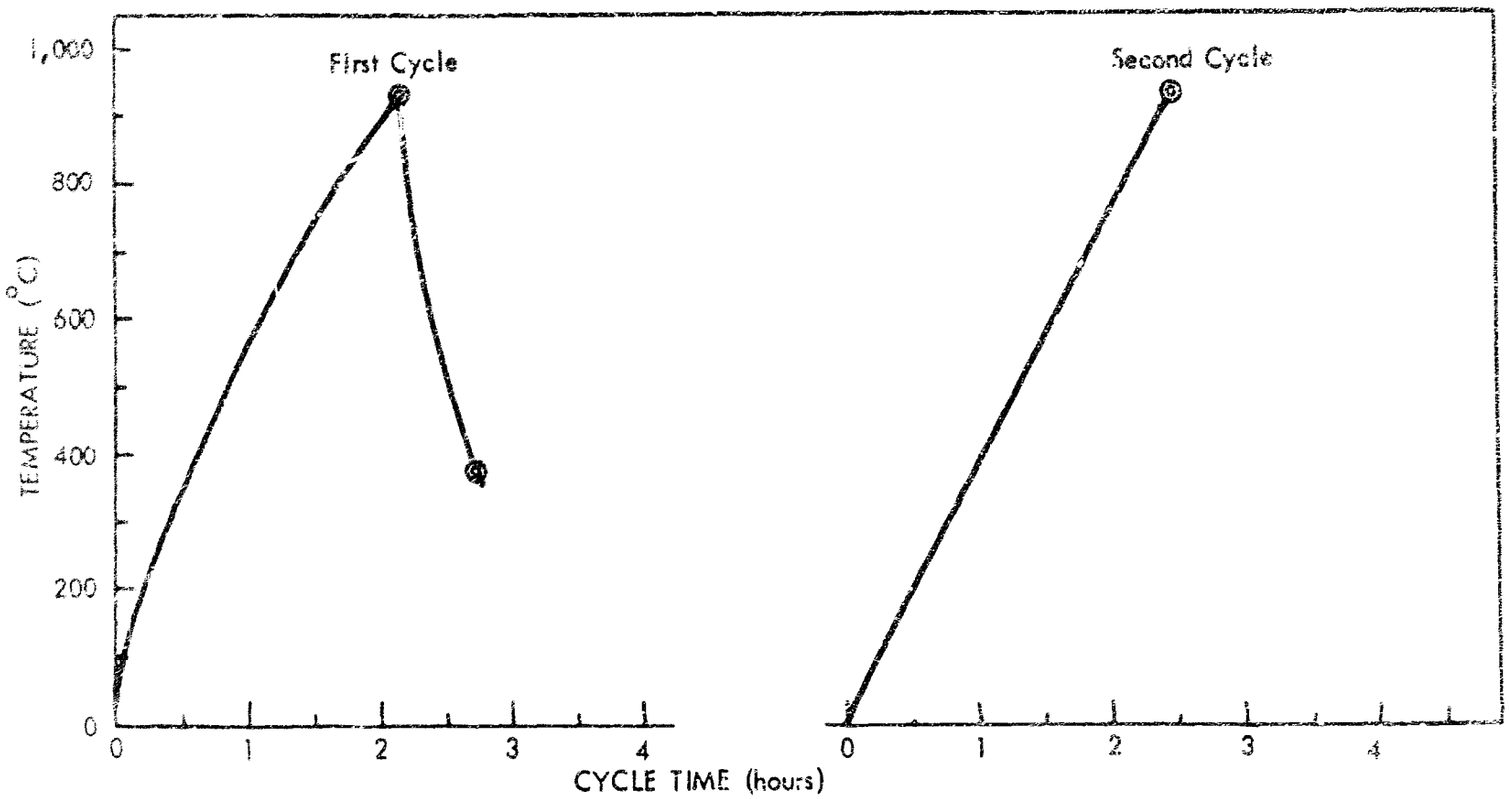

Figure 11-8: OVEN TEMPERATURE DURING MOLYBDENUM TRIOXIDE TESTS

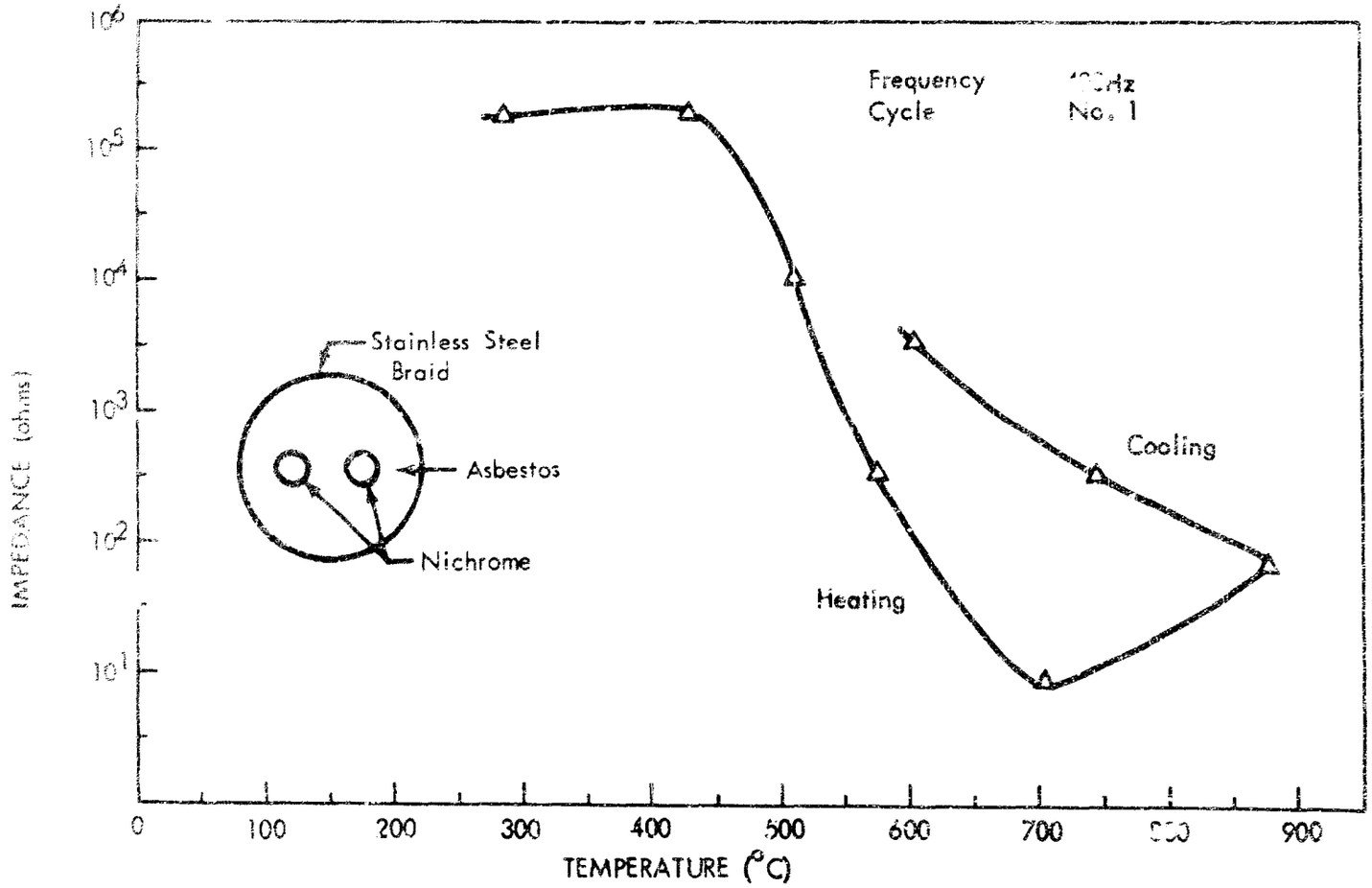

Figure 11-9: IMPEDANCE OF 2-CONDUCTOR SHIELDED CABLE IN MOLYBDENUM TRIOXIDE VAPOR

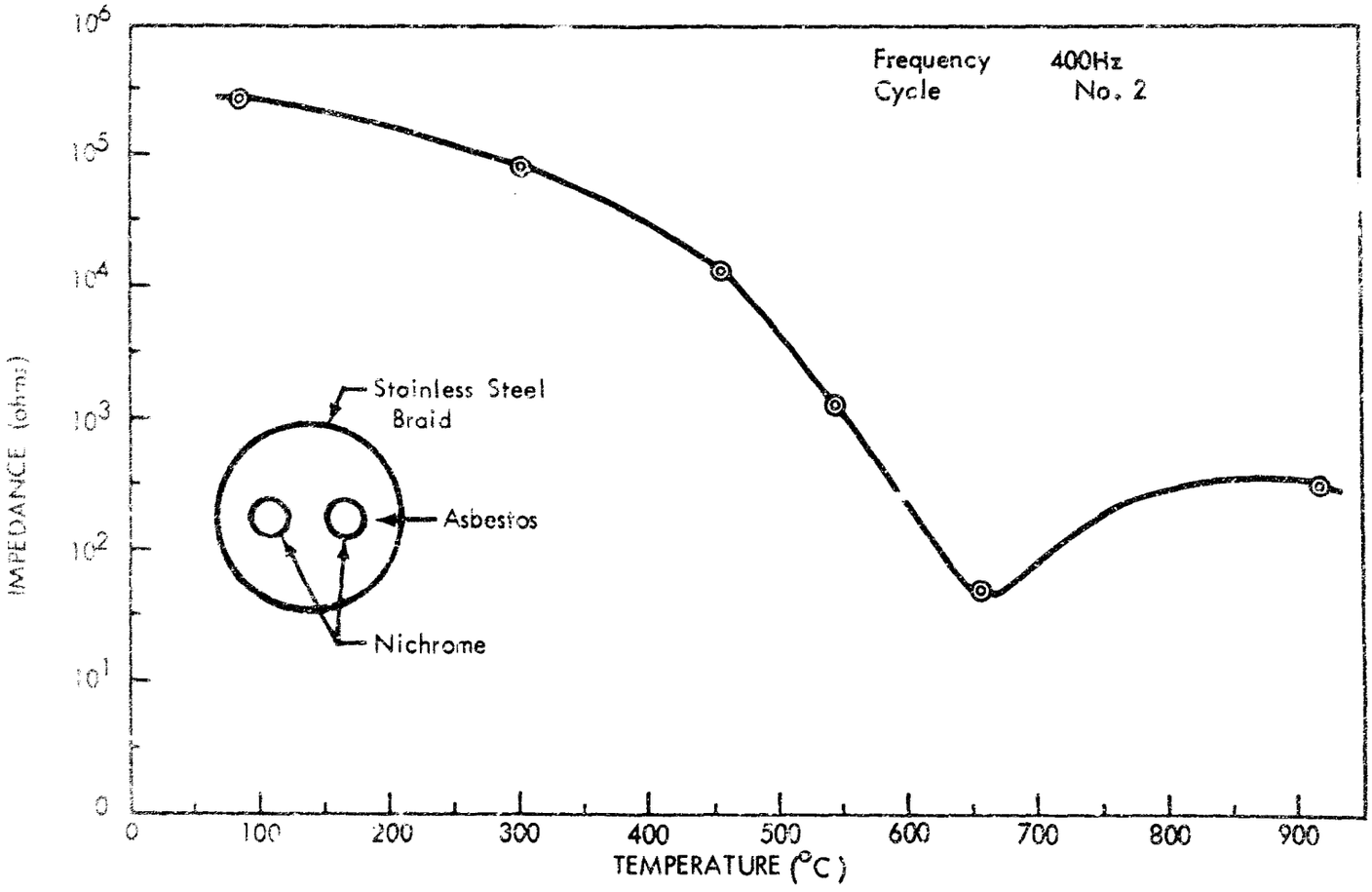

Figure 11-10: IMPEDANCE OF 2-CONDUCTOR SHIELDED CABLE IN MOLYBDENUM TRIOXIDE VAPOR

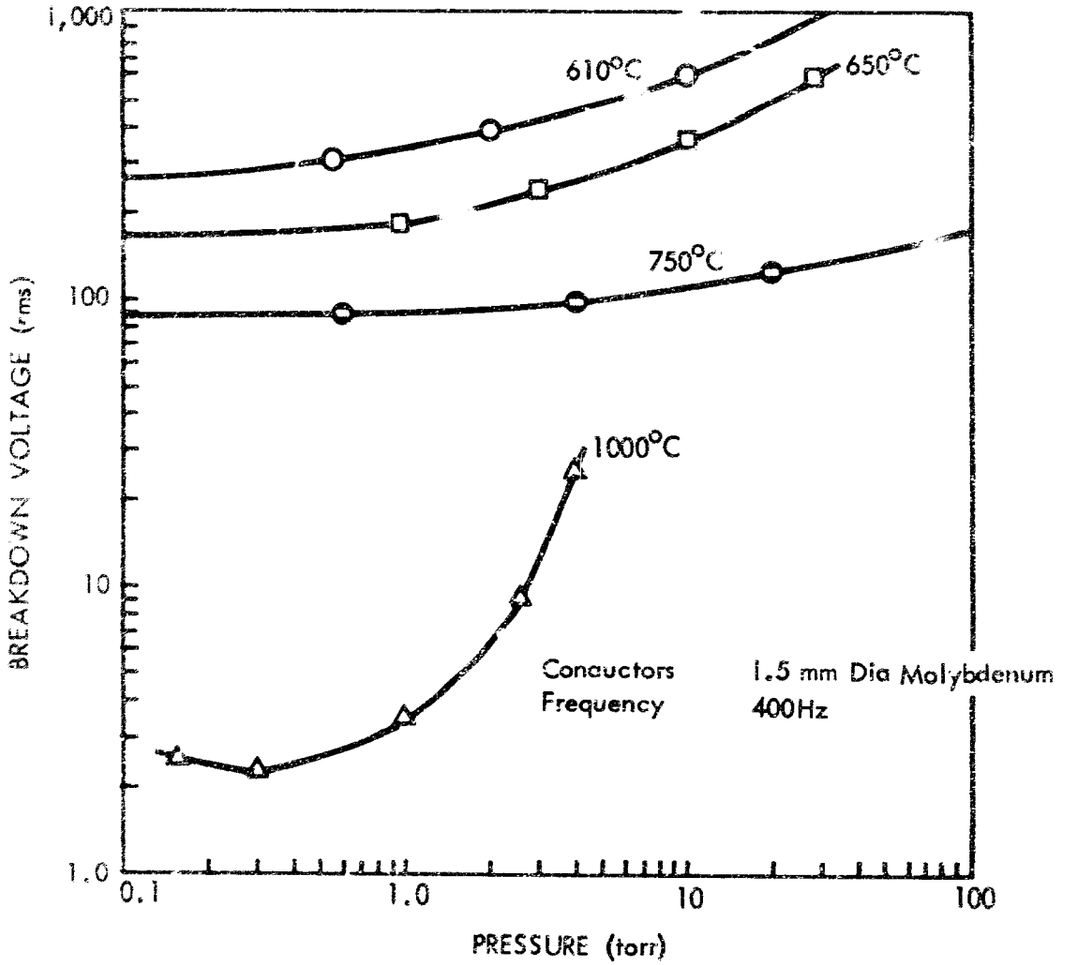

Figure II-11: MOLYBDENUM WIRES SPACED mm IN AIR

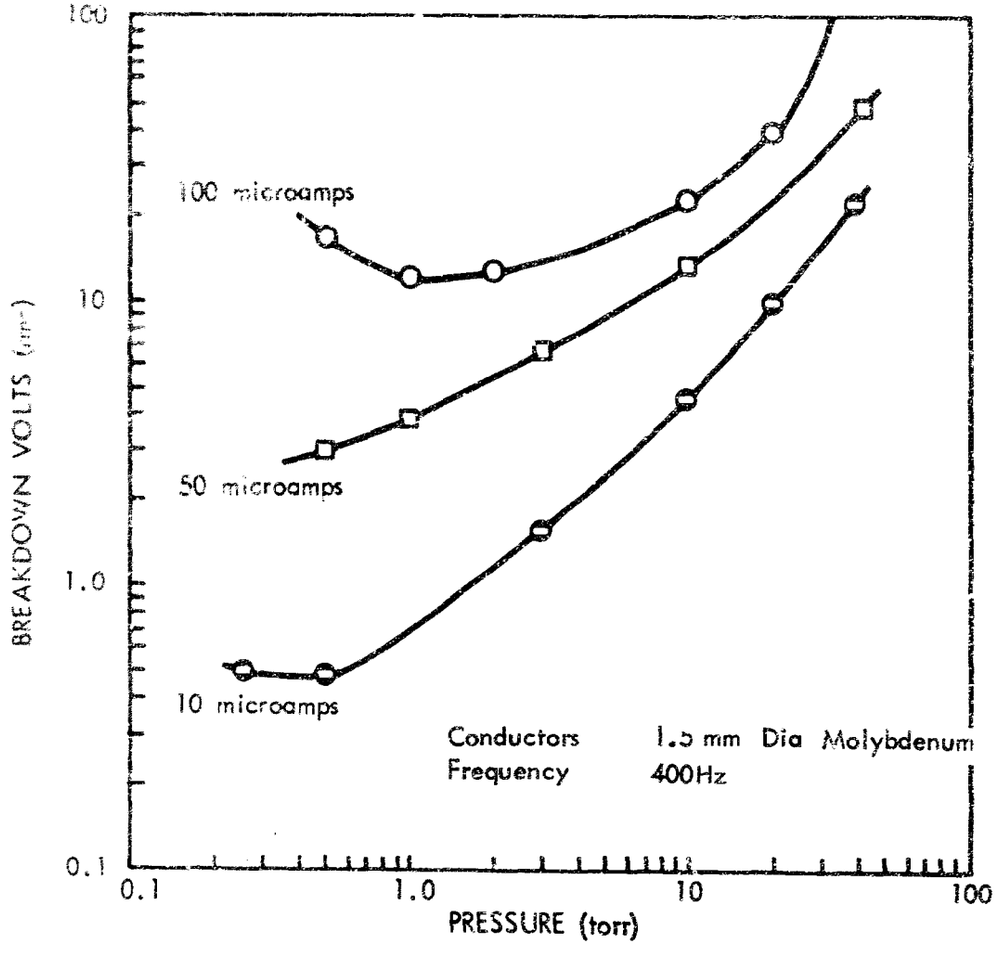

Figure 11-12: CURRENT BETWEEN MOLYBDENUM WIRES SPACED 6 mm IN AIR AT 975°C

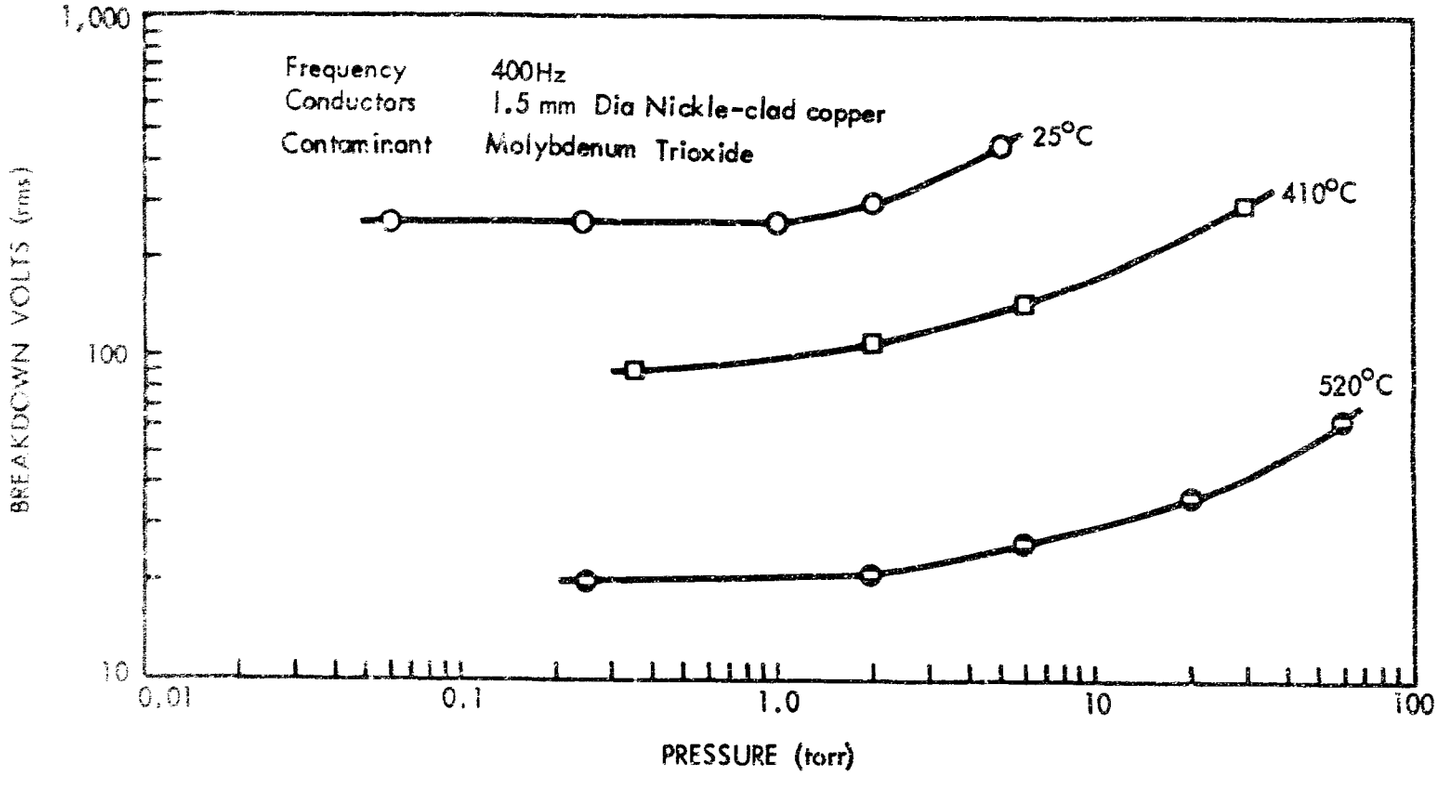

Figure 11-13. NICKEL-CLAD COPPER WIRES SPACED 6 mm IN AIR

Appendix III

INSULATED WIRE TESTS

The corona onset voltage between conductors was measured with twisted and spaced insulated wires, coaxial lines, and cables. The tests were limited to teflon-insulated wires and cables for low-current applications, such as instrumentation, and glass-asbestos-teflon wires for power conductors. The gases used were air, dry nitrogen, and helium-oxygen mixtures. Air was chosen because all X-20A compartments were filled with air prior to flight; nitrogen was chosen because the X-20A electronics compartment was to be pressurized with nitrogen during flight; and helium-oxygen mixtures were chosen because these mixtures are proposed for future manned space vehicles. Nitrogen-oxygen mixtures were not tested because their corona onset voltages were between or above those of air and nitrogen.

Organic insulations such as the silicones, epoxies, and teflon are limited to service temperatures below 300°C; they have a short life at higher temperatures. In temperatures above 300°C, it is necessary to use thermally stable inorganic insulations even though their insulating properties may degrade at very high temperatures.

Teflon conductors spaced 0.64 centimeter apart were tested for corona onset voltage at room temperature and at 260°C. They were also tested when twisted together at one turn every 7.5 centimeters. The voltage applied to the 0.64-centimeter-spaced conductors was limited to 1200 volts (rms) to prevent overstressing the teflon insulation.

One set of power wires was tested for corona at 700°C to find out what happens to the power subsystem during prolonged faults. It was found that the corona onset voltage for a given pressure-times-spacing was much lower when the teflon was ablating at 700°C than at lower temperatures. Experimental corona onset voltage test data for parallel insulated wires are shown in this appendix.

ANALYSIS OF TWO-DIMENSIONAL FIELD

A graphical method of obtaining the two-dimensional field for an insulated wire and ground plane is shown in the text. A mathematical definition of the field lines as a function of dielectric constant, insulation thickness, and conductor-to-central-plane distance is derived in the following paragraphs.

In the sketch under the point x_o, y_o represents the interface between the solid insulation and gaseous medium. Two circles intersect at that point — one representing the field line emanating normal to the conductor, the other in the gaseous medium.

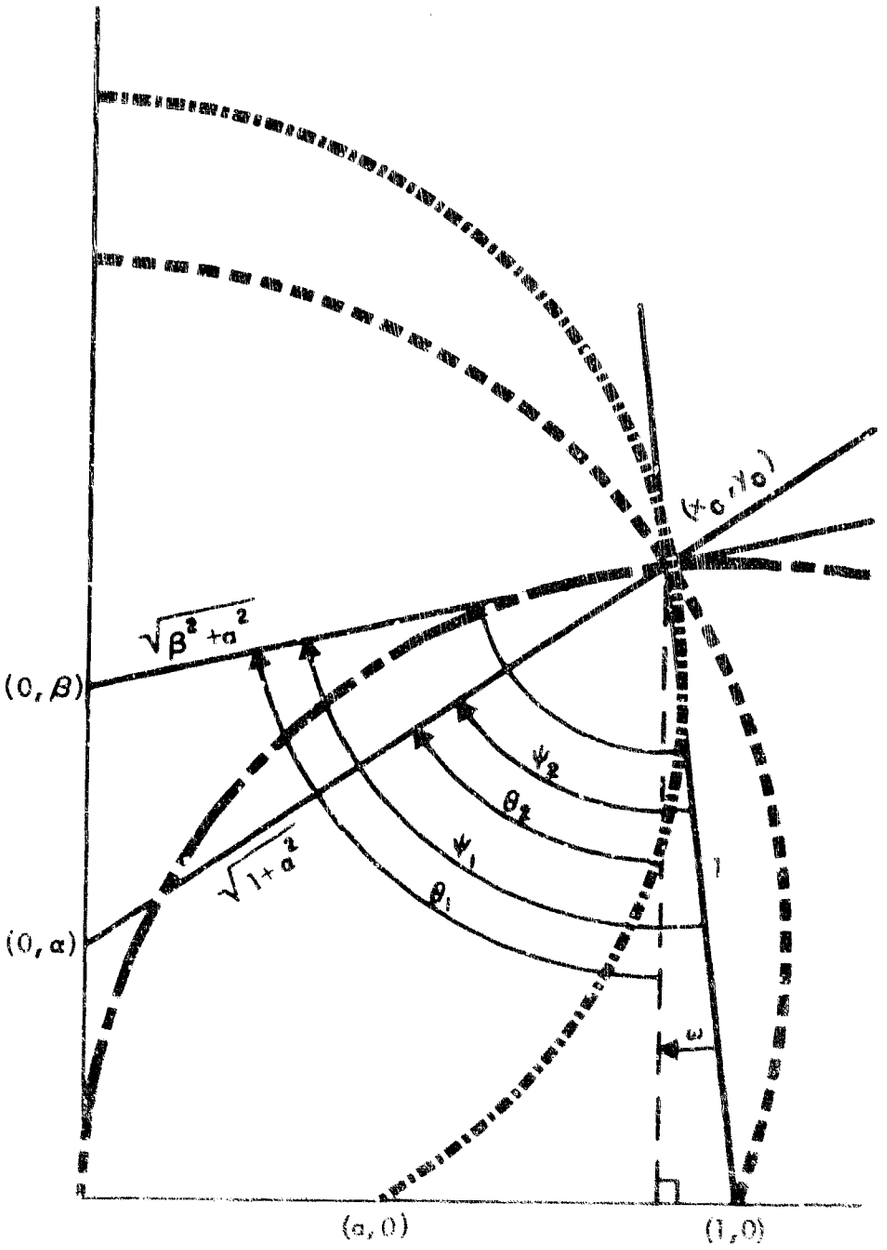

To solve, let

$$x_o^2 + y_o^2 - 2x_o = 0$$

be the equation for the circle representing the outside diameter of the insulation — the interface between the solid and gas media. The equation for the field line inside the solid medium passing through the interface (x_o, y_o) with center at (o, α) is

$$x_o^2 + y_o^2 - 2\alpha y_o = 1 \qquad \text{(III-1)}$$

and the field line through the gas medium passing through the interface (x_o, y_o) with center at ($0, \beta$) is

$$x_o^2 + y_o^2 - 2\beta y_o = a^2 \qquad \text{(III-2)}$$

The angles between the direction lines and the targets to the boundaries of the E field are

$$\frac{\tan \psi 1}{\tan \psi 2} = \frac{\epsilon 2}{\epsilon 1} = \lambda \qquad \text{(III-3)}$$

Letting $x_o = \frac{A}{B}$ $\qquad y_o = \frac{C}{B}$ (III-5A & 5B)

then $A = 2\alpha^2 + 1 + \alpha\sqrt{4\alpha^2 + 3}$

$= B + D$ (III-6)

$B = 2(\alpha^2 + 1)$ (III-7)

$C = \alpha + \sqrt{4\alpha^2 + 3}$ (III-8)

$D = -1 + \alpha\sqrt{4\alpha^2 + 3}$ (III-9)

From the illustration

$\psi_1 \quad \theta_1 + w$ (III-10)

$\psi_2 \quad \theta_2 + w$ (III-11)

Therefore

$$\tan w \quad \frac{y_o}{1 + x_o} \qquad \text{(III-12)}$$

$$\tan \theta_2 = \frac{y_o - \beta}{x_o} \qquad \text{(III-13)}$$

$$\tan \theta_1 = \frac{y_o - \alpha}{x_o} \qquad \text{(III-14)}$$

Solving the equations for the direction lines at the interface, the following can be obtained

$$\frac{\tan \theta_1 + \tan w}{1 - \tan \theta_1 \tan w} = \lambda \frac{\tan \theta_2 + \tan w}{1 - \tan \theta_1 \tan w} \qquad \text{(III-15)}$$

or

$$\frac{y_o - \alpha - x_o y_o + \alpha x_o + x_o y_o}{x_o - x_o^2 - y^2 + \alpha y_o} = \lambda \frac{y_o - \beta - x_o y_o + \beta x_o + x_o y_o}{x_o - x_o^2 - y_o^2 + \beta y_o} \qquad \text{(III-16)}$$

collecting terms

$$\frac{y_o + \alpha (x_o - 1)}{\alpha y_o - x_o} = \lambda \frac{y_o + \beta (x_o - 1)}{\beta y_o - x_o} \qquad \text{(III-17)}$$

abbreviated

$$\frac{\frac{C}{B} + \alpha \frac{D}{B}}{\alpha \frac{C}{B} - \frac{D}{B} - 1} = \lambda \frac{\frac{C}{B} + \beta \frac{D}{B}}{\beta \frac{C}{D} - \frac{D}{B} - 1} \qquad \text{(III-18)}$$

or

$$\frac{C + \alpha D}{\alpha C - D - B} = \lambda \frac{C + \beta D}{\beta C - D - B} \qquad \text{(III-19)}$$

Expanding

$$\beta C(C + \alpha D) - (D + B)(C + \alpha D) = \lambda C(\alpha C - [D + B]) \quad \beta \lambda D(\alpha C - [D + B]) \qquad \text{(III-20)}$$

$$\beta = \frac{\lambda C(\alpha C - [D + B]) + (D + B)(C + \alpha D)}{C(C + \alpha B) - \lambda D(\alpha C - [D + B])}$$

$$\frac{\lambda C\left(-\frac{B}{2}\right) + (D + B)\frac{\rho}{2} B}{C\frac{\rho}{2} B - \lambda D\left(-\frac{B}{2}\right)}$$

$$\frac{\lambda C + \rho (D + B)}{\rho C + \lambda D}$$

$$= \frac{-\lambda(\alpha + \rho) + \rho(2\alpha^2 + 1 + \alpha\rho)}{\rho(\rho + \alpha) + \lambda(-1 + \alpha\rho)} \qquad \text{(III-21)}$$

where

$$\rho = \sqrt{4\alpha^2 + 3} \qquad \text{(III-22)}$$

By knowing β in terms of α and λ, the length of the field line in the gaseous medium can be found. Then the ratio of the portion of the field line in the solid can be compared to that portion in the gas to obtain the voltage drop across the solid.

The solution indicates that for the line through the gas medium at $\beta \gg 1$ (radius outside diameter insulation = 1), the ratio of the line section through the gas is so great that the total voltage drop would be across the gas. Consequently, the corona onset voltage of either twisted or spaced conductor should be equal to that of closely spaced bare electrodes. This fact did not occur experimentally, as is readily shown in the preceding curves. The solution does not take into account second-order effects such as irregularities along the boundary, conductivity at the boundary, and the fact that the breakdown voltage for very long paths, in excess of 20 centimeters, is increased. Obviously these second-order conditions are more significant than originally assumed.

LIST OF FIGURES — APPENDIX III

LIST OF FIGURES -- APPENDIX III

TABLES

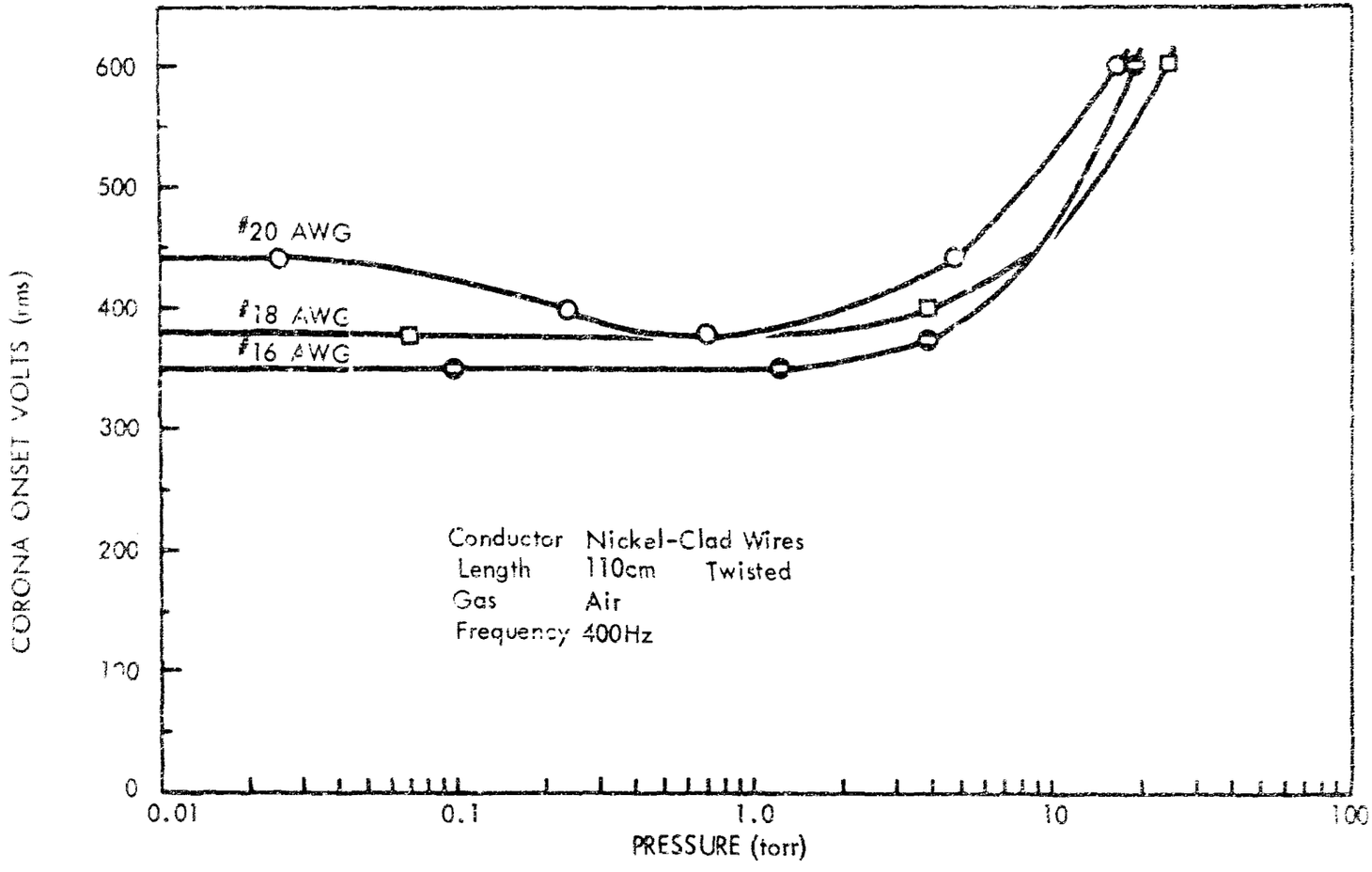

Figure III-1: ASBESTOS-GLASS INSULATED #16 TO 20 WIRES AT 24°C

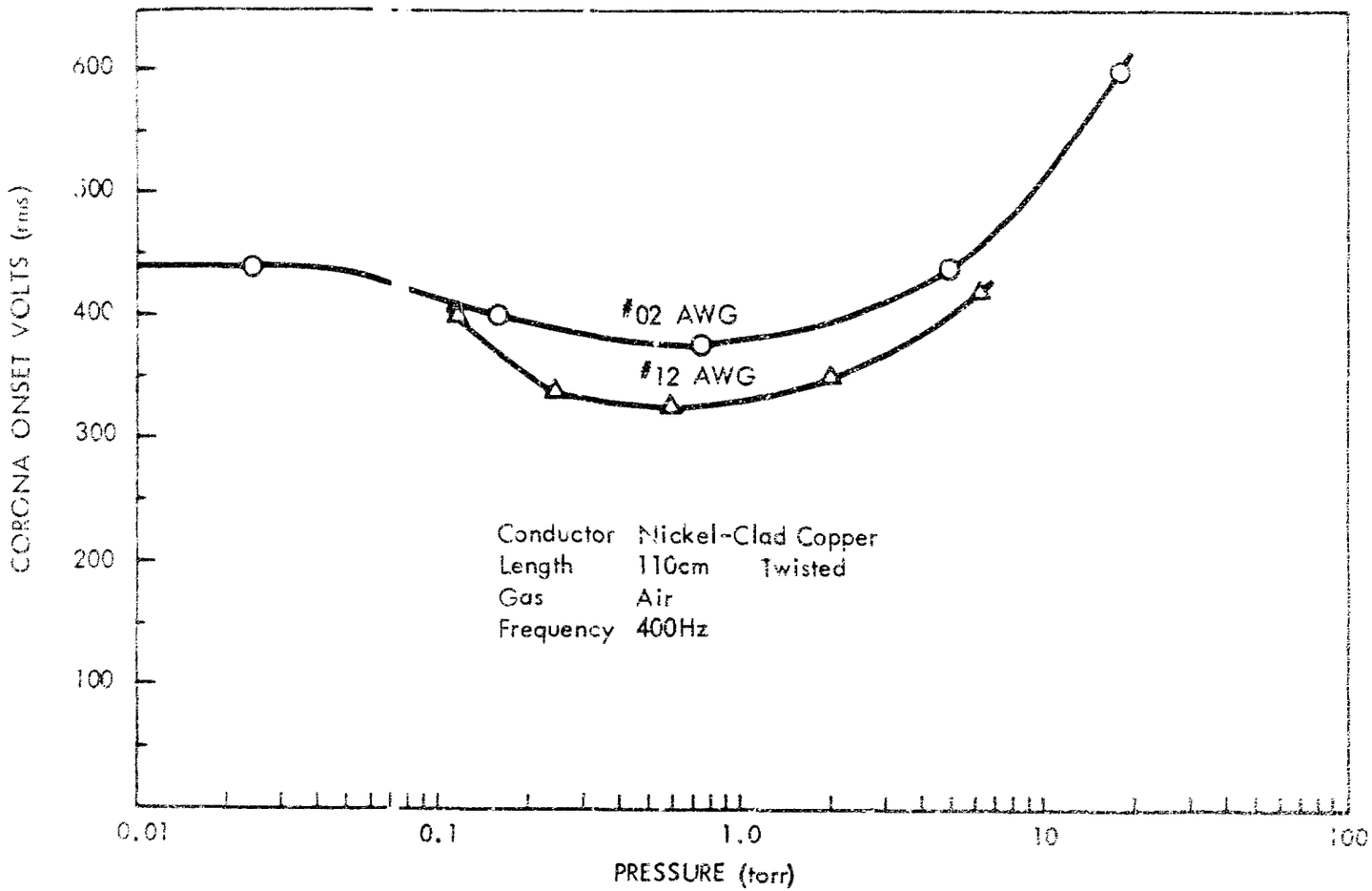

Figure III-2: ASBESTOS-GLASS INSULATED #12 WIRE AT 24°C

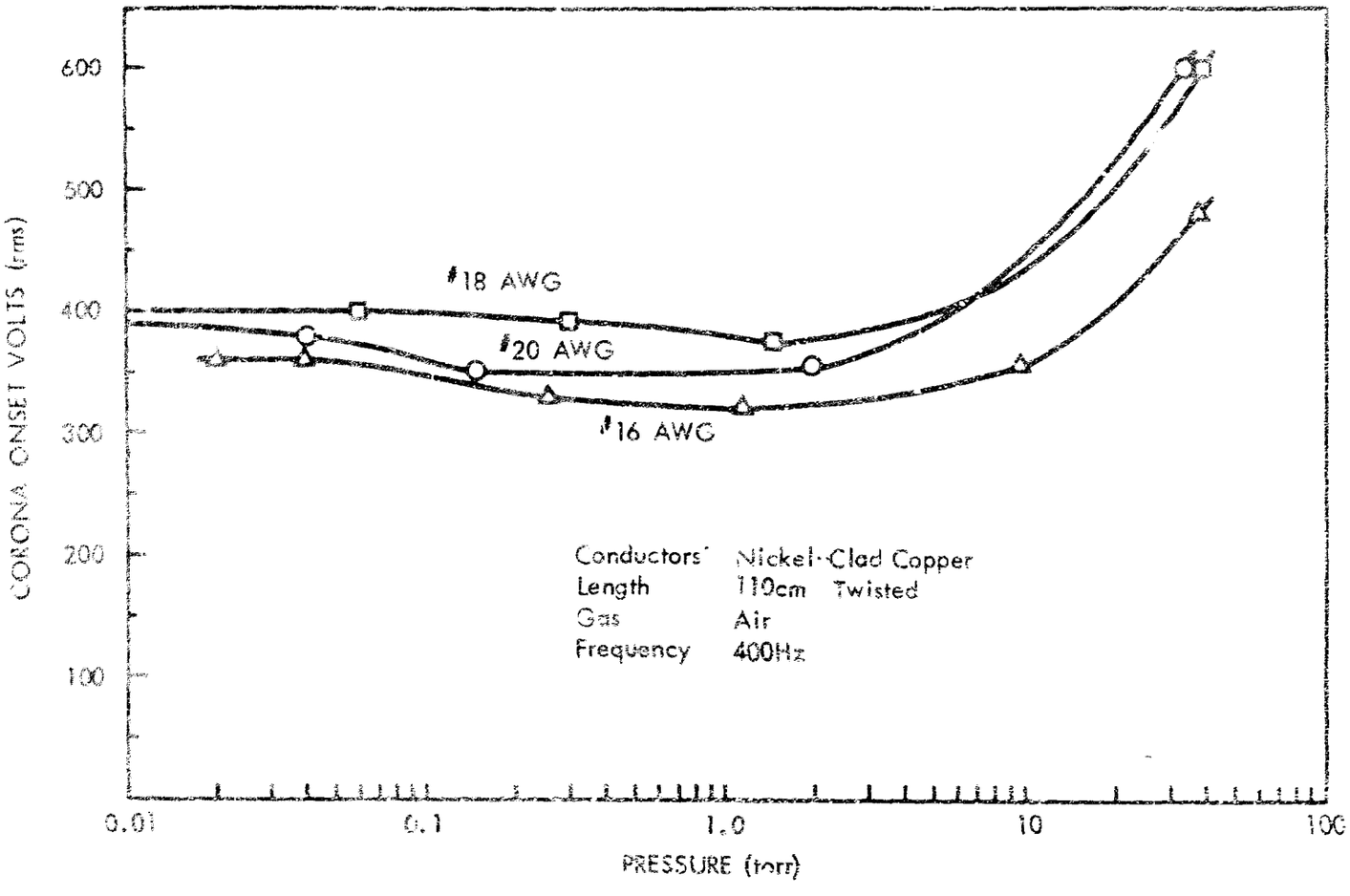

Figure III-3. GLASS-ASBESTOS INSULATED #16 TO 20 WIRES AT 260°C

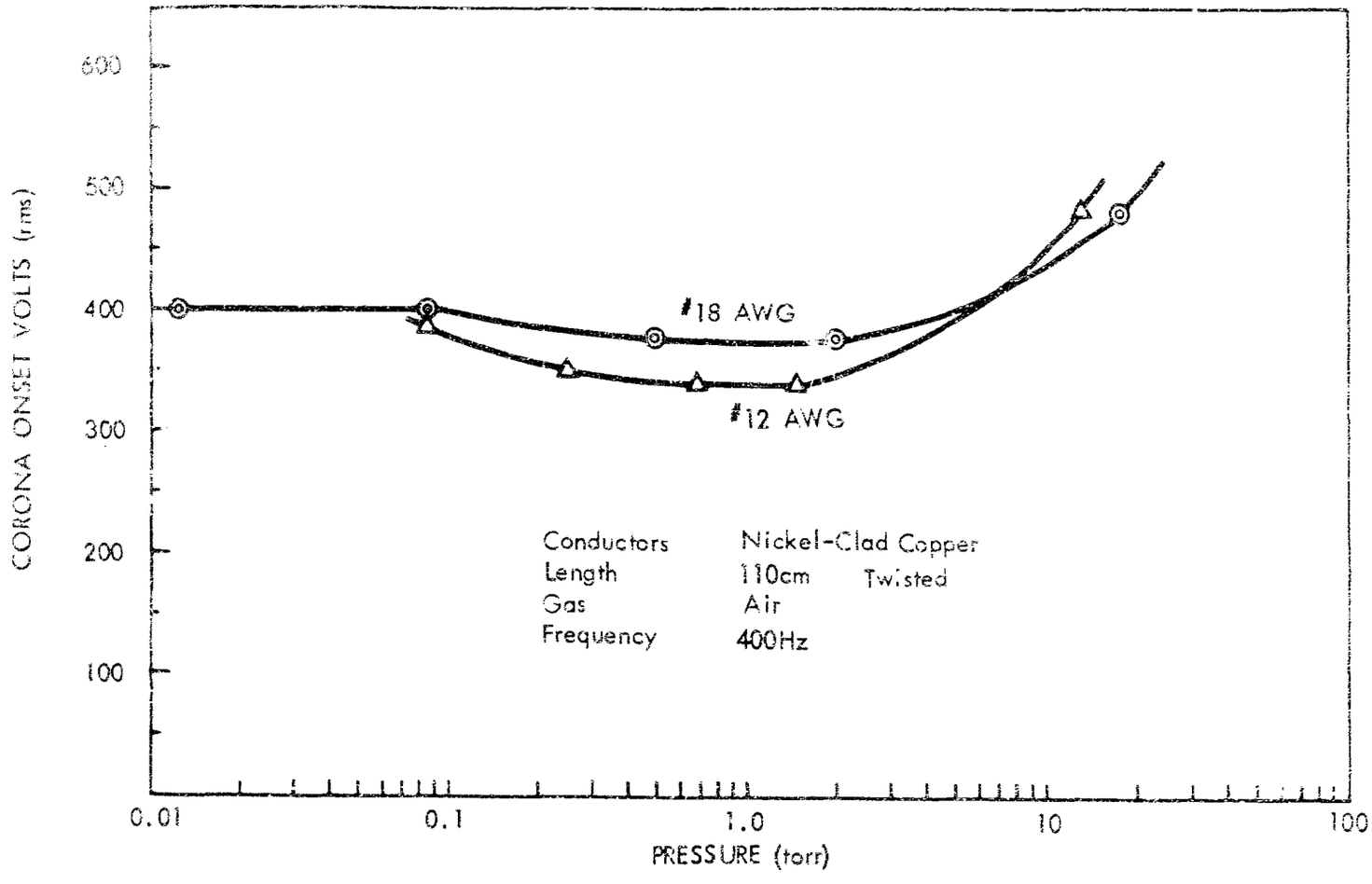

Figure III-4: ASBESTOS-GLASS INSULATED #12 AND #18 WIRE AT 260°C

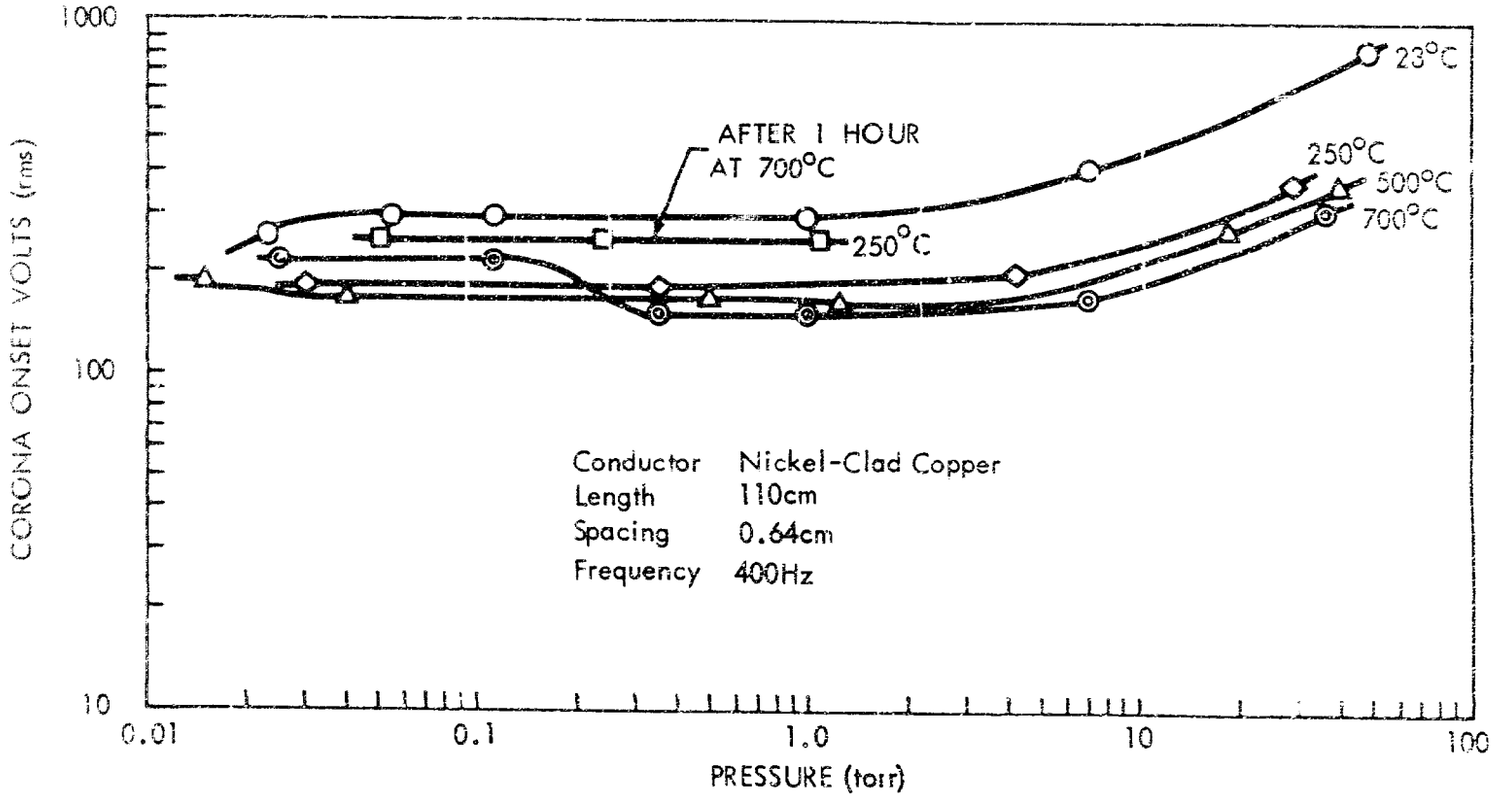

Figure III-5: ASBESTOS-GLASS INSULATED #16 SPACED WIRES IN AIR UP TO 700°C

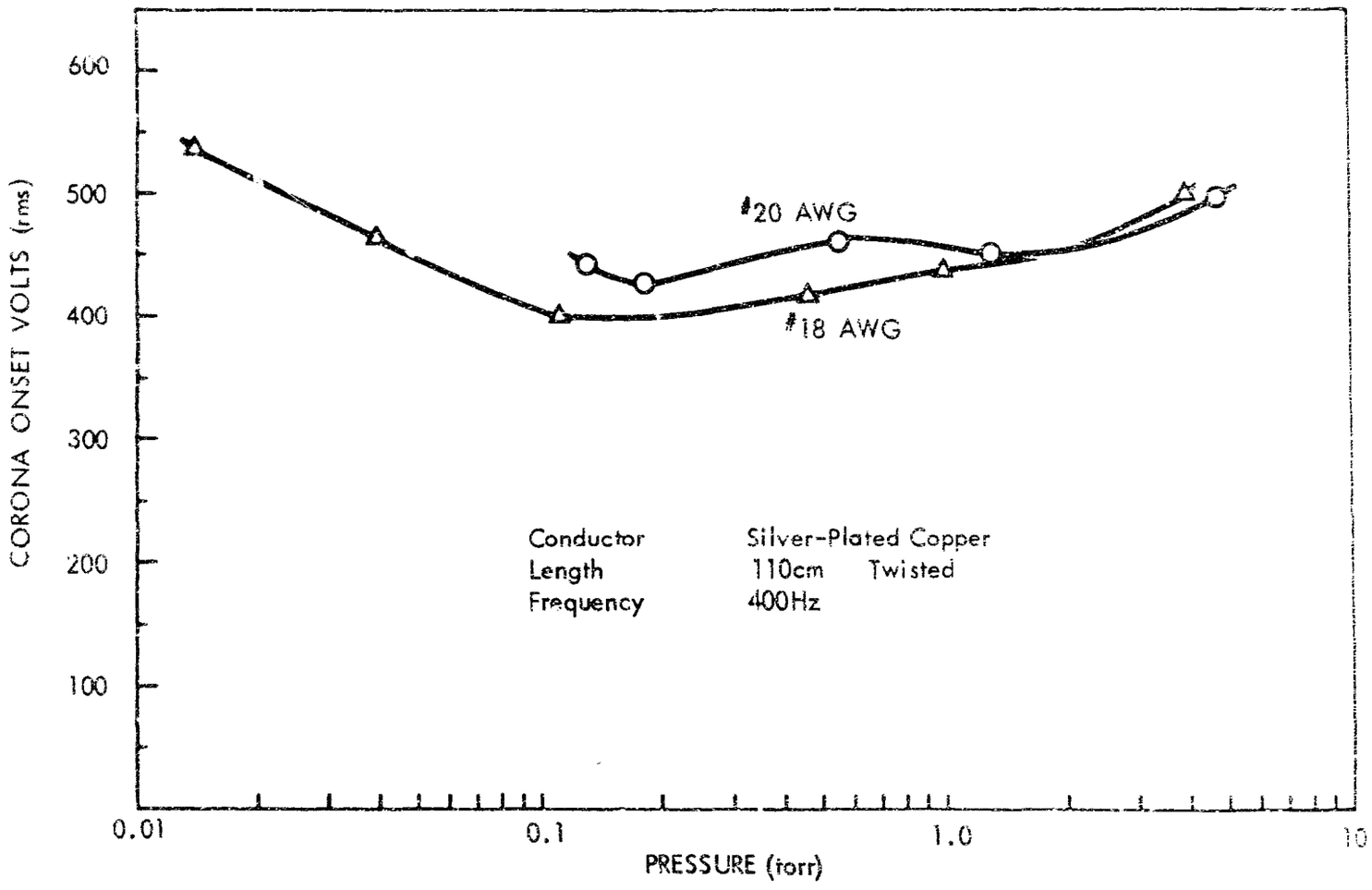

Figure III-6: GLASS-TEFLON INSULATED WIRE TESTS IN AIR AT 24°C

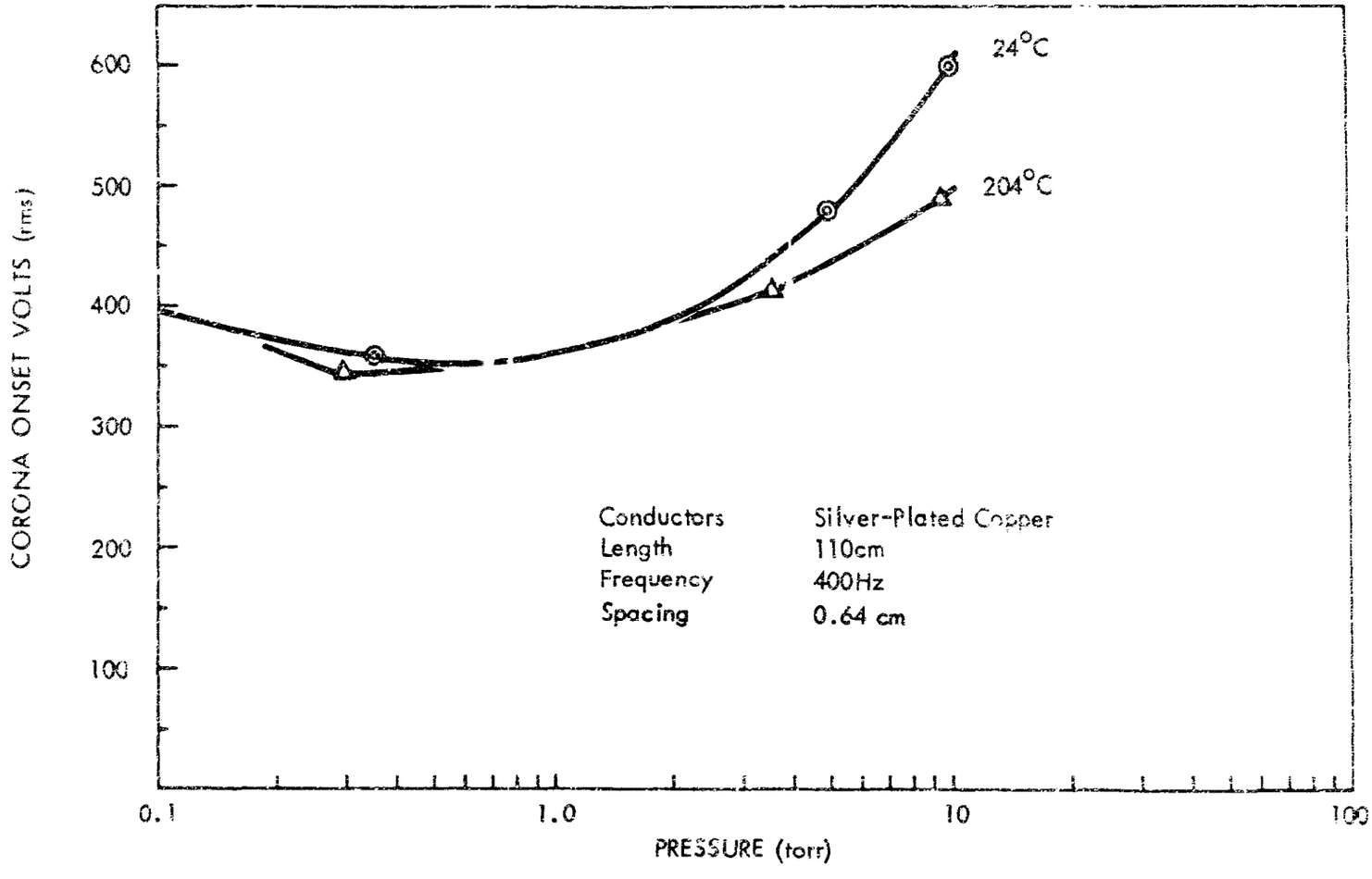

Figure III-7: GLASS-TEFLON INSULATED #16 WIRES IN AIR AT 204°C

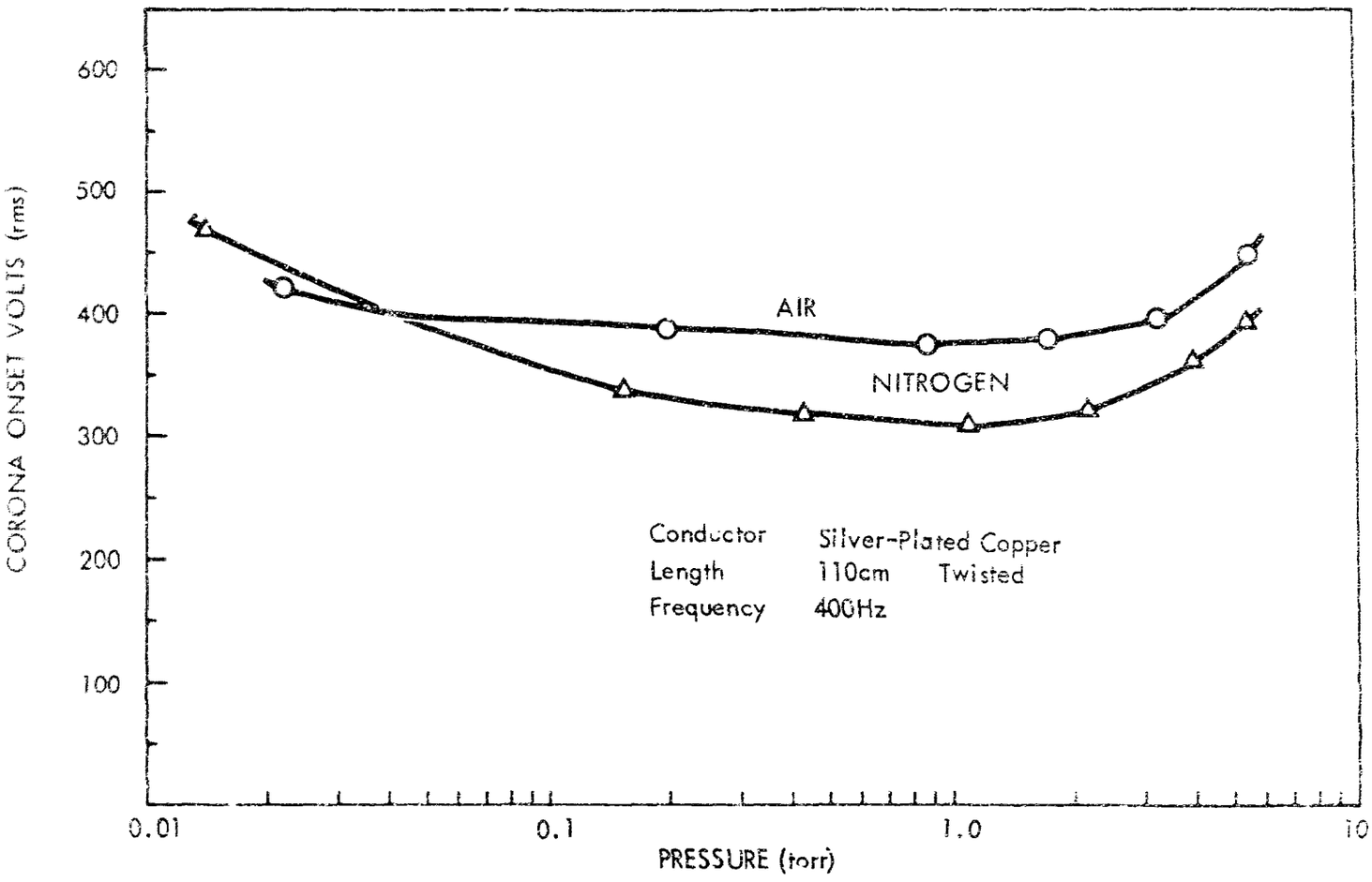

Figure III-8: GLASS-TEFLON INSULATED #8 WIRES IN NITROGEN AT 24°C

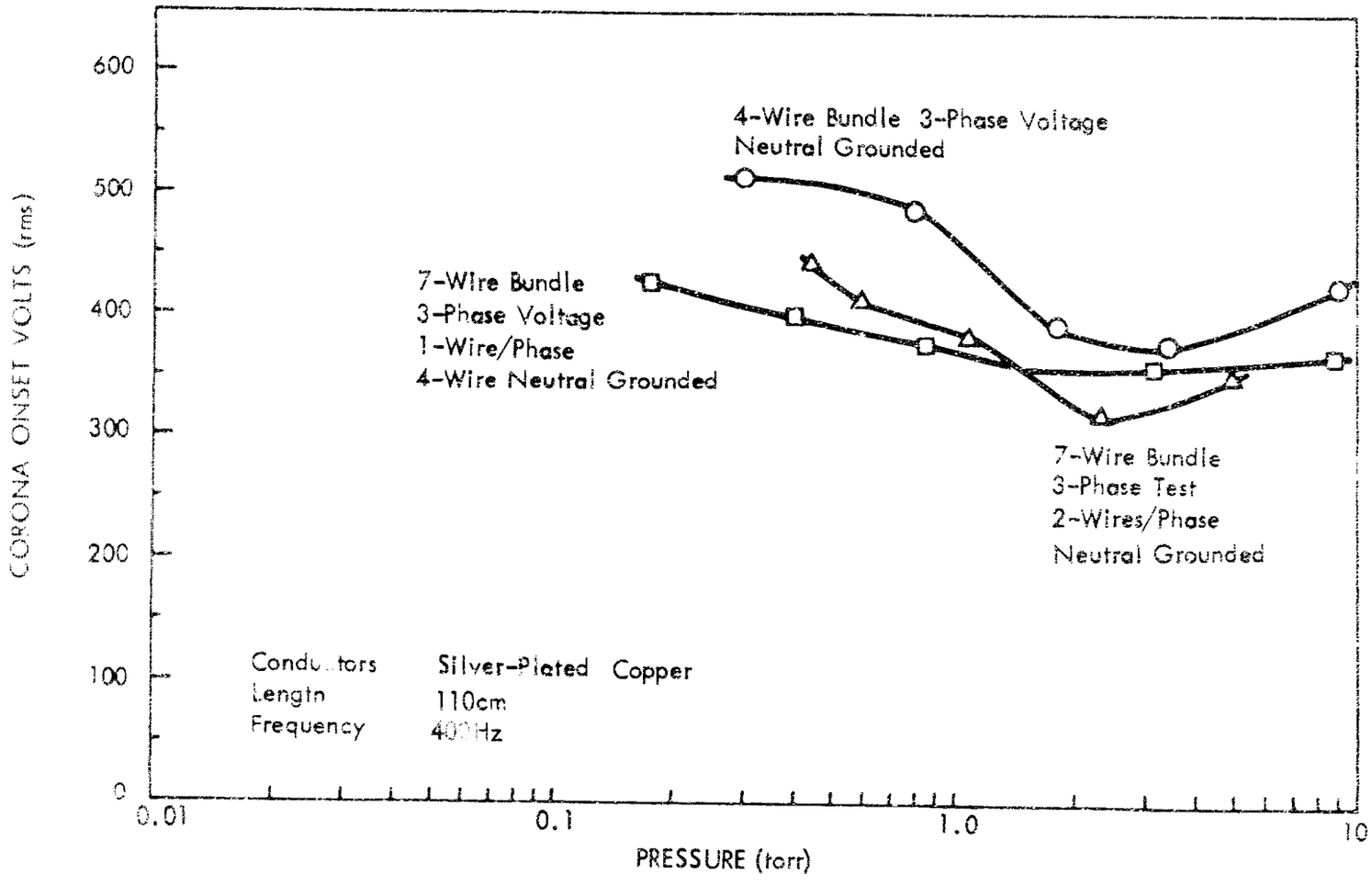

Figure III-9: GLASS-TEFLON INSULATED #20 WIRE CABLES IN AIR AT 24°C

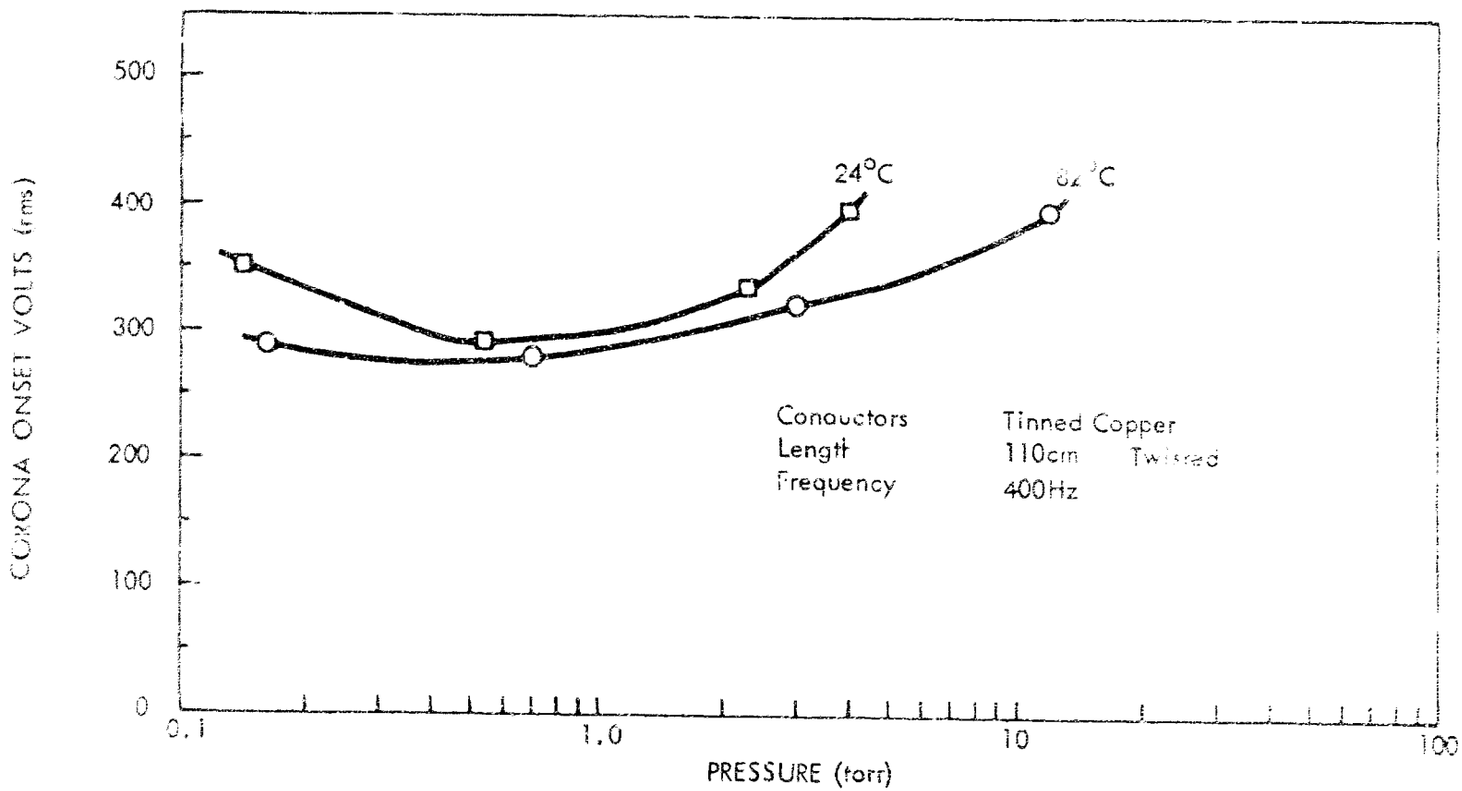

Figure III-10: PVC-GLASS-NYLON INSULATED #10 WIRES IN AIR

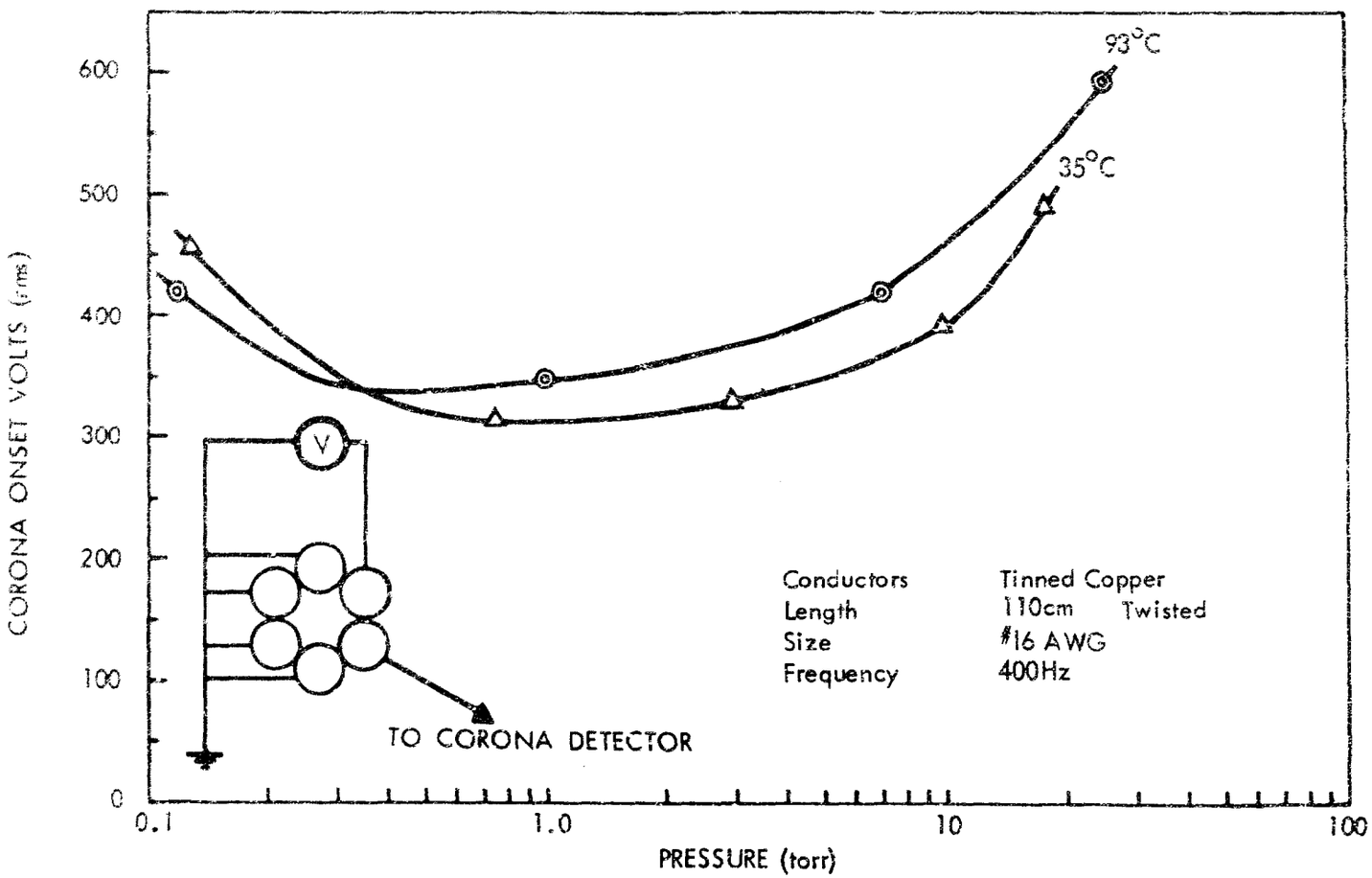

Figure III-11: PVC-GLASS-NYLON INSULATED 6-CONDUCTOR UNSHIELDED CABLE IN AIR

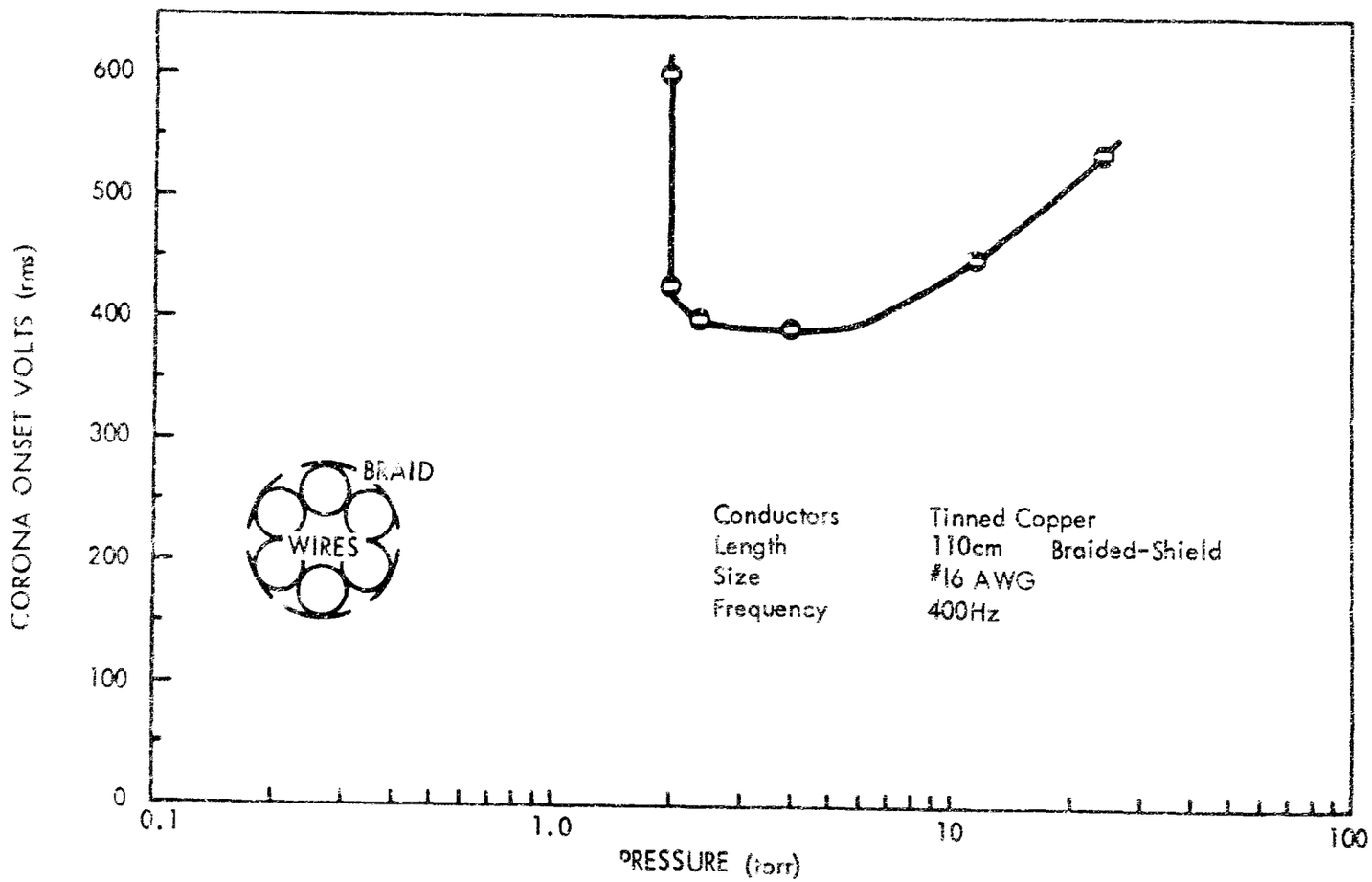

Figure III-12: PVC-GLASS-NYLON INSULATED 6-CONDUCTOR SHIELDED CABLE IN AIR AT 65°C

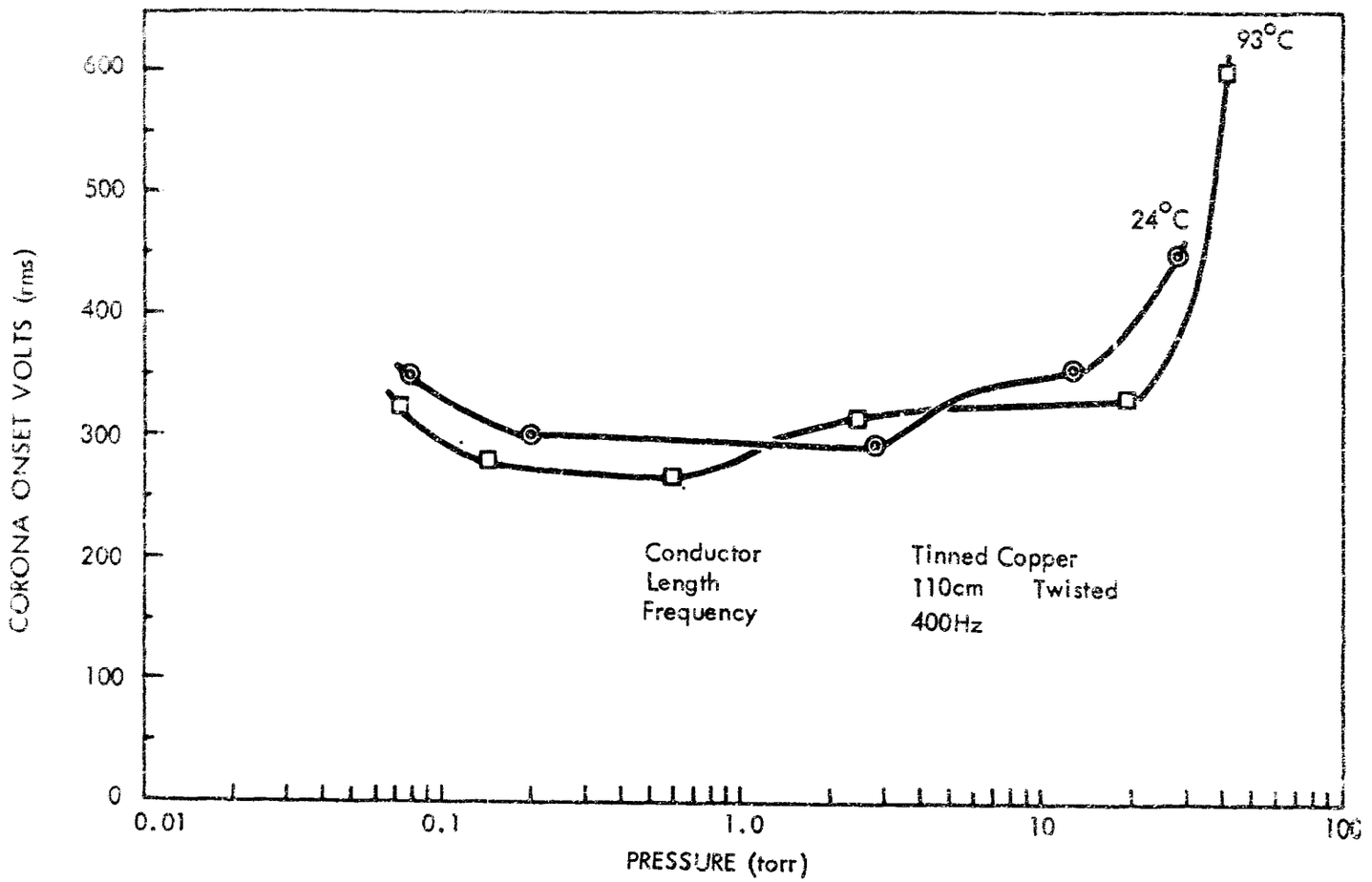

Figure III-13: PVC-NYLON INSULATED #20 WIRES IN AIR

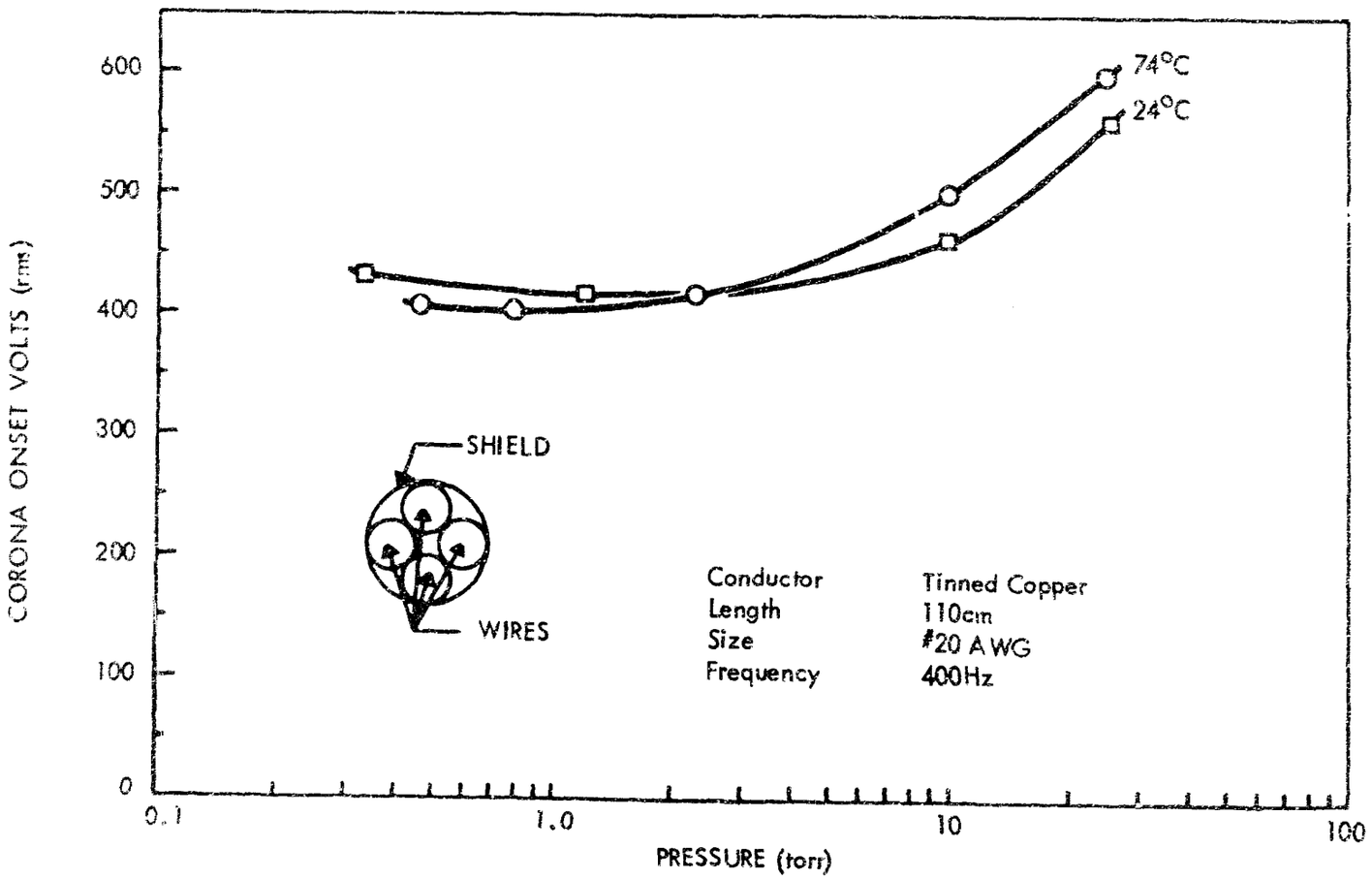

Figure III-14: PVC-NYLON INSULATED 4-CONDUCTOR SHIELDED CABLE IN AIR

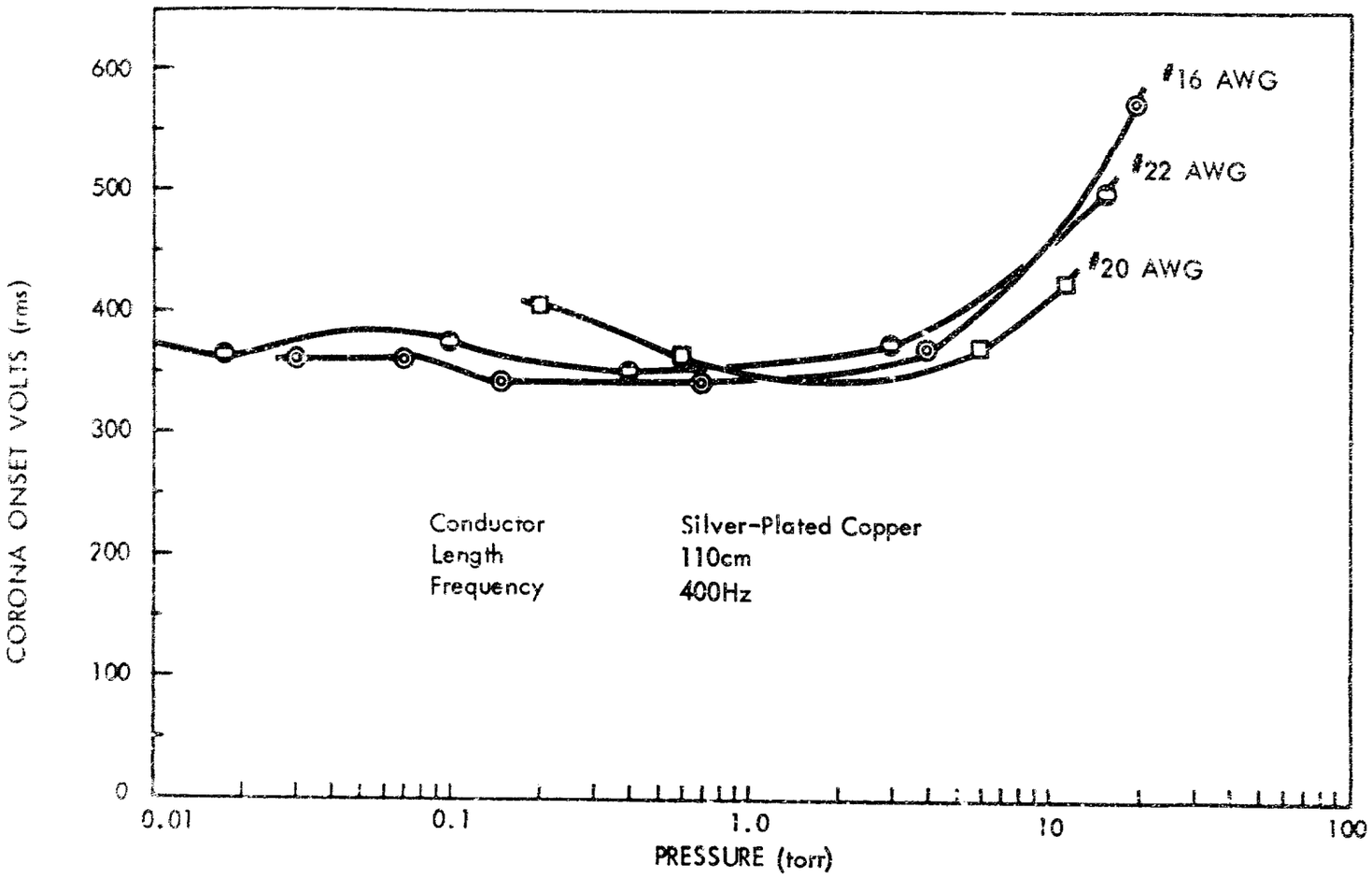

Figure III-15: TEFLON INSULATED #16 TO #22 TWISTED WIRES IN AIR AT 24°C

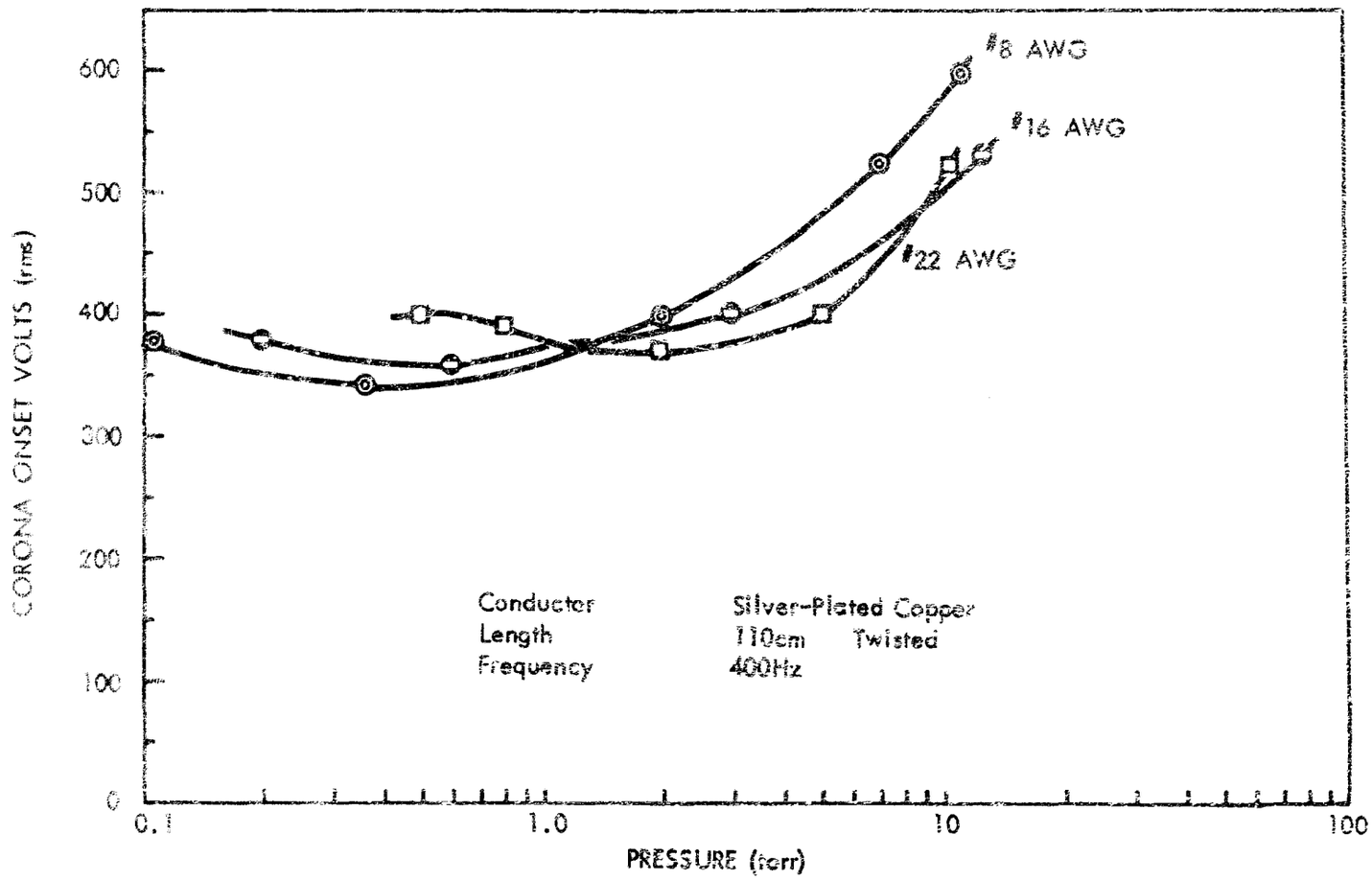

Figure III-16: TEFLON INSULATED WIRES WITH CORONA INHIBITOR IN AIR AT 24°C

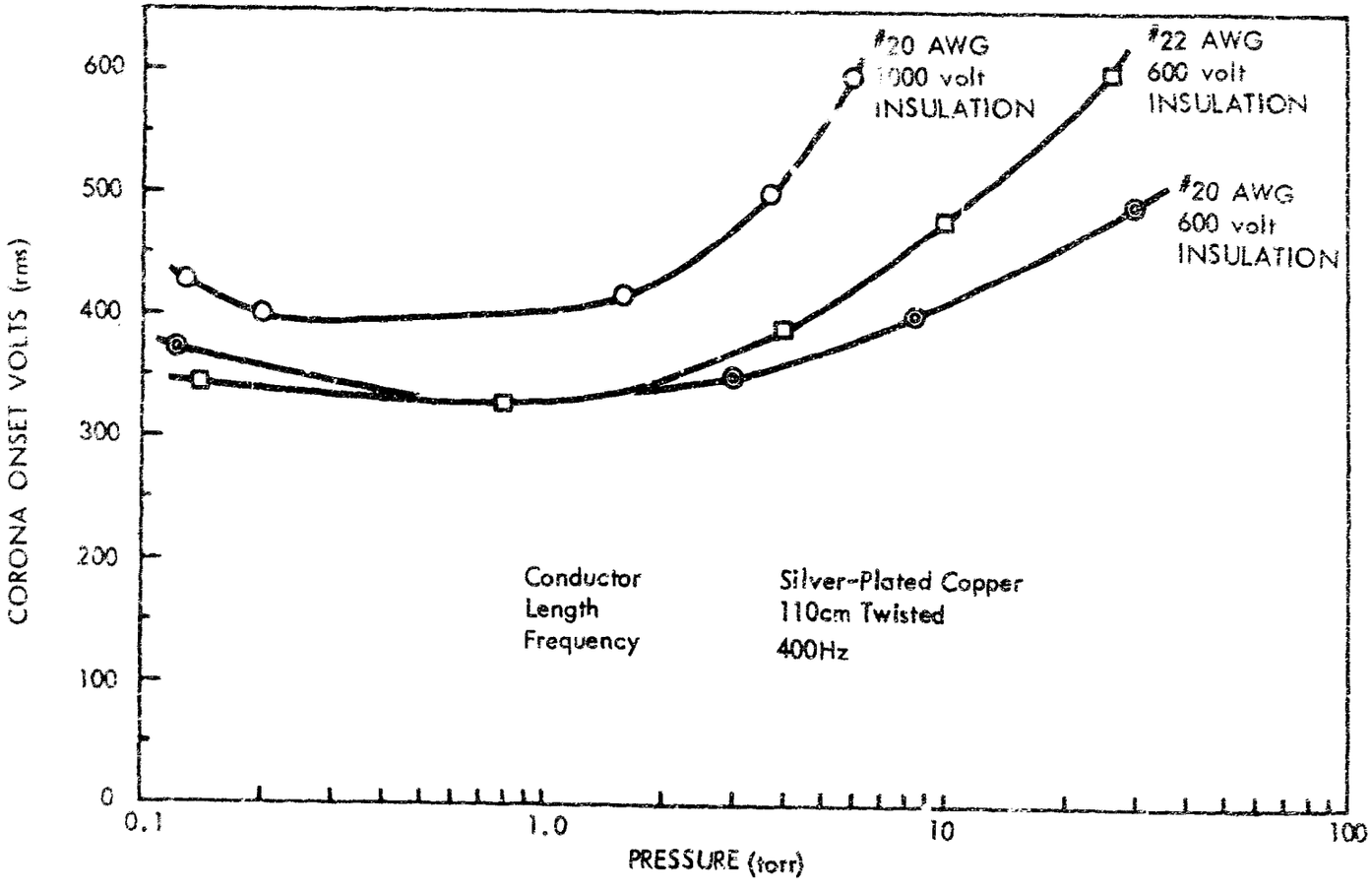

Figure III-17: TEFLON INSULATED WIRES — 1000 VOLTS — WITH CORONA INHIBITOR IN AIR AT 24°C

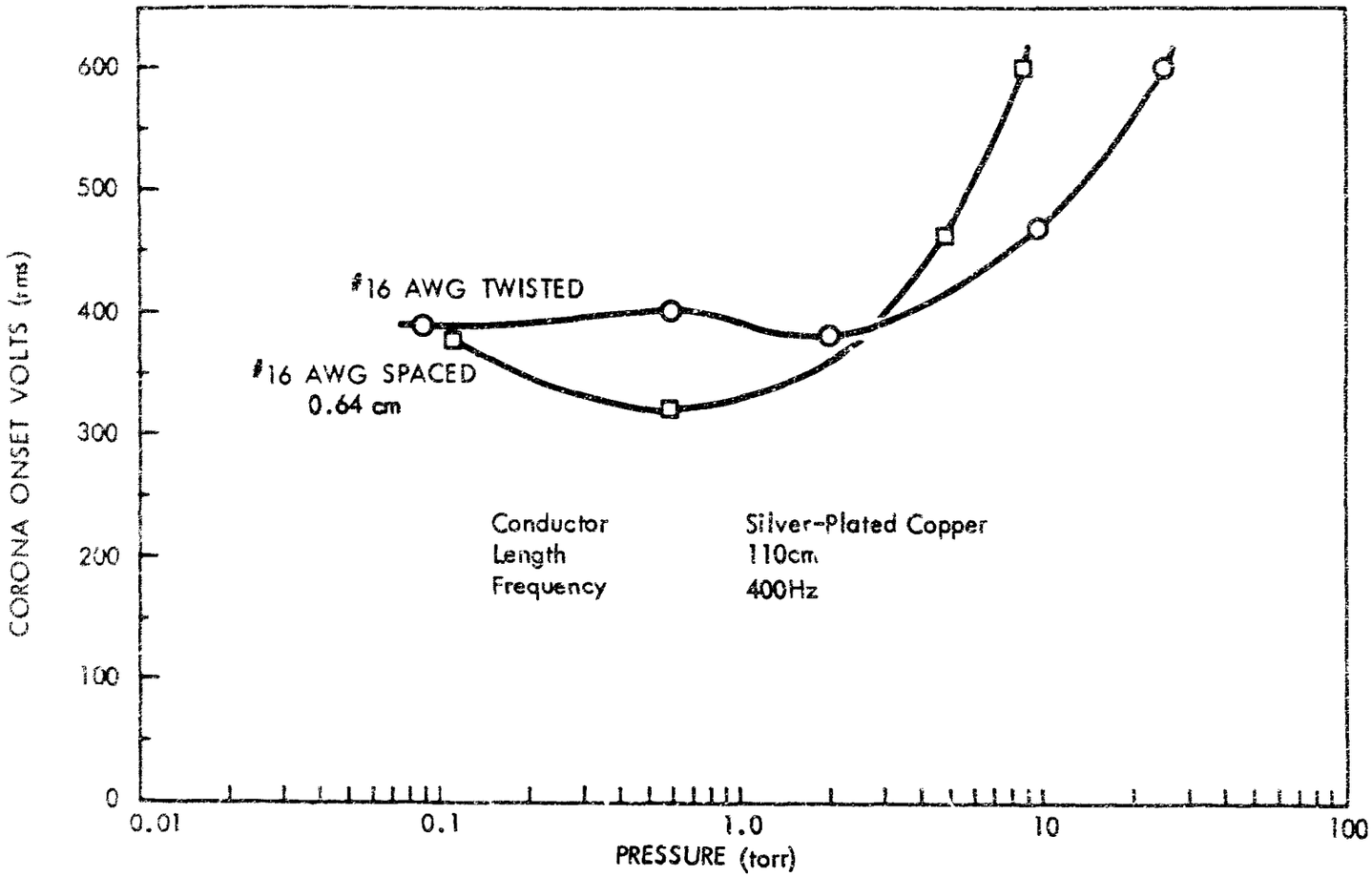

Figure III-18 TEFLON INSULATED #16 SPACED WIRES IN AIR AT 24°C

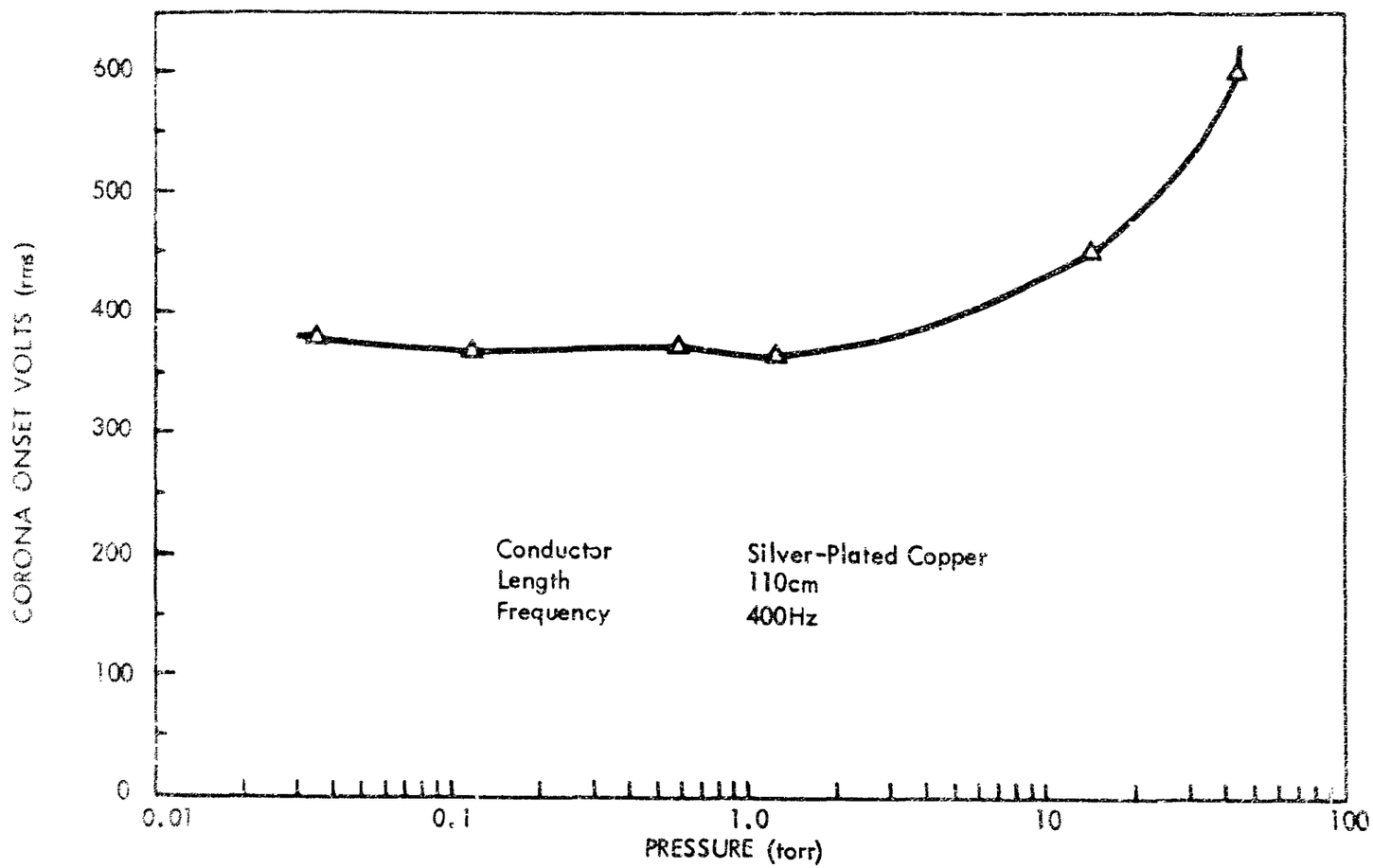

Figure III-19: TEFLON INSULATED #20 TWISTED WIRES IN AIR AT 260°C

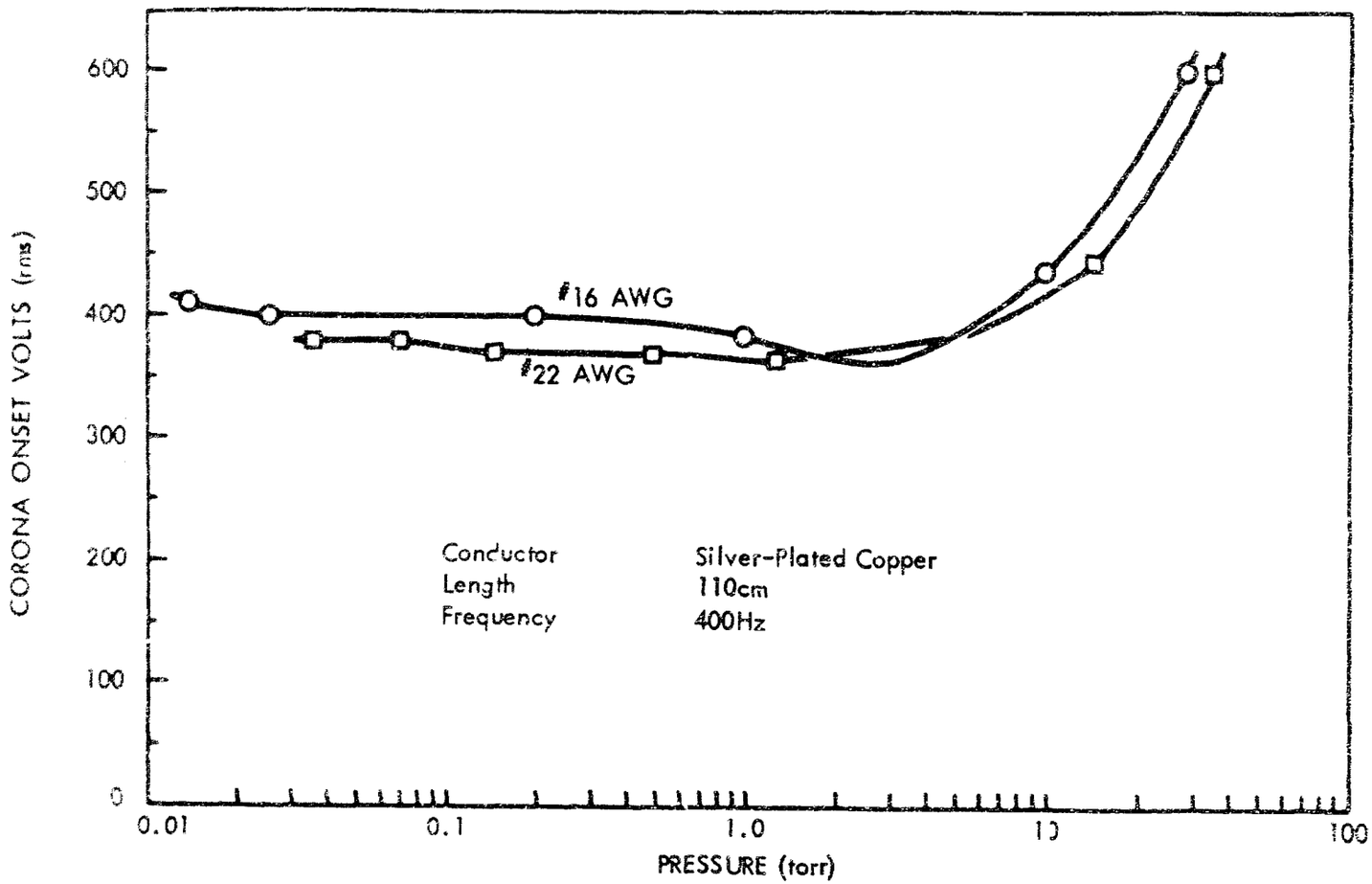

Figure III-20: TEFLON INSULATED #16 AND #22 TWISTED WIRES IN AIR AT 260°C

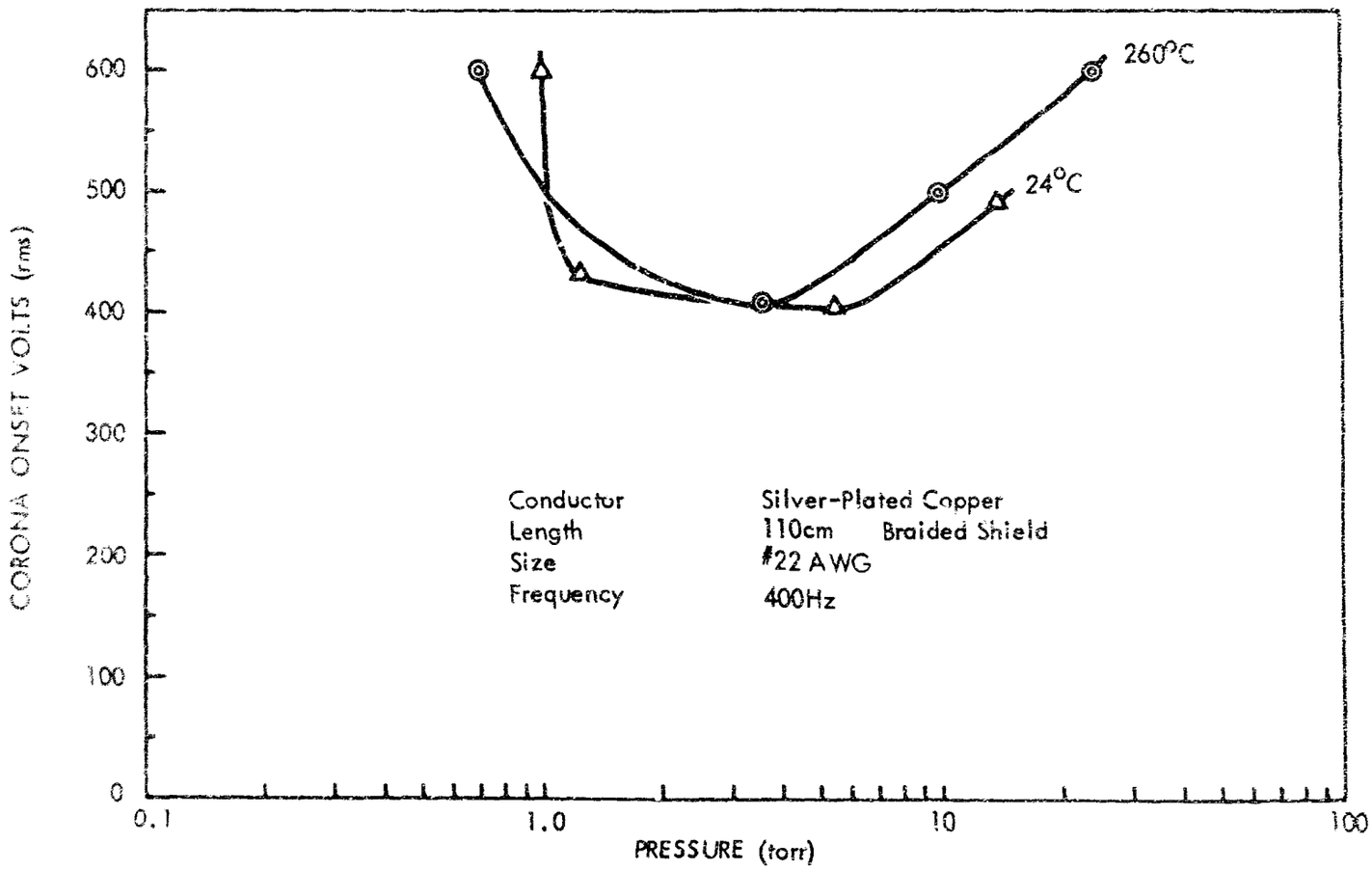

Figure III-21: TEFLON INSULATED COAXIAL CABLE IN AIR AT 24°C AND 260°C

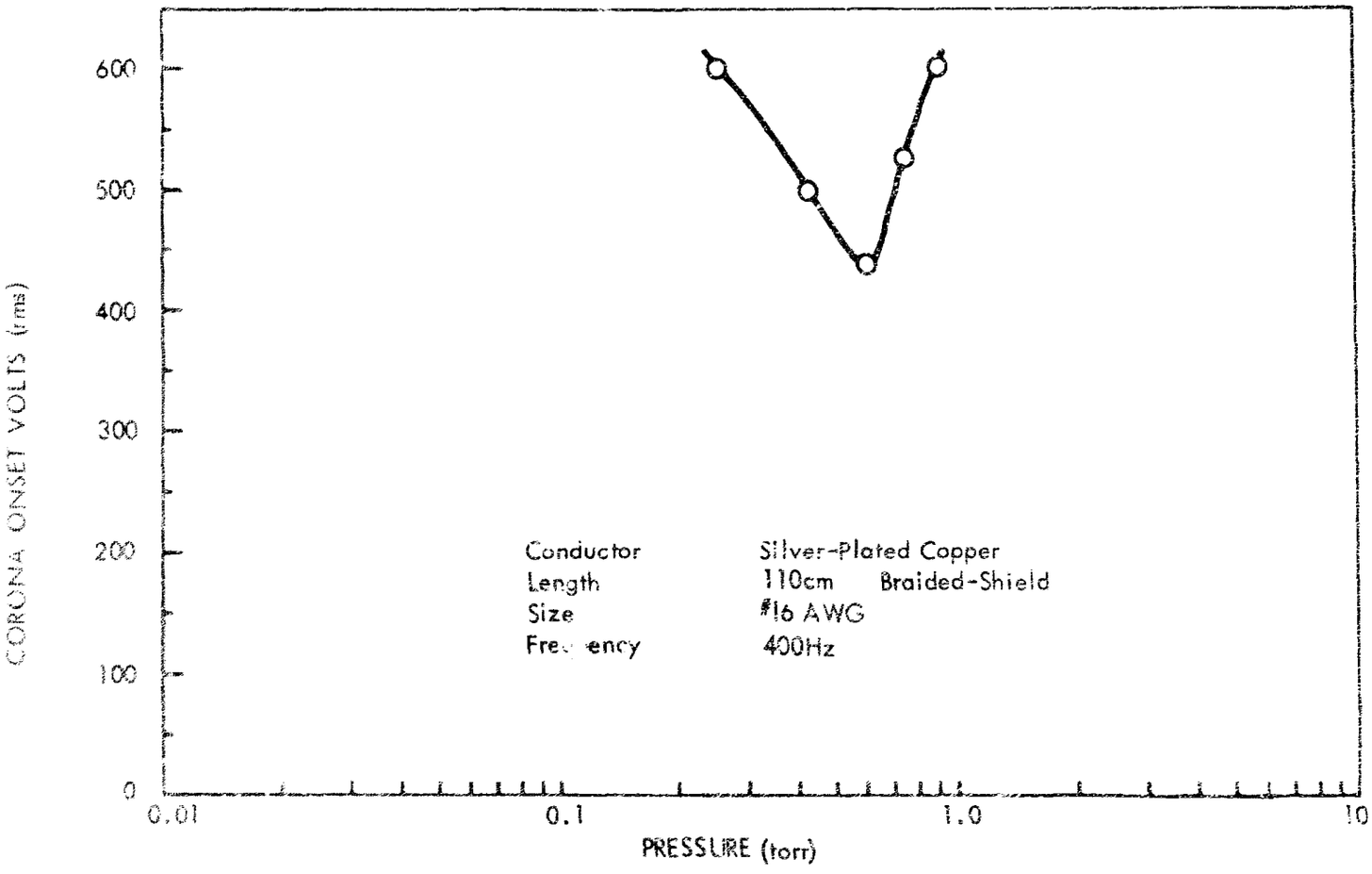

Figure III-22: TEFLON INSULATED COAXIAL LINE IN AIR AT 315°C

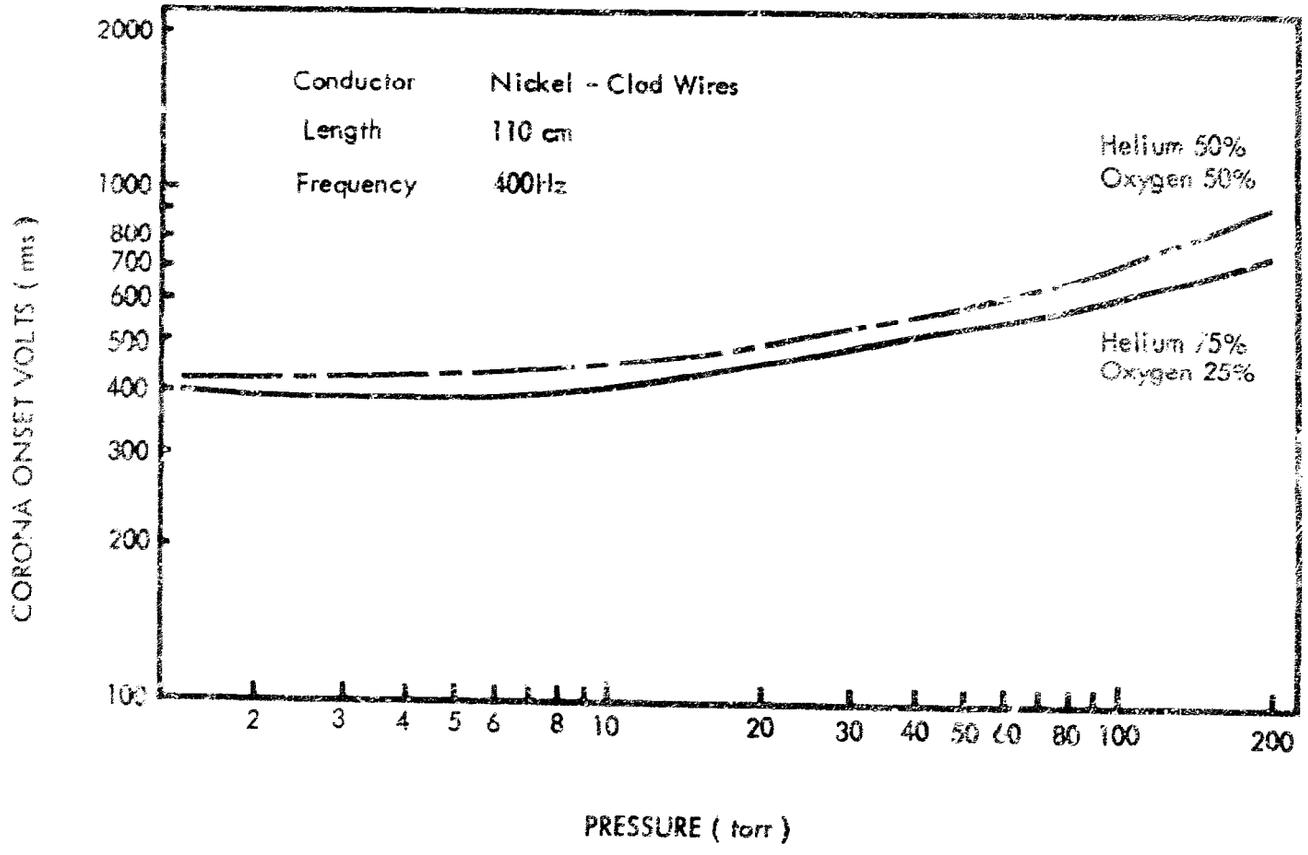

Figure III - 23: TEFLON INSULATED # 16 TWISTED WIRES IN HELIUM - OXYGEN MIXTURES AT 24° C

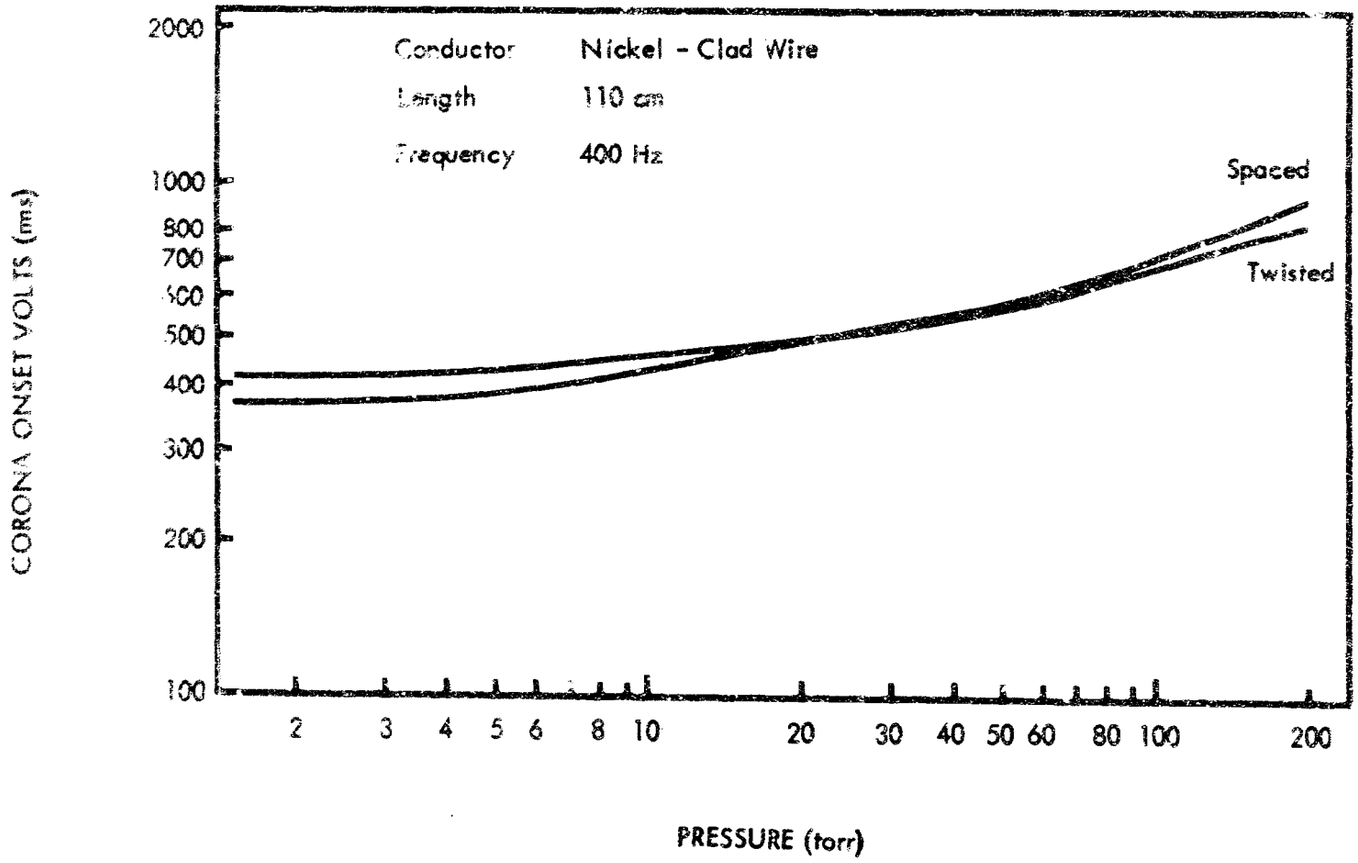

Figure III - 24: TEFLON INSULATED # 16 WIRES IN 50 - 50 HELIUM - OXYGEN MIXTURE AT 24° C

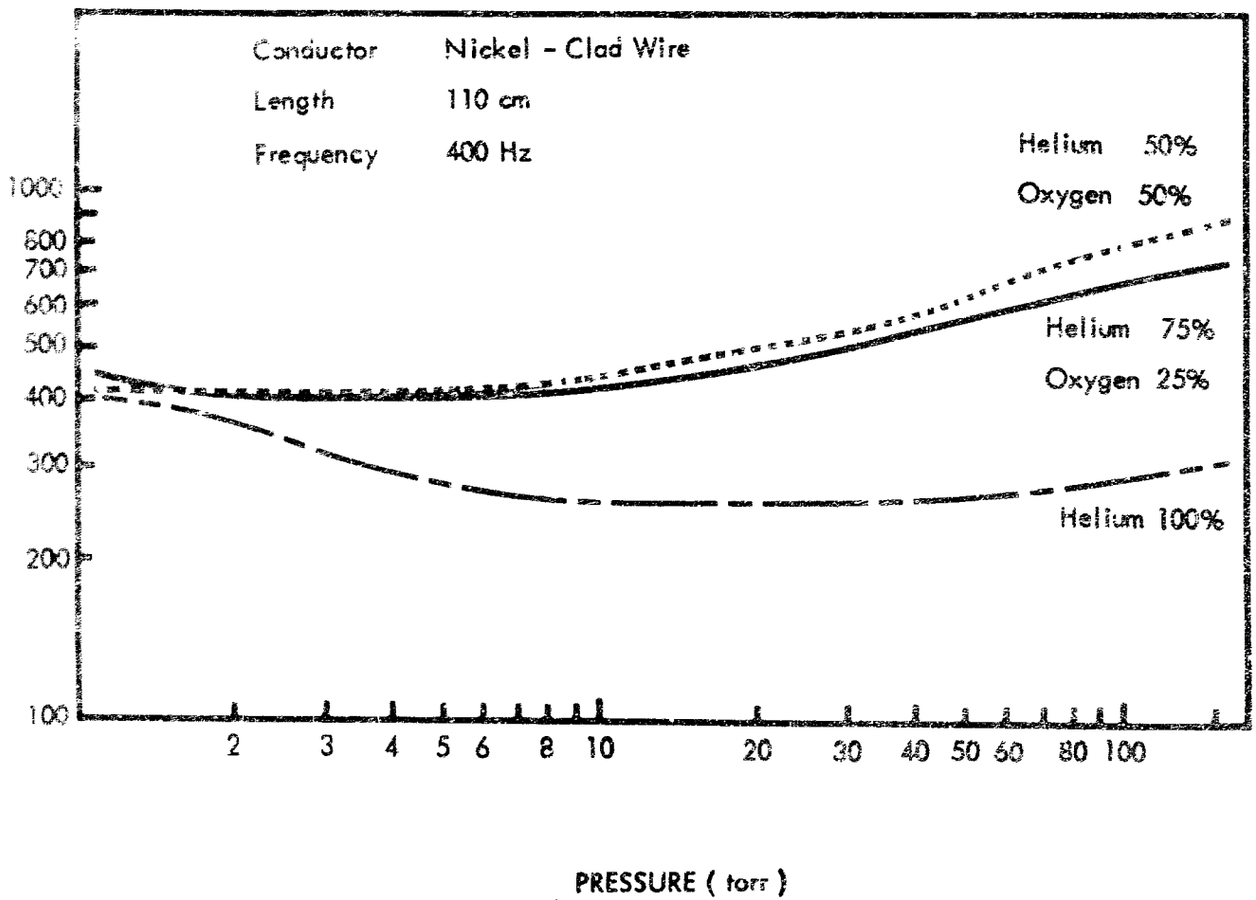

Figure III - 25: TEFLON INSULATED # 20 TWISTED WIRES IN HELIUM-- OXYGEN MIXTURES AT 24° C

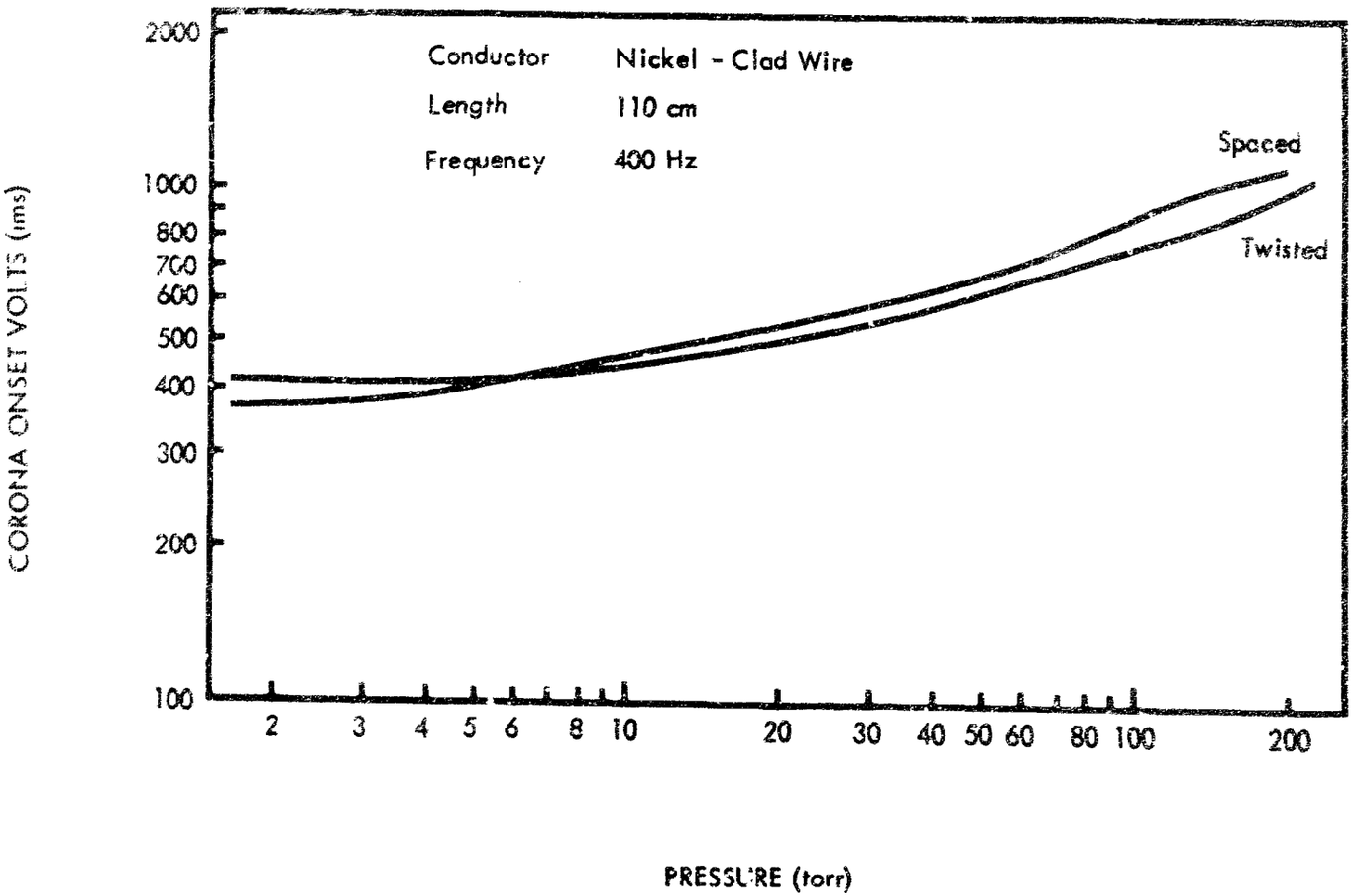

Figure III - 26: TEFLON INSULATED # 20 WIRES IN 50 - 50 HELIUM - OXYGEN MIXTURE AT 24° C

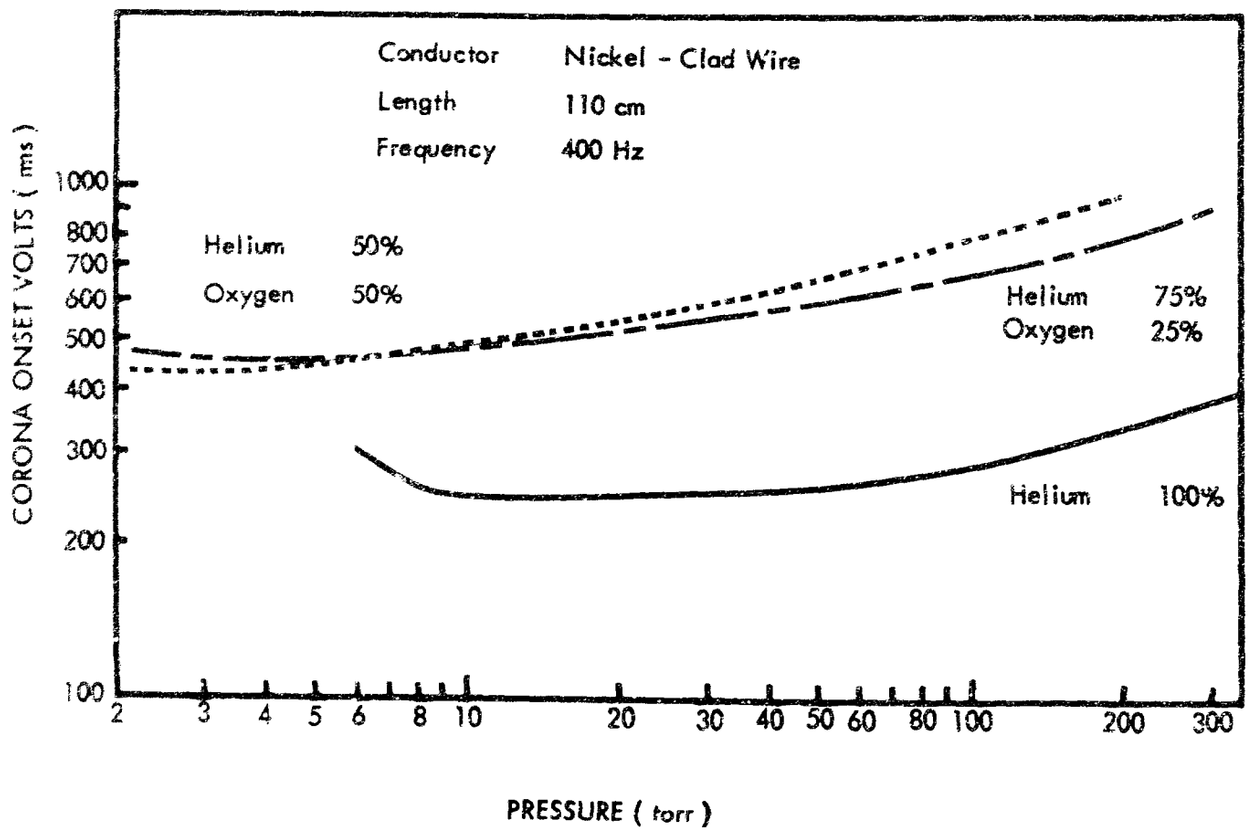

Figure III - 27: TEFLON INSULATED # 22 WIRES IN HELIUM - OXYGEN MIXTURES AT 24° C

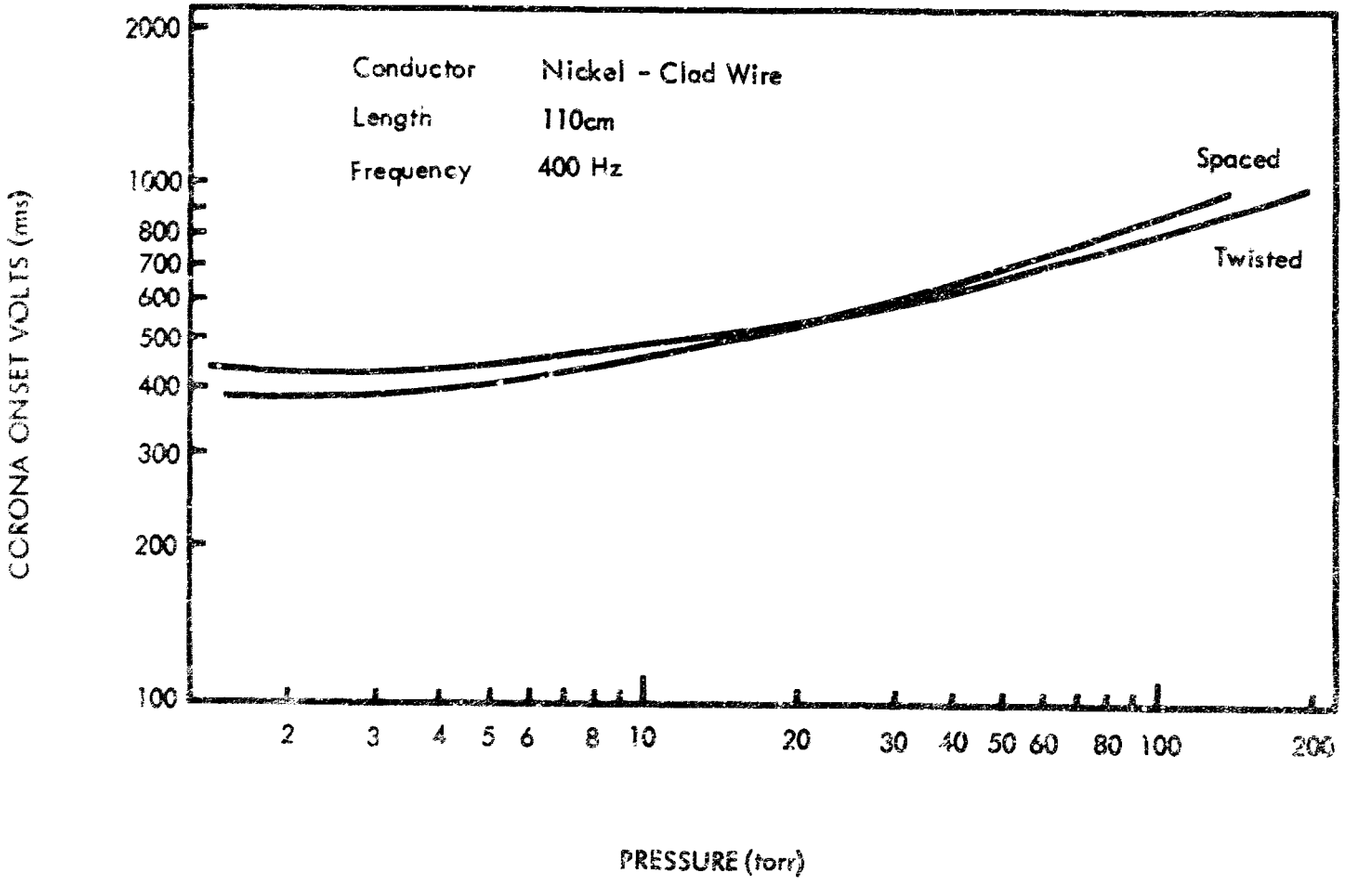

Figure III - 28: TEFLON INSULATED # 22 WIRES IN 50 - 50 HELIUM - OXYGEN MIXTURE AT 24° C

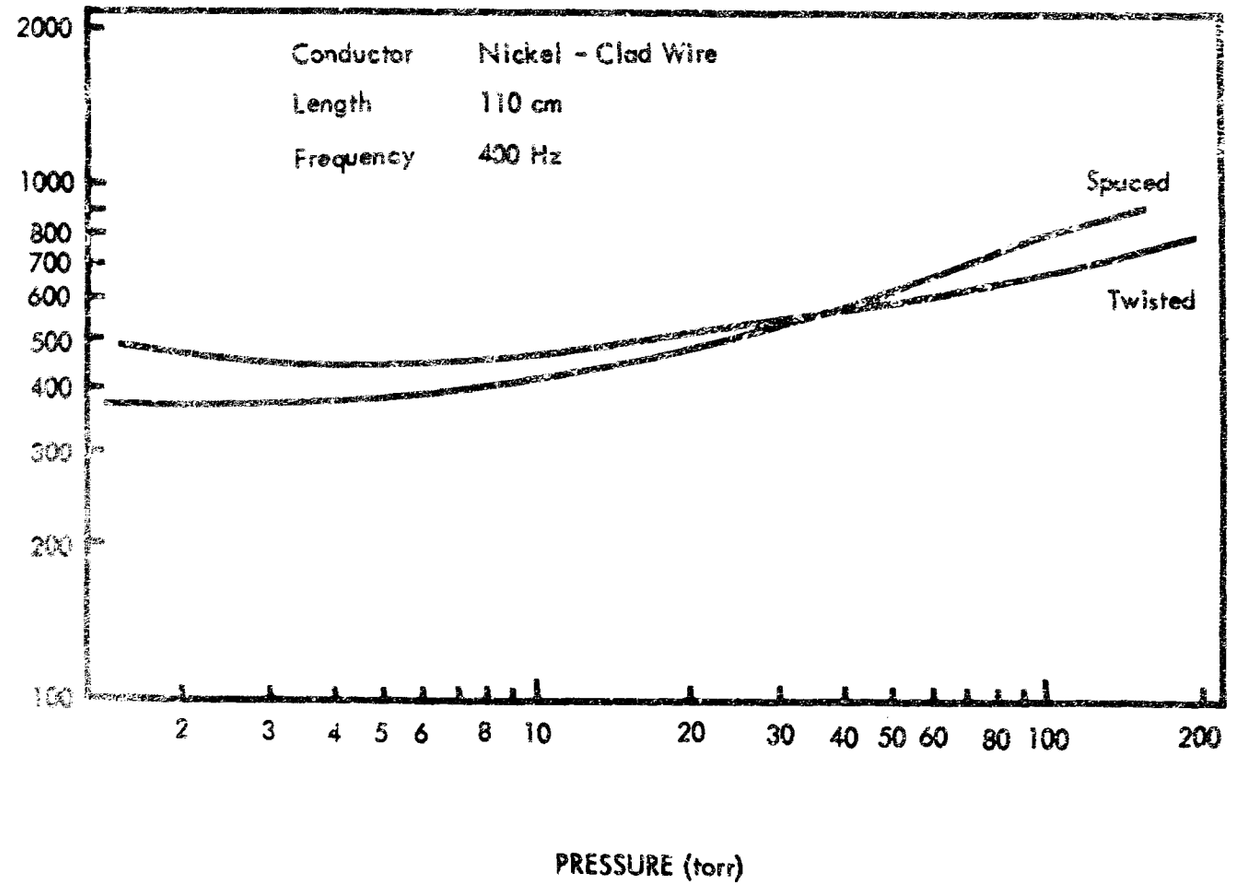

Figure III-29: TEFLON INSULATED # 22 WIRES IN 75 - 25 HELIUM - OXYGEN MIXTURE AT 24° C

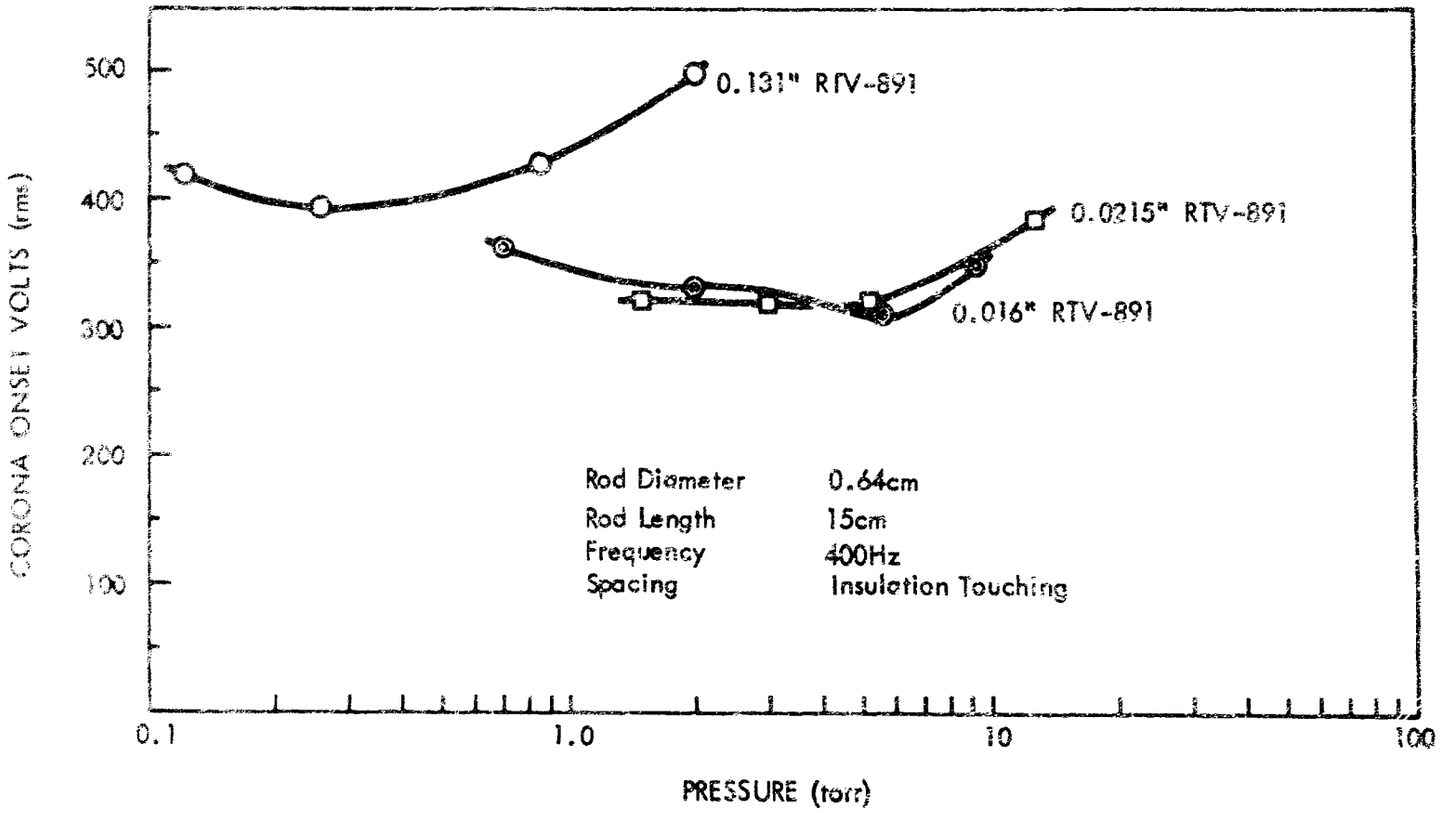

Figure III-30: RTV-RUBBER INSULATED BRASS RODS IN AIR AT 24°C

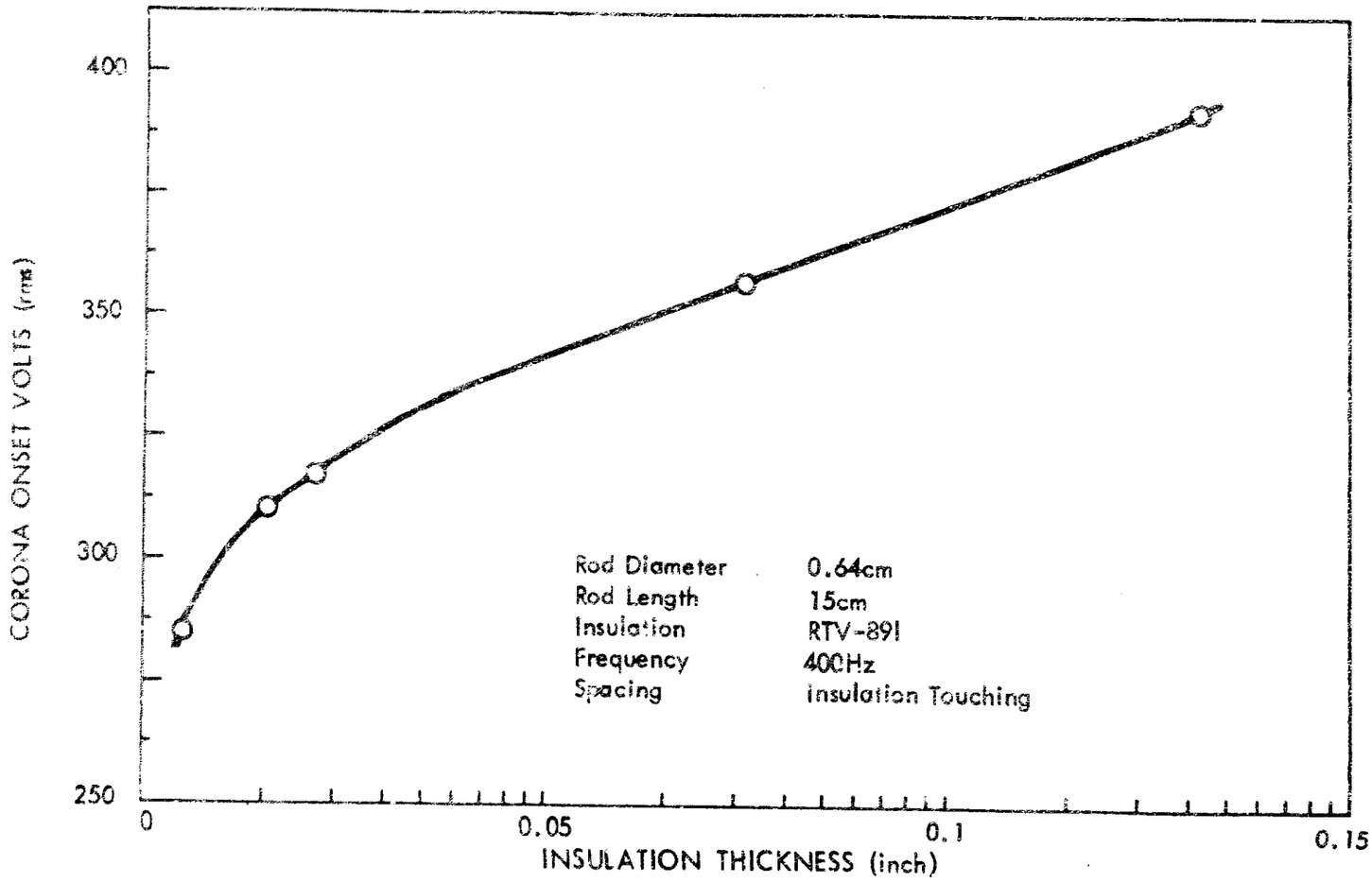

Figure III-31: CRITICAL COV BETWEEN RTV-RUBBER INSULATED RODS IN AIR AT 24°C

Table III-1: RELATION OF COV ACROSS INSULATED WIRES AND BARE ELECTRODES

Gas	Bare Electrode COV (Volts)	Insulated Wire COV (Volts)	Difference (Volts)
Helium	132	245	113
75% Helium 25% Oxygen	285	395	110
50% Helium 50% Oxygen	295	405	110
Air	232	340	108

Appendix IV

COMPONENT TESTS

The X-20A components were installed on a baseplate with terminals wired. In many cases it was discovered that the wire connection and installation established the corona onset voltage of the assembly. The special connector test, described in the text, shows the influence of wiring on the corona onset voltage of an installed connector.

The curves on the figures in this appendix are self-explanatory; they indicate the type of wiring and potting used. The wires for each test unit were closely bound to the ground planes of the component and to the vacuum-system baseplate. Furthermore, the spaced portions of the wire near the terminations and the terminations themselves were potted to limit corona in these areas. By wiring the components in this manner the corona onset voltage of the wiring was kept above 340 volts (rms); any lower corona onset voltages could be attributed to the component.

LIST OF FIGURES — APPENDIX IV

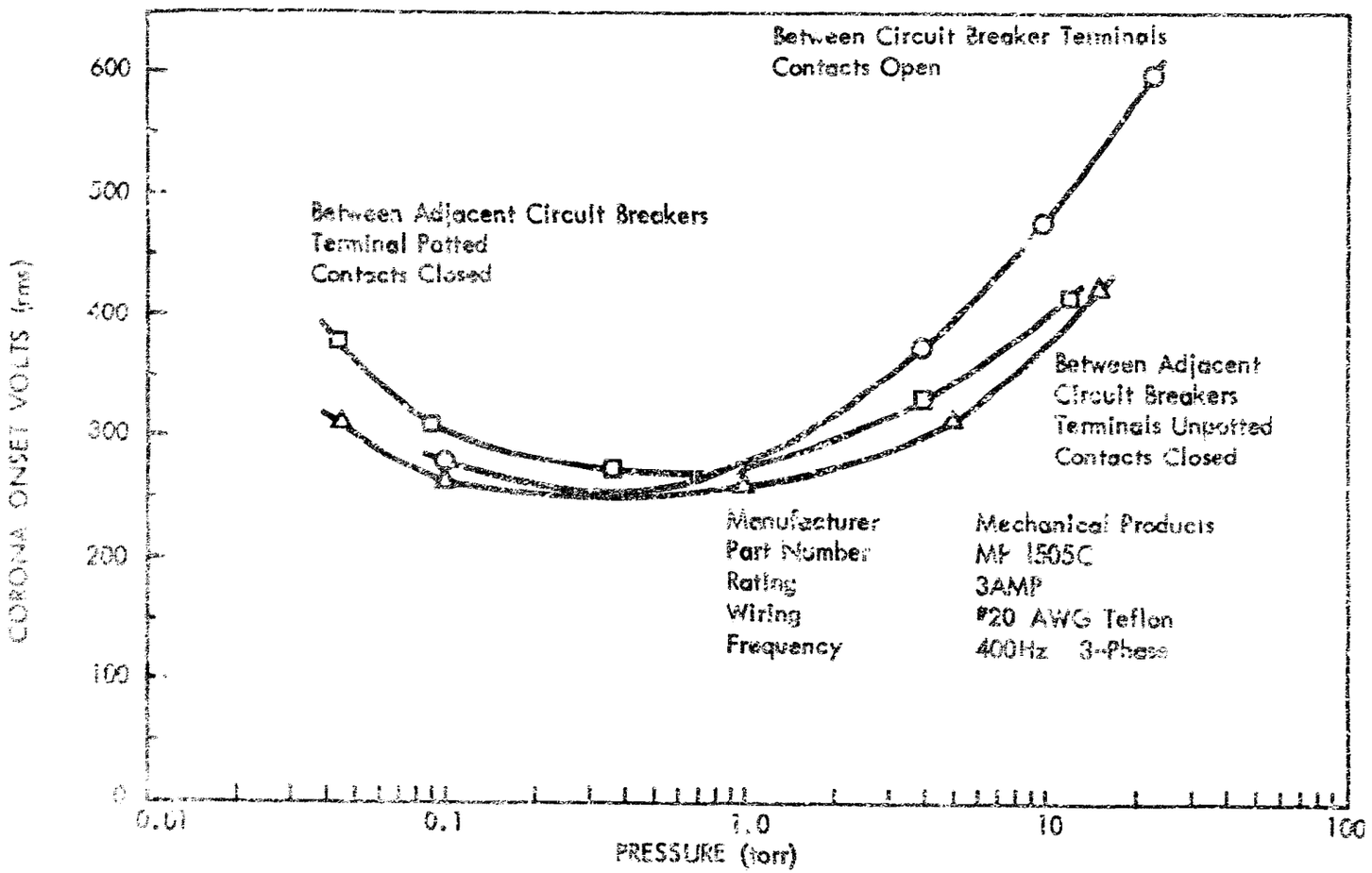

Figure IV-1: CIRCUIT BREAKER IN AIR AT 24°C

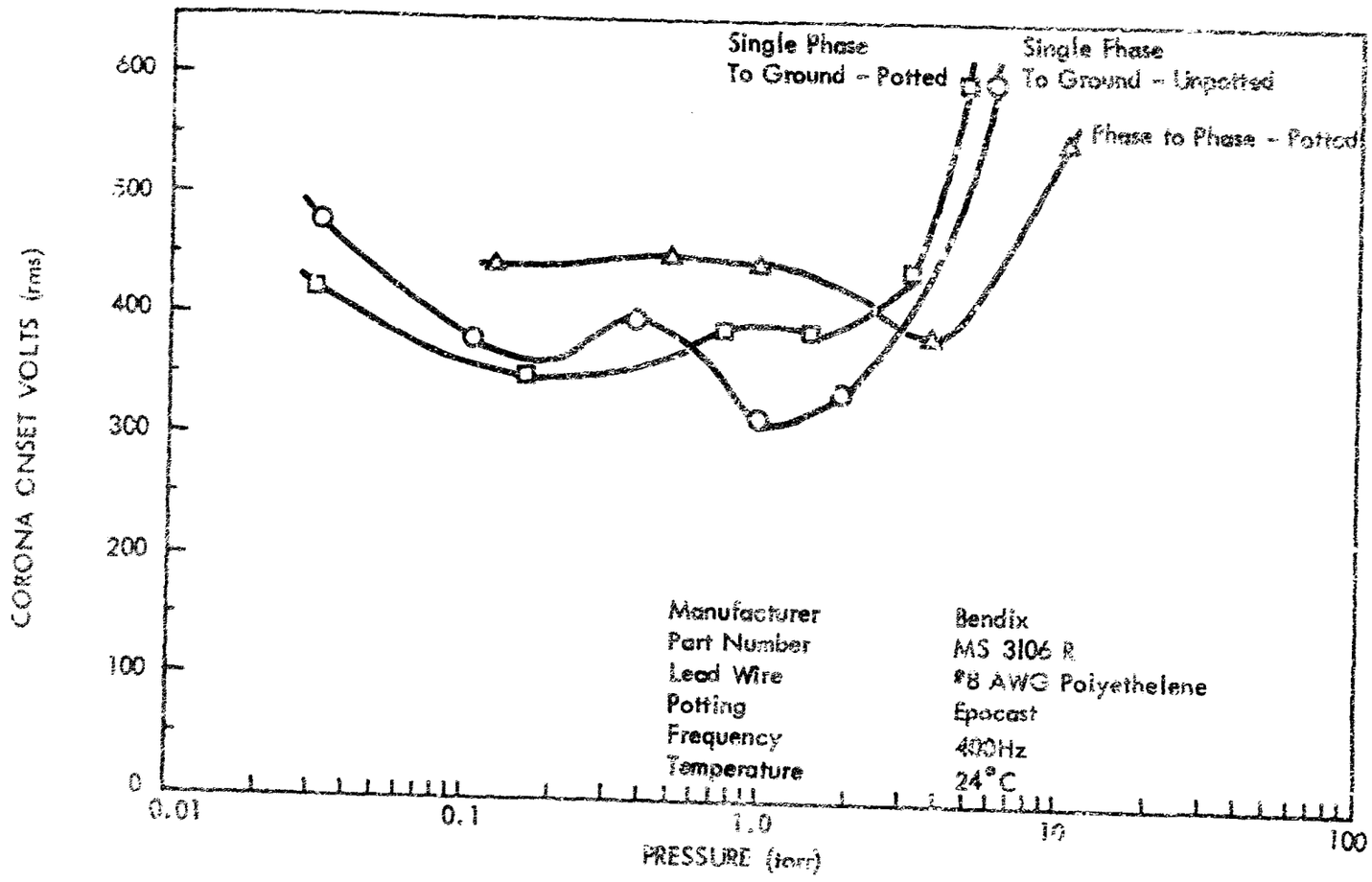

Figure IV-2. POWER CONNECTOR — 7-PINS

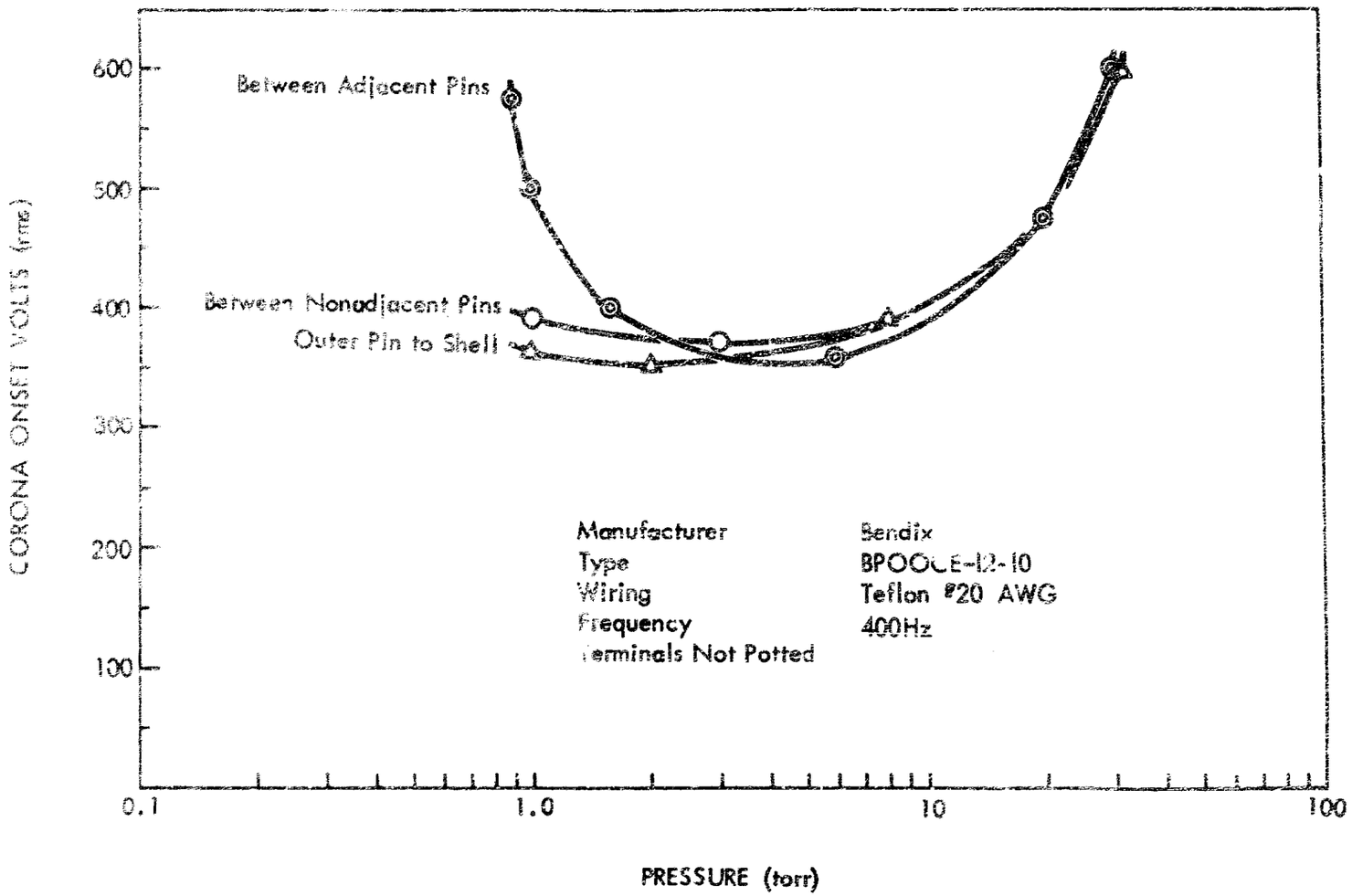

Figure IV-3: CONNECTOR — 10-PINS IN AIR AT 24°C

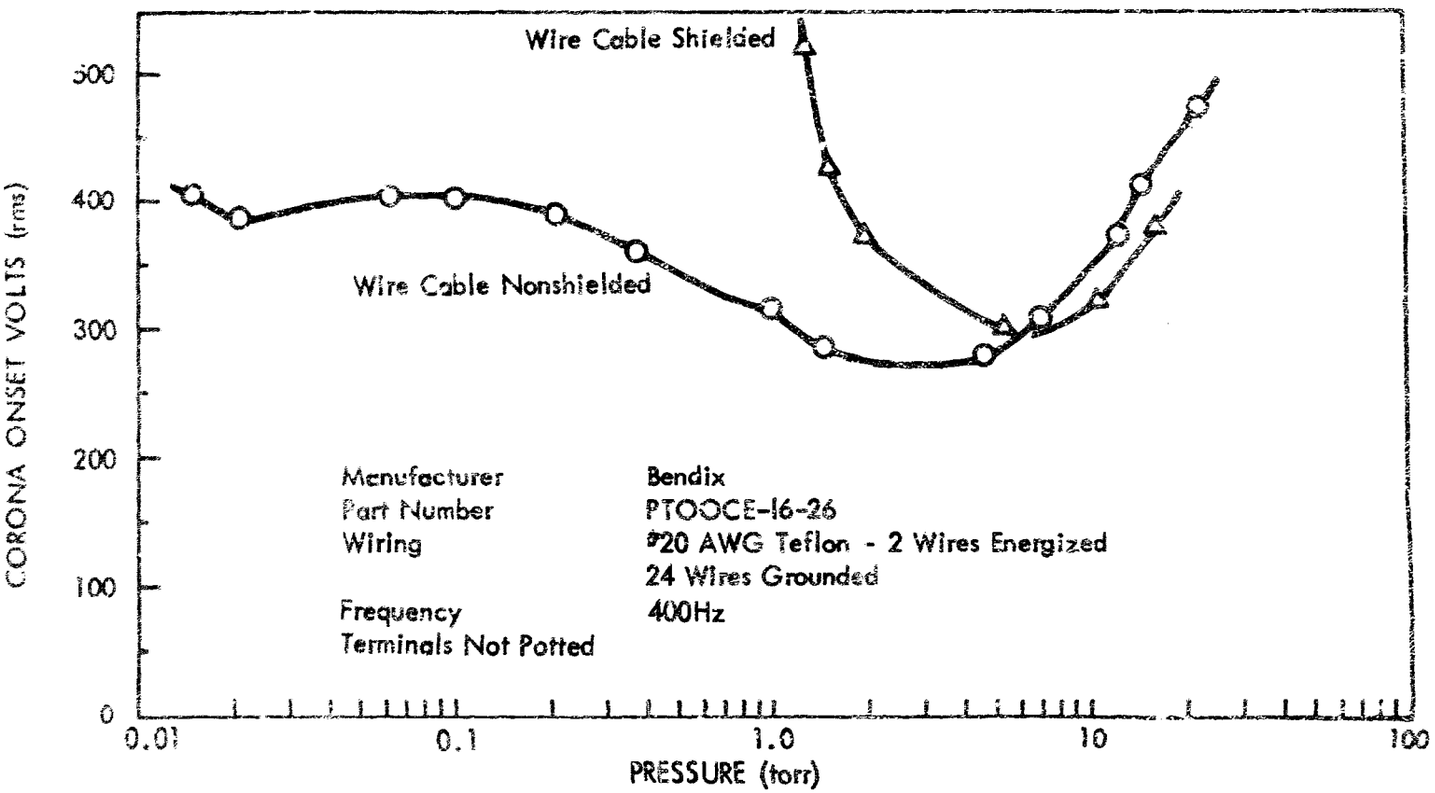

Figure IV-4: CONNECTOR — 26-PINS IN AIR AT 24°C

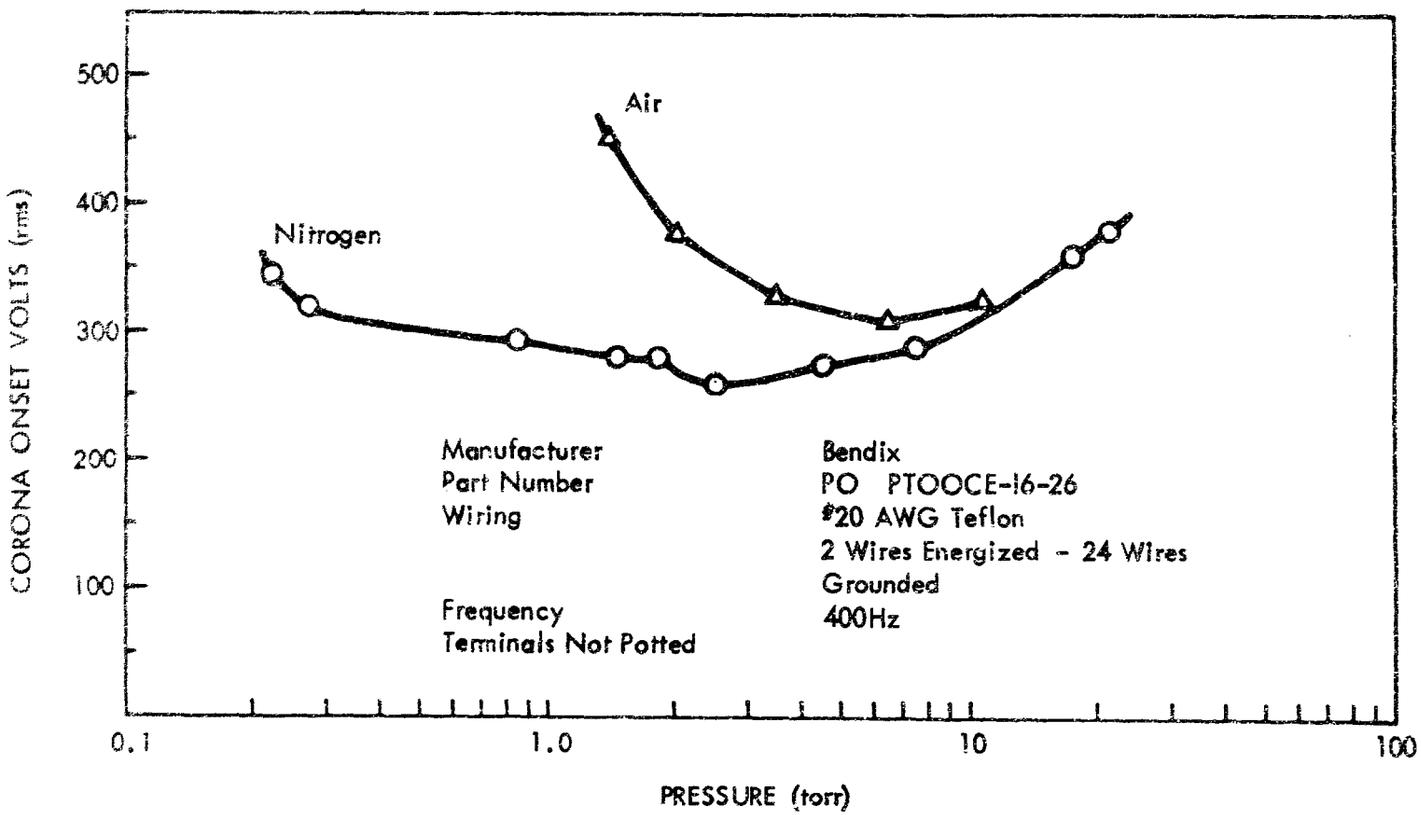

Figure IV-5: CONNECTOR — 26-PINS IN NITROGEN AT 24°C

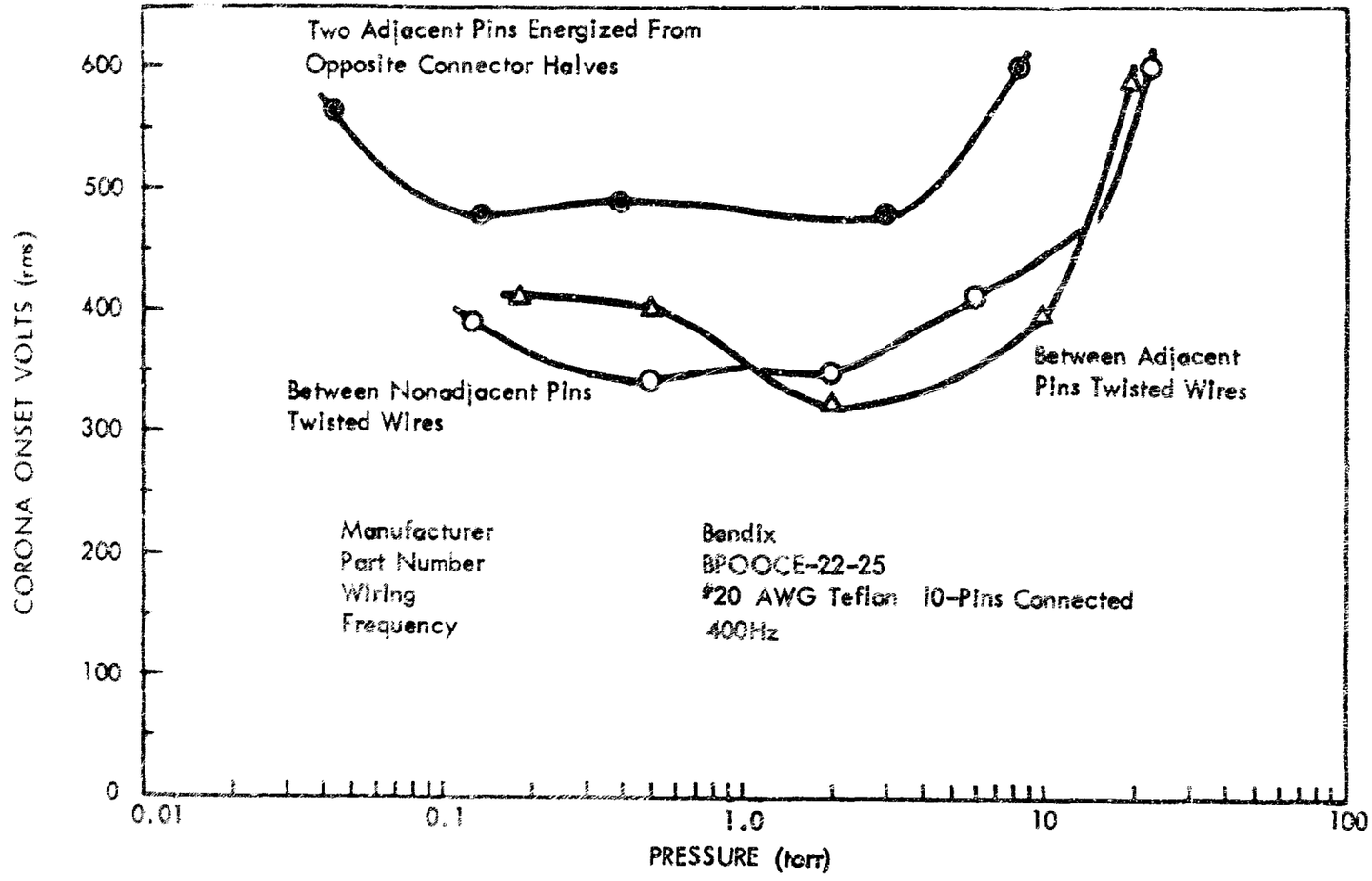

Figure IV-6: CONNECTOR — 55-PINS IN AIR AT 24°C TERMINALS NOT POTTED

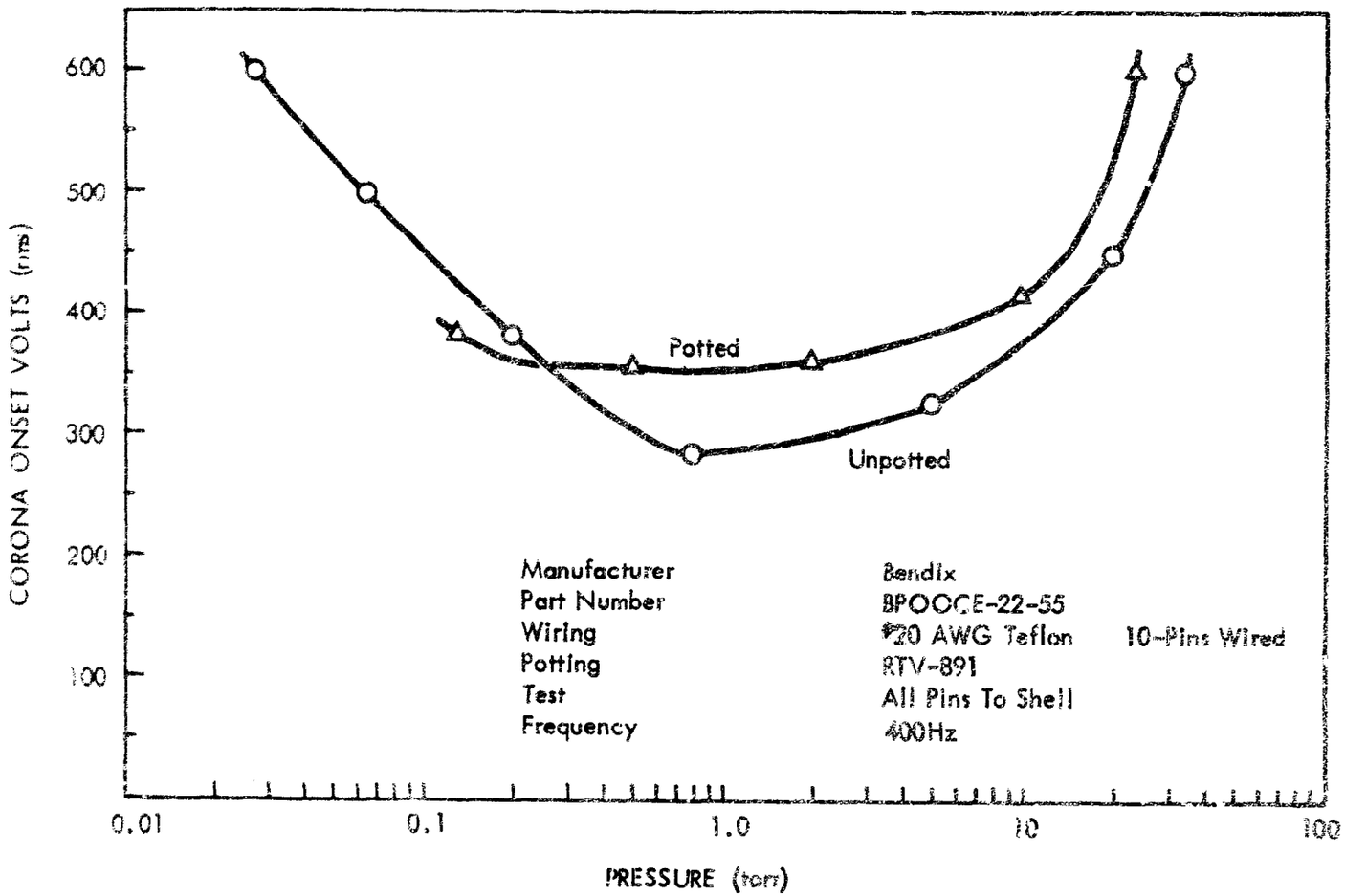

Figure IV-7: CONNECTOR TEST -- 55-PINS IN AIR AT 24°C TERMINALS POTTED

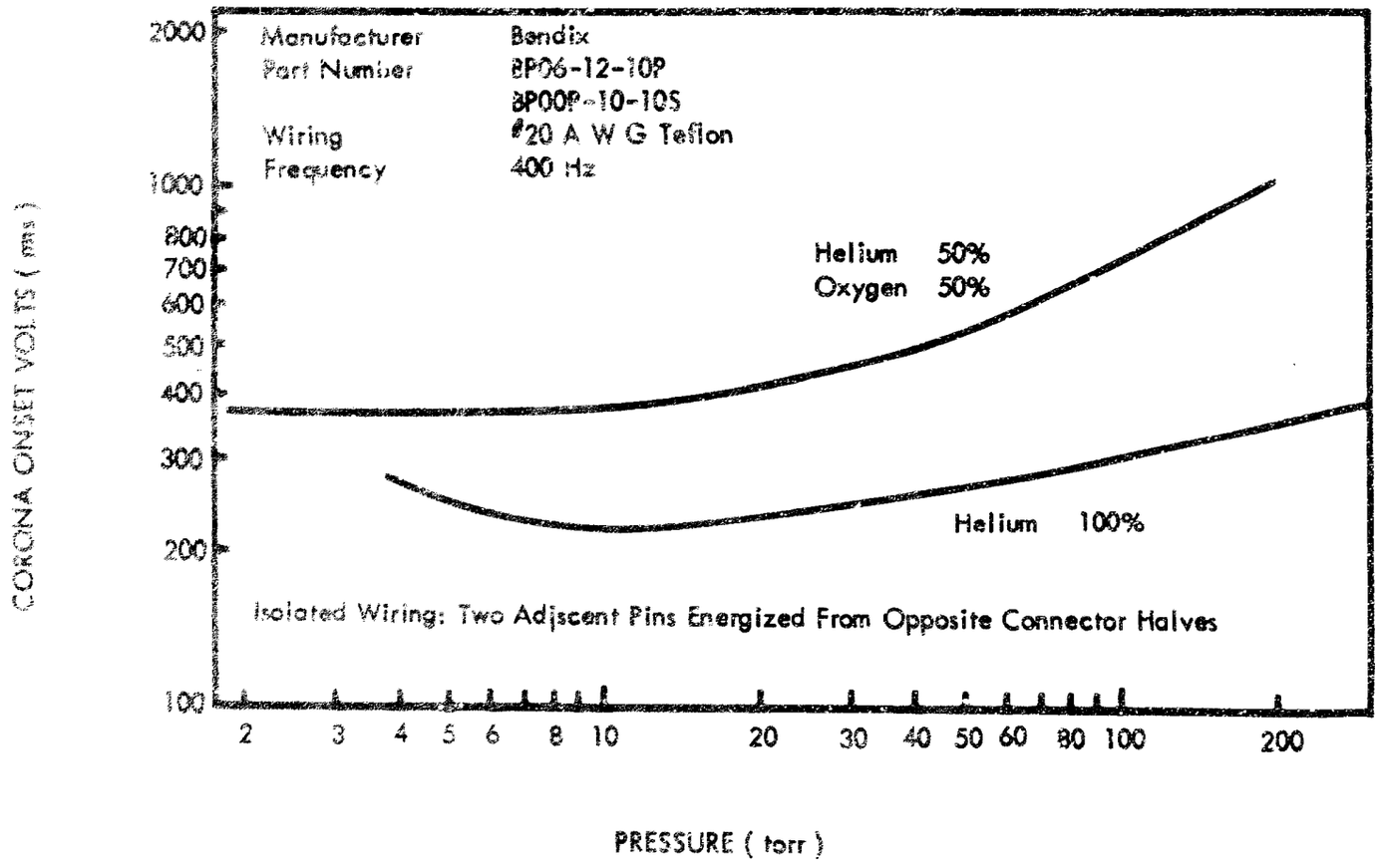

Figure IV - 8: CONNECTOR - 10 - PINS IN HELIUM - OXYGEN MIXTURES AT 24°C TERMINALS UNPOTTED, ISOLATED WIRING

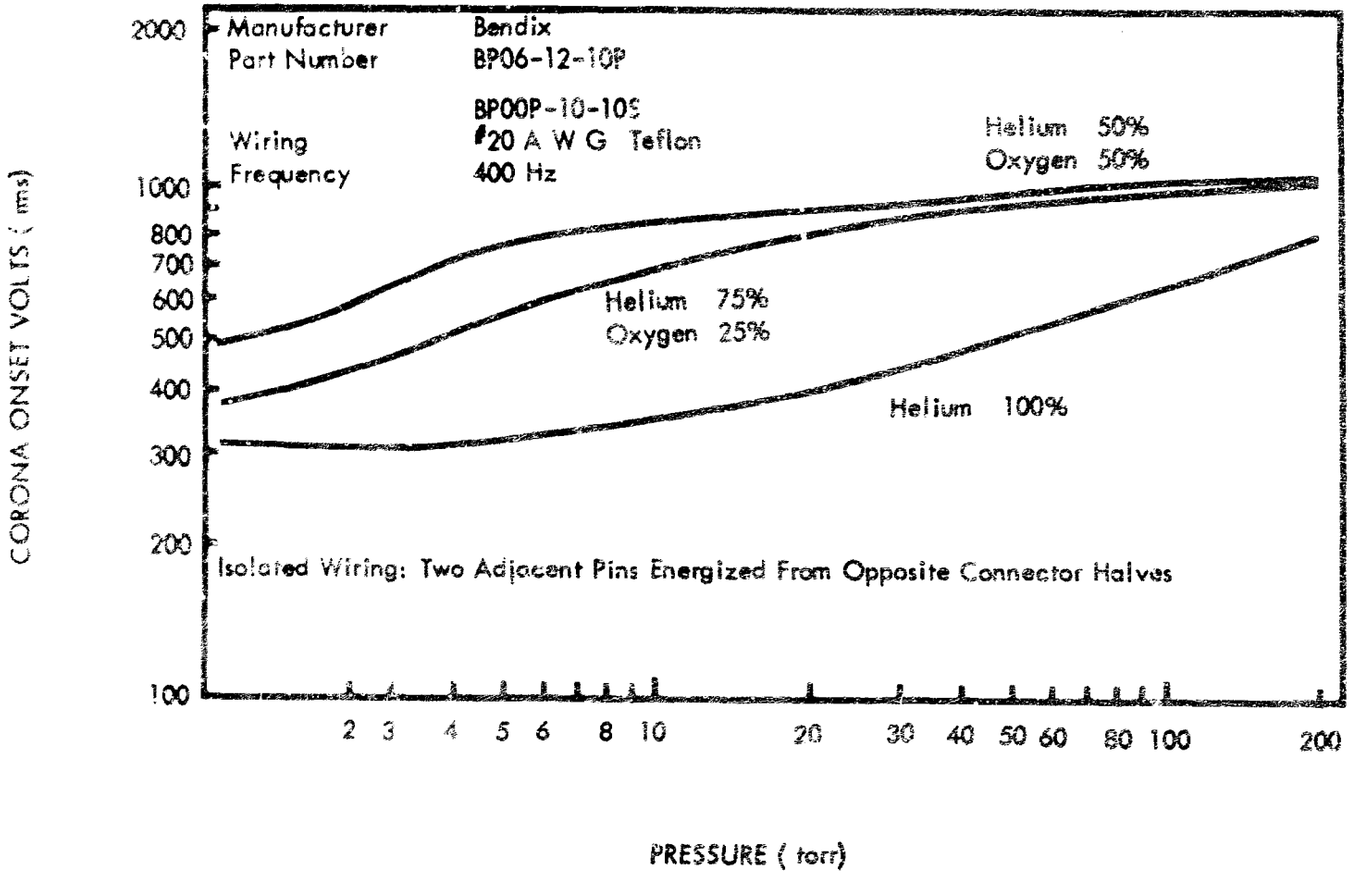

Figure IV - 9. CONNECTOR - 10 - PINS IN HELIUM - OXYGEN MIXTURES AT 24° C
TERMINALS POTTED, ISOLATED WIRING

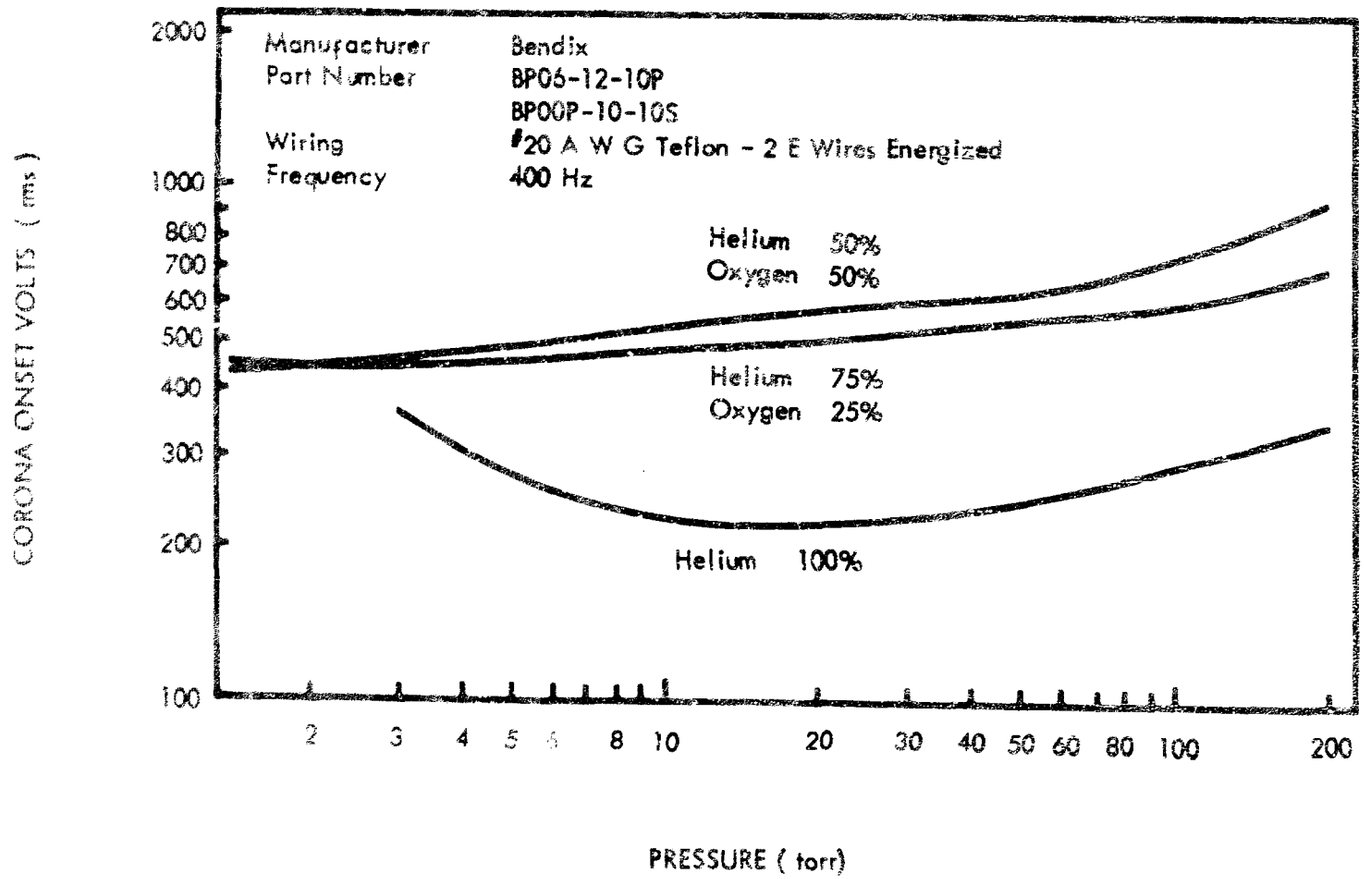

Figure IV - 10: CONNECTOR - 10 - PINS IN HELIUM - OXYGEN MIXTURES AT 24° C TERMINALS POTTED, NORMAL WIRING

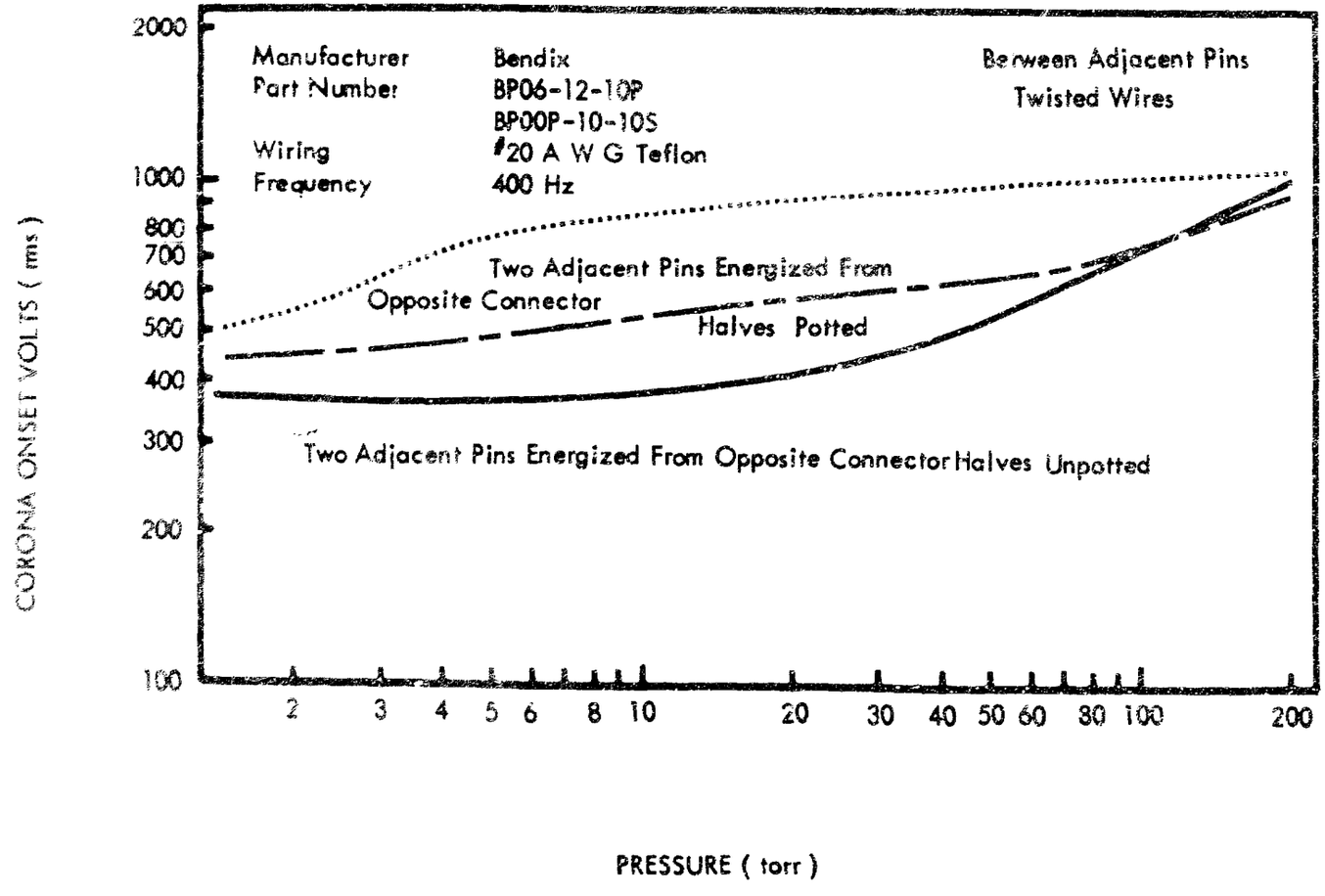

Figure IV - 11: CONNECTOR - 10 - PINS IN 50 - 50 PERCENT HELIUM - OXYGEN MIXTURE AT 24° C

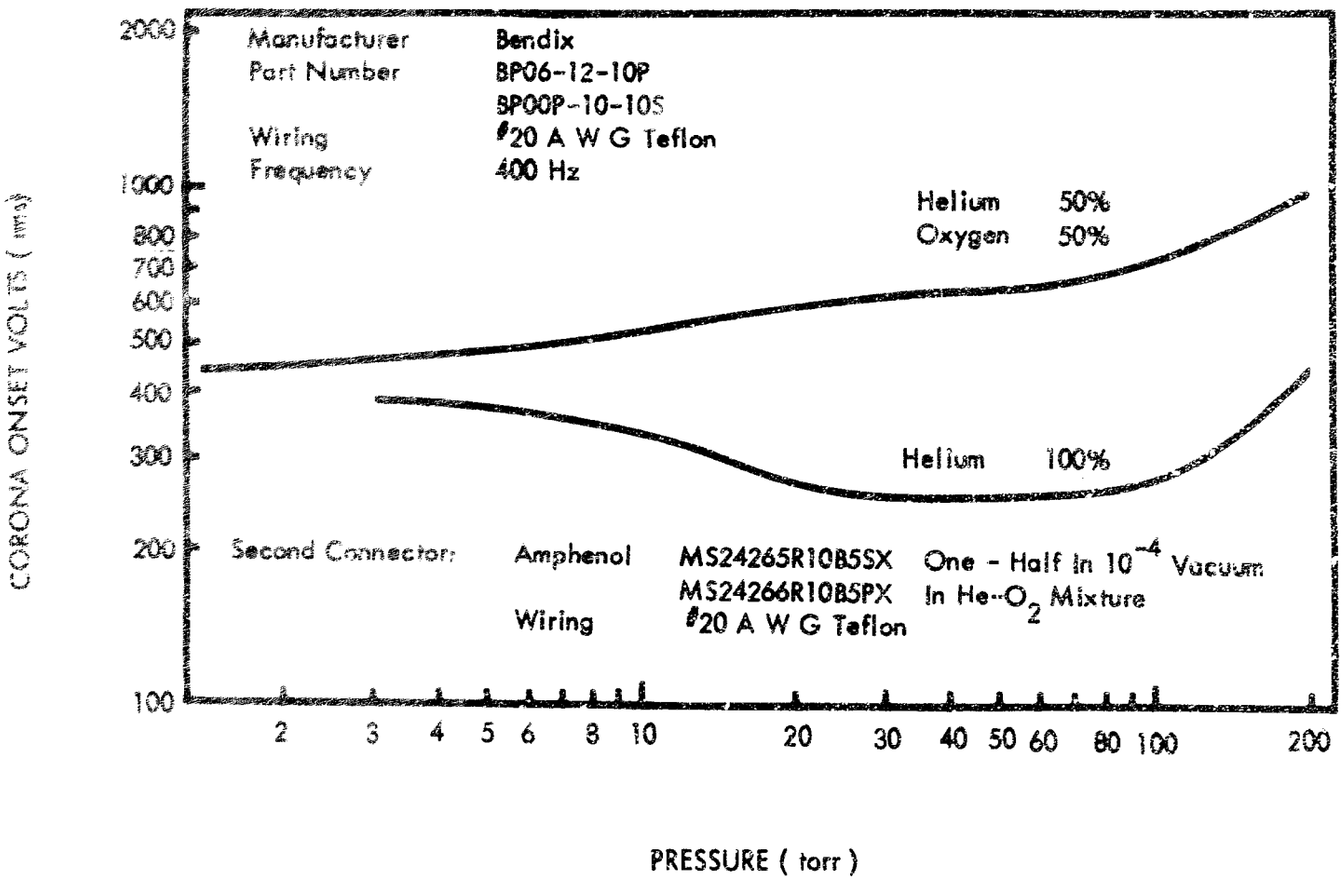

Figure IV - 12: CONNECTOR SYSTEM IN HELIUM - OXYGEN MIXTURES AT 24° C

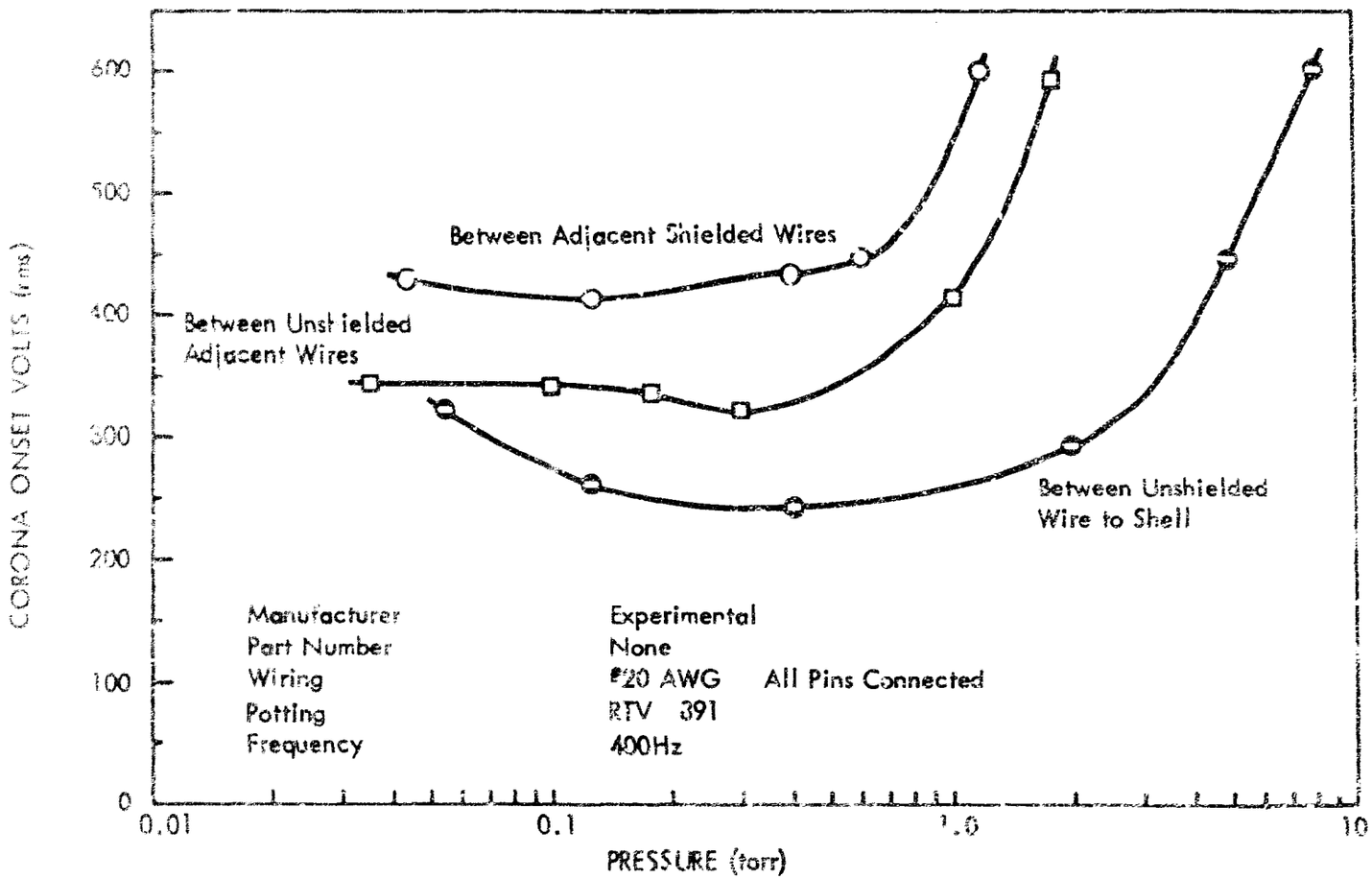

Figure IV-13: EXPERIMENTAL FEEDTHROUGH — 73-PINS IN AIR AT 24°C

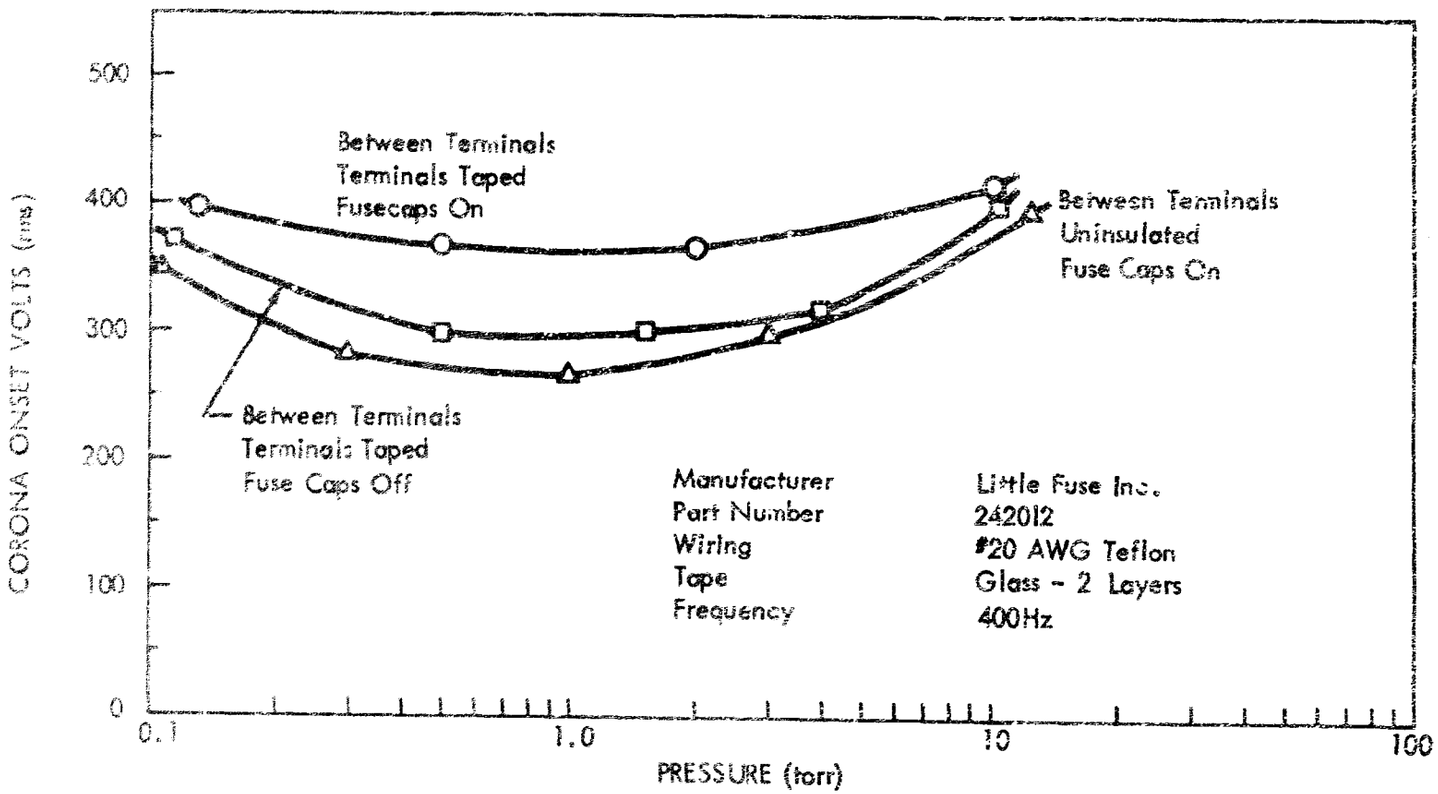

Figure IV-14: SINGLE FUSE HOLDER IN AIR AT 24°C — NO FUSES

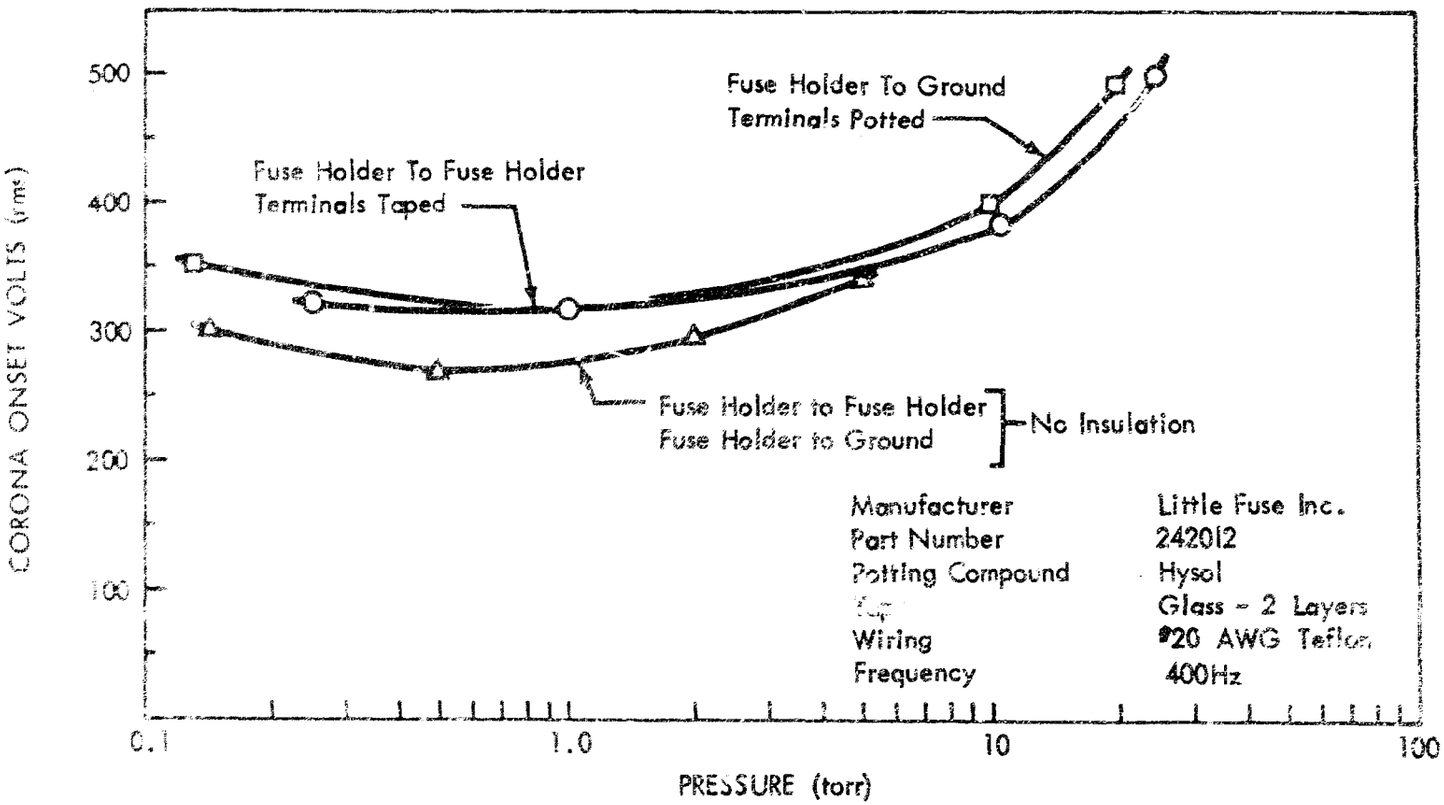

Figure IV-15: FUSE PANEL — 9-FUSE HOLDERS IN AIR AT 24°C

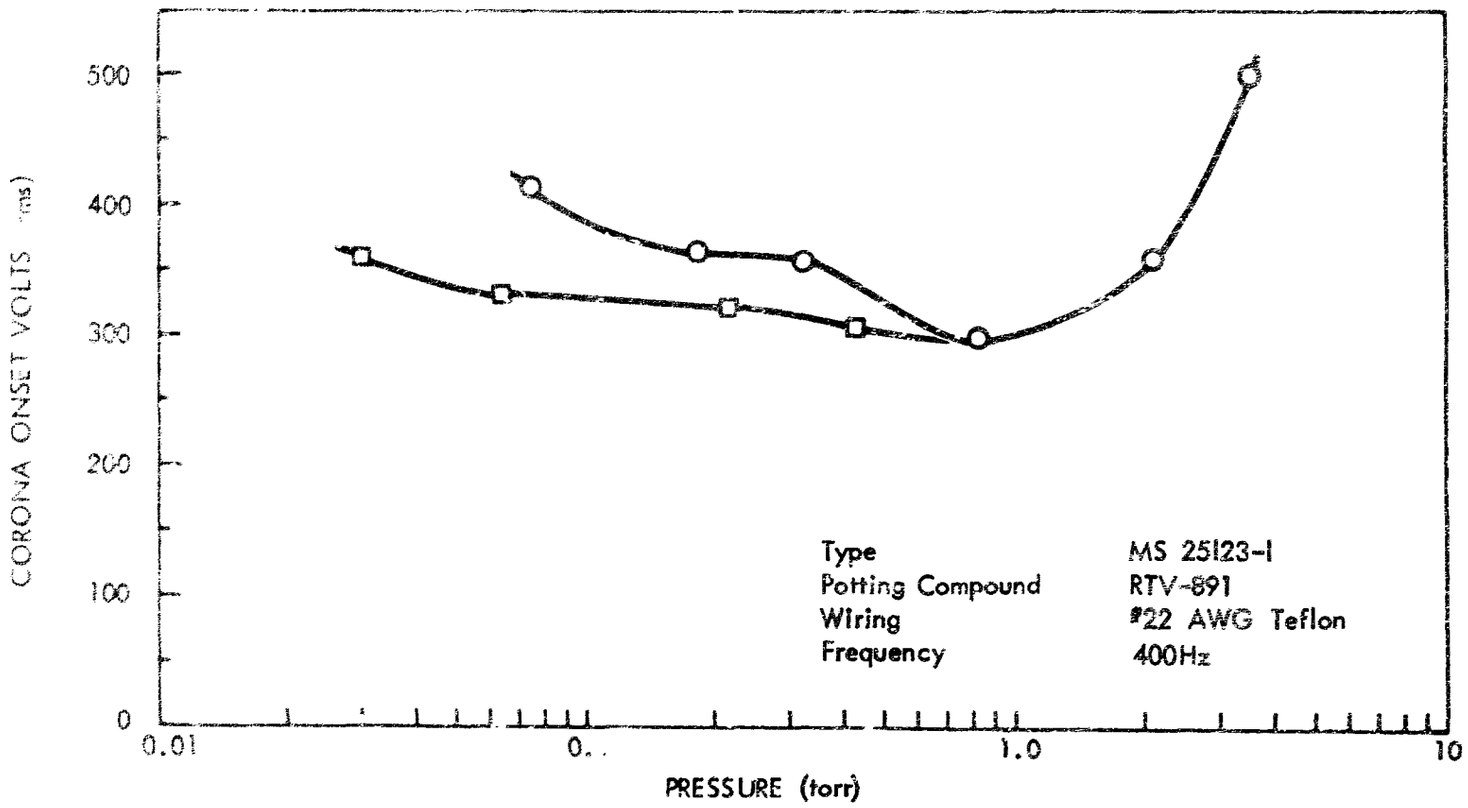

Figure IV-16: TERMINAL STRIP IN AIR AT 24°C

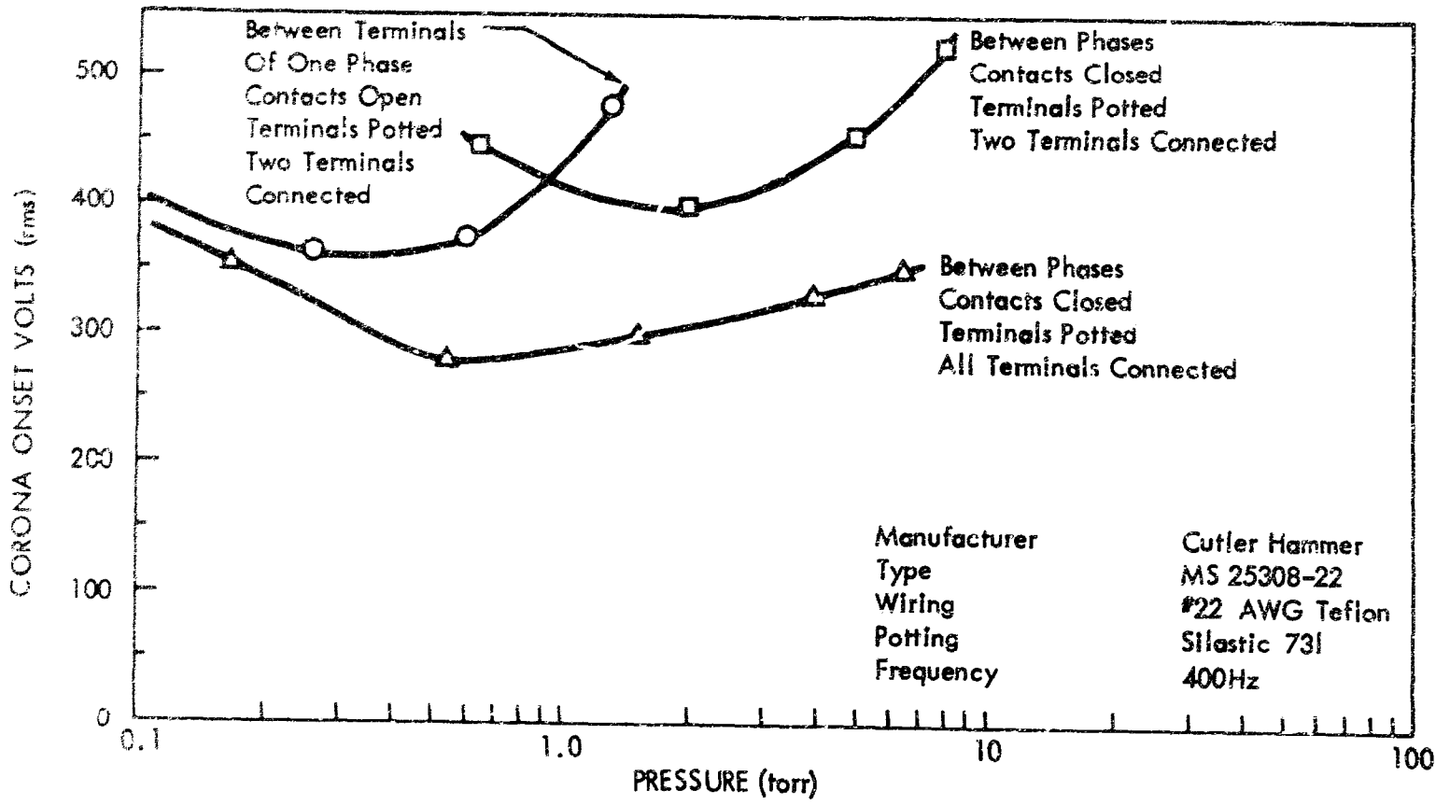

Figure IV-17: TOGGLE SWITCH IN AIR AT 24°C

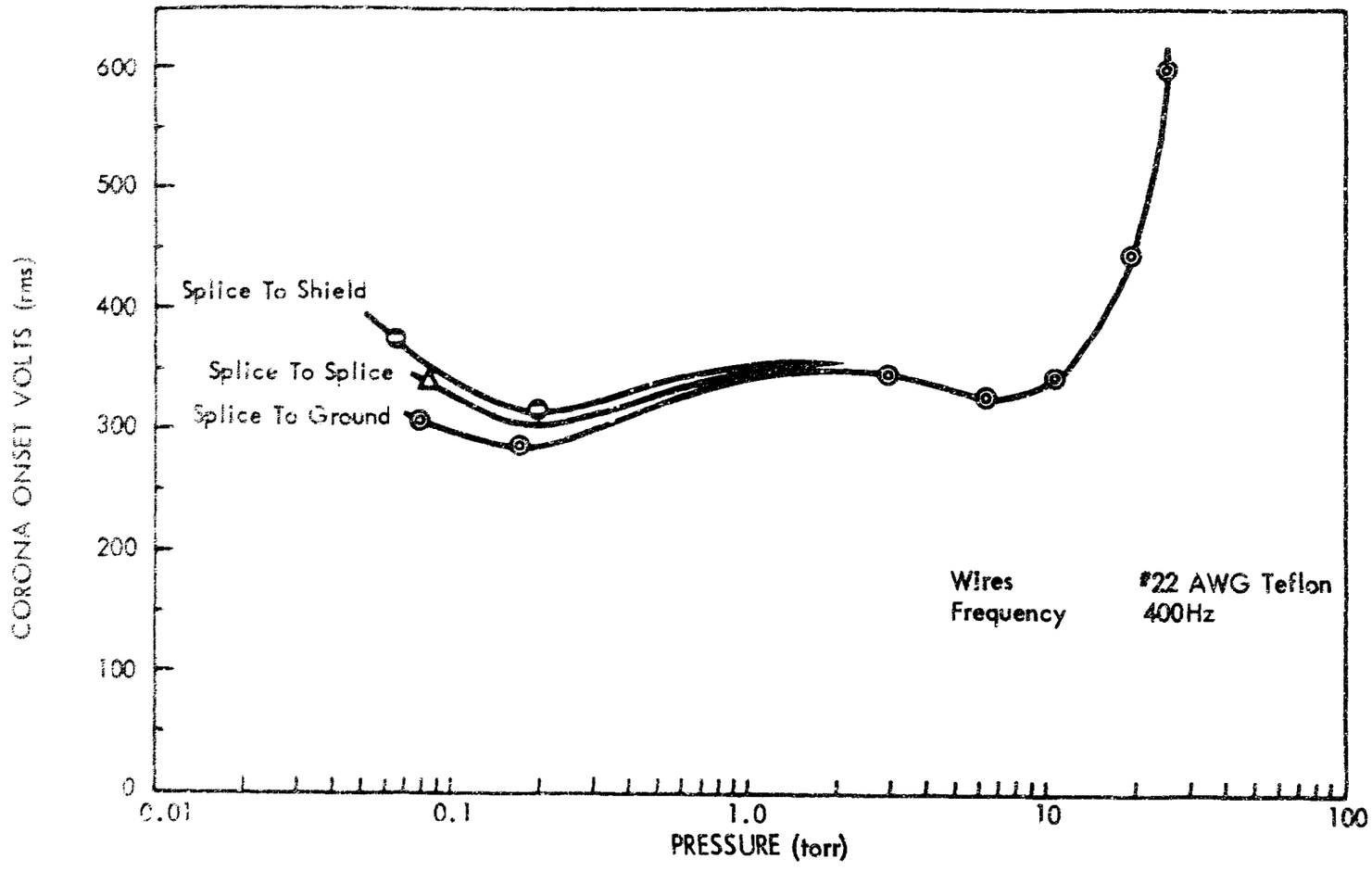

Figure IV-18: WIRE SPLICES IN AIR AT 24°C

Appendix V

U. S. STANDARD ATMOSPHERE

Part of the U. S. Standard Atmosphere for 1962 (Ref. 8) is given in this appendix. The parameters used most in corona work are presented; altitude in feet and meters, pressure in torr, and temperature in degrees Celsius.

Table V-1: ATMOSPHERE ALTITUDE TEMPERATURE PRESSURE

Altitude (feet)	Altitude (meters)	Temperature (°C)	Pressure (torr)
0	0	15.000	760.0000
2,000	609.6	11.038	706.6575
4,000	1,219.2	7.077	656.4012
6,000	1,828.8	3.116	609.0861
8,000	2,438.4	-0.844	564.5802
10,000	3,048.0	-4.803	522.7516
12,000	3,657.6	-8.761	483.4756
14,000	4,267.2	-12.718	446.6330
16,000	4,876.8	-16.675	412.1017
18,000	5,486.4	-20.631	379.7727
20,000	6,096.0	-24.586	349.5340
22,000	6,705.6	-28.540	321.2791
24,000	7,315.2	-32.494	294.9088
26,000	7,924.8	-36.447	270.3217
28,000	8,534.4	-40.399	247.4277
30,000	9,144.0	-44.351	226.1331
32,000	9,753.6	-48.301	206.3508
34,000	10,363.2	-52.251	187.9973
36,000	10,972.8	-56.200	170.9918
38,000	11,582.4	-56.500	155.3739
40,000	12,192.0	-56.500	141.1842
42,000	12,801.6	-56.500	128.2929
44,000	13,411.2	-56.500	116.5808
46,000	14,020.8	-56.500	105.9397
48,000	14,630.4	-56.500	96.2717
50,000	15,240.0	-56.500	87.4876
52,000	15,849.6	-56.500	79.5067
54,000	16,459.2	-56.500	72.2548
56,000	17,068.8	-56.500	65.6658
58,000	17,678.4	-56.500	59.6787
60,000	18,288.0	-56.500	54.2383
62,000	18,897.6	-56.500	49.2950
64,000	19,507.2	-56.500	44.8030
66,000	20,116.8	-56.447	40.7210
68,000	20,726.4	-55.841	37.0174
70,000	21,336.0	-55.235	33.6603
72,000	21,945.6	-54.630	30.6161
74,000	22,555.2	-54.025	27.8551
76,000	23,164.8	-53.419	25.3502
78,000	23,774.4	-52.814	23.0769

Table V-1: (Continued)

Altitude (feet)	Altitude (meters)	Temperature (°C)	Pressure (torr)
80,000	24,384.0	-52.209	21.0133
82,000	24,993.6	-51.604	19.1394
84,000	25,603.2	-51.000	17.4374
86,000	26,212.8	-50.395	15.8911
88,000	26,822.4	-49.790	14.4858
90,000	27,432.0	-49.186	13.2083
92,000	28,041.6	-48.582	12.0466
94,000	28,651.2	-47.977	10.9901
96,000	29,260.8	-47.373	10.0288
98,000	29,870.4	-46.769	9.1540
100,000	30,480.0	-46.165	8.3577
110,000	33,528.0	-40.714	5.3285
120,000	36,576.0	-32.273	3.4481
130,000	39,624.0	-23.840	2.2659
140,000	42,672.0	-15.415	1.5106
150,000	45,720.0	- 6.998	1.0206
160,000	48,768.0	- 2.500	6.9740×10^{-1}
170,000	51,816.0	- 2.500	4.7754
180,000	54,864.0	- 7.280	3.2622
190,000	57,912.0	-13.178	2.2104
200,000	60,960.0	-19.262	1.4848
210,000	64,008.0	-29.979	9.8528×10^{-2}
220,000	67,056.0	-41.924	6.4082
230,000	70,104.0	-53.857	4.0756
240,000	73,152.0	-65.779	2.5285
250,000	76,200.0	-77.69	1.5256
260,000	79,248.0	-89.59	8.9222×10^{-3}
270,000	82,296.0	-92.50	5.0917
280,000	85,344.0	-92.50	2.9040
290,000	88,392.0	-92.50	1.6572
300,000	91,440.0	-88.20	9.4915×10^{-4}
310,000	94,488.0	-79.15	5.5656
320,000	97,536.0	-70.22	3.3464
330,000	100,584.0	-60.30	2.0592
340,000	103,632.0	-45.71	1.3049
350,000	106,680.0	-31.41	8.5196×10^{-5}
360,000	109,728.0	-17.39	5.7102
370,000	112,776.0	9.96	3.9502
380,000	115,824.0	38.24	2.8364
390,000	118,872.0	66.12	2.0999

Table V-1: (Continued)

Altitude (feet)	Altitude (meters)	Temperature (°C)	Pressure (torr)
400,000	121,920.0	112.19	1.6014
410,000	124,968.0	168.61	1.2677
420,000	128,016.0	224.50	1.0334
430,000	131,064.0	279.98	8.6182×10^{-6}
440,000	134,112.0	335.13	7.3200
450,000	137,160.0	390.05	6.3106
460,000	140,208.0	444.81	5.5090
470,000	143,256.0	499.41	4.8598
480,000	146,304.0	553.87	4.3264
490,000	149,352.0	608.13	3.8816
500,000	152,400.0	651.01	3.5050
600,000	182,880.0	897.32	1.5030
700,000	213,360.0	1002.06	7.4221×10^{-7}
800,000	243,840.0	1073.52	3.9520
900,000	274,320.0	1122.99	2.2193
1,000,000	304,800.0	1162.53	1.3027
1,500,000	457,720.0	1216.20	1.4029×10^{-8}
2,000,000	609,600.0	1232.69	2.3292×10^{-9}

REFERENCES

1. Hagenguth, J. H. and Liao, T. W., "Impulse Corona-Detection, Measurement of Intensity and Damage Produced," A.I.E.E. Technical Paper No. 52-105, 1952.

2. Manning, M. L., "New Concepts in Evaluating Electric Equipment Insulation Systems - The Problems Encountered," Paper No. 57-392, A.I.E.E. Transactions, Part I, Vol. 76, 1957.

3. Meek, J. M. and Craggs, J. D., Electrical Breakdown of Gases, Oxford University Press, London, England, 1953.

4. Loeb, L. B., Fundamental Processes of Electrical Discharges in Gases, Wiley, New York, 1939.

5. Mankin, Arthur H., "Corona Suppression Methods," Electrical Manufacturing, Vol. 47, June 1951.

6. Devins, J. C., "High Frequency Pulses Occurring in 60 Cycle Discharges in Dielectric Voids," Annual Report, National Research Council Conference on Electrical Insulation, 1954.

7. Mackenzie, K. J. and Ward, R. A., "Irradiated Polyethylene Insulation Systems," Electrical Manufacturing, Vol. 61, January 1958.

8. U. S. Standard Atmosphere, 1962, NASA, USAF, and U. S. Weather Bureau, 1962.

9. Halleck, M. C., "Calculation of Corona Starting Voltage in Air-Solid Dielectric Systems," A.I.E.E., Vol. 75, Part III, 1956.

10. Mercier, C. E. and Elliott, W. E., "Analysis and Elimination of Corona Effects," Electrical Manufacturing, Vol. 60, No. 5, November 1957.

11. Dakin, T. W. and Lim, J., "Corona Measurement and Interpretation," A.I.E.E. Paper No. 57-690, 1957.

12. Manning, M. L., "Experience with the A.I.E.E. Subcommittee Test Cell for Gaseous Insulation," A.I.E.E. Transaction, Paper No. 59-114, 1959.

13. Engel, A. von, Ionized Gases, Oxford University Press, London, 1955.

14. Loeb, L. B., Basic Processes of Gaseous Electronics, University of California Press, Berkeley, 1955.

15. Druyvesteyn, M. J. and Penning, F. M., "The Mechanism of Electrical Discharges in Gases of Low Pressure," Review of Modern Physics, Vol. 12, No. 2, 1940.

16. Penning, F. M., Electrical Discharges in Gases, The Macmillan Company, New York, New York, 1957.

17. Jones, F. L., Ionization and Breakdown in Gases, John Wiley and Son, 1957.

18. Roth, E. M., "Space Cabin Atmospheres, Part III - Physiological Factors of Inert Gases," Lovelace Foundation, Albuquerque, New Mexico, 1965.

19. Breeze, R. K., "Space Vehicle Environmental Control Requirements Based on Equipment and Physiological Criteria," ASD Technical Report 61-161A, Part 1, Flight Accessories Laboratory, Aeronautical System Division, Wright-Patterson Air Force Base, Ohio.

20. Roth, E. M., "Medical Considerations in the Selection of Space Cabin Atmospheres," Presented at American Chemical Society, Symposium on Atmosphere in Space Cabins, September 13, 1965, Atlantic City, New Jersey.

21. Mason, J. L., "The Two-Gas Spacecraft Cabin Atmosphere," Document SS-3223, Airesearch Manufacturing Company, December 1964, Los Angeles, California.

22. Roth, E. M., "Selection of Space Cabin Atmosphere, Part IV Engineering Tradeoff of Single Versus Mixed Cases," to be published July 1966.

23. Perry, J. H., Chemical Engineers Handbook, McGraw-Hill, 1957.

24. Loeb, L. B., Electrical Coronas Their Basic Physical Mechanisms, University of California Press, 1965.

25. Dunbar, W. G., "High Temperature Effects on Ceramic-Insulated Thermocouple Wires," IEEE Transactions on Aerospace, Vol. 2, No. 2, April 1964.

26. Harwood, J. J., The Metal Molybdenum, American Society for Metals, Cleveland, Ohio, 1958.

UNCLASSIFIED

Security Classification

DOCUMENT CONTROL DATA - R&D

(Security classification of title, body of abstract and indexing annotation must be entered when the overall report is classified)

1. ORIGINATING ACTIVITY (Corporate author) Space Electric Power Systems Aerospace Group, THE BOEING COMPANY Seattle, Washington	2a. REPORT SECURITY CLASSIFICATION Unclassified 2b. GROUP

3. REPORT TITLE

CORONA ONSET VOLTAGE OF INSULATED AND BARE ELECTRODES IN RAREFIED AIR AND OTHER GASES

4. DESCRIPTIVE NOTES (Type of report and inclusive dates)

Final Report July - December 1965

5. AUTHOR(S) (Last name, first name, initial)

Dunbar, William H.

6. REPORT DATE	7a. TOTAL NO. OF PAGES	7b. NO. OF REFS
June 1966	175	26

8a. CONTRACT OR GRANT NO.	9a. ORIGINATOR'S REPORT NUMBER(S)
AF33(615)-3020 b. PROJECT NO. 8128 c. Task 812806 d.	D2-84141-1 9b. OTHER REPORT NO(S) (Any other numbers that may be assigned this report) AFAPL-TR-65-122

10. AVAILABILITY/LIMITATION NOTICES

11. SUPPLEMENTARY NOTES	12. SPONSORING MILITARY ACTIVITY
Report is documentation of corona work by Boeing preceding and during X-20A Program.	Air Force Aero-Propulsion Laboratory, Research and Technology Division, AFSC, Wright-Patterson Air Force Base, Ohio

13. ABSTRACT

Electrical discharges caused by corona, glow discharges, and voltage breakdown were measured under conditions encountered in the X-20A (Dyna-Soar) aerospace vehicle when operating within the 70,000- to 250,000-foot altitude zone. Most measurements were made at the electric-power-system frequency (400 hertz) in gases used to pressurize X-20A compartments. These gases were nitrogen, oxygen, nitrogen-oxygen mixtures, and normal sea level air at reduced pressure.

Test results show that: (1) the corona onset voltage (that voltage at which the electrical discharge is initiated) can be increased by insulating the electrical terminals and by twisting or cabling the insulated wires; (2) the corona onset voltage between insulated wires is increased as the insulation is made thicker and insulation dielectric constant is made lower, and is decreased to that of bare wires as the wire diameter and wire spacing are increased; and (3) the corona onset voltage of components depends on the type of component, its wire connections, its installation, and the gaseous environment.

The corona onset voltage of round, bare, nichrome wires is less at temperatures over 500° than at temperatures between -60°C and 150°C. The corona onset voltage drops to nearly zero when contaminants such as molybdenum-trioxide vapor permeate the air space between wires at temperatures above 500°C and pressures above 1.0 torr.

DD FORM 1473

UNCLASSIFIED

Security Classification

14 KEY WORDS	LINK A		LINK B		LINK C	
	ROLE	WT	ROLE	WT	ROLE	WT
Corona onset voltage						
Voltage breakdown						
Ionization						
Molybdenum trioxide contamination						
High temperature wire						
Insulated wires						
Electric power system components						
X-20A Dyna-Soar						

INSTRUCTIONS

1. ORIGINATING ACTIVITY: Enter the name and address of the contractor, subcontractor, grantee, Department of Defense activity or other organization *(corporate author)* issuing the report.

2a. REPORT SECURITY CLASSIFICATION: Enter the overall security classification of the report. Indicate whether "Restricted Data" is included. Marking is to be in accordance with appropriate security regulations.

2b. GROUP: Automatic downgrading is specified in DoD Directive 5200.10 and Armed Forces Industrial Manual. Enter the group number. Also, when applicable, show that optional markings have been used for Group 3 and Group 4 as authorized.

3. REPORT TITLE: Enter the complete report title in all capital letters. Titles in all cases should be unclassified. If a meaningful title cannot be selected without classification, show title classification in all capitals in parenthesis immediately following the title.

4. DESCRIPTIVE NOTES: If appropriate, enter the type of report, e.g., interim, progress, summary, annual, or final. Give the inclusive dates when a specific reporting period is covered.

5. AUTHOR(S): Enter the name(s) of author(s) as shown on or in the report. Enter last name, first name, middle initial. If military, show rank and branch of service. The name of the principal author is an absolute minimum requirement.

6. REPORT DATE: Enter the date of the report as day, month, year, or month, year. If more than one date appears on the report, use date of publication.

7a. TOTAL NUMBER OF PAGES: The total page count should follow normal pagination procedures, i.e., enter the number of pages containing information.

7b. NUMBER OF REFERENCES: Enter the total number of references cited in the report.

8a. CONTRACT OR GRANT NUMBER: If appropriate, enter the applicable number of the contract or grant under which the report was written.

8b, 8c, & 8d. PROJECT NUMBER: Enter the appropriate military department identification, such as project number, subproject number, system numbers, task number, etc.

9a. ORIGINATOR'S REPORT NUMBER(S): Enter the official report number by which the document will be identified and controlled by the originating activity. This number must be unique to this report.

9b. OTHER REPORT NUMBER(S): If the report has been assigned any other report numbers *(either by the originator or by the sponsor)* also enter this number(s).

10. AVAILABILITY/LIMITATION NOTICES: Enter any limitations on further dissemination of the report, other than those imposed by security classification, using standard statements such as:

(1) "Qualified requesters may obtain copies of this report from DDC."

(2) "Foreign announcement and dissemination of this report by DDC is not authorized."

(3) "U. S. Government agencies may obtain copies of this report directly from DDC. Other qualified DDC users shall request through

_____."

(4) "U. S. military agencies may obtain copies of this report directly from DDC. Other qualified users shall request through

_____."

(5) "All distribution of this report is controlled. Qualified DDC users shall request through

_____."

If the report has been furnished to the Office of Technical Services, Department of Commerce, for sale to the public, indicate this fact and enter the price, if known.

11. SUPPLEMENTARY NOTES: Use for additional explanatory notes.

12. SPONSORING MILITARY ACTIVITY: Enter the name of the departmental project office or laboratory sponsoring *(paying for)* the research and development. Include address.

13. ABSTRACT: Enter an abstract giving a brief and factual summary of the document indicative of the report, even though it may also appear elsewhere in the body of the technical report. If additional space is required, a continuation sheet shall be attached.

It is highly desirable that the abstract of classified reports be unclassified. Each paragraph of the abstract shall end with an indication of the military security classification of the information in the paragraph, represented as *(TS)*, *(S)*, *(C)*, or *(U)*.

There is no limitation on the length of the abstract. However, the suggested length is from 150 to 225 words.

14. KEY WORDS: Key words are technically meaningful terms or short phrases that characterize a report and may be used as index entries for cataloging the report. Key words must be selected so that no security classification is required. Identifiers, such as equipment model designation, trade name, military project code name, geographic location, may be used as key words but will be followed by an indication of technical context. The assignment of links, roles, and weights is optional.